Characterization of drug disposition in humans using novel *in vitro* methodologies based on the Extended Clearance Model

Inauguraldissertation

zur

Erlangung der Würde eines Doktors der Philosophie

vorgelegt der

Philosophisch-Naturwissenschaftlichen Fakultät

der Universität Basel

von

Julia Riede

aus Deutschland

Basel, 2018

Genehmigt von der Philosophisch-Naturwissenschaftlichen Fakultät

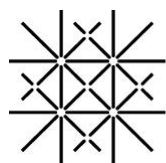auf Antrag von

Prof. Dr. Jörg Huwyler (Fakultätsverantwortlicher)

Dr. Gian Camenisch (Dissertationsleiter)

Prof. Dr. Gerd Kullak-Ublick (Korreferent)

Basel, den 23. Mai 2017

Prof. Dr. Martin Spiess (Dekan)

To my mother

for making everything possible

Table of Contents

Abbreviations

ABC	ATP binding cassette
ADMET	absorption, distribution, metabolism, excretion, and toxicity
AMP	adenosine monophosphate
ATP	adenosine triphosphate
BCRP	breast cancer resistance protein
BSEP	bile salt export pump
CAR	constitutive androstane receptor
C_b	drug concentration in whole blood
$C_{b,u}$	unbound drug concentration in whole blood
$C_{hep,u}$	unbound intrahepatic drug concentration
CL	clearance
CL_{hep}	hepatic clearance
$CL_{h,int}$	intrinsic hepatic clearance
$CL_{int,met,app}$	apparent intrinsic metabolic clearance
$CL_{int,met}$	intrinsic metabolic clearance
$CL_{int,sec,app}$	apparent intrinsic biliary clearance
$CL_{int,sec}$	intrinsic biliary clearance
CL_{other}	non-hepatic/non-renal clearance
CL_{ren}	renal clearance
$CL_{ren,fil}$	glomerular filtration clearance
$CL_{ren,sec}$	tubular secretion clearance
CL_{tot}	total clearance
C_p	drug concentration in plasma
$C_{p,u}$	unbound drug concentration in plasma
CYP	cytochrome P450
DDI	drug-drug interaction
DILI	drug-induced liver injury
DNA	deoxyribonucleic acid
ECCCS	Extended Clearance Concept Classification System
ECM	Extended Clearance Model
EMA	European Medicine Agency
F	bioavailability
F_a	fraction absorbed
FDA	Food and Drug Administration
F_g	fraction escaping gut wall metabolism
F_h	fraction escaping hepatic clearance
FMO	flavin-containing monooxygenase

fu_b	unbound fraction in blood
fu_p	unbound fraction in plasma
fu_{hep}	unbound fraction in hepatocytes
fu_{mic}	unbound fraction in microsomes
f_{reab}	fraction of drug that is reabsorbed from the tubule fluid back into the blood
FXR	farnesoid-X receptor
GST	glutathione S-transferase
HMG-CoA	3-hydroxy-3-methylglutaryl-coenzyme A
IC_{50}	concentration of inhibitor to achieve half-maximal transporter inhibition
IVIVC	*in vitro-in vivo* correlation
IVIVE	*in vitro-in vivo* extrapolation
K_i	reversible inhibition constant
K_m	Michaelis-Menten constant
Kp	liver-to-blood concentration ratio for total drug at steady-state
Kp_{uu}	liver-to-blood concentration ratio for unbound drug at steady-state
$logD_{7.4}$	distribution coefficient at pH 7.4
logP	octanol-to-water partition coefficient
MATE	multidrug and toxin extrusion protein
MRP	multidrug resistance-associated protein
NADPH	nicotinamide adenine dinucleotide phosphate
NAT	N-acetyltransferases
NTCP	sodium taurocholate co-transporting polypeptide
OAT	organic anion transporter
OATP	organic anion transporting polypeptide
OCTN	organic/carnitine cation transporter
OCT	organic cation transporter
OST	organic solute transporter
PBPK	physiologically-based pharmacokinetic
PEPT	peptide transporter
PFIC-2	progressive familial intrahepatic cholestasis type 2
P-gp	P-glycoprotein
pK_a	acid dissociation constant
PS_{app}	apparent hepatic uptake permeability
PS_{eff}	total hepatic efflux permeability
$PS_{eff,act}$	active hepatic efflux permeability
$PS_{eff,pas}$	passive hepatic efflux permeability
PS_{inf}	total hepatic uptake permeability
$PS_{inf,act}$	active hepatic uptake permeability
$PS_{inf,pas}$	passive hepatic uptake permeability
PXR	pregnane X receptor

Q_h	hepatic blood flow
R_b	blood-to-plasma partition coefficient
SLC	solute carrier
SULT	sulfotransferase
UDP	uridine diphosphate
UDPGA	uridine diphosphate glucuronic acid
UGT	UDP-glucuronosyltransferase
ULN	upper limit of normal
V_{max}	maximum velocity

CHAPTER 1

Summary

Safety and efficacy of drugs depend on their exposure in the body, which is determined by dose and bioavailability, but also by drug disposition as a result of tissue distribution and elimination processes. Knowledge about drug disposition in humans is therefore critical for the successful development of new drugs, with clinical information being unavailable at early development stages. To overcome this limitation, the pharmacokinetic properties of new drug candidates are routinely characterized using cell-based *in vitro* methods and *in vitro-in vivo* extrapolation (IVIVE) models. However, the assessment of drug distribution and elimination remains challenging. It was therefore the aim of this thesis to 1) establish a mechanistic *in vitro* model to study the hepatic distribution of unbound drug and to validate the model by predicting the clinical risk of drug-induced cholestasis, 2) investigate the applicability of additional *in vitro* methods for the determination of hepatic distribution of unbound drug, and 3) develop an *in vitro* model for the prediction of total (hepatic and renal) drug clearance and elimination pathway contributions in humans.

Knowledge about the drug distribution into tissues and the corresponding unbound intracellular drug concentrations is of particular interest in the context of intracellular drug effects related to toxicity, pharmacokinetics, and pharmacodynamics. For instance, prediction of drug-induced cholestasis due to inhibition of the intrahepatic bile salt export pump (BSEP) is commonly conducted using the unbound systemic drug exposure as a surrogate for the unbound intrahepatic concentration following the "free-drug hypothesis". However, this assessment offers limited translatability to the clinical cholestasis risk since the effective unbound intrahepatic drug concentration is affected by active transport and/or metabolic processes. To improve such evaluations of intrahepatic drug interactions, the determination of the liver-to-blood partition coefficient for unbound drug at steady-state (Kp_{uu}) was established based on *in vitro* measurements of active and passive sinusoidal uptake permeability, sinusoidal efflux permeability, hepatic metabolism, and biliary secretion according to the Extended Clearance Model (ECM). Following successful validation of the ECM-based Kp_{uu} approach by *in vitro-in vivo* correlation in rats, human Kp_{uu} data of 18 drug compounds were used to calculate unbound intrahepatic drug concentrations based on clinical drug exposure. This assessment significantly improved the translation of BSEP inhibition *in vitro* data to human and allowed the prediction of the clinical cholestasis frequency. Moreover, usefulness of the ECM as a drug classification system and for the quantitative evaluation of genetic and physiological risk factors for the development of cholestasis was demonstrated. The determination of unbound intrahepatic drug concentrations using the ECM-based hepatic Kp_{uu} is therefore expected to improve early risk assessment of drug-induced cholestasis as well as of other intrahepatic drug interactions.

The ECM-based determination of Kp_{uu} was successfully established and validated. However, this approach is labor and cost-intensive. A second project therefore aimed at comparing alternative *in vitro* Kp_{uu} determination methods for the previously investigated compound set. For this purpose, three straightforward approaches were selected that rely on separate *in vitro* measurements of the liver-to-blood partition coefficient for total drug at steady-state (Kp) and the unbound fraction in hepatocytes (fu_{hep}). Kp was generally determined in hepatocellular drug accumulation experiments in the absence of intrinsic metabolic and biliary clearance processes, whereas fu_{hep} was either measured in hepatocellular drug accumulation experiments on ice (temperature method), using homogenized hepatocytes in equilibrium dialysis experiments (homogenization method), or calculated from the distribution coefficient $logD_{7.4}$ using an empirical model ($logD_{7.4}$ method). All investigated methods indicated deviations to ECM-derived Kp_{uu} data, which were closely linked to the pharmacokinetic and physicochemical compound properties, namely the extent of intrinsic hepatic clearance, $logD_{7.4}$, and molecular weight. The usefulness of the alternative Kp_{uu} determination methods is therefore limited, with the ECM remaining the preferred approach for an integrated assessment of hepatic Kp_{uu}. Nevertheless, the alternative methods can provide valid fu_{hep} data if the physicochemical compound properties are considered for the selection of the appropriate method.

During drug development, hepatic drug clearance is routinely predicted using *in vitro* approaches such as the ECM. In contrast, appropriate *in vitro* models for the prediction of renal drug clearance are lacking. Thus, the assessment of total clearance for new drug candidates is strongly limited. To overcome this drawback, an empirical *in vitro* model was established that provides estimates of the relative hepatic metabolic, biliary, and renal elimination pathway contributions in humans, based on *in vitro* sinusoidal uptake permeability data. This assessment subsequently allows the extrapolation of hepatic into total drug clearance. Under consideration of ECM-based hepatic clearances, the model provided accurate predictions of total human clearance for 10 developmental compounds. Moreover, it was demonstrated that the Extended Clearance Concept Classification System (ECCCS) is applicable to evaluate the relevance of metabolic, biliary, and renal drug elimination, which provides useful guidance for the design of follow-up enzyme and transporter phenotyping studies. Thus, the established model allows a simple and highly reliable assessment of total drug clearance and relative elimination pathway contributions in humans based solely on hepatic *in vitro* data, facilitating a tailor-made pharmacokinetic assessment during early drug development.

CHAPTER 2

Introduction

2.1. Drug transport across biological membranes

Permeation across cellular membranes is a key determinant for the ADMET (absorption, distribution, metabolism, excretion, and toxicity) properties of drugs. Membrane permeation occurs either via the transcellular route through the cells or via the paracellular route between the cells (Figure 2.1). Paracellular permeability represents a passive process, which is restricted to small hydrophilic compounds by intercellular tight junctions (Camenisch et al., 1997; Pade and Stavchansky, 1997). Transcellular permeation occurs by passive diffusion (passive membrane permeability) and/or by carrier-mediated (active or facilitated) transport. Passive membrane permeability is driven by a concentration gradient and is mainly dependent on physicochemical properties such as lipophilicity, polarity, ionization, and molecular size of a drug. Thereby, small, lipophilic, and uncharged drugs generally exhibit higher passive membrane permeability (Oostendorp et al., 2009; Sugano et al., 2010). Active transport of drugs across cell membranes is mediated by transport proteins of the solute carrier (SLC) family and the adenosine triphosphate (ATP) binding cassette (ABC) family, whereby SLC transporters mainly facilitate uptake into cells and ABC transporters mediate efflux out of cells.

2.1.1. SLC transporters

The human SLC superfamily consists of 52 subfamilies (SLC1 - SLC52) with about 400 transporter genes (Hediger et al., 2013). SLC transporters are membrane-bound proteins that primarily mediate cellular uptake of their substrates by facilitated diffusion or secondary active transport (DeGorter et al., 2012). Facilitated diffusion is energy-independent and driven by an electrochemical gradient that determines the direction of transport. Secondary active transport occurs against an electrochemical gradient and is coupled to the symport or antiport of ions (Hediger et al., 2013; Sahoo et al., 2014). SLC transporters are important determinants for the absorption, tissue distribution, and elimination of endogenous substances including sugars, amino acids, peptides, nucleotides, and ions. Therefore, they have been recognized as potential therapeutic drug targets due to their physiological functions and role in numerous diseases (Cesar-Razquin et al., 2015; Lin et al., 2015). In addition, many drugs have been identified as substrates for SLC transporters in different organs.

In the context of drug transport, SLC transporters of the organic anion transporting polypeptides (OATP, SLCO (previously SLC21A)) family, the organic anion transporters (OAT, SLC22A), organic cation transporters (OCT, SLC22A) family, and the multidrug and toxin
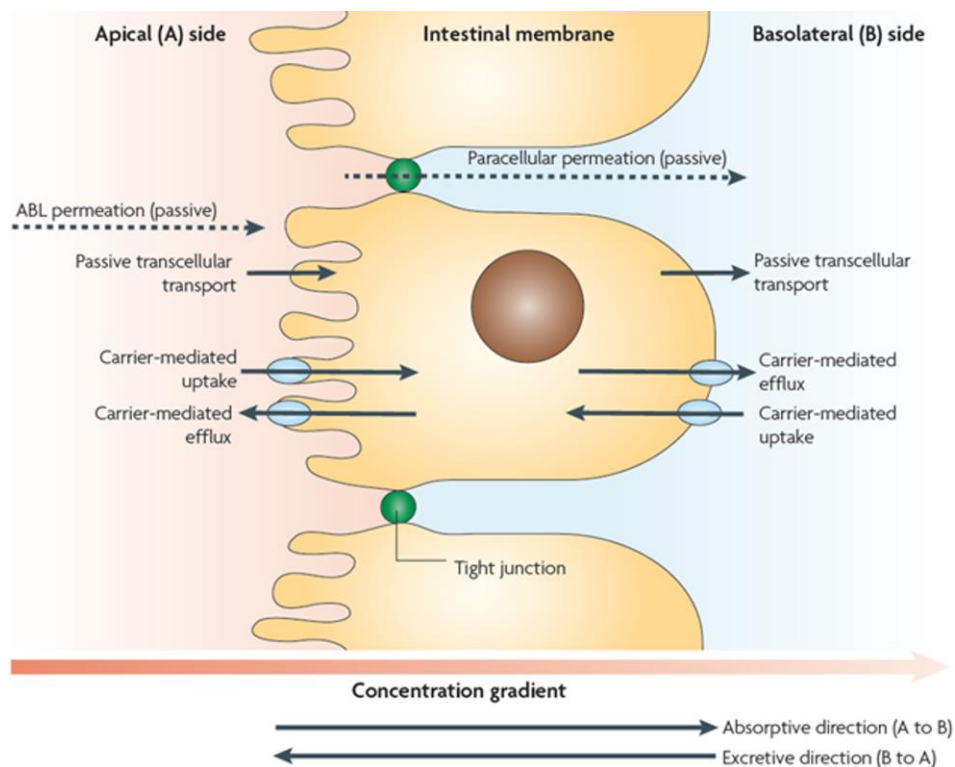
Figure 2.1. Transport mechanisms in epithelial cells. Drugs permeate across epithelial membranes via the paracellular or the transcellular route in either an absorptive (apical to basolateral) or excretory (basolateral to apical) direction. Passive paracellular and transcellular permeability is driven by a concentration gradient and depends on physicochemical properties, with tight junctions between cells limiting paracellular permeability. Active transcellular permeability is mediated by efflux transporters of the ABC superfamily and uptake transporters of the SLC superfamily. Taken from Sugano et al. (2010).

extrusion protein (MATE, SLC47A) family are considered to be of high clinical relevance. These SLC transporters are predominantly expressed in the plasma membrane of polarized epithelial cells in tissues with barrier or excretory function such as intestinal epithelia, hepatocytes, kidney proximal tubules, and the blood-brain barrier where they regulate the systemic and tissue exposure of drugs (Figure 2.2). In addition, interactions between drugs and transporters are generally associated with a risk for drug-drug interactions (DDI) that might change the exposure profile of drugs and therefore alter their safety and efficacy. Thereby, transporter substrates are potential DDI victim drugs and transporter inhibitors can become perpetrators of DDIs. The evaluation of new drug candidates regarding their interaction with clinically relevant drug transporters is therefore recommended by American and European health authorities (Food and Drug Administration (FDA), European Medicine Agency (EMA)) as well as by the International Transporter Consortium (EMA, 2012; FDA, 2012; Hillgren et al., 2013). The role and characteristics of these SLC drug transporters is described in the following sections.

2.1.1.1. OATP family

The OATP family consists of 11 members, with OATP1B1 (SLCO1B1) and OATP1B3 (SLCO1B3) representing the most important isoforms with regard to the transport of drugs (EMA, 2012; FDA, 2012; Hillgren et al., 2013). OATP1B1 and 1B3 are exclusively expressed in the sinusoidal plasma membrane of hepatocytes where they mediate the hepatic uptake of their substrates (Kullak-Ublick et al., 2001). The transport mechanism of OATPs is not fully understood, but they likely function as electroneutral exchangers (Roth et al., 2012). OATP1B1 and 1B3 have an overlapping substrate range including endogenous substances, such as bile acids or conjugated and unconjugated bilirubin, as well as various drugs (DeGorter et al., 2012; Roth et al., 2012). Hence, they enhance the access to drug-metabolizing enzymes and biliary secretion in the liver and mediate the first step in hepatic drug elimination. In addition, OATP1B1 and 1B3 are known to contribute to drug efficacy for intrahepatic targets, as in the case for the hepatic uptake of statins, facilitating their lipid-lowering effect as inhibitors of 3-hydroxy-3-methylglutaryl-coenzyme A (HMG-CoA) reductase (Niemi et al., 2005). On the other hand, reduced OATP1B1 and 1B3 function is linked to increased systemic exposure and drug toxicity, exemplified by statin-induced myopathy (Neuvonen, 2010; DeGorter et al., 2012). This condition can be caused by OATP1B1 and 1B3 inhibition due to co-medication or by the presence of nonsynonymous polymorphisms. The latter is particularly relevant for OATP1B1 (Link et al., 2008; Elsby et al., 2012).

2.1.1.2. OAT and OCT family

The SLC22 gene family is composed of over 30 members in mammals including OATs, OCTs, and organic/carnitine cation transporter (OCTNs) (Liu et al., 2016). Among the SLC22 family, OAT1 (SLC22A6), OAT3 (SLC22A8), OCT1 (SLC22A1), and OCT2 (SLC22A2) are considered the most relevant drug transporters (EMA, 2012; FDA, 2012; Hillgren et al., 2013). OAT1 and OAT3 mediate the cellular uptake of hydrophilic anionic and zwitterionic molecules with low molecular weight including various drugs. They function as antiporters and mediate the membrane transport of their substrates in exchange for the counter ion α-ketoglutarate (Roth et al., 2012; Koepsell, 2013; Liu et al., 2016). Both transporters are primarily localized at the basolateral plasma membrane of renal proximal tubule cells, with OAT1 expression having additionally been observed in skeletal muscle cells (Takeda et al., 2004; DeGorter et al., 2012).

OCT1 and OCT2 facilitate bidirectional diffusion of their substrates down the electrochemical gradient (Roth et al., 2012). Their range of substrates covers organic cations with low molecular weight, including several drugs, and endogenous compounds like monoamine neurotransmitters and creatinine (DeGorter et al., 2012). OCT1 is primarily expressed in the sinusoidal plasma membrane of hepatocytes. In addition, OCT1 is located in the basolateral plasma membrane of intestinal epithelial cells and in the apical plasma membrane of kidney proximal tubule and lung cells (Lips et al., 2005; Muller et al., 2005; Nies et al., 2008; Tzvetkov et al., 2009). Large inter-individual variability in hepatic OCT1 expression has been observed, which could be linked to genetic variations and cholestasis (Nies et al., 2009). OCT2 is mainly expressed in the basolateral

plasma membrane of kidney distal tubule cells and to a lesser extent in the lung and brain (Gorboulev et al., 1997; Lips et al., 2005; DeGorter et al., 2012). Hence, OATs and OCT mediate the elimination of drugs and limit their systemic exposure, whereby OAT1, OAT3, and OCT2 contribute to active renal tubular secretion and OCT1 primarily facilitates hepatic drug uptake.

2.1.1.3. MATE family

The MATE family consists of MATE1 (SLC47A1), MATE2 (SLC47A2), and the splicing variants MATE2K and MATE2B. Among the MATE2 variants, MATE2K is the active form, whereas the physiological role of MATE2 and MATE2B is unknown (Masuda et al., 2006). MATE1 and MATE2K are mainly expressed in the apical plasma membrane of kidney proximal tubule cells. MATE1 is also located at the canalicular hepatocyte membrane and in skeletal muscle, adrenal gland, and testis (Otsuka et al., 2005; Masuda et al., 2006). MATEs are electroneutral transporters that typically facilitate bidirectional transport of organic cations with low molecular weight against a proton gradient (Tanihara et al., 2007). They function in cooperation with hepatic OCT1 and renal OCT2 and mediate the secretion of organic cations into bile and urine (Otsuka et al., 2005). In addition, transport of anions and zwitterions has been observed, likely working together with OAT-mediated cellular uptake (Yonezawa and Inui, 2011; Hillgren et al., 2013).

2.1.2. ABC transporters

ABC transporters are membrane-bound transport proteins that mediate energy-dependent cellular efflux against a concentration gradient by binding and hydrolysis of ATP. So far, 52 human ABC transporters have been identified, categorized in seven subfamilies (ABCA - ABCG) (Saier et al., 2016). Similar to SLC transporters, clinically relevant ABC transporters are mainly located in the plasma membrane of polarized epithelial cells in intestinal epithelia, hepatocytes, kidney proximal tubule cells, and at the blood-brain barrier (Figure 2.2). ABC transporters play a pivotal role in limiting the absorption and distribution or mediating the excretion of drugs and other xenobiotics, protecting the body from potentially harmful substances (Giacomini et al., 2010). Interactions with ABC transporters are also associated with a potential risk for DDIs (Chan et al., 2004; Konig et al., 2013). ABC drug transporters of particular clinical importance are P-glycoprotein (P-gp, ABCB1), breast cancer resistance protein (BCRP, ABCG2), members of the multidrug resistance protein (MRP, ABCC) family, and bile salt export pump (BSEP, ABCB11) (Hillgren et al., 2013). These transporters are described in the following section.

2.1.2.1. P-gp and BCRP

P-gp and BCRP are expressed in the apical plasma membrane of polarized epithelial tissues and mediate the excretory transport of drugs and xenobiotics, thereby limiting their bioavailability and systemic and intracellular exposure. P-gp and BCRP are present in the intestinal epithelium,

hepatocytes, kidney proximal tubule cells, endothelial cells in the blood-brain barrier as well as in blood-nerve, blood-testis, and maternal-fetal barriers. BCRP is also expressed in mammary tissue where it secretes vitamins but also drugs and toxins into breast milk (Schinkel and Jonker, 2003). The substrate spectrum of P-gp and BCRP is large and includes endogenous substrates and xenobiotics such as numerous drugs and carcinogens. P-gp substrates are frequently hydrophobic cationic or neutral molecules. For BCRP, no definite substrate-structure relationship has been established (Schinkel and Jonker, 2003; Robey et al., 2009; Giacomini et al., 2010; Wessler et al., 2013). In addition, several inhibitors and inducers of P-gp and BCRP have been identified, including pharmaceutical drugs, herbal medicines, and food and juice components (Marchetti et al., 2007; Muller and Fromm, 2011).
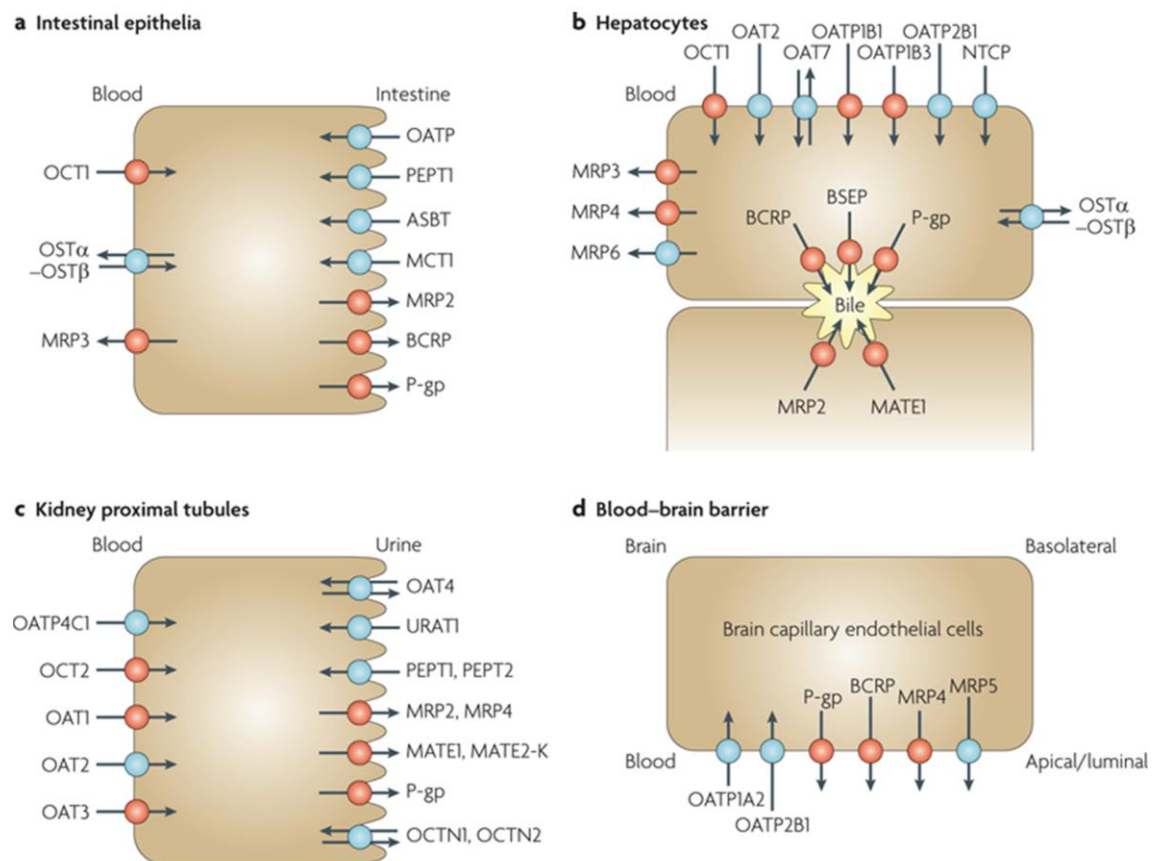
Figure 2.2. Drug transporters in intestinal epithelia (a), hepatocytes (b), kidney proximal tubules (c), and blood-brain barrier (d). Red highlighted transporters have high clinical relevance and evaluation of their interaction potential with new drug candidates is requested by health authorities (EMA, 2012; FDA, 2012; Hillgren et al., 2013). ASBT, sodium/bile acid co-transporter; BCRP, breast cancer resistance protein; BSEP, bile salt export pump ; MATE, multidrug and toxin extrusion protein; MCT, monocarboxylic acid transporter; MRP, multidrug resistance protein; NTCP, sodium taurocholate co-transporting peptide; OAT, organic anion transporter; OATP, organic anion transporting polypeptide; OCT, organic cation transporter; OCTN, organic/carnitine cation transporter; OSTα-OSTβ, heteromeric organic solute transporter; PEPT, peptide transporter; P-gp, P-glycoprotein; URAT, urate transporter. Modified from Giacomini et al. (2010).

2.1.2.2. MRP family

The MRP family comprises 9 members (MRP1 - MRP9), which primarily mediate cellular efflux of endogenous organic anionic substances such as glucuronide, glutathione, and sulfate conjugates, and steroids, as well as drugs and their conjugated metabolites (Slot et al., 2011). Among the MRP family, MRP2 (ABCC2), MRP3 (ABCC3), and MRP4 (ABCC4) are considered the most clinically relevant members (Hillgren et al., 2013). MRP2 is apically expressed in the canalicular plasma membrane of hepatocytes, kidney proximal tubule cells, small intestinal epithelium, colon, gall bladder, bronchi, and placenta. On the contrary, MRP3 and MRP4 are located in the sinusoidal hepatocyte membrane and mediate efflux towards to bloodstream. Further localizations of MRP3 and MRP4 are the plasma membrane of intestinal epithelial cells, kidney proximal tubule cells, and various other tissues (Schinkel and Jonker, 2003; Hillgren et al., 2013). MRP2-mediated efflux is of particular importance for the hepatobiliary, renal, and intestinal elimination of conjugated drug metabolites and endogenous substances such as bilirubin glucuronides (Konig et al., 1999). For instance, patients with Dubin-Johnson syndrome display conjugated hyperbilirubinemia due to mutations in the ATP-binding regions of MRP2, resulting in complete MRP2 deficiency (Erlinger et al., 2014; Keppler, 2014). Similarly, MRP2 inhibition by drugs may induce conjugated hyperbilirubinemia (Chang et al., 2013). Under such conditions, MRP3 and MRP4-mediated efflux act as compensatory pathways by increased sinusoidal efflux and renal excretion of conjugated bilirubin (Vlaming et al., 2006; Kock and Brouwer, 2012; Keppler, 2014).

2.1.2.3. BSEP

BSEP is exclusively expressed in the canalicular plasma membrane of hepatocytes and primarily mediates the biliary secretion of monovalent conjugated bile salts, which works in cooperation with sinusoidal expressed sodium taurocholate co-transporting polypeptide (NTCP, SLC10A1) and OATPs. Thus, BSEP has a central function in the vectorial hepatobiliary transport of bile acids, bile formation, and driving bile flow (Kullak-Ublick et al., 2000; Dawson et al., 2009). Impairment of BSEP function is linked to intrahepatic cholestasis, a pathophysiological condition characterized by reduced bile flow as well as potential intrahepatic accumulation of cytotoxic bile acids and hepatocellular damage (Kosters and Karpen, 2008; Stieger, 2010). So far, more than 100 different mutations in the ABCB11 gene have been identified that are partly linked to severe hereditary cholestatic syndromes (Dietrich and Geier, 2014). For instance, complete absence of functional BSEP protein is represented by progressive familial intrahepatic cholestasis type 2 (PFIC-2), which can result in liver cirrhosis, liver failure, and ultimately the need for liver transplantation (Srivastava, 2014). In addition, acquired and transient forms of cholestasis exist. Intrahepatic cholestasis during pregnancy commonly arises in the third trimester and resolves after delivery. Variations in the ABCB11 gene as well as in other genes of bile acid transporters and the nuclear bile acid-sensitive farnesoid-X receptor (FXR) likely contribute to a genetic predisposition. Furthermore, inhibition of bile acid transporters by hormones such as estrogens

and progesterones plays a role in the development of intrahepatic cholestasis of pregnancy (van der Woerd et al., 2010; Dietrich and Geier, 2014).

With regard to the role of BSEP in hereditary and acquired forms of cholestasis, BSEP inhibition has been recognized as a key factor for the development of intrahepatic drug-induced cholestasis (Stieger et al., 2000; Fattinger et al., 2001; Funk et al., 2001a; Dawson et al., 2012). Drug-induced cholestasis represents one form of drug-induced liver injury (DILI), alternative phenotypes are hepatocellular or mixed DILI. Every type of DILI is characterized by a different pattern of elevated liver enzymes, namely alkaline phosphatase (AP), alanine transaminase (ALT), and aspartate transaminase (AST), in the serum (CIOMS, 1999). Drug-induced cholestasis is characterized by a predominant elevation of AP compared to no or only moderate increases of ALT and AST. On the contrary, increases in AST or ALT compared to AP indicate a hepatocellular pattern of DILI, whereas all three liver enzymes are elevated during mixed DILI. The severity of drug-induced cholestasis ranges from asymptomatic elevations of liver enzymes to acute liver failure and is reported to account for up to 26% of all hepatic adverse reactions (Bjornsson and Olsson, 2005; Hussaini and Farrington, 2007; Yang et al., 2013). Hence, drug interactions with BSEP are of high relevance, although BSEP has a minor role in the hepatobiliary elimination of drugs. Accordingly, the evaluation of the BSEP inhibition potential is recommended for new drug candidates (EMA, 2012; Hillgren et al., 2013; Kullak-Ublick et al., 2017). If clinically relevant BSEP inhibition is expected, biochemical monitoring of cholestasis markers in clinical studies should be considered. Yet, recent studies have demonstrated limited predictability of drug-induced cholestasis from *in vitro* BSEP data since there is no direct correlation with the effective cholestasis risk in humans (Dawson et al., 2012; Morgan et al., 2013; Shah et al., 2015).

2.2. Drug absorption and bioavailability

Absorption generally refers to the passage of a drug from its site of application into the bloodstream and is an important process in terms of bioavailability and systemic exposure of drugs. While intravenously, intramuscularly, or subcutaneously administered drugs commonly feature complete bioavailability, different processes influence the gastrointestinal absorption and can reduce the systemic bioavailability of orally administered drugs (Figure 2.3). Gastrointestinal absorption mainly takes place in the small intestine due to the large surface area, high permeability of intestinal membranes compared to that of the stomach, and high blood flow in the intestinal capillaries (Rowland and Tozer, 1995; Pang et al., 2010). The absorption process itself is defined as permeation of a drug into the enterocytes of the intestinal epithelium, which is denoted as the fraction of absorbed drug (F_a). The systemic bioavailability of orally administered drugs (F) further depends on metabolic first-pass effects in the gut wall and in the liver, which are represented by the fraction escaping gut wall metabolism (F_g) and the fraction escaping hepatic clearance (F_h) as summarized in Eq. (2.1) (Kwon, 2001):

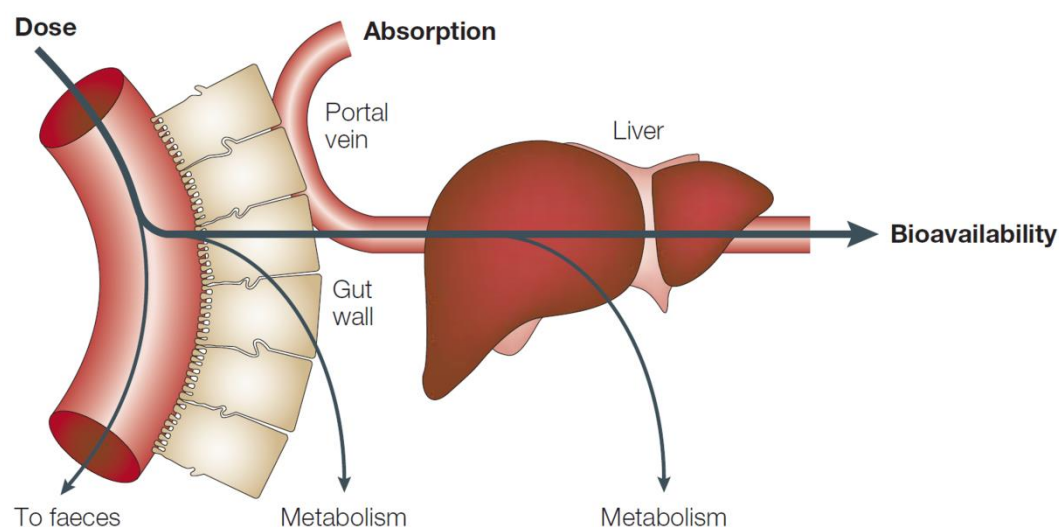$$F = F_a \times F_g \times F_h \tag{2.1}$$

Figure 2.3. Absorption and bioavailability of orally administered drugs. A solute drug in the gastrointestinal lumen enters the blood capillaries via transcellular or paracellular permeation through the intestinal epithelium. Gut wall metabolism and active transport by efflux transporters in the luminal enterocyte membrane reduce drug absorption and systemic bioavailability. The absorbed drug is transported to the liver via the portal vein and undergoes hepatic-first pass elimination before reaching the systemic circulation. Taken from van de Waterbeemd and Gifford (2003).

Prerequisites for absorption of an orally dosed drug are the disintegration of the oral dosage form and the dissolution of the released drug in gastrointestinal fluids, which is mainly determined by the aqueous solubility (van de Waterbeemd and Gifford, 2003). Once dissolved, the absorption of drugs into or across the intestinal epithelium occurs either via transcellular or the paracellular route (Figure 2.1). Transcellular permeation is mediated by passive membrane permeability and by luminal uptake by OATPs, OCTNs, and peptide transporter 1 (PEPT1, SLC15A1) and by basolateral efflux by MRPs (Oostendorp et al., 2009; Estudante et al., 2013) (Figure 2.2, panel A). While passing the intestinal epithelium, drugs can undergo active excretion by luminal efflux transporters back into the intestinal lumen, which reduces the fraction of absorbed drug. In particular, P-gp but also BCRP and MRP2 are known to limit the intestinal absorption of their substrates (Schinkel and Jonker, 2003; Robey et al., 2009). In addition, these molecules are also potential substrates of phase I and phase II drug-metabolizing enzymes in enterocytes (Benet et al., 2004; Chan et al., 2004). Although the intestinal expression levels of drug-metabolizing enzymes are relatively low compared to the liver, gut wall metabolism may lead to a substantial reduction in oral bioavailability (Gertz et al., 2010; Jones et al., 2016). Among all intestinal drug-metabolizing enzymes, cytochrome P450 (CYP) 3A is the most abundant subfamily and accounts for 82% of the total intestinal CYP content in humans (Paine et al., 2006). Further enzymes with relevant contributions to intestinal drug metabolism are other CYP isoforms, sulfotransferases (SULT), uridine diphosphate (UDP) glucuronosyltransferases (UGT), and N-acetyltransferases (NAT) (Gundert-Remy et al., 2014).

The fraction of drug that is absorbed and escaping gut wall metabolism (F_a x F_g) enters the blood capillaries and reaches the liver via the portal vein before entering the systemic circulation. The liver represents the major organ for drug elimination, with hepatic first-pass extraction by metabolism and hepatobiliary secretion further substantially reducing the oral bioavailability of a drug. A detailed description of the mechanisms that contribute to hepatic drug elimination is provided in section 2.4.1.

2.3. Drug distribution

Upon entering the systemic blood circulation, drugs are reversibly distributed into the different tissues and compartments of the body. The rate and extent of drug distribution is determined by the blood perfusion rate, permeability across tissue membranes, and binding within blood and tissues (Rowland and Tozer, 1995; Smith et al., 2010). Drug distribution into tissues and organs and the resulting intracellular drug concentrations are of particular interest with regard to the large amount of intracellular drug targets (Overington et al., 2006). Besides affecting pharmacological efficacy, the tissue distribution of drugs is an important determinant for drug elimination and toxicity (Chu et al., 2013).

In the systemic circulation, drugs are partly bound to different blood components and it has been widely accepted that only free (unbound) drug is able to interact and to exert any pharmacological, pharmacokinetic, or toxicological effect ("free-drug hypothesis") (Pang and Rowland, 1977; Smith et al., 2010). Blood consists of cellular elements (red blood cells, white blood cells, and platelets), which are suspended in an extracellular matrix (plasma). Red blood cells account for ~99% of the cellular blood components and as such, drug partitioning into red blood cells represents the major cellular binding process in blood (Hinderling, 1997). Blood plasma accounts for approximately half of the total blood volume and is composed of water, proteins, and other solutes. Within plasma, acidic drugs are mainly bound to albumin, whereas basic drugs are often bound to α1-acid glycoprotein and lipoproteins (Shen et al., 2013; Liu et al., 2014). Plasma protein binding generally depends on non-specific hydrophobic interactions or hydrogen bonding and is reversible (Bohnert and Gan, 2013). Due to the different binding properties in whole blood and plasma, the total (i.e. unbound and bound) drug concentrations and the unbound fractions in whole blood (C_b and fu_b) and in plasma (C_p and fu_p) can vary substantially, which is represented by the blood-to-plasma partition coefficient (R_b). The unbound drug concentrations in whole blood ($C_{b,u}$) and plasma ($C_{p,u}$) are equal, as outlined in Eq. (2.2) (Kwon, 2001):

$$C_{b,u} = C_b \times fu_b = C_p \times R_b \times fu_b = C_p \times fu_p = C_{p,u} \qquad (2.2)$$

The "free-drug hypothesis" further implies that unbound drug can freely diffuse across cellular membranes and that unbound drug concentrations in the blood and in cells are equal at steady-

state (Pang and Rowland, 1977; Smith et al., 2010). This assumption is traditionally used to justify the assessment of intracellular drug interactions based on unbound drug concentrations in the blood as a surrogate for unbound intracellular concentrations, which cannot be measured in humans (Muller and Milton, 2012; Zamek-Gliszczynski et al., 2013). However, unbound drug concentrations in blood do not necessarily reflect unbound intracellular drug concentrations in tissues such as the liver, brain, kidney, intestine, or tumor cells, where active transport by uptake and efflux transporters or metabolism can disturb the distribution equilibrium (Chu et al., 2013; Pfeifer et al., 2013a). In particular, the liver expresses a large number of drug transporters and drug-metabolizing enzymes that affect the unbound intrahepatic drug concentration ($C_{hep,u}$). In this context, the liver-to-blood partition coefficient for unbound drug at steady-state (Kp_{uu}) was introduced in order to account for the hepatic distribution of unbound drug (Shitara et al., 2006; Parker and Houston, 2008; Kusuhara and Sugiyama, 2009; Yabe et al., 2011; Chu et al., 2013; Pfeifer et al., 2013a; Shitara et al., 2013; Varma et al., 2014; Morse et al., 2015; Riccardi et al., 2016; Iwasaki et al., 2017):

$$C_{hep,u} = Kp_{uu} \times C_{b,u} \tag{2.3}$$

Under the assumption of a homogenous ("well-stirred") drug distribution in the liver, Kp_{uu} is governed by active hepatic uptake and efflux by sinusoidal transporters, passive membrane permeability into and out of the hepatocyte, hepatic metabolism, and biliary secretion by canalicular efflux transporters (Figure 2.4) (Chu et al., 2013; Pfeifer et al., 2013a). The same processes are involved in the hepatic elimination of drugs and are described in full detail in section 2.4.1.

In addition, different intrahepatic partitioning and binding processes affect the hepatic drug distribution (Figure 2.4), which is represented by the liver-to-blood partition coefficient of total drug at steady-state (Kp) and the unbound fraction in hepatocytes (fu_{hep}). However, the extent of intrahepatic partitioning processes is reflected by both parameters and only affects the hepatic distribution of total drug, whereas Kp_{uu} and unbound intrahepatic drug concentrations are solely determined by membrane permeability and intrinsic elimination processes at steady-state (Chu et al., 2013). The relationship between Kp_{uu}, Kp and fu_{hep} is outlined in Eq. (2.4):

$$Kp_{uu} = Kp \times \frac{fu_{hep}}{fu_b} \tag{2.4}$$

Drug partitioning into membranes or binding to intrahepatic proteins and other cellular structures is usually attributed to non-specific hydrophobic interactions, which are mainly dependent on the physicochemical drug properties such as lipophilicity and molecular charge (Kilford et al., 2008; Yabe et al., 2011; Nagar and Korzekwa, 2012; Fan and de Lannoy, 2014; Poulin, 2015). Specific binding to cellular structures such as proteins or deoxyribonucleic acid (DNA) generally occurs in form of drug-target interactions and rarely contributes to intracellular drug accumulation (Terasaki

et al., 1984). In addition, pH and electrochemical gradients across plasma membranes or organelle membranes affect the cellular and subcellular drug distribution. While the cytosolic pH is ~7.2, ATPases in the lysosomal membranes maintain low pH values of 4 - 5 within the lysosomal compartments. Lipophilic weak bases (octanol-to-water partition coefficient (logP) > 1 and acid dissociation constant (pK_a) > 6 (Kazmi et al., 2013)) that are uncharged in the cytosol, freely diffuse into lysosomes and become charged in the acidic environment. This substantially reduces their membrane permeability and results in lysosomal trapping and enhanced cellular accumulation of these drugs (Ohkuma and Poole, 1981; Trapp et al., 2008; Chu et al., 2013; Kazmi et al., 2013; Mateus et al., 2013). In addition, polar acids (pK_a = 5 - 9) and lipophilic bases (pK_a > 11) are trapped in mitochondria due to the alkaline mitochondrial pH (~8) or the electrochemical gradient across the inner mitochondrial membrane (-160 mV), respectively (Trapp and Horobin, 2005; Chu et al., 2013).
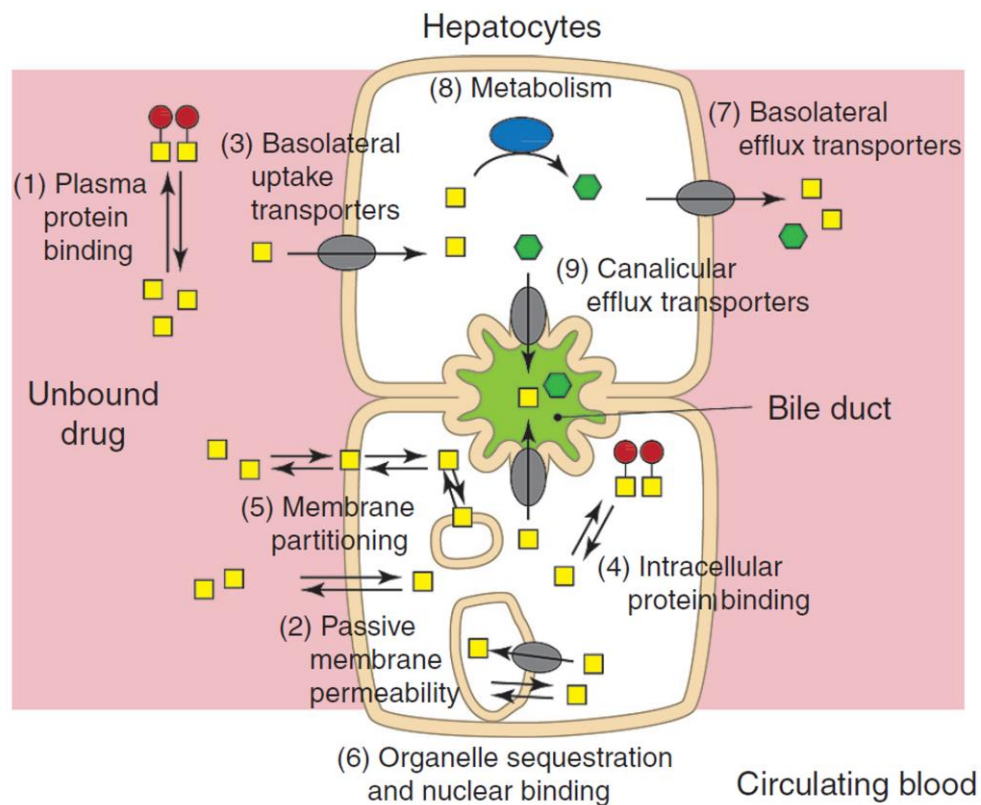
Figure 2.4. Processes affecting hepatic drug distribution and the intrahepatic drug concentration. Only unbound drug, which is not associated with plasma proteins or red blood cells (1), can cross the sinusoidal (basolateral) hepatocyte membrane via passive membrane permeability (2) or via transporter-mediated active uptake (3). Within the hepatocyte, drugs bind to intracellular proteins (4) or membranes (5) and distribute into subcellular organelles such as lysosomes or mitochondria (6). Unbound intrahepatic drug fractions undergo sinusoidal (basolateral) efflux via passive membrane permeability (2) or via transporter-mediated active efflux (7), are subject to biotransformation by drug-metabolizing enzymes (8) or biliary secretion by canalicular (apical) efflux transporters (9). Taken from Chu et al. (2013).

2.4. Drug elimination

Drug elimination denotes the irreversible removal of a parent drug compound from the systemic circulation, which occurs either by metabolic processes or by direct excretion into bile or urine, primarily mediated by the liver and the kidneys. The combination of drug distribution and drug elimination is referred to as drug disposition. The capacity of drug elimination is described by the drug clearance (CL), which is defined as the volume of blood or plasma being cleared from a drug over time. As such, clearance relates the elimination rate to the drug concentrations (Pang and Rowland, 1977; Rowland and Tozer, 1995). Clearance can refer to an individual organ or elimination pathway, i.e. hepatic (CL_{hep}) and renal clearance (CL_{ren}) or to the overall drug elimination in the body, i.e. total clearance (CL_{tot}), which is the sum of each individual organ clearance as outlined in Eq. (2.5) (Rowland and Tozer, 1995):

$$CL_{tot} = CL_{hep} + CL_{ren} + CL_{other} \tag{2.5}$$

The liver and kidneys are the most important drug-eliminating organs, whereas drug clearance by other elimination pathways (CL_{other}) is generally of less relevance. The liver expresses a broad range of drug-metabolizing enzymes and hepatic metabolism is the major elimination pathway for most drugs. Metabolic biotransformation of drugs generally describes the conversion of lipophilic compounds into more hydrophilic metabolites that are subsequently excreted into urine or bile. The most common metabolic reactions with drugs are oxidation, reduction, hydrolysis, and conjugation (Rowland and Tozer, 1995; Fan and de Lannoy, 2014). More hydrophilic drugs undergo direct urinary and/or biliary excretion, which is mediated by renal and hepatic transporters. In addition, transporters play an important role in the hepatic and renal uptake of drugs and regulate the access to hepatic and renal drug elimination. The underlying physiological mechanisms in the liver and kidneys are described in full detail in sections 2.4.1 and 2.4.2, respectively.

Non-hepatic/non-renal drug elimination mainly occurs by extra-hepatic drug metabolism in the respiratory tract, gastrointestinal tract, skin, brain, heart, blood, and in various other organs and tissues. Enzymes in tissues that act as a boundary between the external and internal environment such as skin, respiratory tract, and gastrointestinal tract protect the body by preventing the entry of xenobiotics. The relevance of these drug-metabolizing enzymes strongly depends on the site of drug application (Ding and Kaminsky, 2003; Walsh et al., 2013; Costa et al., 2014; Gundert-Remy et al., 2014). Special attention is required if extra-hepatic metabolism occurs in target tissues, which may affect the respective tissue drug concentration and therefore reduce the drug efficacy (e.g. in cancer cells, brain, or lung) (Foti et al., 2015). Besides drug excretion into bile and urine, excretion can occur via the breath, sweat, tears, salvia, and breast milk, however, these pathways generally do not considerably contribute to overall drug elimination (Costa et al., 2014).

2.4.1. Hepatic drug elimination

The liver is the main organ for detoxification and elimination of endogenous and xenobiotic substances. In addition, the liver plays an important role in the absorption and digestion of fats and vitamins though production and excretion of bile, metabolism of gastrointestinal absorbed nutrients including glycogen storage and regulation, decomposition of red blood cells, and synthesis of proteins and hormones (Corless and Middleton, 1983; Malarkey et al., 2005). Lobules are the functional units of the liver (Figure 2.5). They are composed of parenchymal cells, called hepatocytes, and non-parenchymal cells such as sinusoidal endothelial cells, Kupffer cells, stellate cells, dendritic cells, and lymphocytes (McCuskey, 2008; Godoy et al., 2013). Hepatocytes account for 60% of hepatic cells and surround the sinusoid and the bile canaliculi, which face the sinusoidal and canalicular hepatocyte membranes, respectively. Peripheral oxygen-rich blood reaches the liver via branches of the hepatic artery, whereas branches of the portal vein deliver blood containing absorbed nutrients and potential harmful substances from the gastrointestinal tract. Within the sinusoids, arterial and venous blood is mixed and leaves the liver via the central vein (Malarkey et al., 2005; Eipel et al., 2010). The hepatocytes produce and secrete bile into bile canaliculi, which merge into bile ductules and form the common bile duct. The common bile duct transports and releases the bile into the duodenum in order to facilitate the absorption and digestion of fats and lipid-soluble vitamins (Kosters and Karpen, 2008; Li and Chiang, 2014).

The hepatic elimination of drugs takes place in the hepatocytes and represents a complex interplay between drug-metabolizing enzymes and drug transporters. As outlined above, drug from the systemic circulation reaches the sinusoidal blood via the hepatic artery, whereas gastrointestinal absorbed drug is delivered to the sinusoid via the portal vein and undergoes hepatic first-pass extraction. The rate of delivery is determined by the hepatic blood flow (Q_h) (Pang and Rowland, 1977). Within the sinusoid, unbound drug can become subject to intrinsic hepatic clearance ($CL_{h,int}$), which results from the interplay between sinusoidal membrane permeability into the hepatocytes and back into the blood, biliary secretion at the canalicular membrane and hepatic metabolism. Assuming that the liver is a homogenous compartment, these relationships can be described by the "well-stirred" liver model (Pang and Rowland, 1977):

$$CL_{hep} = \frac{Q_h \times fu_b \times CL_{h,int}}{Q_h + fu_b \times CL_{h,int}}$$

(2.6)

2.4.1.1. Sinusoidal membrane permeability

The permeation through the sinusoidal plasma membrane into the hepatocyte represents the first step in hepatic drug elimination. Small, lipophilic, and uncharged drugs mainly enter the hepatocytes via passive membrane permeability (Sugano et al., 2010). These drugs will partly
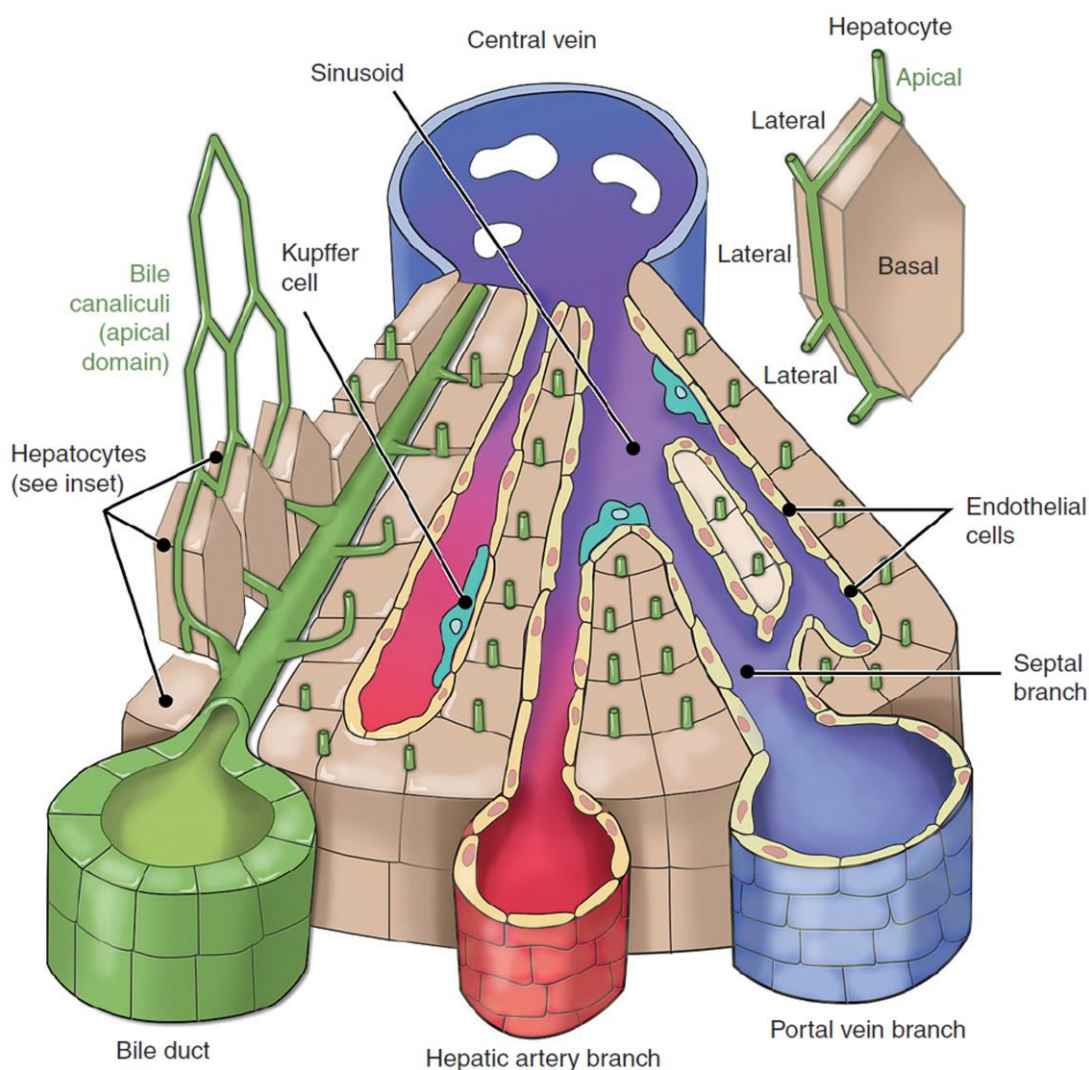
Figure 2.5. Microanatomy of the liver. Lobules are the functional units of the liver and are primarily composed of hepatocytes, sinusoids, and bile ductules. Blood enters the liver via branches of the hepatic artery and the portal vein, reaches the sinusoidal (basolateral) membrane of hepatocytes via the sinusoid and is collected in the central vein. Bile canaliculi transport secreted bile from the hepatocytes via the bile ductules and the common bile duct to the intestine. Taken from Chu et al. (2013).

diffuse back into the sinusoidal blood and probably enter other hepatocytes (Iusuf et al., 2012; van de Steeg et al., 2012). In addition, hepatocytes express a variety of uptake transporters at the sinusoidal membrane that mediate the cellular uptake of less lipophilic and charged drugs. Among these transporters, OATP1B1, OATP1B3, and OCT1 are most important for the hepatic uptake of drugs (Figure 2.2, panel B and section 2.1.1). Active sinusoidal back flux has likely minor relevance for drugs, whereas endogenous substances such as bile acids or bilirubin glucuronides potentially undergo sinusoidal efflux by MRPs (section 2.1.2.2).

2.4.1.2. Hepatic metabolism

Hepatic metabolism is the most common route of drug elimination and is mediated by numerous drug-metabolizing enzymes from different families. The metabolic biotransformation of drugs is categorized into phase I ("functionalization" by oxidation, reduction, and hydrolysis) and phase II reactions ("conjugation", e.g. by glucoronidation, sulfation, and acetylation), where the phase of metabolism does not necessarily provide information on the order of reactions (Rowland and Tozer, 1995; Fan and de Lannoy, 2014).

Phase I reactions are mainly catalyzed by members of the CYP family, with additional phase I drug-metabolizing enzymes such as flavin-containing monooxygenase (FMO), alcohol dehydrogenase, carbonyl reductase, carboxylesterase, epoxide hydrolase, and others (Pang et al., 2010). The CYP family has more than 50 members and is organized into five subfamilies (CYP1 - CYP4 and CYP7), which are responsible for the metabolism of ~90% of all clinically used medications (Xu et al., 2005; Lynch and Price, 2007; Chen et al., 2011). The isoforms CYP1A2, 2B6, 2C9, 2C19, 2D6, and 3A4 are considered to be of particular importance for the elimination of drugs, whereby CYP3A4 is the most abundant and relevant isoform (Zhou, 2008). CYPs mediate oxidative metabolism and are located in the endoplasmatic reticulum membrane in hepatocytes, oriented towards the cytosol, but can be found in virtually all tissues in the body (Neve and Ingelman-Sundberg, 2010; Gundert-Remy et al., 2014). Similar to drug transporters, drug-metabolizing enzymes are associated with DDIs through enzyme inhibition or induction as well as with polymorphisms. In particular CYP3A4 has a high DDI potential due to the large number of substrates, inhibitors, and inducers that partly overlap with the specificity of P-gp (Benet et al., 2004; Marchetti et al., 2007; Zhou, 2008). The most relevant polymorphisms have been identified for the CYP isoforms 1A2, 2B6, 2C9, 2C19, and 2D6 (Lynch and Price, 2007; Pang et al., 2010; van Leeuwen et al., 2013).

Phase II reactions are mediated by members of the UGT, SULT, glutathione S-transferase (GST), and NAT families of which UGT and SULT enzymes are particularly important for the elimination of drugs (Pang et al., 2010; Hardwick et al., 2013). UGT and SULT enzymes catalyze the covalent linkage to glucuronic acid (glucoronidation) or sulfate (sulfation) in order to increase the water-solubility and subsequent excretion of their substrates. UGT1A1, UGT2B7, SULT1A1, and SULT1B1 have the highest clinically relevance with regard to the glucoronidation and sulfation of drugs and endogenous substrates (e.g. bilirubin glucoronidation) (Pang et al., 2010; Rowland et al., 2013; Coughtrie, 2016). UGTs are predominately expressed in hepatocytes where they are localized in endoplasmatic membrane facing the luminal side (Radominska-Pandya et al., 1999). SULTs are likewise expressed in hepatocytes as well as in other tissues but are located in the cytosol (Gundert-Remy et al., 2014; Coughtrie, 2016).

2.4.1.3. Biliary secretion and enterohepatic circulation

Biliary secretion represents another hepatic drug clearance process that refers to the active efflux of parent drug compound into the bile canaliculi (Figure 2.5). The biliary secretion of drugs as well

as drug metabolites and endogenous substances like bile acids or bilirubin is mediated by P-gp, BCRP, MRP2, MATE1, and BSEP (Figure 2.2, panel B and sections 2.1.2 and 2.1.1.3), whereas passive permeability across the canalicular plasma membrane is considered to be negligible (Yang et al., 2009). The common physicochemical property of biliary secreted drugs is a high molecular weight with reported cut-off values between 400 and 600 g/mol (Levine, 1978; Yang et al., 2009; Varma et al., 2012). In addition, biliary secreted drugs frequently have a large polar surface area, high number of rotatable bonds, and high hydrogen-bond count. Lipophilic and highly permeable drugs are typically not biliary secreted since such compound properties increase the affinity to drug-metabolizing enzymes and promote metabolic drug elimination (Benet et al., 2008; Varma et al., 2012). Besides the common substrate affinity to canalicular efflux transporters, biliary secreted drugs are frequently OATP substrates (Varma et al., 2012).

Within the bile duct, drugs and other bile constituents are transported to the duodenum where bile constituents such as bile acids and cholesterol are efficiently reabsorbed (Kosters and Karpen, 2008; Dawson et al., 2009). Drugs are commonly excreted into feces but can potentially be reabsorbed in the intestine as well. In addition, conjugated metabolites might undergo deconjugation by intestinal bacteria and can be reabsorbed as the parent drug compound (Gao et al., 2014). Reabsorbed drugs return to the liver via the portal vein where they are again subject to hepatic elimination processes before reaching the systemic circulation. The repeating process of absorption, biliary secretion, and reabsorption (with or without hepatic metabolism and intestinal deconjugation) is called enterohepatic circulation.

2.4.2. Renal drug elimination

The kidneys have an important role in the general detoxification of blood, maintenance of fluid, electrolyte and base/acid homeostasis in the body, and regulation of blood pressure (Sherwood, 2015). The kidneys are divided into the outer cortex and the inner medulla. The nephrons are the functional units of the kidney and span across the cortex and medulla. They are composed of a glomerulus and a tubule consisting of different segments (proximal convoluted tubule, loop of Henle, and distal convoluted tubule) where the urinary filtrate is formed and delivered to the collecting duct (Figure 2.6) (Kriz, 1981; Morrissey et al., 2013; Scotcher et al., 2016).

Renal excretion of parent drug compounds is a major elimination pathway for many drugs and depends on glomerular filtration, tubular secretion, and reabsorption. These processes take place in the nephron and are determined by physicochemical drug properties as well as by interactions with uptake and efflux transporters (Masereeuw and Russel, 2001b; Feng et al., 2010). Renal clearance is defined as the net result of glomerular filtration ($CL_{ren,fil}$) and tubular secretion clearance ($CL_{ren,sec}$) and the fraction of drug that is reabsorbed from the tubule fluid back into the blood (f_{reab}), as summarized in Eq. (2.7) (Rowland and Tozer, 1995):

$$CL_{ren} = \left(CL_{ren,fil} + CL_{ren,sec}\right) \times (1 - f_{reab}) \tag{2.7}$$
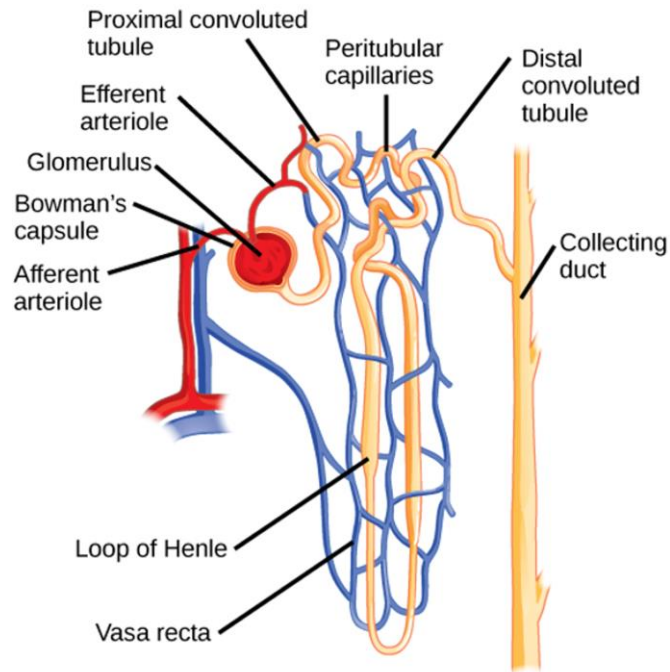
Figure 2.6. Microphysiology of the kidney. Nephrons are the functional units of the kidney and consist of a glomerulus and a tubule with different regions (proximal convoluted tubule, loop of Henle, and distal convoluted tubule). Blood is filtered within the glomerulus. The filtrate passes the tubule where water and lipophilic molecules are reabsorbed. Transporters in renal tubule cells secrete molecules into the glomerular filtrate. The filtrate from several nephrons flows together in the collecting duct. Taken from http://cnx.org/.

Peripheral blood enters the nephron via branches of the renal artery (afferent arterioles) and reaches the glomerulus, a network of blood capillaries surrounded by the Bowman`s capsule (Figure 2.6). Within the glomerulus, the blood is filtered (glomerular filtration) into the Bowman`s capsule, which releases the glomerular filtrate into the proximal tubule (Lote, 2012). The rate of glomerular filtration depends on the renal blood flow and binding in blood (Feng et al., 2010; Fan and de Lannoy, 2014). Glomerular filtration is a passive, unidirectional, and size-dependent process that prevents the excretion of blood cells and large molecules such as plasma proteins. Hence, only unbound and small molecules (molecular weight < 500 g/mol) undergo glomerular filtration, representing the counterpart to the biliary secretion of larger molecules (Varma et al., 2012). Following filtration, the blood leaves the glomerulus via efferent arterioles that form a network of peritubular capillaries around the tubular segments (Lote, 2012).

The renal tubule is formed by epithelial cells, constituting a barrier between blood in the peritubular capillaries and the glomerular filtrate inside the tubule. It is divided into three segments: the proximal convoluted tubule, the loop of Henle, and the distal convoluted tubule (Figure 2.6). Along the different segments, water and nutrients are reabsorbed by osmotic processes, passive diffusion, and active transport, whereas certain substances in the blood are actively secreted into the tubular fluid (Lote, 2012). These processes likewise affect the net renal excretion of drugs. Active tubular secretion of drugs mainly takes place in the proximal tubule and contributes to their

elimination (Masereeuw and Russel, 2001b; Scotcher et al., 2016). Proximal tubule cells express a large number of uptake and efflux transporters of which OAT1, OAT3, OCT2, MATE1, MATE2K, P-gp, MRP2, and BCRP primarily work as combined carrier systems for the secretory transport of anionic and cationic drugs (Figure 2.2, panel C and sections 2.1.1 and 2.1.2). Thereby OATs and OCT2 act as uptake transporters at the basolateral plasma membrane, whereas MATEs, P-gp, MRP2, and BCRP mediate the apical efflux of drugs into the tubular fluid. In addition, tubular epithelial cells express phase I and II drug-metabolizing enzymes including members of the CYP, UGT, and GST families. Thereby, glucoronidation of drugs by UGT2B7 and UGT1A9 seems to be the most important metabolic pathway in the kidney (Di, 2014; Gundert-Remy et al., 2014; Scotcher et al., 2016). However, in general, renal metabolism does not contribute to a large extent to the overall drug elimination (Rowland and Tozer, 1995; Fan and de Lannoy, 2014).

Following glomerular filtration and active secretion processes, drugs and endogenous substances can be subject to reabsorption back into the systemic circulation (Lote, 2012). Passive reabsorption mainly occurs in the distal tubules due to high concentration gradients between the tubular fluid and the blood in peritubular capillaries that result from the reabsorption of water (Fan and de Lannoy, 2014). The extent of passive tubular reabsorption depends on physicochemical properties. Lipophilic and uncharged molecules are reabsorbed to a large extent by passive diffusion, whereas hydrophilic and charged compounds are efficiently eliminated into the urine (Feng et al., 2010; Scotcher et al., 2016). In this context, the pH of tubular fluid (ranging between 5 and 8) has a high impact on the degree of ionization and thus on the extent of reabsorption (Levy, 1976). Active reabsorption of drugs is uncommon although different apical uptake (e.g. OCTN1 and OCTN2) and basolateral efflux transporters (e.g. MRP1) are expressed along the renal tubule (Launay-Vacher et al., 2006; Morrissey et al., 2013; Kunze et al., 2014b; Scotcher et al., 2016). However, the process of active reabsorption is primarily relevant for the recovery of nutrients such as glucose via the apical sodium/glucose cotransporter SGLT2 and basolateral glucose transporter GLUT1 (Masereeuw and Russel, 2001a; Vallon et al., 2011). The primary urine containing non-reabsorbed constituents enters the collecting duct and is further concentrated and transported to the bladder (Lote, 2012).

2.5.   *In vitro* methods to study hepatic drug disposition

Within the human body, drugs are subject to various active and passive processes that influence their ADMET properties as outlined in the sections 2.1 to 2.4. Knowledge about these processes is therefore required to understand the pharmacokinetic and toxicological behavior of drugs in order to anticipate an appropriate drug dose and to ensure drug safety and efficacy. Furthermore, interactions with transporters and enzymes are associated with the risk of drugs becoming victims of DDIs, which potentially alters their ADMET properties. However, clinical pharmacokinetic data are not or only rarely available at early stages of drug development, while pharmacokinetic and toxicological data from preclinical animals often show large species-dependent differences to humans (Chaturvedi et al., 2001; Deguchi et al., 2011; Watanabe et al., 2011; Dave and Morris,

2015). To overcome this gap, different *in vitro* systems based on human cells or subcellular fractions have been developed. These systems allow the investigation of clearance processes, interactions with specific transporters and drug-metabolizing enzymes, and drug binding in order to quantitatively predict the pharmacokinetic behavior of drugs in humans using mechanistic *in vitro-in vivo* extrapolation (IVIVE) models. The following section provides on overview of *in vitro* methods for the study of hepatic drug disposition that were applied within the scope of this work.

2.5.1. Drug binding

The binding of drugs within blood and tissues has high impact on their intra- and extracellular distribution and elimination in humans (section 2.3). In addition, different binding processes are present in *in vitro* systems requiring correction of the measured (apparent) pharmacokinetic parameters. In the following section, common methods for the determination of drug binding are introduced using the examples of binding in whole blood, plasma, and liver microsomes.

2.5.1.1. Binding in whole blood and plasma

Drug binding in plasma and whole blood is routinely determined during drug development. fu_p is commonly measured using equilibrium dialysis, ultracentrifugation, ultrafiltration, or gel filtration, whereas fu_b is indirectly determined from experimental measures of R_b and fu_p (Hinderling, 1997; Pelkonen and Turpeinen, 2007; Bohnert and Gan, 2013; Fan and de Lannoy, 2014).

In order to obtain plasma for the determination of fu_p, whole blood is centrifuged to remove blood cells and platelets. Equilibrium dialysis is the most common method for the measurement of plasma protein binding. An equilibrium dialysis device consists of two chambers that are separated by a semi-permeable membrane (Figure 2.7). The membrane allows the diffusion of drug but not of plasma proteins (the molecular cut-off value commonly ranges between 6 to 20 kDa, depending on the system). The chambers are either filled with plasma and the test drug (donor chamber) or buffer solution (receiver chamber). Hence, only unbound drug can reach the receiver chamber and the unbound drug concentration equilibrates between both chambers. Following equilibration, the ratio between the drug concentrations in both chambers represents fu_p (Bailey, 1997; Bohnert and Gan, 2013). Equilibrium dialysis is generally considered as the gold-standard for measuring plasma protein binding of drugs. It can be conducted at physiological temperature (37°C), is easy in handling, and suitable for high throughput screenings. On the other hand, fu_p can be affected by non-specific binding of drugs to membrane inserts and long incubations are required to establish the concentration equilibrium, which limits the analysis of drugs with low stability (Bohnert and Gan, 2013).

R_b is obtained from incubations of whole blood with test drugs, followed by centrifugation to separate plasma from cellular blood components (Figure 2.7). The ratio between drug concentrations in whole blood and plasma represents R_b and subsequently allows the calculation of fu_b (Eq. (2.2)) (Laznicek and Laznickova, 1995; Hinderling, 1997).

$$fu_p = \frac{C_{receiver}}{C_{donor}} \qquad R_b = \frac{C_b}{C_p} \qquad fu_b = \frac{R_b}{fu_p}$$
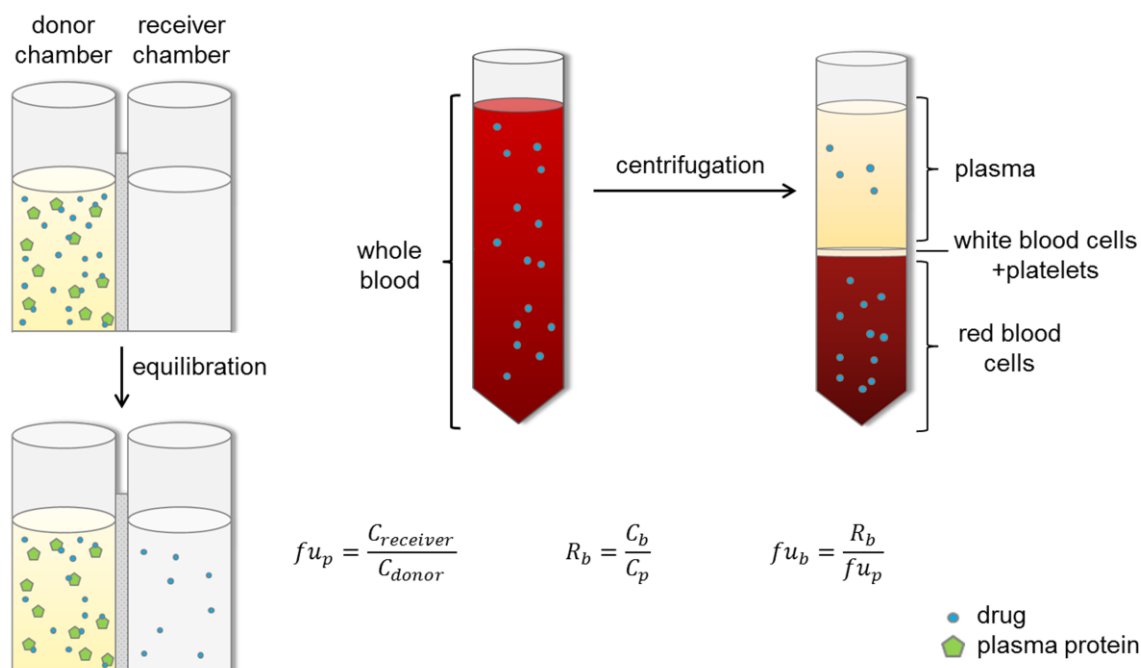
Figure 2.7. Determination of unbound fractions in plasma (fu_p) and whole blood (fu_b) using equilibrium dialysis and centrifugation. The dialysis devices consist of two chambers, which are separated by a semi-permeable membrane that allows diffusion of drug but not of plasma proteins. After equilibrium of unbound drug is reached, fu_p is calculated from measured drug concentrations in the receiver ($C_{reveiver}$) and donor chambers (C_{donor}). In order to obtain R_b, drug concentrations in whole blood (C_b) (before centrifugation) and plasma (C_p) (following centrifugation) are compared. fu_b is calculated from R_b and fu_p.

2.5.1.2. Binding in (sub)cellular *in vitro* systems

During *in vitro* incubations using (sub)cellular systems such as liver microsomes or hepatocytes, drugs are subject to different binding processes. Drugs can bind to cellular structures as well as to plastic surfaces in the assay device, thereby affecting the obtained kinetic parameters, which are commonly calculated using total applied drug concentration (apparent parameters) (Pelkonen and Turpeinen, 2007; Kilford et al., 2008). However, intrinsic kinetic parameters depend on the unbound drug concentration in the *in vitro* system. Hence, the unbound fraction of drug needs to be assessed in order to correct apparent parameters and to obtain unbound intrinsic parameters.

For instance, the metabolic drug clearance is commonly determined in human liver microsomes that are composed of endoplasmic membranes and associated proteins. Accordingly, the drug concentration in microsomes is affected by membrane partitioning and protein binding, which is reflected by the unbound fraction in microsomes (fu_{mic}) (Pelkonen and Turpeinen, 2007). In principle, all methods for the measurement of plasma protein binding are applicable to determine the unbound fraction in a (sub)cellular system (Kilford et al., 2008). Ultracentrifugation is the most common method for the measurement of fu_{mic}. This method is based on the separation of unbound and bound drug by high centrifugal forces. The microsomal membranes,

including associated microsomal protein and bound drug, sediment during the centrifugation and unbound drug can be quantified in the supernatant. Ultracentrifugation is applicable to drugs that exhibit high non-specific binding but has low through-put and centrifugation cannot be conducted at physiological temperature (Bohnert and Gan, 2013). As an alternative, mathematical models have been developed in order to predict drug binding in different systems from physicochemical drug properties (Austin et al., 2005; Kilford et al., 2008; Yabe et al., 2011).

2.5.2. Hepatobiliary drug transport and transporter inhibition

Three clearance processes predominately contribute to the hepatobiliary transport of drugs, namely passive sinusoidal membrane permeability, active sinusoidal uptake permeability, and active canalicular efflux permeability (biliary secretion). These processes are commonly assessed in freshly isolated or cryopreserved primary hepatocytes that are derived using collagenase perfusion of the human liver (Lecluyse and Alexandre, 2010). Suspended hepatocytes are generally used for the measurement of sinusoidal transport processes, whereas canalicular transport is investigated in plated sandwich-cultured hepatocytes. The obtained information is subsequently used to predict hepatic drug clearance in humans. In contrast, the interaction with individual transporters is investigated using membrane vesicles or recombinant cell lines that express only the transporter of interest (Brouwer et al., 2013).

2.5.2.1. Sinusoidal transport and passive membrane permeability

Isolated human hepatocytes express the majority of sinusoidal uptake transporters and phase I and II drug-metabolizing enzymes similar to the situation in the liver. In contrast, the function of canalicular efflux transporters is strongly limited due to loss of cell polarization and internalization of canalicular transporters during isolation (Bow et al., 2008; Di et al., 2012). Plated hepatocytes additionally lose their uptake transporter activity in culture (Ishigami et al., 1995; Sahi et al., 2010). Therefore, primary suspended hepatocytes are used to investigate the sinusoidal uptake permeability of drugs. To limit the impact of interindividual variability in transporter expression, hepatocytes from multiple human donors are pooled within experiments (Brouwer et al., 2013).

The total sinusoidal uptake permeability into hepatocytes (PS_{inf}) represents the sum of active transporter-mediated ($PS_{inf,act}$) and passive uptake permeability ($PS_{inf,pas}$):

$$PS_{inf} = PS_{inf,act} + PS_{inf,pas} \qquad (2.8)$$

PS_{inf} is determined by incubating hepatocytes with medium containing the test drug at a low concentration to avoid saturation of active transport. In order to prevent passive diffusion back into the medium, hepatic uptake is measured in short incubations within the initial uptake phase. The influence of metabolism can generally be neglected due to the short incubation times. The

incubation is terminated by separating cells and medium e.g. by filtration through an oil layer (oil-spin method) followed by quantification of the drug amount in cells and medium (Umehara and Camenisch, 2012; Kunze et al., 2014a). The apparent uptake permeability (PS_{app}) is calculated by normalizing the amount of drug in cells to the nominal drug concentration, incubation time, and cell number. PS_{app} is potentially affected by non-specific binding to plastic surfaces in the assay device or by saturable binding to cell surfaces. Non-specific binding to plastic surfaces is corrected based on the total recovery of radiolabeled substrates. The extent of saturable binding to cell surfaces can be measured in control incubations at 4°C in order to correct PS_{app} into the intrinsic parameter PS_{inf} (Umehara and Camenisch, 2012; Kunze et al., 2014a).

Three approaches are available to discriminate between active and passive uptake permeability: the use of uptake transporter inhibitors, high substrate concentrations in order to saturate active transport, or incubation at 4°C where transporters are not active. It has been widely accepted that incubation at 4°C is not suitable to measure passive membrane permeability because membrane fluidity is temperature-sensitive, which also affects the membrane permeability (Frezard and Garnier-Suillerot, 1998; Pang et al., 2010; Brouwer et al., 2013; Zamek-Gliszczynski et al., 2013). Therefore, active uptake permeability is usually abolished using uptake transporter inhibitors or high substrate concentrations (Sugano et al., 2010; EMA, 2012). However, attempts to saturate active transport can be limited by low substrate solubility, whereas uptake transporter inhibitors do not necessarily suppress the full activity of all relevant transporters.

The sinusoidal efflux permeability (PS_{eff}) of drugs is difficult to assess. Therefore, $PS_{inf,pas}$ is commonly used as a surrogate measure for passive sinusoidal efflux permeability ($PS_{eff,pas}$). Active sinusoidal efflux permeability ($PS_{eff,act}$) seems to have limited relevance for the hepatic disposition of drugs and this process is generally neglected in IVIVE models (Jones et al., 2012; Nordell et al., 2013; Zamek-Gliszczynski et al., 2013; Kunze et al., 2015; Varma et al., 2015).

The limitations of suspended hepatocytes as *in vitro* system for sinusoidal drug transport are mainly related to the expression of transporters. Although isolated hepatocytes are generally considered to have an appropriate pattern of transporter expression, recent studies demonstrated that cryopreservation of hepatocytes can reduce the expression and activity of OATPs, OCTs, and NTCP, which potentially affects the quality of measured *in vitro* parameters (Kimoto et al., 2012; Lundquist et al., 2014b). Therefore, freshly isolated hepatocytes are considered the gold-standard for measuring sinusoidal drug transport. However, the availability of freshly isolated human hepatocytes is limited and transport studies are commonly conducted using cryopreserved hepatocyte batches with confirmed uptake transporter activity (Chiba et al., 2009; Brouwer et al., 2013; Nordell et al., 2013; Kunze et al., 2015). In addition, it has been shown that P-gp, BCRP, MRP2, and BSEP exhibit remaining activity in suspended hepatocytes due to incomplete internalization, which can also affect the assessment of hepatic uptake permeability. Yet, residual activity of efflux transporters seems to be substantially lower in cryopreserved than in freshly isolated hepatocytes (Lundquist et al., 2014a).

2.5.2.2. Biliary secretion by canalicular efflux transporters

Biliary secretion of drugs is mediated by canalicular efflux transporters and is commonly investigated in sandwich-cultured human hepatocytes (Pan et al., 2012; Brouwer et al., 2013). For this purpose, freshly isolated or cryopreserved hepatocytes are seeded on collagen-coated plates and overlaid with an additional layer of collagen (e.g. Matrigel). Although isolated hepatocytes lose their cell polarization upon plating, they recover their polarization after 6 to 7 days in the sandwich-culture system including functional expression of the major transporters at the sinusoidal and canalicular membranes as well as formation of bile canaliculi in form of bile pockets. Tight junctions between the hepatocytes separate the bile pockets from the extracellular medium and prevent diffusion of the test drug between both compartments (Figure 2.8) (Liu et al., 1999; Schaefer et al., 2012; Brouwer et al., 2013). This system therefore allows measuring canalicular and sinusoidal drug transport under physiologically relevant conditions. Additional
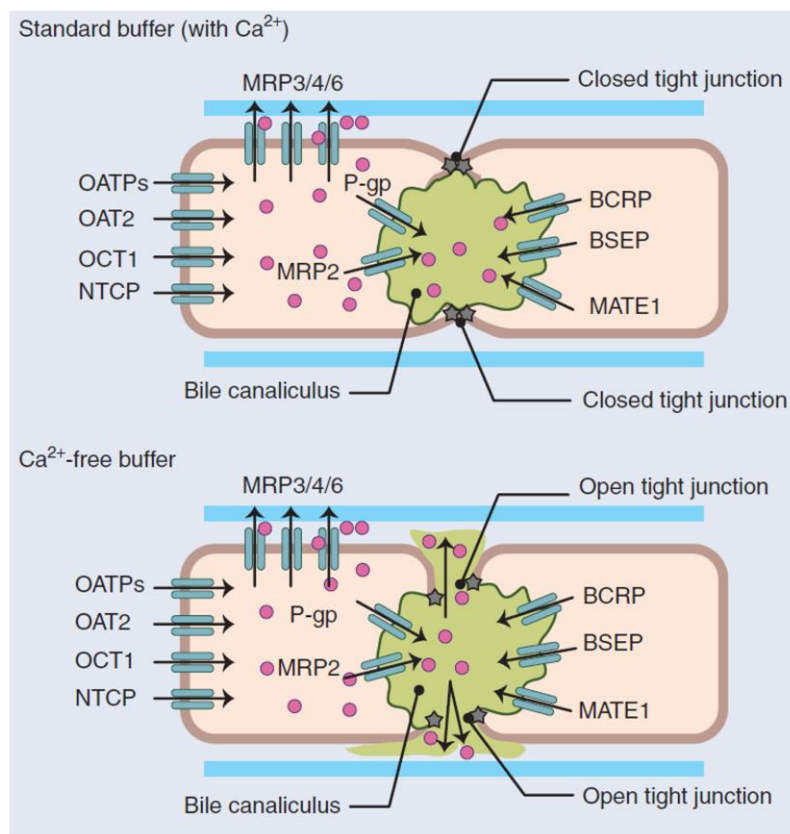

Figure 2.8. Sandwich-cultured hepatocytes express sinusoidal and canalicular transporters and form bile canaliculi (bile pockets). Test drug is taken up by sinusoidal uptake transporters and/or passive uptake permeability and canalicular efflux transporters mediate the secretion of drug into bile canaliculi. In the presence of Ca^{2+}-containing standard buffer, intercellular tight junctions are maintained and prevent the diffusion of drug into the extracellular medium, whereas tight junctions are disrupted in the presence of Ca^{2+}-free buffer. The extent of biliary secretion is represented by differences in the cellular drug accumulation in the presence of the Ca^{2+}-containing and Ca^{2+}-free buffers. Taken from Brouwer et al. (2013).

applications of sandwich-cultured hepatocytes include the investigation of hepatic drug metabolism and its interplay with sinusoidal and canalicular transport processes, bile acid transport, and hepatotoxicity (Swift et al., 2010; Schaefer et al., 2012). However, sandwich-cultured hepatocytes exhibit reduced function of sinusoidal uptake transporters and drug-metabolizing enzymes compared to primary suspended hepatocytes (Mathijs et al., 2009; Kotani et al., 2011). Therefore, and due to the labor- and cost-intensive culturing procedure, sandwich-cultured hepatocytes are mainly used for the investigation of canalicular drug transport, whereas sinusoidal transport and hepatic metabolism are assessed in suspended hepatocytes (section 2.5.2.1) and using liver microsomes (section 2.5.3), respectively (Obach, 2001; Swift et al., 2010; Brouwer et al., 2013; Yang et al., 2016).

In order to measure biliary secretion, sandwich-cultured hepatocytes are incubated with the test drug at a low substrate concentration to prevent saturation of active transport. The drug is taken up from the extracellular medium by sinusoidal uptake transporters and/or passive uptake permeability and secreted into the bile pockets by canalicular efflux transporters. The initial rate of biliary secretion depends on the unbound intracellular concentration (Swift et al., 2010; Chu et al., 2013; Pfeifer et al., 2014). Following the incubation, the cells are washed and the drug amount in cells and associated bile pockets is quantified. In order to discriminate between drug in hepatocytes and in the bile pockets, different buffers are used in sandwich-culture experiments. In Ca^{2+}-containing standard buffer, the intercellular tight junctions are maintained, whereas the tight junctions are disrupted upon incubation in a Ca^{2+}-free buffer (Figure 2.8). The drug accumulation in bile pockets is represented by the difference between the cellular drug accumulation in Ca^{2+}-containing buffer (cells and bile pockets) and the cellular accumulation in Ca^{2+}-free buffer (cells only) (Liu et al., 1999). The apparent intrinsic biliary clearance ($CL_{int,sec,app}$) is calculated by normalizing the amount of drug in the bile pockets to the intracellular drug concentration and incubation time (Brouwer et al., 2013). The intracellular drug concentration can be obtained based on the cellular accumulation in Ca^{2+}-free buffer and the hepatocellular volume (Lee et al., 2003). In order to account for intracellular binding processes, $CL_{int,sec,app}$ is subsequently corrected into the intrinsic biliary clearance ($CL_{int,sec}$) using fu_{hep} (section 2.5.1.2).

The sandwich-culture system has limited use for drugs with low sinusoidal uptake permeability since they might not achieve sufficient intracellular levels in order to become subject to canalicular efflux. As a consequence, the process of biliary secretion might be underestimated (Brouwer et al., 2013). In addition, parameters obtained in the sandwich-culture are liable to interindividual variability in transporter expression. Hepatocytes from multiple donors cannot be pooled for sandwich-culture experiments since cells from different donors do not homogeneously grow on culture plates. Thus, parameters from sandwich-culture experiments should be determined using multiple hepatocyte batches in independent experiments and the functional activity of uptake and efflux transporters has to be carefully monitored by the use of reference substrates (i.e. taurocholate) (Brouwer et al., 2013; De Bruyn et al., 2013; Yang et al., 2016).

2.5.2.3. Transporter inhibition

Primary hepatocytes are suitable to determine hepatic process clearances such as sinusoidal uptake permeability or biliary secretion (sections 2.5.2.1 and 2.5.2.2). However, the expression of many transporters makes it difficult to characterize individual transporters, especially since selective inhibitors are only available for a limited number of transporters (Sahi et al., 2010; Swift et al., 2010; Brouwer et al., 2013; Yang et al., 2016). Therefore, recombinant cell lines or inside-out oriented membrane vesicles have been developed that express only individual transporters. Thus, these systems allow identifying drugs as substrates or inhibitors of individual transporters.

The interaction between transporters and their substrates is described by the maximum velocity (V_{max}) of transport and Michaelis-Menten constant (K_m). K_m represents the substrate affinity and refers to the substrate concentration that is associated with the half-maximal transport velocity. K_m and V_{max} are obtained in concentration-dependent phenotyping experiments under initial rate conditions (Zamek-Gliszczynski et al., 2013). Transporter inhibition by a drug is also characterized in concentration-dependent experiments under initial rate conditions but in the presence of a specific reference substrate. Alterations in the transport of the reference substrate indicate an inhibitory effect of the test drug. The inhibition potency of the test drug is described by the concentration of inhibitor to achieve half-maximal transporter inhibition (IC_{50}) or the reversible inhibition constant (K_i) (Zamek-Gliszczynski et al., 2013).

The selection of recombinant cell lines or membrane vesicles as *in vitro* test systems depends on compound properties and transport mechanism. Uptake transporter interactions are commonly studied in recombinant cell lines (Brouwer et al., 2013). In addition, interactions between efflux transporters and highly permeable drugs (i.e. lipophilic substrates of P-gp and BCRP) should be investigated in recombinant cells lines (Tweedie et al., 2013; Zamek-Gliszczynski et al., 2013). However, such cellular systems are not suitable to measure interactions between efflux transporters and low permeable drugs. In order to reach the intracellular binding site of an efflux transporter, such drugs often require uptake transporters *in vivo*, which might not be expressed in the recombinant cell line. Therefore, inside-out oriented membrane vesicles, where efflux transporters directly interact with the test drug in the extracellular medium, are the preferred *in vitro* system for low permeable drugs (Figure 2.9). For instance, inhibition of the efflux transporter BSEP is commonly investigated in inside-out oriented membrane vesicles since BSEP substrates are typically low permeable hydrophilic molecules that cannot be characterized or used as reference substrates (i.e. the BSEP reference substrate taurocholate) in recombinant cell lines (Stieger et al., 2000; Morgan et al., 2010; Dawson et al., 2012; Pedersen et al., 2013; Cheng et al., 2016).

Inside-out oriented membrane vesicles are typically prepared from recombinant cells lines that were transfected with complementary DNA (cDNA) encoding the human ABC transporter of interest (Brouwer et al., 2013; Cheng et al., 2016). Alternatively, membrane vesicles can be obtained from human tissue (Funk et al., 2001a). In order to measure the inhibition potential of
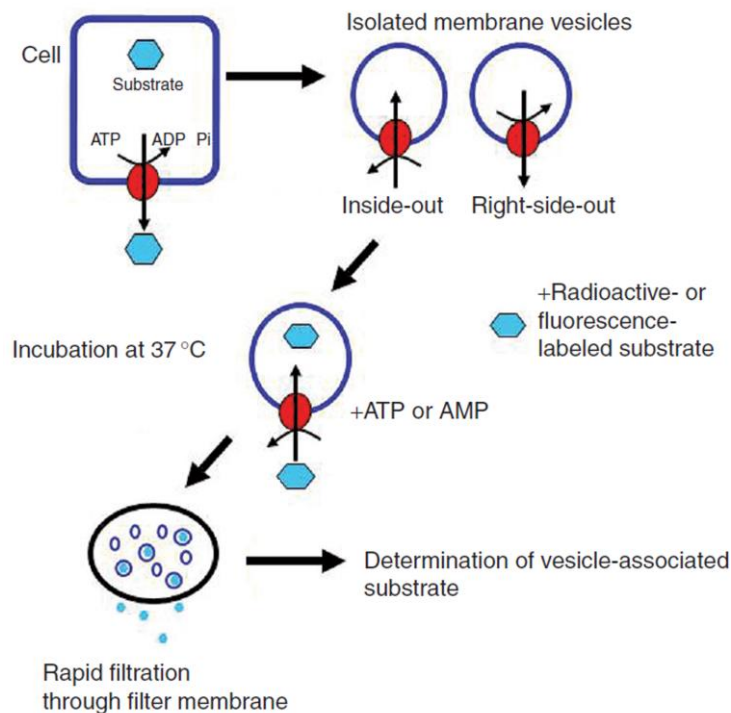
Figure 2.9. Vesicular transport assay. Inside-out oriented membrane vesicles are obtained from recombinant cell lines that express the efflux transporter of interest. Membrane vesicles are incubated with a transporter substrate in the presence of ATP or AMP. The efflux transporter reacts with ATP and mediates the vesicular uptake of substrate. Vesicles and non-associated substrate are separated by filtration and the amount of vesicle-associated substrate is quantified. Altered transport kinetics of a reference substrate in the presence of a test drug indicate transporter inhibition. Modified from Brouwer et al. (2013).

drugs, membrane vesicles are incubated with the test drug at various concentrations and in the presence of a reference substrate and ATP. The ABC transporter mediates the vesicular uptake of the reference substrate by hydrolysis of ATP unless the test drug inhibits the transport process. Parallel incubations with adenosine monophosphate (AMP) serve as a negative control for passive permeation of substrate into the vesicles. The incubation is terminated by separation of membrane vesicles and medium (e.g. by filtration) and the amount of substrate in the vesicles is quantified (Figure 2.9) (van Staden et al., 2012; Brouwer et al., 2013). The IC_{50} value for the test drug is obtained by non-linear regression analysis of the concentration-dependent inhibition of vesicular uptake (van Staden et al., 2012; Volpe et al., 2014).

2.5.3. Hepatic drug metabolism

The metabolic clearance of drugs is routinely measured in human hepatocytes or in liver subcellular fractions. Freshly isolated or cryopreserved hepatocytes express the majority of phase I and II drug-metabolizing enzymes (Sahi et al., 2010; Vildhede et al., 2015). Cultured primary

hepatocytes are not suitable to determine metabolic drug clearance since metabolic activity is lost within a short time, but these cells can be used for metabolite identification, enzyme induction or toxicity studies (Pelkonen and Turpeinen, 2007; Fasinu et al., 2012). As an alternative to hepatocytes, liver subcellular fractions such as microsomes, S9, and cytosolic fractions are available, which, however, contain only certain drug-metabolizing enzymes. In order to prepare liver subcellular fractions, human liver tissue is homogenized and centrifuged at low speed. The supernatant (S9 fraction) contains the microsomal and cytosolic fractions that can be separated by ultracentrifugation (Jia and Liu, 2007; Fasinu et al., 2012; Richardson et al., 2016). The S9 fraction covers the same range of drug-metabolizing enzymes like intact hepatocytes but co-factors that are required for metabolic processes like nicotinamide adenine dinucleotide phosphate (NADPH) or uridine diphosphate glucuronic acid (UDPGA) for CYP and UGT enzymes, respectively, are not available in S9 and subsequent fractions. Compared to hepatocytes, the plasma membrane, which limits the access to drug-metabolizing enzymes, is removed in S9 and subsequent fractions (Richardson et al., 2016). The microsomal fraction is mainly composed of membranes from the endoplasmatic reticulum. Microsomes therefore contain all phase I and II drug-metabolizing enzymes that are bound to endoplasmatic membranes including CYP, UGT, and FMO enzymes. The cytosolic fraction contains soluble drug-metabolizing enzymes such as SULT, GST, and NAT (Fasinu et al., 2012).

Human liver microsomes are the most common system to assess the metabolic drug clearance since they contain phase I CYP enzymes, are cheap, robust, and suitable for high-throughput screenings (Obach, 2001; Pelkonen and Turpeinen, 2007; Di et al., 2013). The influence of interindividual variability in enzyme expression and activity is reduced by using pools of liver microsomes from up to 200 donors for clearance measurements. Liver microsomes are typically incubated with test drug and the co-factor NADPH to determine the CYP-mediated metabolic clearance. The study of additional microsomal enzymes must be conducted in the presence of other co-factors. For instance, UGT-dependent metabolism is analyzed in the presence of UDPGA and requires the pre-treatment of microsomes with the pore-forming peptide alamethicin to increase the access to the luminal-orientated UGT in the endoplasmatic membranes (Obach, 2001; Walsky et al., 2012). In order to prevent saturation or product inhibition of drug-metabolizing enzymes, the metabolic clearance is measured in the linear time, substrate, and enzyme concentration range (Obach, 2001; Fujiwara et al., 2008; Chiba et al., 2009). K_m and V_{max} of enzyme substrates can be assessed in concentration-dependent phenotyping experiments under initial rate conditions. However, incubations with recombinant enzymes (i.e. using supersomes) are more suitable to characterize substrate kinetics for individual enzymes (Kuehl et al., 2005; Jia and Liu, 2007; Pelkonen and Turpeinen, 2007). Following the incubation, the formation of major metabolites or the decrease of parent drug concentration is quantified by high-performance liquid chromatography or liquid chromatography coupled to tandem mass spectrometry, respectively. The apparent intrinsic metabolic clearance ($CL_{int,met,app}$) is calculated by normalizing the concentration of major metabolites or the decrease of parent drug concentration to the applied

concentration of parent drug, incubation time, and microsomal protein. In order to account for binding processes in the incubation, $CL_{int,sec,app}$ is subsequently corrected into the intrinsic metabolic clearance ($CL_{int,sec}$) using fu_{mic} (section 2.5.1.2).

2.5.4. Processing of hepatic process clearances

The prediction of hepatic drug clearance in humans from *in vitro* data requires four different steps. In the first step, the hepatic process clearances for sinusoidal uptake and efflux, hepatic metabolism, and biliary secretion are measured *in vitro* (sections 2.5.1 to 2.5.3). In the second step, the individual process clearances must be scaled to the human organ level in order to account for the capacity of the whole liver (Obach, 2011). Thereby, each *in vitro* system has its specific scaling factor. The following scaling factors are commonly applied: 99 x10^6 cells/g liver for suspended human hepatocytes, 116 mg protein/g liver for sandwich-cultured hepatocytes, 53 mg microsomal protein/g liver for human liver microsomes, and 25.7 g liver/kg body weight for liver weight (Carlile et al., 1997; Houston and Galetin, 2008; Swift et al., 2010).

In the third step, the up-scaled hepatic process clearances are feed into a mechanistic IVIVE model in order to investigate their interplay and to calculate the intrinsic hepatic clearance. In the last step, liver models such as the "well-stirred" liver model (Eq. (2.6)) are used to relate the intrinsic hepatic clearance to physiological parameters (i.e. hepatic blood flow and binding in blood) in order to predict the hepatic drug clearance (Pang and Rowland, 1977).

In this work, the Extended Clearance Model (ECM) was used as mechanistic IVIVE model. The use and different applications of the ECM are reviewed in full detail in the section 2.6.

2.6. The Extended Clearance Model and its use for the interpretation of hepatobiliary elimination data

Gian Camenisch[1], Julia Riede[1,2], Annett Kunze[1], Jörg Huwyler[2], Birk Poller[1], Ken-ichi Umehara[1]

[1] Division of Drug Metabolism and Pharmacokinetics, Integrated Drug Disposition Section, Novartis Institutes for BioMedical Research, CH-4056 Basel, Switzerland

[2] Department of Pharmaceutical Sciences, Division of Pharmaceutical Technology, University of Basel, CH-4056 Basel, Switzerland

ADMET

Review

The extended clearance model and its use for the interpretation of hepatobiliary elimination data

Gian Camenisch*,[1], Julia Riede[1,2], Annett Kunze[1], Jörg Huwyler[2], Birk Poller[1] and Kenichi Umehara[1]

[1]*Division of Drug Metabolism and Pharmacokinetics, Integrated Drug Disposition Section, Novartis Institutes for BioMedical Research, CH-4056 Basel, Switzerland*
[2]*Department of Pharmaceutical Sciences, Division of Pharmaceutical Technology, University of Basel, CH-4056 Basel, Switzerland*

*Corresponding Author: E-mail: gian.camenisch@novartis.com; Tel.: +41-79-278-58-17; Fax: +41-61-696-85-83

Abstract

Hepatic elimination is a function of the interplay between different processes such as sinusoidal uptake, intracellular metabolism, canalicular (biliary) secretion, and sinusoidal efflux. In this review, we outline how drugs can be classified according to their in vitro determined clearance mechanisms using the extended clearance model as a reference. The approach enables the determination of the rate-determining hepatic clearance step. Some successful applications will be highlighted, together with a discussion on the major consequences for the pharmacokinetics and the drug-drug interaction potential of drugs. Special emphasize is put on the role of passive permeability and active transport processes in hepatic elimination.

Keywords

extended clearance concept classification system; hepatic elimination; passive permeability; transporters

Extended clearance model

Historically, hepatic clearance models assumed that (i) the unbound drug concentration in blood is determining the hepatic clearance (metabolism and/or biliary excretion) and that (ii) there is no membrane transport barrier limiting access to the enzymes or transporters in the hepatocyte. Improved models, however, reflect the physiological reality more precisely. In the liver drugs first have to overcome the membrane barrier separating the blood in the sinusoid from the cytosol of the hepatocytes. Permeation across this barrier might occur by passive diffusion and/or active carrier-mediated transport. Once in the cytosol drugs are subject to metabolism, efflux transporter-mediated canalicular (biliary) secretion and/or back-flux (active or passive) into the sinusoid. Consequently, generally referred as the extended clearance model (ECM), the overall hepatic intrinsic drug clearance ($CL_{h,int}$) can be described as the interplay between all these processes as follows [1,2]:

$$CL_{h,int} = \frac{PS_{inf} \cdot CL_{int}}{PS_{eff} + CL_{int}} = \frac{(PS_{inf,act} + PS_{inf,pas}) \cdot (CL_{int,met} + CL_{int,sec})}{PS_{eff,act} + PS_{eff,pas} + CL_{int,met} + CL_{int,sec}} \tag{1}$$

where, $PS_{inf,act}$ and $PS_{inf,pas}$ are the active and passive hepatic influx clearances from the blood, respectively, $CL_{int,sec}$ is the intrinsic biliary secretion clearance, and $CL_{int,met}$ is the intrinsic metabolic clearance. $PS_{eff,act}$ and $PS_{eff,pas}$ describe the active and passive sinusoidal efflux from the hepatocytes back into the blood, respectively. PS_{inf} is the sum of $PS_{inf,act}$ and $PS_{inf,pas}$, PS_{eff} is the sum of $PS_{eff,act}$ and $PS_{eff,pas}$, CL_{int} is the sum of $CL_{int,sec}$ and $CL_{int,met}$ and $CL_{int,h}$ is the overall intrinsic hepatic clearance.

The extended clearance model allows the identification of the rate-determining hepatic clearance step for a given drug molecule [1]. Depending on the relative contributions of the individual processes in Eq. (1), four different cases can be distinguished (Fig. 1). While (passive) hepatic uptake is the rate-determining step for ECM class 1 compounds, the sum of metabolism and efflux transporter-mediated biliary elimination is predicted to be the rate-limiting step for ECM class 2 compounds. The overall hepatic uptake (sum of active and passive) is projected to be rate-determining for ECM class 3 compounds, whereas the overall intrinsic clearance of ECM class 4 compounds is dependent on the interplay of all processes involved in hepatic elimination (namely metabolism, uptake, and efflux).
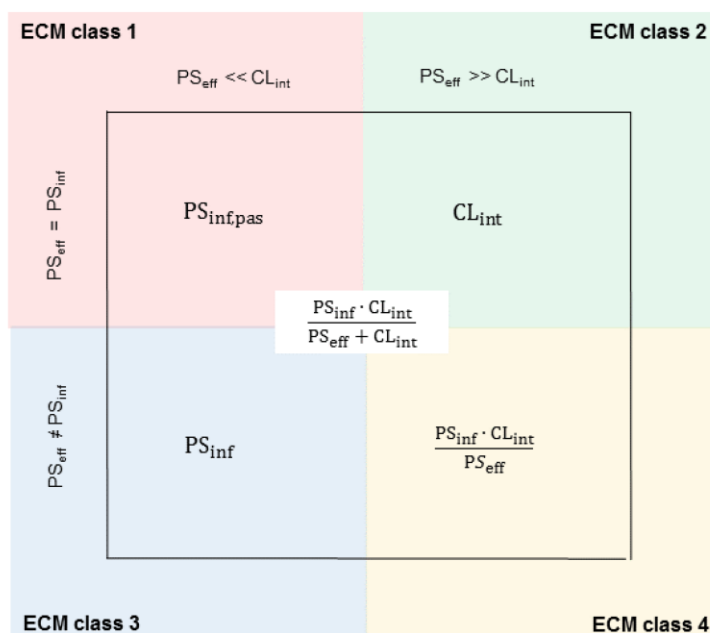

Figure 1. Rate-determining hepatic clearance processes (inner panels) derived from the extended clearance model (ECM) based on different pre-requisites (outer panels) and the assumption thyat $PS_{eff,pas}$ is equal to $PS_{inf,pas}$ and that $PS_{eff,act}$ equals zero (Eq. (1)).

Viewing the liver as a single compartment and assuming that drug molecules are distributing instantaneously and homogeneously within the liver upon entering (well-stirred liver model) the hepatic blood clearance (CL_h) can be calculated with:

$$CL_h = \frac{Q_h \cdot f_{u,b} \cdot (PS_{inf,act} + PS_{inf,pas}) \cdot (CL_{int,met} + CL_{int,sec})}{Q_h \cdot (PS_{eff,act} + PS_{eff,pas} + CL_{int,met} + CL_{int,sec}) + f_{u,b} \cdot (PS_{inf,act} + PS_{inf,pas}) \cdot (CL_{int,met} + CL_{int,sec})} \qquad (2)$$

where Q_h is the hepatic blood flow (20.7 mL/(min·kg)) and $f_{u,b}$ is the unbound fraction in blood. The clearance parameters of the extended clearance model can be determined experimentally as discussed in full detail elsewhere [1,3]. In brief, $PS_{inf,act}$ and $PS_{inf,pas}$ can be assessed by uptake experiments in suspended human hepatocytes (SHH), $CL_{int,sec}$ can be determined in human sandwich-cultured hepatocyte incubations (generally assuming that metabolism in this system is negligible) whereas $CL_{int,met}$, assuming absence of non-oxidative metabolism, is usually experimentally evaluated in human liver microsomal (HLM) incubations. Efflux over the sinusoidal membrane from hepatocytes back into the blood is frequently assumed to occur via passive diffusion only (i.e. $PS_{eff,act}$ = 0). The experimental determination of this parameter is difficult. In the absence of measured data, the passive sinusoidal efflux is usually assumed to be equal to the passive influx (i.e. $PS_{eff,pas}$ = $PS_{inf,pas}$). The individual clearances can finally be fed into Eq. (1) and Eq. (2) to predict $CL_{h,int}$ and CL_h of a drug. Table 1 provides a compilation of experimentally determined intrinsic clearances for a dataset of 19 physicochemically diverse compounds from the literature together with corresponding *in vivo* reference data and the ECM classification according to Fig. 1 [1, 4-7].

Table 1. Experimental human hepatic process clearances from in vitro assays and corresponding in vivo reference data.

compounds	ECM/ECC	$PS_{inf,act}$	$PS_{eff} = PS_{inf,pas}$	$CL_{int,met,HLM}$	$CL_{int,met,HH}$	$CL_{int,sec}$	$f_{u,b}$	$CL_{h,obs}$	fn_{ren}	fn_{met}
	-	mL/(min·kg)	mL/(min·kg)	mL/(min·kg)	mL/(min·kg)	mL/(min·kg)	-	mL/(min·kg)	-	-
lovastatin acid	3/1	165.1	145.5	459.0	119.6	0.0	0.08	11.4	0.10	0.90
simvastatin acid	3/1	116.1	297.9	769.2	ND	1.7	0.11	25.2	0.13	0.87
propanolol	4/2	300.7	276.3	110.8	29.2	6.8	0.11	12.8	0.01	0.99
quinidine	4/2	229.4	109.3	28.4	18.0	5.1	0.27	8.7	0.19	0.81
verapamil	2/2	0.0	258.2	127.7	33.4	8.1	0.13	13.7	0.03	0.97
ketoconazole	2/2	0.0	1568.5	97.4	ND	29.6	0.02	3.9	0.03	0.97
cerivastatin	4/2	221.5	243.8	46.9	ND	0.0	0.02	3.4	0.00	1.00
fluvastatin	4/2	218.7	325.5	146.8	ND	0.0	0.04	7.0	0.00	1.00
pitavastatin	4/2	364.3	258.7	17.7	ND	0.0	0.07	3.5	0.00	ND
aliskiren	3/3	32.3	25.4	89.2	ND	31.2	0.70	11.3	0.25	0.10
cimetidine	3/3	3.0	3.6	528.7	3.2	0.2	0.84	2.7	0.84	0.14
digoxin	3/3	20.0	6.9	24.2	ND	18.4	0.82	4.6	0.66	0.04
cyclospsorine A	3/4	113.2	41.9	77.6	13.5	9.1	0.03	3.1	0.01	0.96
atorvastatin	4/4	140.4	57.7	64.6	254.4	11.8	0.08	5.9	0.02	0.69
furosemide	4/4	11.1	23.9	19.0	0.9	1.2	0.03	0.4	0.66	0.01
ciprofloxacin	4/4	7.0	22.9	22.0	ND	0.0	0.69	4.5	0.60	0.12
valsartan	4/4	16.0	18.5	4.1	ND	21.5	0.09	0.6	0.29	0.11
pravastatin	4/4	57.9	36.0	0.9	5.3	2.2	0.97	10.4	0.47	0.30
rosuvastatin	4/4	27.2	24.8	1.5	ND	5.7	0.17	ND	0.30	0.10

ND: Not determined or experimental data subject to a high degree of uncertainty as discussed elsewhere [4]. With exception of the hepatocyte turn-over data [5,6] all hepatic in vitro and in vivo data were taken from previous in-house manuscripts [1,4,7]. ECM and ECC class assignment was performed according to Fig. 1 and Fig. 6, respectively (underlying working principle: class 1 or 3 if $2 \cdot PS_{eff} <$ ($CL_{int,met,HLM}$ + $CL_{int,sec}$), otherwise class 2 or 4). Metabolic clearance data from human liver microsomes and human hepatocytes are labeled with the subscripts HLM and HH, respectively. fn_{met} (= $CL_{met,obs}/CL_{tot,obs}$) and fn_{ren} (= $CL_{ren,obs}/CL_{tot,obs}$) values were calculated from the observed total ($CL_{tot,obs}$), renal ($CL_{ren,obs}$) and metabolic ($CL_{met,obs}$) clearances as derived from peroral human mass balance studies taking into consideration the estimated absolute oral bioavailability (F). Thereof, fn_h (=1- fn_{ren}) and fn_{sec} (= fn_h- fn_{met}) values discussed in this manuscript can be calculated.

Role of membrane permeability in hepatic elimination

The likelihood that drugs will be subject to enzyme and/or canalicular efflux transporter activities in the liver depends on the extent of their sinusoidal membrane permeation. For the compounds in our dataset (Table 1) this is illustrated in Fig. 2 depicting the relationship between (*in vitro*) sinusoidal passive uptake ($PS_{inf,pas}$) and the fractional contribution of metabolism (fn_{met}, panel A) or biliary secretion (fn_{sec}, panel B) to overall *in vivo* elimination.
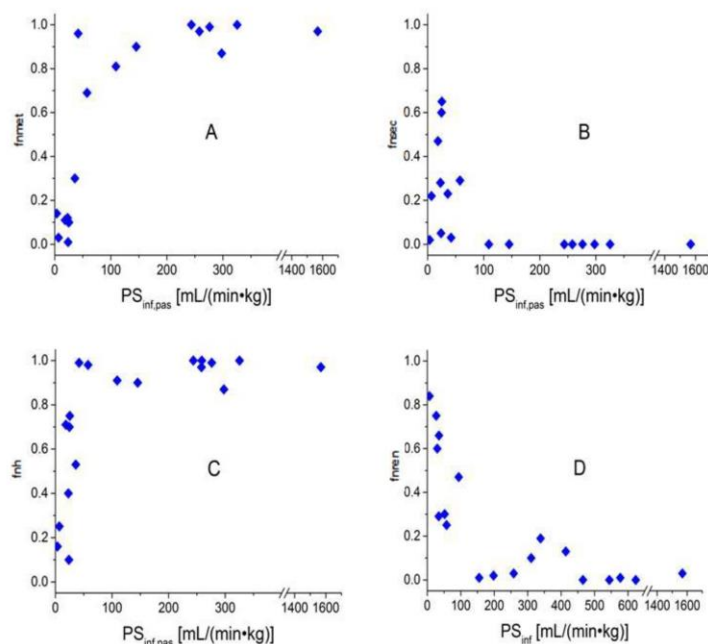

Figure 2. Correlation of sinusoidal hepatic uptake clearances ($PS_{inf,pas}$ or PS_{inf}) with the fractional contributions of metabolic (panel **A**), biliary (panel **B**), hepatic (panel **C**) and renal (panel **D**) clearance to overall in vivo elimination.

An increase in lipophilicity is well known to promote the passive permeability potential of drugs as well as their affinity to drug metabolizing enzymes [8]. Above observed inter-relationship, as depicted in Fig. 2 (panel A), is therefore not very surprising. The association of permeability and enzyme activity allows to define an approximate sinusoidal permeability threshold above which drug elimination seems predominantly driven by metabolism (> 200 mL/(min·kg)). The corresponding plot of $PS_{inf,pas}$ vs fn_{sec} reveals that compound recognition by canalicular efflux transporters, in contrast to fn_{met}, is by some means inversely correlated with rising sinusoidal permeability (Fig. 2, panel B). Fig. 3 shows the contribution of the measured *in vivo* metabolic clearance to the *in vivo* hepatic clearance (= fn_{met}/fn_h) for the compounds in our dataset. Not astonishingly, the compounds with a high (total) sinusoidal permeability are predominantly cleared via hepatic metabolism, while the contribution of metabolism generally decreases for lower permeability compounds apparently accompanied by an increasing contribution of active canalicular secretion.
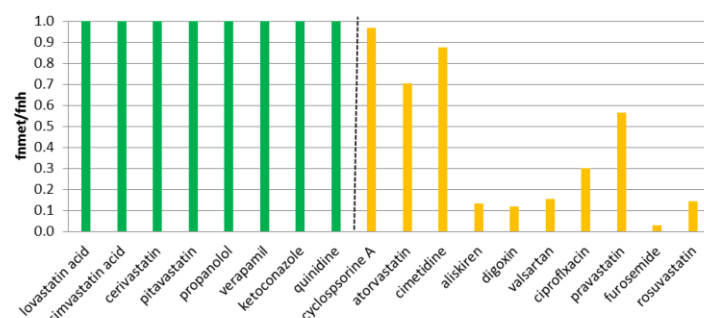
Figure 3. Contribution of in vivo metabolism to overall hepatic clearance for the dataset in Table 1. The dotted line separates the high permeability compounds (green bars) from the low permeability drugs (orange bars) as determined by uptake experiments in suspended hepatocytes (PS_{inf} threshold: 200 mL/(min·kg)).

Hepatic versus non-hepatic elimination

Figure 2 (panel C) illustrates the relationship between passive sinusoidal uptake ($PS_{inf,pas}$) and the observed (*in vivo*) fractional contribution of hepatic clearance to overall drug elimination fn_h. From this illustration it appears that a sinusoidal permeability of above 40-60 mL/(min·kg) will result in predominant hepatic clearance (> 80 %). Numerous data demonstrates that permeability also exerts a key role in renal elimination similar to the one discussed here for liver [4]. It could be demonstrated that for the highly permeable compounds, despite significant tubular secretion, reabsorption from the tubule back into the blood is so extensive that overall renal clearance for these compounds will be low. For the low permeable compounds on the other hand reabsorption, in agreement with their reduced permeability potential, will be much less. As illustrated in Fig. 4, for all compounds in our dataset with a (passive) sinusoidal permeability beyond 40 mL/(min·kg) renal clearance is a minor route of elimination (fn_{ren} < 20 %). For the lower permeable compounds the fractional contribution of renal clearance to total body clearance exceeds 20% or even represents the predominant route of elimination suggesting that hepatic and renal elimination are somehow complementary with regards to the role of sinusoidal permeability in drug elimination.
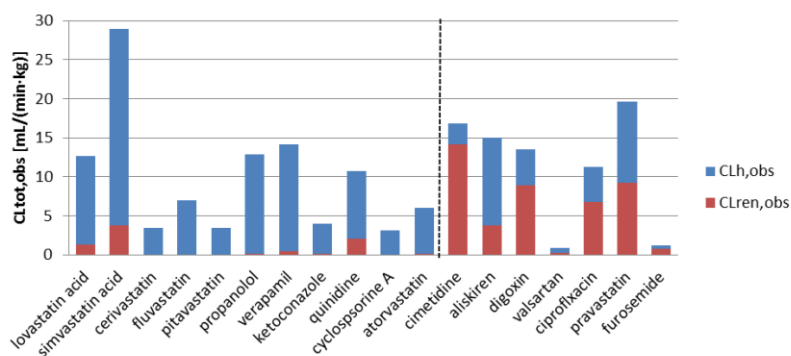

Figure 4. Contributions of the observed renal (red bars) and hepatic (blue bars) clearance pathways to the total body clearance ($CL_{tot,obs} = CL_{h,obs} + CL_{ren,obs}$) for the compounds in Table 1. The dotted line separates the compounds with a $PS_{inf,pas}$ value greater (left part) or lower (right part) than 40 mL/(min·kg).

Fig. 2 (panel D) illustrates the relationship between fn_{ren} and total sinusoidal uptake (PS_{inf}) for the present dataset. As discussed above, a low permeability is hindering hepatic elimination pushing drugs towards alternative elimination routes (with decreasing lipophilicity plasma protein binding usually decreases which would result in increased glomerular filtration process, possibly increased active tubular secretion and less reabsorption) [4]. Beyond a PS_{inf} value of 100 mL/(min·kg)) renal elimination becomes very unlikely. Consequently, following integration of the information from this and the previous chapter, it becomes apparent that total sinusoidal uptake is THE predominant gatekeeper between almost exclusive metabolic hepatic elimination (> 200 mL/(min·kg)), mixed hepatic (metabolism plus biliary secretion, 100-200 mL/(min·kg)) and mixed hepatic/renal elimination (metabolism plus biliary and urinary secretion, < 100 mL/(min·kg)) (Fig. 5). Exclusive renal clearance is expected only if PS_{inf} is approaching a very low value or if substantial entero-hepatic circulation is taking place. Yet, renal excretion might become the predominant elimination pathway for low permeable compounds with about $PS_{inf} < 30$ mL/(min·kg) (Fig. 2, panel D). For compounds with sinusoidal uptake between 30-60 mL/(min·kg), mixed urinary/biliary elimination seems to be the most probable clearance pathway. Consequently, the relationship between $PS_{inf,pas}$ and fn_{sec} as shown in Figure 2 (panel B) likely needs to be interpreted as a bell-shaped curve with a $PS_{inf,pas}$ maximum at around 30 mL/(min·kg) (maximal $fn_{sec} \approx 0.6$-0.7).
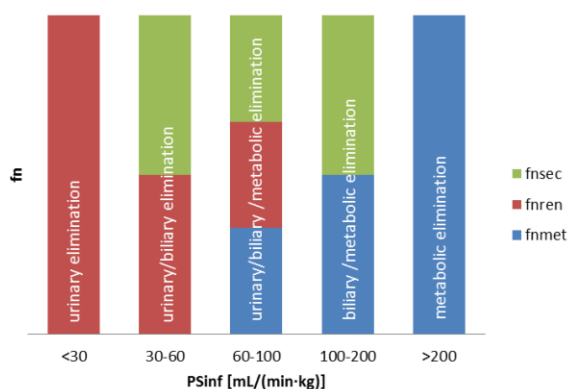

Figure 5. Schematic illustration of the change in elimination route as a function of sinusoidal uptake (PS_{inf}). fn_{met}, fn_{ren} and fn_{sec} denote the fractional contributions of (hepatic) metabolic, urinary and biliary elimination to overall clearance, respectively. Above a PS_{inf} threshold of about 60 mL/(min·kg) liver is the expected primary clearance organ whereas below 30 mL/(min·kg) renal elimination is likely predominant.

Extended Clearance Concept Classification System

The extended clearance concept (ECC) is the intangible attempt to complete the principles of the extended clearance model (Fig. 1) with the gatekeeping role of sinusoidal influx as discussed above (Fig. 5) to allow prediction of *in vivo* pharmacokinetic performance of drugs from *in vitro* permeability and metabolism data as illustrated in Fig. 6. Drugs with a high apparent hepatic intrinsic clearance are removed from the blood essentially as fast as they can be delivered to the liver, i.e. independent of protein binding and intrinsic enzyme and canalicular efflux transporter activities. Therefore, the elimination of such drugs is highly dependent upon liver blood flow and the inherent ability to cross the sinusoidal membrane rapidly. Consequently, according to the well-stirred liver model, a compound can be ranked as highly permeable if

$CL_{h,int} = PS_{inf,pas} \gg Q_h$ (Eq. (1) and Eq. (2)). From above discussion it is evident that a (passive) sinusoidal permeability above 60 mL/(min·kg) results in an almost complete hepatic clearance (Fig. 2, panel C and Fig. 5). Thus, a compound can be ranked as highly permeable if $PS_{inf,pas} \geq$ 3-fold Q_h, a threshold substantiating the conceptual approximation $PS_{inf} \approx PS_{eff} \approx PS_{inf,pas}$ pertinent to all compounds identified to be hepatic uptake transporter substrates besides demonstrating a high intrinsic permeation potential across the sinusoidal membrane of hepatocytes. Hence, it becomes evident that uptake transporter effects for highly permeable compounds are minimally contributing to overall hepatic clearance while they are expected to become important/predominant for the hepatic clearance of lower permeable compounds. Applying this fundamental relationship, the 19 compounds in our dataset were assigned to the four different ECC classes as summarized in Table 1.

Figure 6. Predominant routes of drug elimination and potential transporter effects on (hepatic) drug disposition according to the Extended Clearance Concept Classification System (ECCCS). Thresholds as defined by the Biopharmaceutics Drug Disposition Classification system (BDDCS) are provided for comparative reasons also [1,8].

Taking all above principles into account it is appropriate to conclude that the major route of elimination for ECC class 3 and 4 compounds is renal and biliary excretion of unchanged drug whereas metabolism is the predominant elimination pathway for ECC class 1 and 2 compounds as previously concluded by others also [8]. However, ECC allows a compound classification of drug molecules based on their *in vitro* determined (hepatic) clearance parameters in contrast to the Biopharmaceutics Drug Disposition Classification System (BDDCS) which allocates drugs into four classes according to their *in vivo* metabolism and solubility potential. Both concepts are closely related and have in common that they recognize that the fundamental parameter controlling (hepatic) drug disposition is the compound class-dependent interplay between transporters, enzymes and membrane permeability. Both systems provide a similar rational on the predominant routes of drug elimination and the potential effect of transporters on (hepatic) drug disposition as illustrated in Fig. 6. Yet, assignment into BDDCS relies on clinical elimination information and is therefore not really applicable for early Drug Development.

ECC and IVIVE

The correlation between the *in vitro* predicted ($CL_{h,pred}$) and *in vivo* observed ($CL_{h,obs}$) hepatic clearances for our dataset based on the mechanistic *in vitro-in vivo* extrapolation (IVIVE) method represented by Eq. (1) and Eq. (2) is illustrated in Fig. 7 (panel A). The approach reveals an excellent correlation with 11 out of 18 drugs predicted within two-fold deviation from the clinically observed value. The prediction accuracy in terms of average fold error (afe) and geometric mean fold error (gmfe) was 0.92 and 1.55, respectively. Present results demonstrate that the extended clearance concept model is by far exceeding the accuracy and performance of other IVIVE prediction methods for hepatic clearance based only on *in vitro* metabolism (Fig. 7, panels B and C for microsomes (afe = 0.76, gmfe = 2.11)) and hepatocytes (afe = 0.32, gmfe = 3.56), respectively) or sinusoidal uptake (Fig. 7, panel D, afe = 1.71, gmfe = 1.84) data.
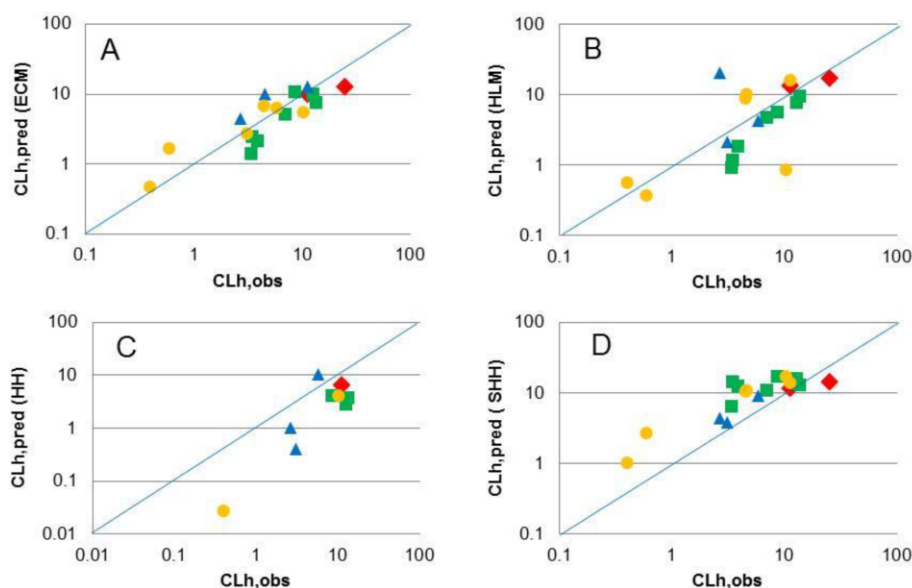

Figure 7. Comparison of the reported ($CL_{h,obs}$) and predicted ($CL_{h,pred}$) hepatic clearances using different IVIVE methods. Panel **A** represents the relationship according to the extended clearance model (ECM). The panels **B** and **C** show the predictions based on in vitro metabolism data from human microsomes (HLM) and hepatocytes (HH), respectively, whereas panel **D** is the representation based on sinusoidal uptake data from suspended human hepatocytes (SHH). Red diamonds, green squares, blue triangles and orange circles show the class 1, 2, 3 and 4 assignments according to ECC (Table 1). The blue line represents the line of unity for each panel.

In accordance with previous research, the correlation analysis in Fig. 7 reveals a systematic under-prediction of *in vivo* hepatic clearance when using metabolic turn-over data from human hepatocyte incubations whereas sinusoidal uptake data from suspended human hepatocytes tend to over-predict the *in vivo* situation [9,10]. Metabolic clearance data from human liver microsomes on the other hand are highly scattered along the line of unity providing under- and over-estimations of the observed human hepatic clearance. The potential rate-determining role of the hepatocyte membrane (missing in the microsomal system) is extensively discussed in literature. In line with this theory more in-depth data examination reveals that metabolism information from microsomes and hepatocytes generally provide reasonable results for the ECC class 1 and 2 compounds while hepatocyte uptake data seem to be highly predictive for the *in vivo* hepatic clearance of ECC class 3 compounds. IVIVE based on the extended mechanistic model surely works best for ECC class 4 compounds though. Imposing these observations on

the principles of ECC the expected performance of the different IVIVE approaches can be summarized as depicted in Fig. 8. It is self-explanatory that with increasing contribution of renal clearance the predictability of all hepatobiliary IVIVE tools for overall (total) clearance is decreasing (tendency for underestimation). Based on above discussion, this is mainly true for ECC class 3 and 4 compounds while the overall prediction performance for ECC class 1 and 2 compounds likely remains good. In-house research intending to improve bottom-up predictions for overall human clearance using different *in vitro* and *in vivo* approaches is currently ongoing.

Figure 8. Anticipated hepatobiliary IVIVE accuracy of different in vitro tools: Metabolism assessment in human liver microsomes (HLM) or human hepatocytes (HH), uptake data from suspended human hepatocytes (SHH) and integrated approach with the extended clearance model (ECM). For the assignment the following assumptions were made: (i) absence of significant biliary secretion (i.e. CL$_{int,sec}$ << CL$_{int,met}$), (ii) absence of phase II metabolism and, (iii) no or down-regulated transporter activity in HH.

Static DDI predictions

A perpetrator drug may inhibit any active clearance pathway contributing to the total hepatic elimination of a substrate. Accordingly, based on Eq. (1) (assuming PS$_{eff,act}$ = 0 and PS$_{eff,pas}$ = PS$_{inf,pas}$), the overall hepatic intrinsic clearance in the presence of a perpetrator (CL$_{h,int,i}$) can be expressed as follows [1,7]:

$$CL_{h,int,i} = \frac{\left[(1-f_{i,inf})\cdot PS_{inf,act} + PS_{inf,pas}\right] \cdot \left[(1-f_{i,met})\cdot CL_{int,met} + (1-f_{i,sec})\cdot CL_{int,sec}\right]}{\left[PS_{inf,pas} + (1-f_{i,met})\cdot CL_{int,met} + (1-f_{i,sec})\cdot CL_{int,sec}\right]} \quad (3)$$

where $f_{i,inf}$, $f_{i,sec}$ and $f_{i,met}$ denote the inhibited fractions of active influx, canalicular secretion, and metabolism, respectively. A f$_i$ value of zero thereby indicates no inhibition whereas a value of one refers to

complete inhibition. Based on this relationship the hepatic clearance in the presence of any perpetrator compound ($CL_{h,i}$) can be anticipated in accordance with Eq. (2).

Following oral (po) administration of a drug and its perpetrator, assuming the presence of hepatic and a non-hepatic (e.g. renal) elimination pathways and that the perpetrator drug only affects active processes in the liver, the exposure (AUC) fold-change (expressed as $AUC_{po,i}/AUC_{po}$) can be described as follows:

$$\frac{AUC_{po,i}}{AUC_{po}} = \frac{F_{h,i}}{F_h} \cdot \frac{1}{fn_h \cdot CL_{h,i}/CL_h + 1 - fn_h} \tag{4}$$

where, $F_h (= 1-CL_h/Q_h)$ and $F_{h,i} (= 1-CL_{h,i}/Q_h)$ are the fractions of the oral dose escaping hepatic first-pass in the absence and presence of a perpetrator, respectively.

Under the additional assumption that the liver is the only clearance organ (i.e. $fn_h = 1$) Eq. (4) simplifies to:

$$\frac{AUC_{po,i}}{AUC_{po}} = \frac{CL_{h,int}}{CL_{h,int,i}} \tag{5}$$

In an abbreviated manner, based on Eq. 5 and previous discussion, the drug-drug interaction (DDI) potential for the four ECM cases in Fig. 1 can therefore be represented as shown in Fig. 9.
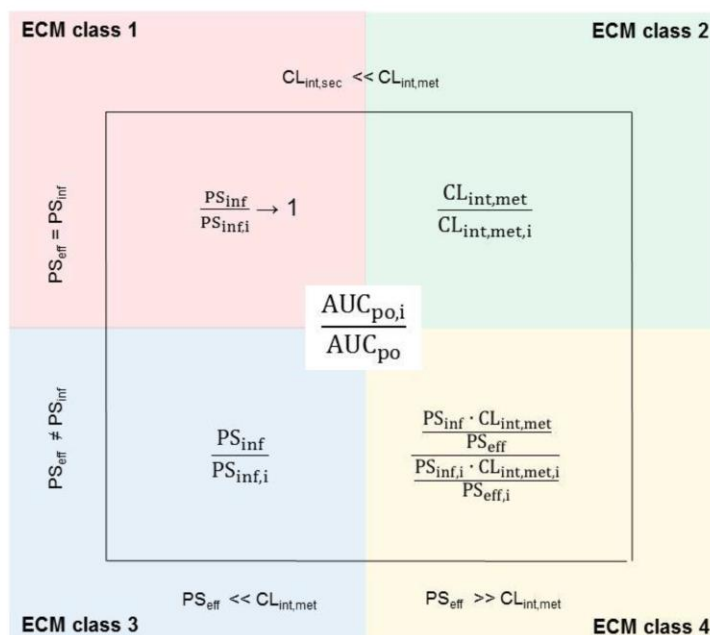
Figure 9. Compound class-dependent DDI prediction (inner panel) according to Eq. 5 for the four different ECM cases based on different pre-requisites (outer panel). i refers to a change in clearance in the presence of any perpetrator compound.

Fig. 10 depicts the predicted static DDI risk assessment of 3 representative compounds from our dataset (namely the ECM class 2 compound verapamil, digoxin as a typical ECM class 3 compound and pravastatin representing the ECM class 4) according to Eq. (4) and Eq. (5), assuming 90% inhibition of the respective

processes (i.e. $f_{i,inf}$ = $f_{i,met}$ = $f_{i,sec}$ = 0.9, not taking into consideration fractional contributions of different enzymes or transporters to overall metabolic or transport clearance). In the absence of a renal clearance contribution (Fig. 10, panel A), in accordance with the extended clearance model, for the ECM class 2 compound in our selection, metabolism is identified as the major clearance mechanism primarily responsible for causing DDI's. Selective inhibition of active hepatic influx or biliary secretion has no significant effect on exposure though. A similarly distinct overall DDI behavior can be derived for the ECM class 3 compound digoxin with sinusoidal transporter inhibition being the major mechanism causing the interaction. For the ECM class 4 compound pravastatin, assuming absence of a renal clearance contribution, we predict a substantial AUC change upon concomitant inhibition of hepatic uptake, biliary secretion and metabolism whereas inhibition of the single clearance pathways results in comparatively moderate AUC ratios. Taking the clinically observed fn_h values according to Eq. (4) into account, the individual as well as the overall DDI risk assessment of verapamil is only marginally effected whereas the impact on the projected exposure changes for digoxin and pravastatin is significant (e.g. the overall $AUC_{po,i}/AUC_{po}$ ratio for pravastatin decreases about 8-fold) (Fig. 10, panel B). This concept is well reflected by ECM and can be rationalized by the process inter-dependencies as discussed above. It is noteworthy to mention at this point, that the extended clearance model represents the four extremes of hepatobiliary elimination and that most drugs settle somewhere in-between the ultimate limits given in Fig. 1. To eventually predict the overall DDI potential of drug molecules it is therefore essential to (quantitatively) assess all the individual hepatic process contributions as defined by Eq. (1).
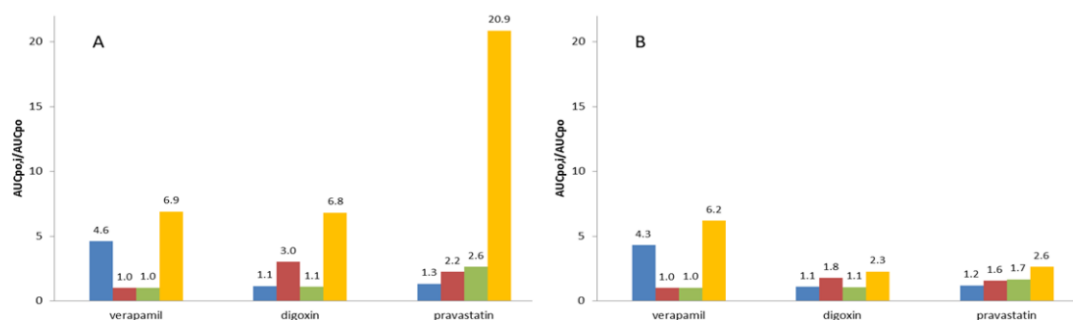

Figure 10. Static victim drug DDI predictions for verapamil (CYP2C8, CYP3A and P-gp), digoxin (P-gp, CYP3A and unknown sodium-dependent sinusoidal uptake transporter) and pravastatin (BCRP, MRP2, OATP1B1, OATP1B3, OATP2B1 and CYP3A4) according to Eq. (5) (panel **A**) and Eq. (4) (panel **B**). The projected AUC fold-changes with $f_{i,inf}$ = $f_{i,met}$ = $f_{i,sec}$ = 0.9 are represented as follows: metabolism inhibition only (blue bars), exclusive sinusoidal active uptake inhibition (red bars), inhibition of canalicular efflux (light green bars) and, simultaneous inhibition of all active processes together (yellow bars).

Neglecting time-dependent concentration changes, static DDI predictions are expected to provide conservative (worst-case) estimates for the effective *in vivo* situation [1]. Nevertheless, DDI assessments according to Eq. (4) are generally in good agreement with clinical DDI data for ECM class 1 and 2 compounds as discussed elsewhere [7]. However, with increasing fn_{ren} (i.e. decreasing fn_h), the predictions become less reliable for ECM class 3 and 4 compounds, often resulting in significant under-estimations of the effective DDI risk observed in clinics (e.g. pravastatin exposure in the presence of cyclosporine A (inhibitor of OATP's, OAT's, NTCP, P-gp, BCRP, MRP2, CYP3A4 and UGT's) was reported to increase about 20-fold, significantly exceeding the theoretically possible hepatic DDI potential of 2.6-fold (Fig. 10)) [7]. The main reason for this observation is that a significant renal secretion process for these low permeable

compounds is typically governed by active transporter processes which often are concomitantly inhibited by perpetrator drugs also interfering with the sinusoidal uptake carrier system in the liver. Consequently, for conservative bottom-up DDI estimates the physiologically less appropriate Eq. (5) should be preferred as it accommodates for possible cross-reactivity on hepatic and renal (transporters) systems (e.g. the clinical observation for pravastatin in the presence of cyclosporine A is well predicted with Eq. (5) (Fig. 10)). Nevertheless, in combination with clinical DDI data and applying a top-down approach, comparative static DDI assessments according to Eq. (4) and Eq. (5) can be extremely helpful in revealing alternative (extra-hepatic) active elimination processes as discussed in full detail elsewhere [7].

Prediction of unbound intracellular hepatic drug concentrations
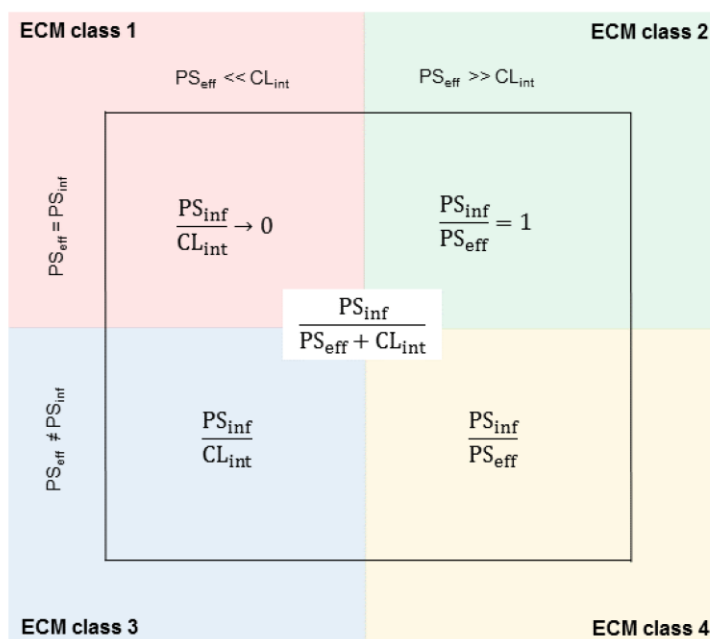
Figure 11. ECM class-dependent effect on the unbound liver-to-capillary blood concentration ratio (Kp_{uu}) according to Eq. 6.

According to the so-called free drug hypothesis, at steady-state and in the absence of a membrane transport barrier limiting access to the hepatocyte, the unbound (free) intracellular concentration $C_{h,u}$ is equal to the unbound blood concentration $C_{b,u}$ (i.e. $C_{h,u}/C_{b,u}$ = 1). However, according to the extended clearance model, $C_{h,u}$ is not only governed by uptake and protein binding but also by all intracellular elimination processes. Therefore, based on Eq. (1), for the liver this relationship needs to be rewritten as follows [11]:

$$\frac{C_{h,u}}{C_{b,u}} = Kp_{uu} = \frac{PS_{inf}}{PS_{eff} + CL_{int}} \tag{6}$$

Extended Clearance Concept Classification System (ECCCS)

where, Kp_{uu} is the unbound liver-to-capillary blood concentration ratio. In line with ECM, the impact of the relative process contributions on Kp_{uu} can be summarized as shown in Fig. 11. The knowledge of the relevant (effective) intrahepatic concentrations is important when performing DDI risk assessments (compound acting as inhibitor) on active processes such as metabolism and/or canalicular efflux. However, due to experimental inaccessibility of $C_{h,u}$, static perpetrator risk calculations for the liver generally refer to $C_{b,u}$ (usually expressed as $C_{b,u}/K_i$, where K_i denotes the inhibition constant on a particular process). Based on the extended clearance model it becomes evident that the use of this substitute might lead to a considerable misjudgment of the DDI potential of perpetrator drugs though. Depending on the major rate-determining process driving hepatic elimination significant under- (e.g. Kp_{uu} equals 2.4 for ECM class 4 compound pravastatin) or over- (e.g. $C_{h,u}$ is about 80-fold less than $C_{b,u}$ for ECM class 3 compound cimetidine) estimations of the real interaction risk might result. The use of systemic unbound drug concentrations (or unbound drug concentrations in the portal vein) is thus likely insufficient to properly assess the actual drug-drug interaction potential on intracellular enzymes/transporters for class 1, 3 and 4 compounds as illustrated in Table 2.

Table 2. Effect of Kp_{uu} on $C_{h,u}$ and the DDI risk outcome for perpetrator drugs.

ECM class	Effect of Kp_{uu} on $C_{h,u}$ (Eq. (6))	Risk assessment with $C_{b,u}/K_i$
1	$C_{h,u} << C_{b,u}$	overestimation
2	$C_{h,u} = C_{b,u}$	predictive
3	$C_{h,u} <$ or $> C_{b,u}$	under- or overestimation (generally overestimation as usually $PS_{inf} < CL_{int}$)
4	$C_{h,u} <$ or $> C_{b,u}$	under- or overestimation (generally underestimation as usually $PS_{inf} > PS_{eff}$)

Although currently not requested by health authorities present ECM-based principles might change the way we are doing perpetrator DDI risk assessments for intracellular hepatic processes in the future, all the more the mechanistic IVIVE method presented in this manuscript was demonstrated to provide quantitative reliable estimates of $CL_{h,obs}$ and therewith of Kp_{uu} (see above). Further in-house research on this this topic is currently ongoing.

Conclusions

In this review, we have illustrated the usefulness of the extended clearance model for classifying drug compounds depending on the relative contributions of the individual hepatic elimination processes. The ECM classification system based upon easily accessible *in vitro* data for metabolism, sinusoidal transport and canalicular efflux allows the quantitative bottom-up assessment of a series of (pharmacokinetic) parameters such as the hepatic clearance, the unbound liver-to-capillary blood concentration ratio and the static prediction of the DDI potential of drug molecules. The method reveals the major role of sinusoidal uptake as a gatekeeper for drug elimination, provides insight into the performance of different IVIVE approaches for hepatic clearance prediction and highlights potential limitations of currently applied drug-drug interaction risk assessment approaches. Consequently, following a thoughtful implementation, the approach may facilitate the compound selection process in Pharmaceutical Research and improve some of the compound profiling methodologies (e.g. DDI risk assessment) applied in Drug Development.

References

[1] G. Camenisch and K. Umehara, *Biopharmaceutics & Drug Disposition* **33** (2012) 179-1940.

[2] Y. Shitara, H. Sato and Y. Sugiyama, *Annual Review of Pharmacology and Toxicology* **45** (2005) 689-723.

[3] K. Umehara and G. Camenisch, *Pharmaceutical Research* **29** (2012) 603-617.

[4] A. Kunze, B. Poller, J. Huwyler and G. Camenisch, *Drug metabolism and drug interactions* In Press.

[5] D. McGinnity, M. Soars, R. Urbanowicz and R. Riley, *Drug Metabolism and Disposition* **32** (2004) 1247-1253.

[6] D. Hallifax, E. Turlizzi, U. Zanelli and J. Houston, *European Journal of Pharmaceutical Sciences* **45** (2012) 570-574.

[7] A. Kunze, J. Huwyler, B. Poller, H. Gutmann and G. Camenisch, *Journal of Pharmaceutical Sciences* **103** (2014) 994-1001.

[8] L. Benet, G. Amidon, D. Barends, H. Lennernas, J. Polli, V. Shah, S. Stavchansky and L. Yu, *Pharmaceutical Research* **25** (2008) 483-48.

[9] M. Chiba, Y. Ishii and Y. Sugiyama, *AAPS Journal* **11** (2009) 262-276.

[10] D. Hallifax, H. Rawden, N. Hakooz and J. Houston, *Drug Metabolism and Disposition* **33** (2005) 1852-1858.

[11] Y. Shitara, K. Maeda, K. Ikejiri, K. Yoshida, T. Horie and Y. Sugiyama, *Biopharmaceutics & Drug Disposition* **34** (2013) 45-78.

CHAPTER 3

Aim of the thesis

Drug disposition processes are important determinants for drug safety and efficacy since they directly influence the drug exposure in the different compartments of the human body. Understanding the pharmacokinetic behavior of new drug candidates is therefore of critical importance for the development of efficacious and safe drugs. However, clinical information about the pharmacokinetic properties of new drug candidates is rarely available at early preclinical development stages. Hence, *in vitro* systems and IVIVE models are valuable tools to provide estimates of human pharmacokinetic data. This work focused on the development of new *in vitro* methods to predict drug disposition in humans. The individual objectives were defined as follows:

1. **Establishment of a mechanistic *in vitro* Kp_{uu} model to predict drug-induced cholestasis**

   In the absence of tissue concentration data in humans, systemic drug exposure is commonly used as surrogate for unbound intracellular drug concentrations. However, this approach is inappropriate for the liver where unbound intracellular drug concentrations are affected by active transport and metabolic processes (section 2.3). This study aimed at establishing an *in vitro* Kp_{uu} approach under consideration of all hepatic processes based on the ECM concept. As a proof-of-concept, the resulting estimates of unbound intrahepatic drug concentrations were validated by predicting the clinical risk of drug-induced cholestasis upon inhibition of the intrahepatic transporter BSEP.

2. **Investigation of alternative *in vitro* Kp_{uu} methods**

   Besides the ECM approach, different alternative *in vitro* Kp_{uu} determination methods have been described that rely on separate measurements of hepatocellular drug accumulation and the unbound fraction in hepatocytes. These methods are based on simplified *in vitro* systems that neglect intrinsic hepatic drug elimination by metabolism and biliary secretion, though they represent straightforward and less labor-intensive approaches. The aim of this study was to investigate the applicability of three alternative Kp_{uu} determination methods in comparison to the ECM approach. Deviations between the applied methods were investigated with regard to pharmacokinetic and physicochemical drug properties.

3. **Development of an *in vitro* model for the prediction of total drug clearance in humans**

   Sophisticated hepatic IVIVE approaches have been developed to study hepatic elimination and DDIs (sections 2.5 and 2.6). Nevertheless, the usefulness of corresponding renal IVIVE approaches is limited and the prediction of total drug clearance is hampered. Alternatively,

knowledge about hepatic and renal elimination pathway contributions allows extrapolating the ECM-based hepatic clearance to total clearance. Thus, this strategy can compensate the lack of appropriate renal IVIVE models. This study aimed at establishing the quantitative prediction of hepatic metabolic, biliary, and renal elimination pathway contributions in humans from *in vitro* sinusoidal uptake permeability data and to demonstrate the validity of the Extended Clearance Concept Classification System (ECCCS) for elimination pathway predictions. The predicted data were compared with observed total drug clearances in order to validate the developed approach.

CHAPTER 4

Results

The results of this thesis were published in the following articles:

1. **Assessing the risk of drug-induced cholestasis using unbound intrahepatic concentrations**

   Riede et al., Drug Metabolism and Disposition (2017), 45 (5), 523-531

2. **Current *in vitro* methods to determine hepatic Kp_{uu}: a comparison of their usefulness and limitations**

   Riede et al., Journal of Pharmaceutical Sciences (2017), 106 (9), 2805-2814

3. **New IVIVE method for the prediction of total human clearance and relative elimination pathway contributions from *in vitro* hepatocyte and microsome data**

   Riede et al., European Journal of Pharmaceutical Sciences (2016), 86, 96-102

4.1. Assessing the risk of drug-induced cholestasis using unbound intrahepatic concentrations

Julia Riede[1,2], Birk Poller[1], Jörg Huwyler[2], Gian Camenisch[1]

[1] Division of Drug Metabolism and Pharmacokinetics, Integrated Drug Disposition Section, Novartis Institutes for BioMedical Research, Basel, Switzerland

[2] Department of Pharmaceutical Sciences, Division of Pharmaceutical Technology, University of Basel, Basel, Switzerland

Assessing the Risk of Drug-Induced Cholestasis Using Unbound Intrahepatic Concentrations[S]

Julia Riede, Birk Poller, Jörg Huwyler, and Gian Camenisch

Division of Drug Metabolism and Pharmacokinetics, Integrated Drug Disposition Section, Novartis Institutes for BioMedical Research, Basel, Switzerland (J.R., B.P., G.C.); and Department of Pharmaceutical Sciences, Division of Pharmaceutical Technology, University of Basel, Basel, Switzerland (J.R., J.H.)

ABSTRACT

Inhibition of the bile salt export pump (BSEP) has been recognized as a key factor in the development of drug-induced cholestasis (DIC). The risk of DIC in humans has been previously assessed using in vitro BSEP inhibition data (IC_{50}) and unbound systemic drug exposure under assumption of the "free drug hypothesis." This concept, however, is unlikely valid, as unbound intrahepatic drug concentrations are affected by active transport and metabolism. To investigate this hypothesis, we experimentally determined the in vitro liver-to-blood partition coefficients (Kp_{uu}) for 18 drug compounds using the hepatic extended clearance model (ECM). In vitro–in vivo translatability of Kp_{uu} values was verified for a subset of compounds in rat. Consequently, unbound intrahepatic concentrations were calculated from clinical exposure (systemic and hepatic inlet) and measured Kp_{uu} data. Using these values, corresponding safety margins against BSEP IC_{50} values were determined and compared with the clinical incidence of DIC. Depending on the ECM class of a drug, in vitro Kp_{uu} values deviated up to 14-fold from unity, and unbound intrahepatic concentrations were affected accordingly. The use of in vitro Kp_{uu}-based safety margins allowed separation of clinical cholestasis frequency into three classes (no cholestasis, cholestasis in ≤2%, and cholestasis in >2% of subjects) for 17 out of 18 compounds. This assessment was significantly superior compared with using unbound extracellular concentrations as a surrogate for intrahepatic concentrations. Furthermore, the assessment of Kp_{uu} according to ECM provides useful guidance for the quantitative evaluation of genetic and physiologic risk factors for the development of cholestasis.

Introduction

The liver is the major organ involved in the elimination of potentially harmful endogenous and xenobiotic substances, including pharmaceutical drugs, and is itself predisposed to toxicity resulting from high exposure to drugs and their metabolites. Drug-induced liver injury (DILI) is a leading cause of acute liver failure, termination of compounds in drug development, and drug withdrawal from the market (Lee, 2003; Food and Drug Administration, 2009). The severity of DILI ranges from asymptomatic elevations of liver enzymes to acute liver failure and manifests with hepatocellular, cholestatic, or mixed (hepatocellular/cholestatic) patterns.

Although drug-induced cholestasis (DIC) usually represents a less severe form of DILI, it is nevertheless reported to account for up to 26% of all hepatic adverse reactions (Bjornsson and Olsson, 2005; Hussaini and Farrington, 2007). Cholestasis is characterized by reduced bile flow, potentially resulting in accumulation of cytotoxic bile salts within

hepatocytes, leading to liver damage (Stieger, 2010). The bile salt export pump (BSEP), a member of the ATP-binding cassette super-family encoded by the ABCB11 gene, is expressed at the canalicular membrane of hepatocytes and plays a fundamental role in bile homeostasis by secreting bile acids from the hepatocyte into bile ducts. Impairment of BSEP function due to inhibition by drugs or genetic defects was previously identified as a key factor in the development of DIC, hereditary cholestatic syndromes, or intrahepatic cholestasis of pregnancy (Stieger et al., 2000; Fattinger et al., 2001; Funk et al., 2001; Pauli-Magnus et al., 2010; Dietrich and Geier, 2014). Several attempts have been made to predict DIC or DILI in humans from in vitro BSEP inhibition data due to limited translatability of hepatic adverse events from preclinical models (Olson et al., 2000). Recently, Dawson et al. (2012) and Morgan et al. (2013) demonstrated that potent BSEP in vitro inhibition and high systemic drug exposure correlate with the occurrence of DIC. However, the assessments did not allow clear separation of cholestatic/mixed from non-cholestatic drugs, and thus reliable prediction of DIC remains challenging.

Clinical drug toxicity, drug-drug interactions (DDIs), and pharmacological drug-target interactions are commonly anticipated by relating the in vitro target potency (IC_{50}, K_i, or EC_{50} value) to the unbound (i.e., free)

524   Riede et al.
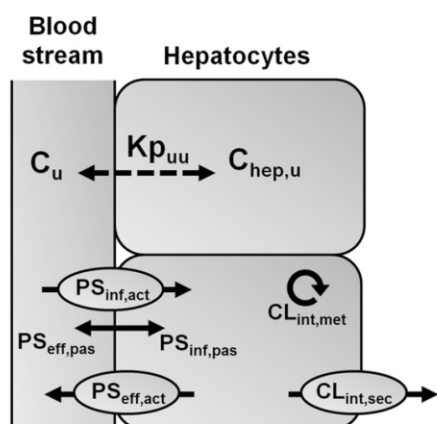
Blood stream **Hepatocytes**

Fig. 1. ECM and Kp_{uu}. Schematic diagram of hepatic clearance processes determining the liver-to-blood partition coefficient for unbound drug at steady state (Kp_{uu}). The unbound intrahepatic concentration ($C_{hep,u}$) is determined by the unbound extracellular concentration (C_u) and the interplay between all hepatic process clearances, where $C_{hep,u} = C_u \times Kp_{uu}$. Unbound drug in the blood stream is taken up into hepatocytes (PS_{inf}) by transporters ($PS_{inf,act}$) and/or by passive diffusion ($PS_{inf,pas}$). Elimination of drug from the hepatocyte (CL_{int}) occurs via hepatic metabolism ($CL_{int,met}$), by active secretion into bile ($CL_{int,sec}$), and by sinusoidal efflux (PS_{eff}) via active transport ($PS_{eff,act}$) and/or passive diffusion ($PS_{eff,pas}$).

systemic drug concentration due to limited availability of tissue concentration data in humans (Muller and Milton, 2012; Zamek-Gliszczynski et al., 2013). This assessment is based on the "free drug hypothesis," which assumes complete distribution equilibrium of the unbound drug between blood and tissue at steady state. This assumption, however, is unlikely to apply to organs such as the liver, where the distribution equilibrium is affected by active cellular transport and metabolic processes (Chu et al., 2013). Therefore, recent publications proposed estimating the unbound intracellular liver concentration using the liver-to-blood partition coefficient for unbound drug at steady state (Kp_{uu}) in vitro (Yabe et al., 2011; Mateus et al., 2013; Pfeifer et al., 2013; Shitara et al., 2013; Nicolai et al., 2015). Following the concept of the hepatic extended clearance model (ECM), the in vitro (hepatocyte-to-medium) Kp_{uu} can be derived from in vitro measurements of individual hepatic elimination process clearances (sinusoidal influx and efflux, metabolism, and biliary secretion), which govern hepatic elimination (Fig. 1) (Shitara et al., 2013; Camenisch et al., 2015; Camenisch, 2016). Measurements of individual hepatic process clearances additionally allow assignment of compounds into four distinct ECM categories to anticipate class-dependent effects on Kp_{uu} and, as a consequence, on the unbound intrahepatic concentration (Fig. 2) (Camenisch et al., 2015; Camenisch, 2016).

The aim of the present study was to identify the reference drug concentration (unbound systemic, unbound hepatic inlet, or unbound intrahepatic concentration) that provides the best anticipation of DIC risk due to BSEP inhibition. Upon assessing in vitro–in vivo correlation (IVIVC) for Kp_{uu} in rat using literature data, we experimentally determined human hepatic in vitro Kp_{uu} values using the ECM concept for 18 drug compounds with diverse physicochemical and pharmacokinetic properties. Unbound intrahepatic concentrations in humans were estimated by applying ECM-based Kp_{uu} to either unbound systemic or hepatic inlet concentrations. The resulting safety margins between in vitro BSEP IC_{50} and the various reference concentrations were compared with the clinical incidence of DIC. In addition, the potential impact of genetic and physiologic risk factors on the induction of cholestasis is discussed using bosentan as tool compound.

Materials and Methods

Materials. Radiolabeled test compounds ([³H] or [¹⁴C]) were obtained from PerkinElmer (Boston, MA), American Radiolabeled Chemicals (St. Louis, MO), and Moravek Biochemicals (Brea, CA). Radiochemical purity of all compounds was ≥95% as determined in-house by high-performance liquid chromatography analysis. All other chemicals were purchased from commercial sources and were of analytical grade.

Determination of Hepatic In Vitro Kp_{uu}. Previous work performed by our group has shown that in vivo hepatic organ clearances (CL_h) were correctly predicted by feeding up-scaled in vitro hepatic process clearances into the ECM (eq. 1) and by applying the "well stirred" liver model (eq. 2) (Camenisch and Umehara, 2012; Umehara and Camenisch, 2012; Kunze et al., 2015):

$$CL_{h,int} = \frac{PS_{inf,act} + PS_{inf,pas}}{PS_{eff,act} + PS_{eff,pas} + CL_{int,met} + CL_{int,sec}} \times (CL_{int,met} + CL_{int,sec})$$

$$= \frac{PS_{inf}}{PS_{eff} + CL_{int}} \times CL_{int} \tag{1}$$

$$CL_h = \frac{Q_h \times fu_b \times CL_{h,int}}{Q_h + fu_b \times CL_{h,int}} \tag{2}$$

where $CL_{h,int}$ is the intrinsic hepatic clearance, PS_{inf} is the sum of active ($PS_{inf,act}$) and passive uptake membrane permeability ($PS_{inf,pas}$), PS_{eff} is the sum of active ($PS_{eff,act}$) and passive sinusoidal efflux membrane permeability ($PS_{eff,pas}$), CL_{int} is the sum of intrinsic metabolic ($CL_{int,met}$) and biliary clearances ($CL_{int,sec}$), Q_h is the hepatic blood flow, and fu_b is the unbound fraction in blood.

This in vitro–in vivo extrapolation approach for human and rat hepatic clearance provided a good prediction accuracy for a diverse data set of 13 compounds with ~80% within 2-fold error (Camenisch and Umehara, 2012; Umehara and Camenisch, 2012). According to the concept of the ECM, the intrinsic clearance is driven by the intracellular concentration (Shitara et al., 2013), and eq. 1 can be rearranged as follows:

$$CL_{h,int} = Kp_{uu} \times CL_{int} \tag{3}$$

Hepatic Process Clearances. Hepatic process clearances for 18 test compounds were experimentally determined as previously described in full detail elsewhere (Camenisch and Umehara, 2012; Umehara and Camenisch, 2012; Kunze et al., 2014, 2015). All presented in vitro data for atorvastatin, cerivastatin, cyclosporine A, fluvastatin, ketoconazole, lovastatin acid, pitavastatin,

Fig. 2. Drug classification according to ECM and expected impact on Kp_{uu} and $C_{hep,u}$. ECM class 1/2 was assigned if $PS_{eff} < CL_{int}$; otherwise, class 3/4 was assigned. Class 1/3 was assigned if $PS_{eff} = PS_{inf}$; otherwise, class 2/4 was assigned. In the present study, PS_{eff} was assumed to occur only via passive diffusion and to be equal to $PS_{inf,pas}$ ($PS_{eff} = PS_{inf,pas}$). Adapted from Camenisch et al. (2015).

pravastatin, rosuvastatin, simvastatin acid, and verapamil were taken from Camenisch and Umehara (2012) and Kunze et al. (2015).

In brief, $PS_{inf,act}$ and $PS_{inf,pas}$ were determined in pooled suspended human hepatocytes using the oil-spin method. $PS_{inf,act}$ and $PS_{inf,pas}$ represent single time-point measurements within the linear time and concentration range, and $PS_{inf,pas}$ was determined in the presence of uptake transporter inhibitors or at high substrate concentrations where active transport processes are known to be saturated. Measured (apparent) uptake clearances were corrected for nonspecific binding to the assay device using radioactivity recoveries and for saturable binding to cell surfaces using data from control incubations at 4°C (Kunze et al., 2014). For the highly lipophilic compounds ketoconazole and atazanvir ($logD_{7.4} > 4$), PS_{inf} was determined from the slope of initial uptake velocity (3 time points between 0.5 and 3 minutes), taking into account initial cellular binding and nonspecific binding to the assay device.

PS_{eff} was assumed to occur only via passive diffusion and to be equal to $PS_{inf,pas}$ ($PS_{eff,act} = 0$, $PS_{eff,pas} = PS_{inf,pas}$).

Apparent metabolic clearance ($CL_{int,met,app}$) was determined using human liver microsomes. Incubations with all test compounds were performed in the presence of nicotinamide adenine dinucleotide phosphate (NADPH). The known uridine diphosphate (UDP) glucuronosyltransferase (substrates cerivastatin, fluvastatin, ibuprofen, pitavastatin, and simvastatin acid) were additionally incubated in the presence of UDP, and $CL_{int,met}$ represents the sum of NADPH and UDP incubations. $CL_{int,met,app}$ values were corrected for the unbound fraction in liver microsomes (fu_{mic}) as follows:

$$CL_{int,met} = \frac{CL_{int,met,app}}{fu_{mic}} \qquad (4)$$

Values for fu_{mic} and corresponding literature references are provided in Supplemental Table 1.

Apparent biliary clearance ($CL_{int,sec,app}$) was determined in sandwich-cultured human hepatocytes (B-CLEAR method; Qualyst, Inc., Durham, NC) and was corrected for the unbound fraction in hepatocytes (fu_{hep}) as given in eq. 5:

$$CL_{int,sec} = \frac{CL_{int,sec,app}}{fu_{hep}} \qquad (5)$$

Values of fu_{hep} were derived from $logD_{7.4}$ as follows (Yabe et al., 2011):

$$\log(fu_{hep}) = -0.9161 - 0.2567 \times logD_{7.4} \qquad (6)$$

Values for $logD_{7.4}$ and corresponding literature references are provided in Supplemental Table 1.

The in vitro clearances were up-scaled to human organ level (ml/min/kg) using the following scaling factors: 99 (10^6 cells/g liver) for suspended hepatocytes, 53 (mg protein/g liver) for human liver microsomes, 116 (mg protein/g liver) for sandwich-cultured hepatocytes, and 25.7 (g liver/kg body weight) for liver weight.

Calculation of Unbound Drug Concentrations in the Systemic Circulation, at the Hepatic Inlet, and in the Hepatocyte. Unbound drug concentrations in blood and plasma are equal (Kwon, 2001) and herein are referred to as unbound systemic drug concentrations ($C_{sys,u}$). $C_{sys,u}$ was calculated from the total maximum available drug plasma concentration (C_{max}) at steady state upon oral administration of the maximum recommended dose in healthy human subjects and the fraction unbound in plasma (fu_p):

$$C_{sys,u} = C_{max} \times fu_p \qquad (7)$$

According to eq. 8, unbound drug concentrations at the hepatic inlet ($C_{inlet,u}$) were calculated as the sum of drug in the systemic circulation reaching the liver via the hepatic artery (i.e., $C_{sys,u}$) and drug that is delivered by the portal vein upon intestinal absorption (Giacomini et al., 2010):

$$C_{inlet,u} = C_{sys,u} + \frac{fu_p \times k_a \times F_a \times F_g \times D}{Q_h \times R_b} \qquad (8)$$

where k_a is the absorption rate constant, F_a is the fraction absorbed, F_g is the fraction escaping gut metabolism, D is the maximum recommended single oral dose, Q_h is the hepatic blood flow (1.45 l/min), and R_b is the blood-to-plasma partition coefficient.

Additionally, maximum unbound hepatic inlet concentrations ($C_{inlet,max,u}$), representing a "worst-case," were calculated according to eq. 8 assuming complete and fast drug absorption (i.e., $F_a \times F_g = 1$ and $k_a = 0.1$ min^{-1}) (Ito et al., 1998).

Unbound intracellular drug concentrations in the hepatocyte [hereafter referred to as unbound intrahepatic concentration ($C_{hep,u}$)] were calculated on the basis of $C_{sys,u}$ (eq. 9), $C_{inlet,u}$ (eq. 10), or $C_{inlet,max,u}$ (eq. 11):

$$C_{hep,sys,u} = Kp_{uu} \times C_{sys,u} \qquad (9)$$
$$C_{hep,inlet,u} = Kp_{uu} \times C_{inlet,u} \qquad (10)$$
$$C_{hep,inlet,max,u} = Kp_{uu} \times C_{inlet,max,u} \qquad (11)$$

All clinical exposure data, pharmacokinetic parameters, and calculations thereof are provided in the Supplemental Material together with the corresponding literature references (Supplemental Tables 1–3).

Human BSEP IC$_{50}$ Values. In vitro IC$_{50}$ data for BSEP inhibition were collected from the literature. In the case of multiple reported values, the lowest one was used for risk assessments (Table 1), whereas Supplemental Table 4 shows the range of reported data. All data were determined under comparable conditions using membrane vesicles expressing human BSEP with [^{3}H]taurocholate as probe substrate.

Cholestasis Classification. Cholestasis annotation was carried out exclusively on the basis of clinical studies, drug labels, and a comprehensive literature search where cholestasis or mixed liver injury was observed under controlled conditions (i.e., declaration of comedication, underlying disease state, known dosing regimen). Drugs were categorized as "cholestatic" based on reports of one of the following adverse events: cholestasis, cholestatic liver injury, cholestatic jaundice, cholestatic hepatitis, mixed liver injury, or biochemical evidence of cholestasis or mixed liver injury in the form of elevated serum alkaline phosphatase (AP) [AP ≥ 2× upper limit of normal (ULN) and ratio between alanine aminotransferase ULN and AP ULN <5] (Council for International Organizations of Medical Sciences, 1999). Based on the reported cholestasis incidence, drugs were assigned to the subclasses "common" (>2% of subjects) or "rare" (≤2% of subjects). In the absence of the previously defined cholestasis events, drugs were categorized as "no cholestasis." The threshold of 2% was selected based on literature information from clinical reports or from the drug label, where rare adverse events were commonly defined as <2%. Detailed cholestasis annotations and literature references are summarized in Supplemental Table 4.

Data Analysis. The DIC risk was assessed based on safety margins, calculated as the ratio between BSEP IC$_{50}$ and the unbound intrahepatic drug concentration. Following the static R-value approach for reversible enzyme or transporter inhibition and using $C_{max,u}$ as the basis for unbound intrahepatic concentrations, the assessment represents a "worst-case" scenario for DIC (Rowland and Matin, 1973). Receiver operating characteristic (ROC) curve analysis (OriginPro 2016; OriginLab Corporation, Northampton, MA) was used to determine the optimal cut-off values (safety margin thresholds) between the three different cholestasis classes and to evaluate the accuracy with which cholestasis classes can be separated. ROC analysis calculates the sensitivity (fraction of true positive (TP) classifications) and specificity (fraction of true negative (TN) classifications) for any possible cut-off value and plots sensitivity against $1 -$ specificity, representing the ROC curve. The optimal cut-off values correspond to the maximum rate of correct positive and negative classifications and were determined by minimizing the distance (d) between point [0,1] in the ROC space (where sensitivity and specificity are maximum) and any point on the ROC curve (Kumar and Indrayan, 2011):

$$d^2 = (1-TP)^2 + (1-TN)^2 \qquad (12)$$

The separation of cholestasis classes by the estimated safety margin thresholds was compared using the area under the ROC curves (ROC AUCs), where 1.0 represents a perfect discrimination between two classes, and 0.5 represents the poorest discrimination.

Quantification of Physiologic and Genetic Factors. A theoretical assessment for the impact of disease state and polymorphic pathways on DIC was conducted using bosentan as an example drug compound. The impact of disease state on $C_{sys,u}$ concentrations was estimated based on literature observations that pulmonary arterial hypertension (PAH) patients show 2-fold increased systemic bosentan concentrations compared with healthy volunteers (Dingemanse and van Giersbergen, 2004). The resulting hepatic inlet and intrahepatic concentrations were calculated according to eqs. 8 and 10 using a $C_{sys,u}$ value of 0.1327 μM.

Riede et al.

TABLE 1

In vitro process clearances, in vitro Kp_{uu}, and human drug exposure

ECM classes were derived as described in Fig. 2. Unbound extracellular (systemic and hepatic inlet) and intrahepatic concentrations were calculated as described in *Materials and Methods*, and all required pharmacokinetic parameters and corresponding literature references are summarized in Supplemental Tables 1–3. Literature references for BSEP IC_{50} values are provided in Supplemental Table 4; presented data represent the lowest available IC_{50} value.

Drug Compounds	Hepatic Process Clearances				In Vitro Kp_{uu}	Unbound Extracellular Concentrations		Unbound Intrahepatic Concentrations		BSEP Inhibition
	$PS_{inf,act}$	$PS_{inf,pas}$ [a]	$CL_{int,met}$	$CL_{int,sec}$		$C_{sys,u}$	$C_{inlet,u}$	$C_{hep,sys,u}$	$C_{hep,inlet,u}$	IC_{50}
	ml/min/kg	ml/min/kg	ml/min/kg	ml/min/kg		μM	μM	μM	μM	μM
ECM class 1										
Ketoconazole	0.0	58.5	97.4	29.6	0.32	0.1661	0.2941	0.0532	0.0941	2.9
ECM class 2										
Imatinib	0.0	300.9	40.9	3.2	0.87	0.4781	1.1534	0.4159	1.0035	<10
Verapamil	0.0	258.2	127.7	8.1	0.66	0.0607	0.2398	0.0401	0.1583	20.5
ECM class 3										
Atazanavir	71.8	20.8	1240.5	81.9	0.07	1.1653	2.3500	0.0816	0.1645	3.1
Atorvastatin	140.3	57.7	64.6	11.1	1.48	0.0226	0.0819	0.0334	0.1212	15.0
Cyclosporine A	113.2	41.9	77.6	9.1	1.21	0.0512	0.1371	0.0620	0.1659	0.4
Erythromycin	10.2	20.3	99.7	8.9	0.24	1.0083	1.1334	0.2420	0.2720	4.1
Ibuprofen	22.2	21.7	34.2	10.3	0.66	3.9289	5.1880	2.5931	3.4241	598.6
Lovastatin acid	165.1	145.5	459.0	0	0.51	0.0050	0.0114	0.0026	0.0058	19.3
Rosiglitazone	45.6	46.6	98.1	0	0.64	0.0036	0.0048	0.0023	0.0031	1.9
Simvastatin acid	116.1	297.9	769.2	1.5	0.39	0.0008	0.0917	0.0003	0.0358	20.9
ECM class 4										
Bosentan (125 mg BID)	30.7	61.5	16.2	0.8	1.17	0.0663	0.0960	0.0776	0.1123	22.0
Bosentan (1000 mg BID)	30.7	61.5	16.2	0.8	1.17	0.4644	0.9312	0.5433	1.0895	22.0
Cerivastatin	221.5	243.8	46.9	0	1.60	0.0003	0.0005	0.0005	0.0008	18.8
Fluvastatin	218.7	325.5	146.8	0	1.15	0.0052	0.0133	0.0060	0.0153	36.1
Glibenclamide	66.4	109.6	41.1	6.3	1.12	0.0094	0.0133	0.0105	0.0149	1.5
Pitavastatin	364.3	258.8	17.7	0	2.25	0.0111	0.0392	0.0245	0.0882	42.2
Pravastatin	58.0	36.0	0.9	2.1	2.41	0.0716	0.7999	0.1726	1.9278	268.4
Rosuvastatin	27.2	24.8	1.5	5.8	1.62	0.0092	0.0670	0.0149	0.1085	197.6

BID, twice daily.
[a]In the present study, PS_{eff} was assumed to occur only via passive diffusion and to be equal to $PS_{inf,pas}$ ($PS_{eff} = PS_{inf,pas}$).

The effect of nonsynonymous polymorphisms of hepatic metabolic enzymes and transporters on the in vitro Kp_{uu} of bosentan was calculated according to eq. 13 using measured in vitro process clearances (Table 1), their fractional in vivo contribution (fn), and reported fold changes in activity compared with the reference genotype (α):

$$Kp_{uu} = \frac{\alpha_{OATP1B1} \times fn_{OATP1B1} \times PS_{inf,act} + \alpha_{OATP1B3} \times fn_{OATP1B3} \times PS_{inf,act} + PS_{inf,pas}}{PS_{eff} + \alpha_{CYP3A4} \times fn_{CYP3A4} \times CL_{int,met} + \alpha_{CYP2C9} \times fn_{CYP2C9} \times CL_{int,met} + \alpha_{MRP2} \times fn_{MRP2} \times CL_{int,sec}}$$

(13)

The α values used were determined from the following data. Increased activity was reported for the organic anion transporting polypeptide (OATP) variants OATP1B1*1b and OATP1B3*2 ($\alpha_{OATP1B1} = \alpha_{OATP1B3} = 2$) (Rowland and Matin, 1973; Letschert et al., 2004). The cytochrome P450 variants CYP3A4*20 and CYP2C9*3 are associated with loss of function ($\alpha_{CYP3A4} = \alpha_{CYP2C9} = 0$) (Lee et al., 2002; Werk and Cascorbi, 2014), similar to the multidrug resistance protein (MRP) 2 variant MRP2*16 (c.2302C>T) ($\alpha_{MRP2} = 0$) (Hulot et al., 2005; Pratt et al., 2015). According to the literature, OATP1B1 and OATP1B3 equally contribute to the total active hepatic uptake of bosentan ($fn_{OATP1B1} = fn_{OATP1B3} = 0.5$) (Treiber et al., 2007). Hepatic metabolism is mediated by CYP3A4 ($fn_{CYP3A4} = 0.6$) and CYP2C9 ($fn_{CYP2C9} = 0.4$) (Dingemanse and van Giersbergen, 2004), and biliary secretion is mediated by MRP2 ($fn_{MRP2} = 1.0$) (Fahrmayr et al., 2013).

To estimate the potential impact of BSEP polymorphisms on the DIC safety margin, reduced BSEP activity was assumed to mimic an increased inhibition potential, where 100% activity corresponds to the BSEP IC_{50} value of bosentan (22 μM). According to the literature, BSEP G855R (c.2563G>A) has <20% transport activity compared with nonpolymorphic BSEP (Lang et al., 2007), which was simulated using a 5-fold reduced BSEP IC_{50} value (4.4 μM).

Results

Kp_{uu} and ECM Class Assignment. In vitro measured hepatic process clearances for the 18 investigated drug compounds are summarized in Table 1 together with the resulting in vitro Kp_{uu} values,

which range from 0.07 to 2.41. Figure 3 displays the corresponding fold change in intrahepatic unbound drug concentrations ($C_{hep,u}$) calculated from extracellular concentrations and in vitro Kp_{uu}, where atazanavir and pravastatin represent the extremes with $\sim$14-fold decreased and $\sim$2.4-fold increased $C_{hep,u}$, respectively.

Compound classification according to ECM is based on the extent of individual hepatic in vitro clearance processes (Fig. 2). As hepatic clearance processes significantly impact intrahepatic concentrations, as illustrated in Figs. 2 and 3, ECM class-dependent effects on Kp_{uu} values can be expected. For the ECM class 1 compound ketoconazole, a Kp_{uu} value <1 was obtained as a result of a predominant intrinsic clearance contribution (i.e., $PS_{eff} + CL_{int} > PS_{inf}$). On the other hand, for ECM class 2 compounds imatinib and verapamil, Kp_{uu} was mainly determined by passive uptake and efflux processes and, consequently, approached values of 1 (i.e., $PS_{eff} + CL_{int} \approx PS_{inf}$). For the ECM class 3 compounds with predominant intrinsic clearance (atazanavir, erythromycin, ibuprofen, lovastatin acid, rosiglitazone, and simvastatin acid), Kp_{uu} values <1 were obtained (i.e., $PS_{eff} + CL_{int} > PS_{inf}$). The ECM class 3 compounds with substantial active hepatic uptake — namely, atorvastatin and cyclosporine A — exhibit Kp_{uu} values >1 (i.e., $PS_{eff} + CL_{int} < PS_{inf}$). Similarly, the ECM class 4 compounds bosentan, cerivastatin, fluvastatin, glibenclamide, pitavastatin, pravastatin, and rosuvastatin reveal Kp_{uu} values >1 due to predominant hepatic uptake (i.e., $PS_{eff} + CL_{int} < PS_{inf}$).

In Vitro–In Vivo Correlation of Kp_{uu} in Rat. Estimation of $C_{hep,u}$ using ECM-based in vitro Kp_{uu} data implies that the in vitro Kp_{uu} directly translates to in vivo Kp_{uu}. We made this assumption based on previous successful applications of the ECM approach for hepatic clearance and DDI predictions (Camenisch and Umehara, 2012; Umehara and Camenisch, 2012; Kunze et al., 2015). To further validate the ECM concept, we performed an IVIVC for Kp_{uu} in rat using
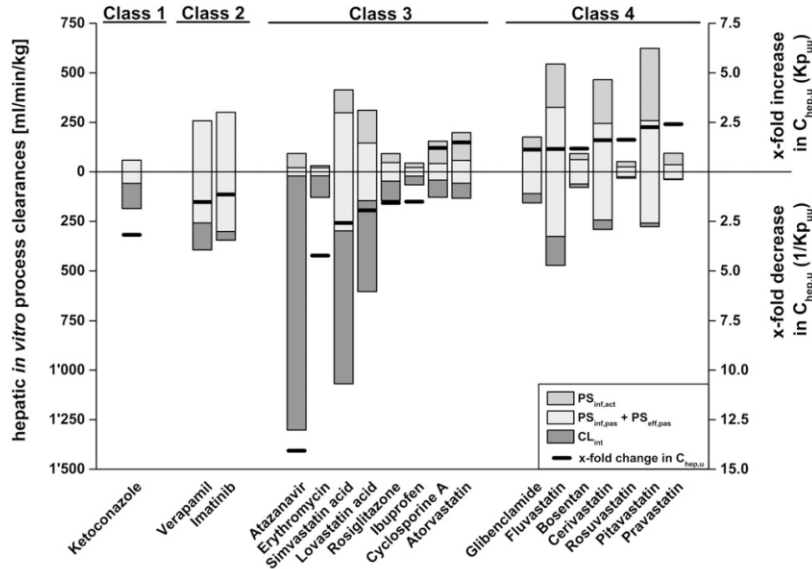
Fig. 3. ECM class-dependent impact of experimentally determined hepatic process clearances on Kp_{uu} and $C_{hep,u}$. The black lines represent the x-fold change of intrahepatic concentrations ($C_{hep,u}$) depending on Kp_{uu}. x-fold increase and decrease in $C_{hep,u}$ correspond to Kp_{uu} and $1/Kp_{uu}$, respectively. Gray, white, and dark-gray bars represent the underlying process clearances (active uptake, sum of passive uptake and efflux, and intrinsic clearance, respectively), which affect Kp_{uu}, as described in Fig. 2. Hepatic process clearances refer to the left y-axis, whereas changes in $C_{hep,u}$ refer to the right y-axis.

published in-house data (Umehara and Camenisch, 2012) (Fig. 4). In addition, IVIVC of reported in vitro Kp_{uu} values from initial rate hepatic uptake clearances in suspended hepatocytes (Yabe et al., 2011; Shitara et al., 2013) and from sandwich-cultured hepatocytes (Pfeifer et al., 2013) is shown in Fig. 4. Observed (in vivo) and predicted (in vitro) Kp_{uu} data following the ECM concept were in good agreement, with all five compounds deviating by less than 2.5-fold. Also, Kp_{uu} from rat sandwich-cultured hepatocytes demonstrated close IVIVC for three compounds. In contrast, in vitro Kp_{uu} from suspended hepatocytes generally provided overestimations of in vivo Kp_{uu}, most likely due to the absence of intrinsic clearance processes (metabolism and biliary secretion).

For atorvastatin, cyclosporine A, and verapamil, different ECM classes were assigned for rat and human due to different contributions of the individual clearance processes. The impact of in vitro and in vivo Kp_{uu} values in rats, however, was in line with the ECM theory described earlier (ECM class 1: $Kp_{uu} < 1$; ECM class 4: $Kp_{uu} > 1$).

Correlation between BSEP Inhibition, Drug Concentrations, and Drug-Induced Cholestasis. The assignments of the 18 test drug compounds into the three cholestasis frequency classes ("no," "rare," "common") are shown in Table 2. Risk assessments with regard to DIC were conducted using safety margins calculated as the ratio of BSEP IC_{50} and either unbound extracellular drug concentrations ($C_{sys,u}$ or $C_{inlet,u}$) or unbound intrahepatic concentrations upon application of Kp_{uu} ($C_{hep,sys,u}$ or $C_{hep,inlet,u}$) (Fig. 5). The risk assessment with unbound systemic concentrations showed a separation between drugs in cholestasis classes "common" and "no cholestasis," whereas drugs in the class "rare" markedly overlapped with drugs in the other classes (Fig. 5A). The separation of drugs in cholestasis class "rare" from "common" or "no cholestasis" was not improved by using the substantially higher unbound drug concentrations at the hepatic inlet (Fig. 5B). This incomplete separation of the cholestasis classes based on extracellular concentrations is reflected by ROC AUC values of 0.83–0.94. In contrast, the use of unbound intrahepatic drug concentrations following Kp_{uu} correction markedly enhanced the separation between the three cholestasis classes. The risk assessment based on $C_{hep,sys,u}$ provided a good separation between the three classes, with only one drug

(rosiglitazone, class "no") being clearly mispredicted (Fig. 5C). The risk assessment was further improved by using Kp_{uu}-corrected unbound hepatic inlet concentrations. Using this reference concentration, an almost complete separation of all drugs into classes "no," "rare," and "common" was achieved (Fig. 5D), as supported by ROC AUC values ≥0.97. Using $C_{hep,inlet,u}$ as a reference, safety margin thresholds
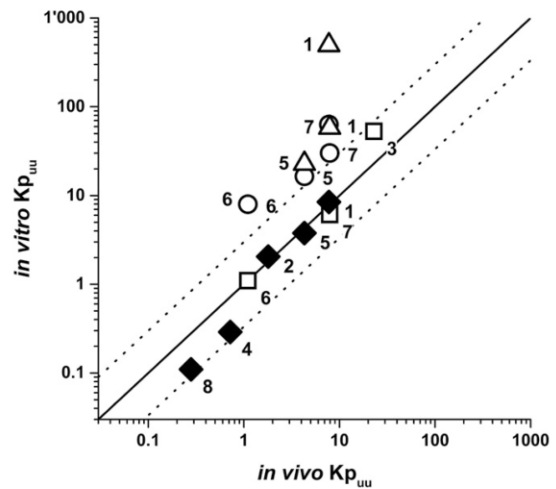
Fig. 4. In vitro–in vivo correlation of hepatic Kp_{uu} in rat. Rat in vitro Kp_{uu} values were calculated according to ECM (eqs. 1 and 3) using published in-house in vitro hepatic process clearance data or were taken from the literature. Rat in vivo Kp_{uu} values were derived from reported liver partition and drug-binding data. Detailed calculations of Kp_{uu} and literature references are summarized in Supplemental Table 5. Black diamonds refer to ECM-based Kp_{uu} (in-house data); white squares, triangles, and circles represent in vitro Kp_{uu} obtained by Pfeifer et al. (2013), Yabe et al. (2011), and Shitara et al. (2013), respectively. The solid line is the line of unity and dotted lines are 3-fold deviations. Numbers represent the investigated drugs: 1, atorvastatin; 2, cyclosporine A; 3, furamidine; 4, ketoconazole; 5, pravastatin; 6, ritonavir; 7, rosuvastatin; 8, verapamil.

528   Riede et al.

TABLE 2

Cholestasis classification

Cholestasis Class	Drug Compounds
Common (>2%)	Bosentan (1000 mg BID), cyclosporine A, erythromycin, imatinib
Rare (≤2%)	Atazanavir, atorvastatin, bosentan (125 mg BID), glibenclamide, ibuprofen, ketoconazole, pitavastatin, pravastatin, verapamil
No cholestasis	Cerivastatin, fluvastatin, lovastatin acid, rosiglitazone, rosuvastatin, simvastatin acid

Bosentan was assigned to the classes "common" and "rare" depending on the administered dose [1000 and 125 mg twice daily (BID), respectively]. Literature references and detailed annotations are summarized in Supplemental Table 4.

between classes "common"/"rare" and "rare"/"no" of 26 and 529, respectively, were obtained (Fig. 5D). These thresholds are clearly lower than those obtained from risk assessments using unbound extracellular concentrations (Fig. 5, A and B; "common"/"rare": 100 and 59, "rare"/

"no": 3821 and 728 for $C_{sys,u}$ and $C_{inlet,u}$, respectively). Using $C_{hep,inlet,u}$, the safety margin of simvastatin was reduced to 584-fold compared with 69,667-fold based on $C_{hep,sys,u}$, representing the largest safety margin change within our test set.

Additionally, maximum (worst-case) unbound hepatic inlet concentrations ($C_{inlet,max,u}$) were calculated to represent the situation during early drug development, where no clinical data are available. Assuming fast and complete intestinal absorption, substantially higher unbound intrahepatic concentrations were obtained compared to using measured clinical parameters. Whereas the resulting ratios still allowed separation of "common" from "rare" cholestasis events, the separation between "no" and "rare" was poorer than that obtained in risk assessments based on measured clinical parameters (Fig. 5D vs. Fig. 5E).

Quantification of Risk Factors for DIC. The theoretical impact of disease state and polymorphic hepatic enzymes and transporters on bosentan-induced cholestasis was estimated based on clinical systemic exposure and in vitro enzyme and transporter polymorphism data (Fig. 6). The systemic exposure of bosentan is reported to be ~2-fold higher in
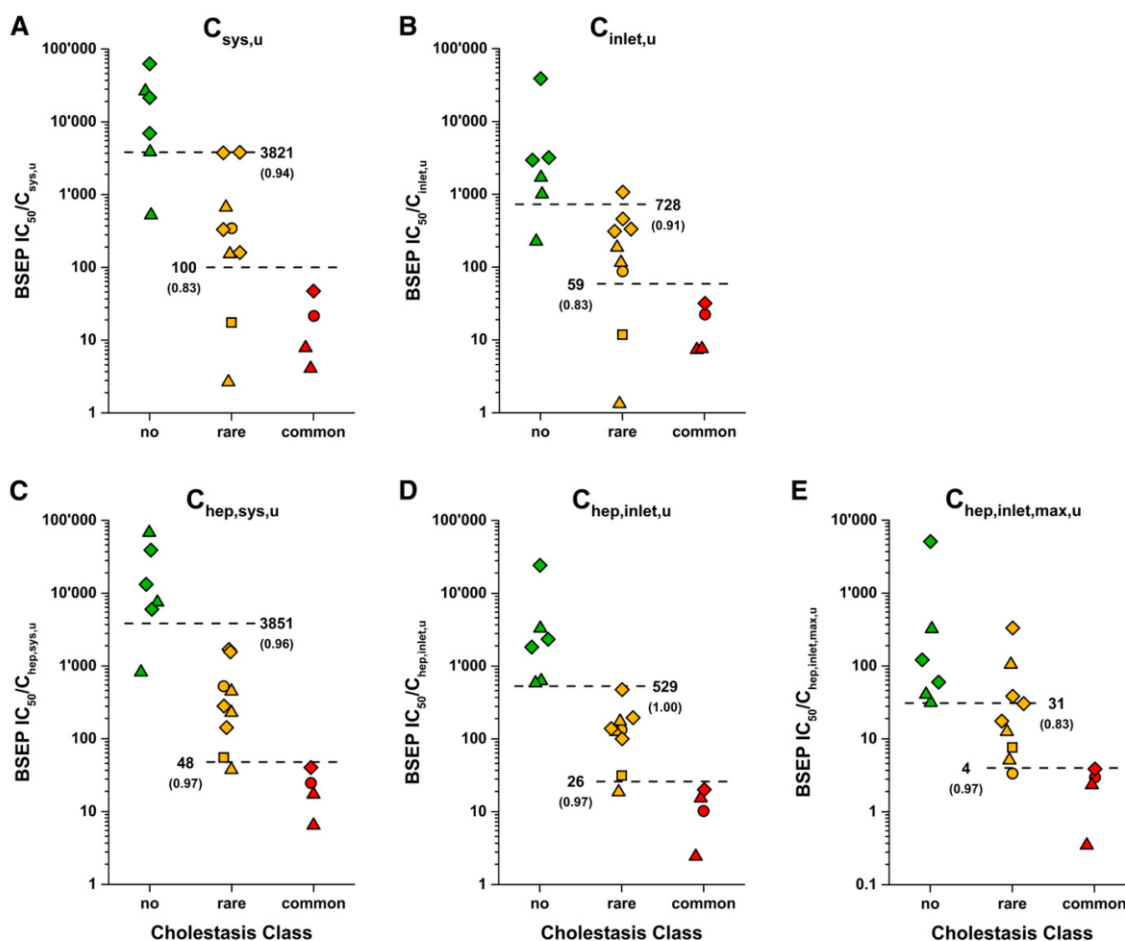
Fig. 5. Correlation between BSEP inhibition, drug concentration, and drug-induced cholestasis. Safety margins for all 18 drug compounds representing the ratio of BSEP IC_{50} value and unbound systemic concentration ($C_{sys,u}$) (A), unbound concentration at the hepatic inlet ($C_{inlet,u}$) (B), unbound intrahepatic concentration on basis of $C_{sys,u}$ ($C_{hep,sys,u}$) (C), unbound intrahepatic concentration on basis of $C_{inlet,u}$ ($C_{hep,inlet,u}$) (D), and worst-case assessment of maximum unbound intrahepatic concentration ($C_{hep,inlet,max,u}$) (E). Red, yellow, and green symbols represent the cholestasis classes "common," "rare," and "no cholestasis," respectively. Squares, circles, triangles, and diamonds represent the ECM classes 1, 2, 3, and 4, respectively. Estimated safety margin thresholds between the cholestasis classes "common"/"rare" and "rare"/"no cholestasis" are shown next to dashed lines with ROC AUCs in brackets.

PAH patients compared with healthy subjects (Dingemanse and van Giersbergen, 2004). Based on this, we calculated the corresponding $C_{hep,inlet,u}$ in PAH patients (0.1901 μM), which is 69% higher than in healthy subjects (Fig. 6, healthy vs. PAH patients). Next, we calculated Kp_{uu}, $C_{hep,inlet,u}$, and corresponding safety margins for bosentan using altered transporter and enzyme activities due to genetic polymorphisms according to eq. 13. Our assessment indicates that the increased transport activity of OATP1B1*1b or OATP1B3*2 variants would increase Kp_{uu} and $C_{hep,inlet,u}$ by 17% (Fig. 6, "PAH patients" vs. "OATP1B1*1b" or "OATP1B3*2"). Loss-of-function mutations in CYP3A4, CYP2C9, and MRP2 would result in increases in both Kp_{uu} and $C_{hep,inlet,u}$ by 14, 9, and 1%, respectively (Fig. 6, "PAH patients" vs. "CYP3A4*20", "CYP2C9*3", or "MRP2*16"). The assumption of concurrence of all these genetic variants leads to predicted increases of Kp_{uu} and $C_{hep,inlet,u}$ by 70% and a reduction of the safety margin from 116 to 68 (Fig. 6, "PAH patients" vs. "CYP3A4*20, CYP2C9*3, MRP2*16, OATP1B1*1b, OATP1B3*2"). Additionally, we evaluated the potential impact of BSEP polymorphisms on the DIC risk assessment. Presence of the low-activity variant BSEP G885R was simulated using a 5-fold reduced BSEP IC$_{50}$ value (4.4 μM). This estimation leads to a 23-fold safety margin (Fig. 6, "PAH patients" vs. "BSEP G885R"). The theoretical combination of the BSEP G885R variant with genetic variants that affect the Kp_{uu} of bosentan would further increase the DIC risk, as shown in Fig. 6 ("PAH patients" vs. "BSEP G885R, CYP3A4*20, CYP2C9*3, MRP2*16, OATP1B1*1b, OATP1B3*2").

Discussion

In the present work, we compare the use of unbound extracellular (systemic and hepatic inlet) or Kp_{uu}–based intrahepatic concentrations in risk assessments of cholestasis upon BSEP inhibition.

Our work follows up on recent studies, which investigated the impact of systemic drug exposure on the clinical manifestation of DIC or DILI. Using safety margin ratios of BSEP IC$_{50}$ to systemic drug concentration, our analyses revealed a generally increased risk of DIC among drugs

with lower safety margins (Fig. 5A). However, no reliable separation of cholestatic and non-cholestatic drugs was obtained from this assessment. The outcome was not improved when hepatic inlet concentrations were used for safety margin calculations (Fig. 5B), even though this concentration is considered most relevant with regard to inhibition of hepatic enzymes or transporters (Zamek-Gliszczynski et al., 2013). These observations based on extracellular concentrations are in line with previous studies using similar approaches (Dawson et al., 2012; Morgan et al., 2013; Shah et al., 2015). However, several differences from previous work are important to highlight. First, following the "free drug hypothesis," we used only unbound drug concentrations rather than total drug concentrations. Indeed, we obtained poorer predictions of DIC using total drug concentrations in plasma or blood (data not shown). Second, we evaluated the association of BSEP inhibition with DIC only and not with other types of liver toxicity. Hepatocellular DILI cases, which are included in other studies, are rather caused by direct toxicity or immune-mediated reactions (Chen et al., 2015) and are likely not explained by BSEP inhibition. Third, we classified the investigated drugs according to the DIC incidence instead of a commonly used DILI severity grading (Chen et al., 2011; Pedersen et al., 2013; Aleo et al., 2014). Fourth, the present assessment represents a worst-case scenario using the lowest reported in vitro BSEP IC$_{50}$ (variability in IC$_{50}$ values was within a 3-fold range for the majority of dugs with the exception of cyclosporine A, erythromycin, glibenclamide, and rosiglitazone) and the maximum reported systemic drug concentration at steady state after administration of the highest recommended oral dose. At least for certain drugs (e.g., $C_{sys,u}$ of atorvastatin and rosiglitazone), our parameters significantly deviate from previous studies (Dawson et al., 2012; Morgan et al., 2013; Shah et al., 2015).

However, relating extracellular drug concentrations to inhibition of an intracellular liver target (BSEP) is not expected to provide meaningful risk estimations if intracellular drug concentrations are affected by active transport or metabolic processes (Dawson et al., 2012; Chu et al., 2013; Camenisch et al., 2015; Camenisch, 2016). Indeed, applying the in vitro Kp_{uu} values to obtain unbound intrahepatic drug concentrations markedly improved the separation of cholestasis classes. This became particularly evident for the correlation with unbound intrahepatic concentrations based on hepatic inlet concentrations, where almost complete separation between the different cholestasis classes was obtained (Fig. 5D). The use of hepatic inlet concentrations is most important for drugs with high hepatic first-pass elimination and significantly reduced systemic concentrations, as observed for simvastatin (115-fold difference between $C_{sys,u}$ and $C_{inlet,u}$). We therefore conclude that the unbound intrahepatic drug concentration based on hepatic inlet concentrations clearly represents the most reliable reference concentration for prediction of the DIC risk using BSEP inhibition assays.

BSEP in vitro inhibition data are commonly generated in early drug development. However, at this stage, clinical drug exposure data are rarely available, and DIC risk assessments based on the presented approach are not possible. We therefore performed an alternative risk assessment assuming that the clinical systemic exposure can be accurately predicted and assuming complete and rapid absorption to obtain worst-case hepatic inlet concentrations (Fig. 5E) (Ito et al., 1998; Giacomini et al., 2010). While the cholestasis classes "common" and "rare" were reasonably well separated by this approach, the separation between classes "no cholestasis" and "rare" failed compared with risk approaches using measured clinical input parameters (Fig. 5D vs. Fig. 5E). Therefore, for DIC risk assessments during preclinical development, we suggest applying unbound intrahepatic drug concentrations derived from in vitro Kp_{uu} and predicted systemic exposure (e.g., using physiologically based pharmacokinetic modeling).

Kp_{uu} and corresponding unbound intrahepatic drug concentrations are affected by the individual contributions of active hepatic transport and
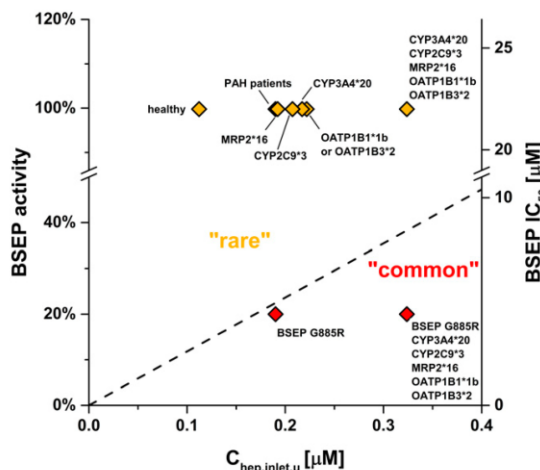
Fig. 6. Theoretical impact of polymorphic hepatic enzymes and transporters on DIC safety margins for bosentan. $C_{hep,inlet,u}$ of bosentan (125 mg twice daily) in PAH patients in various enzyme/transporter polymorphism scenarios was calculated from extracellular $C_{inlet,u}$ and in vitro Kp_{uu} using in vitro activity data (eq. 13). Contributions of transporters and cytochrome P450 enzymes to the hepatic bosentan clearance as well as functional impact of polymorphisms are described in *Materials and Methods*. The dashed line represents the safety margin threshold between the cholestasis classes "common"/"rare" (26-fold).

metabolic processes and correlate well with the four ECM classes (Figs. 2 and 3). For drugs in ECM classes 1 and 3, where hepatic uptake is the rate-limiting elimination step, Kp_{uu} is likely to be below 1 ($C_{hep,u} < C_u$). On the other hand, class 3 drugs can also approach Kp_{uu} above 1 if active hepatic uptake is extensive ($C_{hep,u} > C_u$). As illustrated in Fig. 7, unbound extracellular concentrations of ketoconazole and simvastatin acid markedly overestimated the DIC risk. Use of Kp_{uu}-corrected unbound intrahepatic concentrations shifted ketoconazole (Kp_{uu} = 0.32) and simvastatin acid (Kp_{uu} = 0.39) into their appropriate risk zones ("rare" and "no" cholestasis, respectively). For class 4 drugs, passive uptake/efflux permeability exceeds intrinsic hepatic clearance. In combination with active hepatic uptake processes, drugs accumulate within the hepatocytes, resulting in Kp_{uu} values greater 1 (Figs. 2 and 3). For these drugs, the DIC risk is underestimated by unbound extracellular concentrations, as highlighted for pitavastatin in Fig. 7. After correction with Kp_{uu}, pitavastatin was assigned to the correct risk zone ("rare"). Only for class 2 drugs, such as imatinib, do unbound extracellular concentrations represent an appropriate surrogate for the unbound intrahepatic concentration ($Kp_{uu} \approx 1.0$, $C_{hep,u} \approx C_u$) (Fig. 7).

For the in vitro Kp_{uu} assessment, we generally assumed absence of active sinusoidal efflux. Kp_{uu} values of substrates for basolateral MRP3 and MRP4, which have been shown to be upregulated in human and rat under cholestatic conditions (Soroka et al., 2001; Gradhand et al., 2008), might therefore be overpredicted. However, except for rosuvastatin, the relevance of MRP3 and MRP4 in transport of pharmaceutical drugs is unknown and requires further research. In addition, we assumed that the ECM-based in vitro Kp_{uu} directly translates to in vivo Kp_{uu}. The assumption was based on the good IVIVC for Kp_{uu} in rat (Fig. 4) and on previous hepatic clearance predictions using the ECM, where no systematic underprediction of in vivo hepatic clearance was observed. Similarly, in vitro Kp_{uu} using sandwich-cultured hepatocytes recently provided a close IVIVC in rats for rosuvastatin, ritonavir, and furamidine (Pfeifer et al., 2013), whereas Kp_{uu} from suspended hepatocytes generally overpredicted Kp_{uu} in vivo, likely due to the absence of intrinsic clearance processes. Partial loss of activity in certain in vitro systems has previously been described (Lundquist et al., 2014); however, the need of scaling factors for pharmacokinetic modeling is controversially discussed and likely compound-dependent, requiring clinical data (Jones et al., 2012; Morse et al., 2015; Yoshikado et al., 2016). Especially in an early drug development stage, the direct use of in vitro Kp_{uu} is therefore expected to enable estimations of unbound intrahepatic drug concentrations.

Our risk assessment using unbound hepatic inlet concentrations predicted a DIC risk in more than 2% of subjects for safety margins below ~25 (Fig. 5D). Since unbound intrahepatic concentrations are 25-fold below the IC_{50} of BSEP, no relevant inhibition of BSEP would be expected. However, the occurrence of DIC in a low percentage of patients leads us to the hypothesis that these subjects react more sensitively to BSEP inhibition than the rest of the population. This variability might be explained by various physiologic (e.g., age, gender, underlying diseases), exogenous (e.g., comedication, nutrition), and genetic factors (polymorphisms) that potentially modify intrahepatic drug concentrations or BSEP activity, resulting in increased cholestasis risk. Using bosentan as an example, we evaluated the theoretical impact of disease state and polymorphic hepatic enzymes and transporters on DIC risk (Fig. 6). Physiologic factors, such as increased age and gender, are not associated with altered risk of bosentan-induced cholestasis (Markova et al., 2013). Similarly, increased systemic bosentan exposure in PAH patients could not be linked to higher incidence of liver injury (Dingemanse and van Giersbergen, 2004), which is in line with our assessment (Fig. 6). The present analysis suggests that genetic variants of transporters and enzymes involved in bosentan elimination only marginally affect the DIC risk assessment, even upon the unlikely
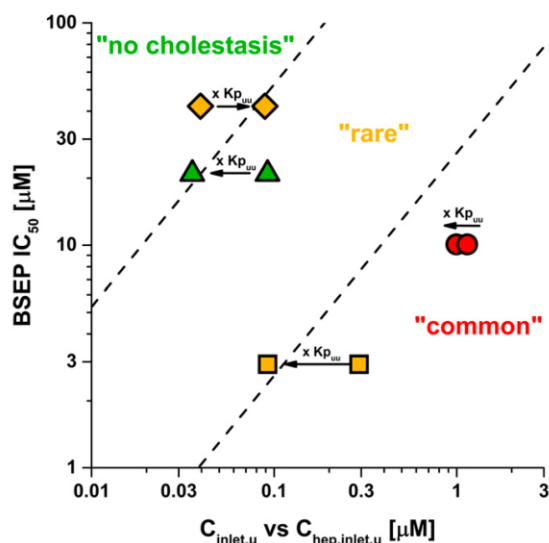

Fig. 7. ECM class-dependent effect of Kp_{uu} on the DIC risk assessment. BSEP IC_{50} values were plotted against unbound hepatic inlet concentrations before ($C_{inlet,u}$) and after correction with in vitro Kp_{uu} to unbound intrahepatic concentrations ($C_{hep,inlet,u}$). Ketoconazole (class 1), imatinib (class 2), simvastatin acid (class 3), and pitavastatin are shown as yellow squares, red circles, green triangles, and yellow diamonds, respectively. Red, yellow, and green symbols represent the cholestasis classes "common", "rare," and "no cholestasis," respectively. Dashed lines represent the safety margin thresholds between cholestasis classes "common"/"rare" (26-fold) and "rare"/"no" (529-fold), respectively.

concurrence of all polymorphisms (Fig. 6). Indeed, bosentan-induced liver injury could not be associated with polymorphic variants of OATP1B1, OATP1B3, CYP2C9, or MRP2 (Markova et al., 2013, 2014; Roustit et al., 2014). In addition, we evaluated the impact of the BSEP variant G885R, which was recently associated with DIC, likely due to substantially reduced activity (<20%) (Lang et al., 2007). Based on these data, we estimated a significantly increased risk of bosentan-induced cholestasis in PAH patients carrying the G885R variant, as indicated by a 23-fold safety margin and the change in cholestasis class from "rare" to "common" (Fig. 6). In summary, the presented risk assessment for bosentan illustrates the utility of ECM-based Kp_{uu} assessments to define the relevance of polymorphic enzymes and transporters in the hepatic elimination of a drug. Especially for drugs with high risk of DIC, such information could guide the selection of genotyping targets in clinics and ultimately allow personalized dosing regimens. However, further research on frequency, global distribution, and in vivo effects of polymorphisms will be required to estimate the incidence of DIC in heterogenic populations.

In conclusion, we demonstrated that the incidence of DIC upon BSEP inhibition correlates with Kp_{uu}-based unbound intrahepatic drug concentrations. To the best of our knowledge, this approach represents the most reliable prediction of DIC available so far, which also allows to account for polymorphisms on hepatic enzymes and transporters associated with DIC risk. Our study represents a proof-of-concept for estimating the inhibition potential of an intracellular transporter and is therefore expected to likewise improve risk assessments for other intrahepatic targets involved in DDI, pharmacologic efficacy, and toxicology, such as hyperbilirubinemia upon MRP2 or UGT1A1 inhibition. The validation of ECM-based risk assessments for other target enzymes or transporters as well as the extension of the approach to other organs, such as the kidney, will require extensive future research.

Unbound Intrahepatic Drug Concentrations Predict Cholestasis   531

References

Aleo MD, Luo Y, Swiss R, Bonin PD, Potter DM, and Will Y (2014) Human drug-induced liver injury severity is highly associated with dual inhibition of liver mitochondrial function and bile salt export pump. *Hepatology* **60**:1015–1022.
Björnsson E and Olsson R (2005) Outcome and prognostic markers in severe drug-induced liver disease. *Hepatology* **42**:481–489.
Camenisch GP (2016) Drug Disposition Classification Systems in Discovery and Development: A Comparative Review of the BDDCS, ECCS and ECCCS Concepts. *Pharm Res* **33**: 2583–2593.
Camenisch G, Riede J, Kunze A, Huwyler J, Poller B, and Umehara K (2015) The extended clearance model and its use for the interpretation of hepatobiliary elimination data. *ADMET DMPK* **3**:1–14.
Camenisch G and Umehara K (2012) Predicting human hepatic clearance from in vitro drug metabolism and transport data: a scientific and pharmaceutical perspective for assessing drug-drug interactions. *Biopharm Drug Dispos* **33**:179–194.
Chen M, Suzuki A, Borlak J, Andrade RJ, and Lucena MI (2015) Drug-induced liver injury: Interactions between drug properties and host factors. *J Hepatol* **63**:503–514.
Chen M, Vijay V, Shi Q, Liu Z, Fang H, and Tong W (2011) FDA-approved drug labeling for the study of drug-induced liver injury. *Drug Discov Today* **16**:697–703.
Chu X, Korzekwa K, Elsby R, Fenner K, Galetin A, Lai Y, Matsson P, Moss A, Nagar S, Rosania GR, et al.; International Transporter Consortium (2013) Intracellular drug concentrations and transporters: measurement, modeling, and implications for the liver. *Clin Pharmacol Ther* **94**: 126–141.
Council for International Organizations of Medical Sciences (1999) Reporting Adverse Drug Reactions: Definitions of Terms and Criteria for their Use, Geneva, Switzerland.
Dawson S, Stahl S, Paul N, Barber J, and Kenna JG (2012) In vitro inhibition of the bile salt export pump correlates with risk of cholestatic drug-induced liver injury in humans. *Drug Metab Dispos* **40**:130–138.
Dietrich CG and Geier A (2014) Effect of drug transporter pharmacogenetics on cholestasis. *Expert Opin Drug Metab Toxicol* **10**:1533–1551.
Dingemanse J and van Giersbergen PL (2004) Clinical pharmacology of bosentan, a dual endo-thelin receptor antagonist. *Clin Pharmacokinet* **43**:1089–1115.
Fahrmayr C, König J, Auge D, Mieth M, Münch K, Segrestaa J, Pfeifer T, Treiber A, and Fromm M (2013) Phase I and II metabolism and MRP2-mediated export of bosentan in a MDCKII-OATP1B1-CYP3A4-UGT1A1-MRP2 quadruple-transfected cell line. *Br J Pharmacol* **169**: 21–33.
Fattinger K, Funk C, Pantze M, Weber C, Reichen J, Stieger B, and Meier PJ (2001) The endo-thelin antagonist bosentan inhibits the canalicular bile salt export pump: a potential mechanism for hepatic adverse reactions. *Clin Pharmacol Ther* **69**:223–231.
Food and Drug Administration (2009) Guidance for Industry. Drug-Induced Liver Injury: Premarketing Clinical Evaluation, Silver Spring, MD.
Funk C, Pantze M, Jehle L, Ponelle C, Scheuermann G, Lazendic M, and Gasser R (2001) Troglitazone-induced intrahepatic cholestasis by an interference with the hepatobiliary export of bile acids in male and female rats. Correlation with the gender difference in troglitazone sulfate formation and the inhibition of the canalicular bile salt export pump (Bsep) by troglitazone and troglitazone sulfate. *Toxicology* **167**:83–98.
Giacomini KM, Huang SM, Tweedie DJ, Benet LZ, Brouwer KL, Chu X, Dahlin A, Evers R, Fischer V, Hillgren KM, et al.; International Transporter Consortium (2010) Membrane transporters in drug development. *Nat Rev Drug Discov* **9**:215–236.
Gradhand U, Lang T, Schaeffeler E, Glaeser H, Tegude H, Klein K, Fritz P, Jedlitschky G, Kroemer HK, Bachmakov I, et al. (2008) Variability in human hepatic MRP4 expression: influence of cholestasis and genotype. *Pharmacogenomics J* **8**:42–52.
Hulot JS, Villard E, Maguy A, Morel V, Mir L, Tostivint I, William-Faltaos D, Fernandez C, Hatem S, Deray G, et al. (2005) A mutation in the drug transporter gene ABCC2 associated with impaired methotrexate elimination. *Pharmacogenet Genomics* **15**:277–285.
Hussaini SH and Farrington EA (2007) Idiosyncratic drug-induced liver injury: an overview. *Expert Opin Drug Saf* **6**:673–684.
Ito T, Iwatsubo T, Kanamitsu S, Ueda K, Suzuki H, and Sugiyama Y (1998) Prediction of pharmacokinetic alterations caused by drug-drug interactions: metabolic interaction in the liver. *Pharmacol Rev* **50**:387–412.
Jones HM, Barton HA, Lai Y, Bi YA, Kimoto E, Kempshall S, Tate SC, El-Kattan A, Houston JB, Galetin A, et al. (2012) Mechanistic pharmacokinetic modeling for the prediction of transporter-mediated disposition in humans from sandwich culture human hepatocyte data. *Drug Metab Dispos* **40**:1007–1017.
Kumar R and Indrayan A (2011) Receiver operating characteristic (ROC) curve for medical researchers. *Indian Pediatr* **48**:277–287.
Kunze A, Huwyler J, Camenisch G, and Poller B (2014) Prediction of organic anion-transporting polypeptide 1B1- and 1B3-mediated hepatic uptake of statins based on transporter protein expression and activity data. *Drug Metab Dispos* **42**:1514–1521.

Kunze A, Poller B, Huwyler J, and Camenisch G (2015) Application of the extended clearance concept classification system (ECCCS) to predict the victim drug-drug interaction potential of statins. *Drug Metab Pers Ther* **30**:175–188.
Kwon Y (2001) *Handbook of Essential Pharmacokinetics, Pharmacodynamics, and Drug Metabolism for Industrial Scientists*, Kluwer Academic/Plenum Publishers, New York.
Lang C, Meier Y, Stieger B, Beuers U, Lang T, Kerb R, Kullak-Ublick GA, Meier PJ, and Pauli-Magnus C (2007) Mutations and polymorphisms in the bile salt export pump and the multidrug resistance protein 3 associated with drug-induced liver injury. *Pharmacogenet Genomics* **17**:47–60.
Lee CR, Goldstein JA, and Pieper JA (2002) Cytochrome P450 2C9 polymorphisms: a comprehensive review of the in-vitro and human data. *Pharmacogenetics* **12**:251–263.
Lee WM (2003) Drug-induced hepatotoxicity. *N Engl J Med* **349**:474–485.
Letschert K, Keppler D, and König J (2004) Mutations in the SLCO1B3 gene affecting the substrate specificity of the hepatocellular uptake transporter OATP1B3 (OATP8). *Pharmacogenetics* **14**:441–452.
Lundquist P, Lööf J, Sohlenius-Sternbeck AK, Floby E, Johansson J, Bylund J, Hoogstraate J, Afzelius L, and Andersson TB (2014) The impact of solute carrier (SLC) drug uptake transporter loss in human and rat cryopreserved hepatocytes on clearance predictions. *Drug Metab Dispos* **42**:469–480.
Markova SM, De Marco T, Bendjilali N, Kobashigawa EA, Mefford J, Sodhi J, Le H, Zhang C, Halladay J, Rettie AE, et al. (2013) Association of CYP2C9*2 with bosentan-induced liver injury. *Clin Pharmacol Ther* **94**:678–686.
Markova SM, Schwartz JB, and Kroetz DL (2014) Response to "CYP2C9 polymorphism is not a major determinant of bosentan exposure in healthy volunteers". *Clin Pharmacol Ther* **95**:252.
Mateus A, Matsson P, and Artursson P (2013) Rapid measurement of intracellular unbound drug concentrations. *Mol Pharm* **10**:2467–2478.
Morgan RE, van Staden CJ, Chen Y, Kalyanaraman N, Kalanzi J, Dunn RT 2nd, Afshari CA, and Hamadeh HK (2013) A multifactorial approach to hepatobiliary transporter assessment enables improved therapeutic compound development. *Toxicol Sci* **136**:216–241.
Morse BL, Cai H, MacGuire JG, Fox M, Zhang L, Zhang Y, Gu X, Shen H, Dierks EA, Su H, et al. (2015) Rosuvastatin liver partitioning in cynomolgus monkeys: measurement in vivo and prediction using in vitro monkey hepatocyte uptake. *Drug Metab Dispos* **43**:1788–1794.
Muller PY and Milton MN (2012) The determination and interpretation of the therapeutic index in drug development. *Nat Rev Drug Discov* **11**:751–761.
Nicolaï J, De Bruyn T, Van Veldhoven PP, Keemink J, Augustijns P, and Annaert P (2015) Verapamil hepatic clearance in four preclinical rat models: towards activity-based scaling. *Biopharm Drug Dispos* **36**:462–480.
Olson H, Betton G, Robinson D, Thomas K, Monro A, Kolaja G, Lilly P, Sanders J, Sipes G, Bracken W, et al. (2000) Concordance of the toxicity of pharmaceuticals in humans and in animals. *Regul Toxicol Pharmacol* **32**:56–67.
Pauli-Magnus C, Meier PJ, and Stieger B (2010) Genetic determinants of drug-induced cholestasis and intrahepatic cholestasis of pregnancy. *Semin Liver Dis* **30**:147–159.
Pedersen JM, Matsson P, Bergström CA, Hoogstraate J, Norén A, LeCluyse EL, and Artursson P (2013) Early identification of clinically relevant drug interactions with the human bile salt export pump (BSEP/ABCB11). *Toxicol Sci* **136**:328–343.
Pfeifer ND, Harris KB, Yan GZ, and Brouwer KL (2013) Determination of intracellular unbound concentrations and subcellular localization of drugs in rat sandwich-cultured hepatocytes compared with liver tissue. *Drug Metab Dispos* **41**:1949–1956.
Pratt VM, Beyer BN, Koller DL, Skaar TC, Flockhart DA, Levy KD, and Vance GH (2015) Report of new haplotype for ABCC2 gene: rs17222723 and rs8187718 in cis. *J Mol Diagn* **17**:201–205.
Roustit M, Fonrose X, Montani D, Girerd B, Stanke-Labesque F, Gonnet N, Humbert M, and Cracowski JL (2014) CYP2C9, SLCO1B1, SLCO1B3, and ABCB11 polymorphisms in patients with bosentan-induced liver toxicity. *Clin Pharmacol Ther* **95**:583–585.
Rowland M and Matin SB (1973) Kinetics of drug-drug interactions. *J Pharmacokinet Biopharm* **1**: 553–567.
Shah F, Leung L, Barton HA, Will Y, Rodrigues AD, Greene N, and Aleo MD (2015) Setting clinical exposure levels of concern for drug-induced liver injury (DILI) using mechanistic in vitro assays. *Toxicol Sci* **147**:500–514.
Shitara Y, Maeda K, Ikejiri K, Yoshida K, Horie T, and Sugiyama Y (2013) Clinical significance of organic anion transporting polypeptides (OATPs) in drug disposition: their roles in hepatic clearance and intestinal absorption. *Biopharm Drug Dispos* **34**:45–78.
Soroka CJ, Lee JM, Azzaroli F, and Boyer JL (2001) Cellular localization and up-regulation of multidrug resistance-associated protein 3 in hepatocytes and cholangiocytes during obstructive cholestasis in rat liver. *Hepatology* **33**:783–791.
Stieger B (2010) Role of the bile salt export pump, BSEP, in acquired forms of cholestasis. *Drug Metab Rev* **42**:437–445.
Stieger B, Fattinger K, Madon J, Kullak-Ublick GA, and Meier PJ (2000) Drug- and estrogen-induced cholestasis through inhibition of the hepatocellular bile salt export pump (Bsep) of rat liver. *Gastroenterology* **118**:422–430.
Treiber A, Schneiter R, Häusler S, and Stieger B (2007) Bosentan is a substrate of human OATP1B1 and OATP1B3: inhibition of hepatic uptake as the common mechanism of its interactions with cyclosporin A, rifampicin, and sildenafil. *Drug Metab Dispos* **35**:1400–1407.
Umehara K and Camenisch G (2012) Novel in vitro-in vivo extrapolation (IVIVE) method to predict hepatic organ clearance in rat. *Pharm Res* **29**:603–617.
Werk AN and Cascorbi I (2014) Functional gene variants of CYP3A4. *Clin Pharmacol Ther* **96**:340–348.
Yabe Y, Galetin A, and Houston JB (2011) Kinetic characterization of rat hepatic uptake of 16 actively transported drugs. *Drug Metab Dispos* **39**:1808–1814.
Yoshikado T, Yoshida K, Kotani N, Nakada T, Asaumi R, Toshimoto K, Maeda K, Kusuhara H, and Sugiyama Y (2016) Quantitative Analyses of Hepatic OATP-Mediated Interactions Between Statins and Inhibitors Using PBPK Modeling With a Parameter Optimization Method. *Clin Pharmacol Ther* **100**:513–523.
Zamek-Gliszczynski MJ, Lee CA, Poirier A, Bentz J, Chu X, Ellens H, Ishikawa T, Jamei M, Kalvass JC, Nagar S, et al.; International Transporter Consortium (2013) ITC recommendations for transporter kinetic parameter estimation and translational modeling of transport-mediated PK and DDIs in humans. *Clin Pharmacol Ther* **94**:64–79.

Address correspondence to: Gian Camenisch, Novartis Pharma AG, Fabrikstr.14, CH-4056 Basel, Switzerland. E-mail: gian.camenisch@novartis.com

Supplemental Data

Assessing the risk of drug-induced cholestasis using unbound intrahepatic concentrations

Julia Riede, Birk Poller, Jörg Huwyler, Gian Camenisch

Drug Metabolism and Disposition

Calculation of pharmacokinetic parameters:

The absorption rate constant (k_a) was calculated based on eq. 1 and 2 [1]:

$$T_{max} = \frac{ln(\frac{k_a}{k_e})}{k_a - k_e} \tag{1}$$

$$k_e = \frac{ln(2)}{T_{1/2}} \tag{2}$$

where T_{max} is the time to reach the maximum plasma concentration, k_e is the elimination rate constant and $T_{1/2}$ is the elimination half-life.

The fraction absorbed and escaping gut metabolism ($F_a \times F_g$) was calculated based on eq. 3 and 4 [1]:

$$F_a \times F_g = \frac{F}{F_h} \tag{3}$$

$$F_h = 1 - \frac{CL_h}{Q_h} \tag{4}$$

where F represents the oral bioavailabilty, F_h is the fraction escaping hepatic clearance, CL_h is the hepatic blood clearance and Q_h is the hepatic blood flow (1.45 l/min).

Pharmacokinetic parameters required for the calculations and literature references for all 18 compounds are summarized in Supplemental Table 2.

Human *in vitro* BSEP inhibition:

K_i values from Hirano et al., 2005 [2] were converted to IC_{50} values according to eq. 5, assuming competitive inhibition [3]:

$$IC_{50} = K_i \times (1 + \frac{[S]}{K_m}) \tag{5}$$

where the substrate concentration of taurocholate [S] = 3 µM and Michealis-Menten constant (K_m) for BSEP-mediated taurocholate transport = 4.64 µM [2].

SUPPLEMENTAL TABLE 1: Hepatic *in vivo* and *in vitro* Kp_{uu} in rat

Drug compound	ECM class	in vitro					in vivo				
		Hepatic process clearances [4]									
		$PS_{inf,act}$	$PS_{inf,pas}$	$CL_{int,met}$	$CL_{int,sec}$	Kp_{uu}	Kp_{uu}	Kp	fu_{liver}	fu_p	fu_b
		[ml/min/kg]									
Atorvastatin	4	2935.3	212.8	158.3	1.2	8.46 63.2 a) [6] 494 a) [7]	7.76	8.2 c) [5]	0.0284 e)	0.03 [4]	0.025 [4]
Cyclosporine A	4	191.3	83.5	37.4	13.1	2.05	1.80	11.0 d) [8]	0.0077 f) [9]	0.06 [4]	0.047 [4]
Furamidine						53 b) [10]	23 [10]				
Ketoconazole	1	0.0	1939.1	4674.6	3.3	0.29	0.72	4.36 d) [11]	0.0035 e)	0.01 [4]	0.014 [4]
Pravastatin	4	185.4	57.3	3.37	3.5	3.78 16.5 a) [6] 22.9 a) [7]	4.30	16.3 c) [12]	0.1689 e)	0.64 [4]	0.84 [4]
Ritonavir						1.1 b) [10]	1.1 [10]				
Rosuvastatin			-			6.1 b) [10] 30.2 a) [6] 58.2 a) [7]	7.9 [10]				
Verapamil	1	0.0	340.6	2636.6	8.8	0.11	0.28	7.67 d) [11]	0.0024 e)	0.06 [4]	0.066 [4]

$PS_{inf,act}$ = active hepatic uptake, $PS_{inf,pas}$ = passive hepatic uptake, PS_{eff} = sinusoidal efflux, $CL_{int,met}$ = intrinsic metabolic clearance, $CL_{int,sec}$ = intrinsic biliary clearance, Kp_{uu} = liver-to-blood partition coefficient for unbound drug, Kp = liver-to-blood partition coefficient, fu_{liver} = fraction unbound in liver, fu_p = fraction unbound in plasma, fu_b = fraction unbound in blood. If not stated otherwise, *in vitro* Kp_{uu} values were calculated according to ECM ($Kp_{uu} = PS_{inf}/(PS_{eff} + CL_{int})$, assuming $PS_{eff} = PS_{inf,pas}$). a) $Kp_{uu} = (CL_{active} + P_{diff})/P_{diff}$, where CL_{active} and P_{diff} are active and passive hepatic uptake clearances, respectively. b) Kp_{uu} values were derived from Kp and fu in sandwich-cultured rat hepatocytes. c) rat liver-to-plasma Kp, *in vivo* Kp_{uu} values were derived from $Kp_{uu} = Kp \times fu_{liver}/fu_p$. d) rat liver-to-blood Kp, *in vivo* Kp_{uu} values were derived from $Kp_{uu} = Kp \times fu_{liver}/fu_b$. e) In-house data for the fraction unbound in suspended human hepatocytes determined from steady-state incubations at 4°C [6]. f) Fraction unbound in homogenized rat liver. Literature references are shown in brackets. DataThief III (http://www.datathief.org) was partially used for extraction of literature data.

SUPPLEMENTAL TABLE 2: Human dose and systemic exposure

Drug compound	maximum daily dose		C_{max} [µM]		C_{max} study conditions
Atazanavir	400 mg qd	[13]	8.3239	[14]	400 mg qd (6 days), healthy subjects
Atorvastatin	80 mg qd	[13]	0.4511	[15]	80 mg qd (14 days), healthy subjects
Bosentan (125 mg bid)	125 mg bid	[13]	3.3193	[16]	125 mg bid (6 days), healthy subjects
Bosentan (1000 mg bid)	1000 mg bid	[17]	23.2209	[18]	1000 mg (extrapolated from C_{max} values after administration of 3 - 1200 mg), healthy subjects
Cerivastatin	0.8 mg qd	[19]	0.0300	[15]	0.8 mg qd (4 weeks), healthy subjects
Cyclosporine A	7.5 mg/kg bid	[20]	0.7317	[21]	5 mg/kg (single dose), healthy subjects, [a]
Erythromycin	1000 mg bid	[20]	20.1655	[22]	1000 mg bid (4 days), healthy elderly subjects
Fluvastatin	80 mg qd	[13]	0.2605	[23]	80 mg qd (repeated), healthy subjects
Glibenclamide	10 mg bid	[13]	0.9372	[24]	7 mg (single dose), diabetic patients
Ibuprofen	800 mg tid	[20]	392.8916	[25]	800 mg (single dose), healthy subjects
Imatinib	400 mg bid	[13]	9.5623	[26]	400 mg qd (4 days), chronic myeloid leukemia patients
Ketoconazole	400 mg qd	[13]	16.6061	[27]	400 mg qd (11 days), healthy subjects
Lovastatin acid	80 mg qd	[13]	0.1006	[15]	80 mg qd (17 days), hypercholesterolemic patients
Pitavastatin	4 mg qd	[13]	0.2769	[28]	4 mg (single dose), healthy subjects
Pravastatin	40 mg qd	[20]	0.1376	[29]	40 mg qd (4 days), healthy subjects
Rosiglitazone	8 mg qd	[13]	1.8241	[30]	8 mg qd (14 days), healthy subjects
Rosuvastatin	40 mg qd	[13]	0.0768	[31]	40 mg qd (11 days), healthy subjects
Simvastatin acid	80 mg qd	[13]	0.0133	[32]	80 mg qd (7 days), healthy subjects
Verapamil	480 mg qd	[20]	0.5521	[33]	180 mg bid (3 days), healthy subjects

C_{max} = maximum available drug plasma concentration in human. qd = once daily; bid = twice daily; tid = three times daily. [a] C_{max} in plasma was converted from C_{max} in blood ($C_{max,plasma}$ = $C_{max,blood}$ / R_b, where R_b is the blood-to-plasma partition coefficient). The literature references are shown in brackets.

3

SUPPLEMENTAL TABLE 3: Human pharmacokinetic parameters

Drug compound	T_{max} [h]	$T_{1/2}$ [h]	k_a [h^{-1}]	k_e [h^{-1}]	CL_{tot} [ml/min/kg]		CL_h [ml/min/kg]		fn_h		F		F_h	F_a x F_g
Atazanavir	2.5	5.9	0.96	0.12	9.59	[34]	8.92	[-]	0.93	[35]	0.60	[36]	0.60	1.00
Atorvastatin	1.6	10.3	2.27	0.07	5.96	[-]	5.90	[37]	0.99	[37]	0.14	[37]	0.71	0.20
Bosentan (125 mg bid)	3.6	5.8	0.54	0.12	3.43	[18]	3.40	[-]	0.99	[38]	0.50	[39]	0.84	0.60
Bosentan (1000 mg bid)	3.0	16.2	1.14	0.04	2.38	[18]	2.36	[-]	0.99	[38]	0.50	[39]	0.89	0.56
Cerivastatin	2.2	2.9	0.77	0.24	3.40	[37]	3.40	[-]	1.00	[37]	0.60	[37]	0.84	0.71
Cyclosporine A	1.7	11.9	2.19	0.06	3.13	[-]	3.10	[40]	0.99	[41]	0.22	[41]	0.85	0.26
Erythromycin	3.6	2.0	0.22	0.35	5.39	[42]	5.12	[-]	0.95	[35]	0.40	[43]	0.75	0.53
Fluvastatin	5.5	5.7	0.26	0.12	7.46	[37]	7.01	[-]	0.94	[37]	0.24	[37]	0.66	0.36
Glibenclamide	2.8	7.9	0.93	0.09	2.21	[44]	2.21	[-]	1.00	[35]	0.93	[45]	0.93	1.00
Ibuprofen	1.3	2.4	1.61	0.29	1.33	[46]	1.33	[-]	1.00	[35]	1.00	[47]	1.00	1.00
Imatinib	3.0	17.3	1.16	0.04	4.17	[48]	3.96	[-]	0.95	[35]	0.98	[49]	0.98	1.00
Ketoconazole	2.2	2.7	0.74	0.26	4.02	[-]	3.90	[40]	0.97	[41]	0.81	[41]	0.81	1.00
Lovastatin acid	4.1	3.4	0.29	0.20	12.60	[37]	11.34	[-]	0.90	[37]	0.05	[37]	0.45	0.11
Pitavastatin	0.8	11.4	6.13	0.06	3.48	[37]	3.48	[-]	1.00	[37]	0.51	[37]	0.83	0.61
Pravastatin	1.2	2.7	1.94	0.26	19.64	[-]	10.41	[37]	0.53	[37]	0.18	[37]	0.50	0.36
Rosiglitazone	1.9	3.8	1.20	0.18	1.20	[50]	1.20	[-]	1.00	[35]	0.99	[51]	0.99	1.00
Rosuvastatin	4.5	20.7	0.71	0.03	16.87	[37]	12.15	[-]	0.72	[37]	0.20	[37]	0.41	0.49
Simvastatin acid	4.3	6.1	0.41	0.11	29.00	[37]	25.23	[-]	0.87	[37]	0.05	[37]	0.05	1.00
Verapamil	9.2	8.9	0.15	0.08	14.10	[-]	13.68	[40]	0.97	[41]	0.26	[41]	0.34	0.76

T_{max} = time to reach the maximum plasma concentration, $T_{1/2}$ = elimination half-life, T_{max} and $T_{1/2}$ values were obtained from Pharmapendium (Elsevier Properties, New York, SA) and represent the average of all reported values after administration of the maximum available recommended single dose in healthy subjects. CL_{tot} = total blood clearance, fn_h = hepatic (non-renal) eliminated fraction, CL_h = hepatic blood clearance, CL_h was either taken from literature or calculated with CL_{tot} x fn_h, assuming a human body weight of 70 kg. F = absolute oral bioavailability, F_h = fraction escaping hepatic clearance, F_a x F_g = fraction absorbed and escaping gut metabolism. bid = twice daily. The literature references are shown in brackets. [-] = calculated parameter.

SUPPLEMENTAL TABLE 4: Binding and physicochemical properties

Drug compound	R_b		fu_p		fu_{mic}		$logD_{7.4}$	
Atazanavir	0.74	[a)]	0.14	[36]	0.84	[a)]	5.77	[52]
Atorvastatin	0.63	[37]	0.05	[37]	0.51	[37]	1.30	[37]
Bosentan	0.57	[a)]	0.02	[53]	0.83	[a)]	1.25	[7]
Cerivastatin	0.60	[37]	0.01	[37]	0.69	[37]	1.90	[37]
Cyclosporine A	2.33	[41]	0.07	[53]	0.73	[4]	2.92	[41]
Erythromycin	0.73	[a)]	0.05	[53]	0.89	[a)]	1.11	[7]
Fluvastatin	0.52	[37]	0.02	[37]	0.31	[37]	1.60	[37]
Glibenclamide	0.55	[a)]	0.01	[53]	0.95	[a)]	2.19	[54]
Ibuprofen	0.57	[a)]	0.01	[53]	0.96	[a)]	0.81	[35]
Imatinib	0.80	[a)]	0.05	[55]	0.48	[a)]	2.40	[56]
Ketoconazole	0.50	[41]	0.01	[53]	0.17	[4]	4.05	[41]
Lovastatin acid	0.57	[37]	0.05	[37]	0.10	[37]	1.51	[37]
Pitavastatin	0.58	[37]	0.04	[37]	0.43	[37]	1.50	[37]
Pravastatin	0.54	[37]	0.52	[37]	0.88	[37]	-0.40	[37]
Rosiglitazone	0.55	[a)]	0.002	[53]	0.72	[a)]	2.60	[57]
Rosuvastatin	0.69	[37]	0.12	[37]	0.98	[37]	-0.89	[37]
Simvastatin acid	0.57	[37]	0.06	[37]	0.05	[37]	1.88	[37]
Verapamil	0.85	[41]	0.11	[41]	0.50	[4]	1.75	[41]

R_b = blood-to-plasma partition coefficient. fu_p = fraction unbound in plasma. fu_{mic} = fraction unbound in liver microsomes. a) in house data. bid = twice daily. The literature references are shown in brackets.

SUPPLEMENTAL TABLE 5: Clinical cholestasis information and BSEP *in vitro* inhibition data

Drug compound	Cholestasis annotation		BSEP IC$_{50}$ values [µM]	
common (cholestasis in > 2% of patients)				
Bosentan (1000 mg bid)	cholestasic/mixed liver injury (elevated AP and bile salts) in 8% of hypertensive patients (1000 mg bid)	[17]	22.0 – 38.1	[53, 58-60]
Cyclosporine A	cholestasis (elevated AP) in 27% of uveitis patients	[61]	0.4 – <10	[53, 58-60, 62]
Erythromycin	cholestasis in 2 - 4% of patients	[63]	4.1 – 13.0	[53, 59]
Imatinib	elevated AP (> 5x ULN) in up to 5% of chronic myeloid leukemia patients	[64]	<10 – 25.1	[59, 60]
rare (cholestasis in ≤ 2% of patients)				
Atazanavir	cholestasis is uncommon[a]	[65]	3.1	[66]
Atorvastatin	cholestatic jaundice in < 2% of patients	[67]	15.0	[2]
Bosentan (125 mg bid)	cholestasic/mixed liver injury (elevated AP and bile salts) in 2% of hypertension (100 mg qd)	[17, 68]	22.0 – 38.1	[53, 59, 60]
Glibenclamide	cholestatic jaundice occurs rarely[a]	[69]	1.5 – 11.3	[53, 58-60, 62]
Ibuprofen	liver injury with cholestatic/mixed pattern occurs very rarely[a]	[70]	598.6 – >789	[53, 60]
Ketoconazole	cholestasis/mixed liver injury occurs very rarely[a] / in 0.023% of patients	[71, 72]	2.9 – 4.1	[53, 59, 60]
Pitavastatin	elevated AP (> 2x ULN) in 0.2% of patients, cholestatic jaundice in 0.5% of patients	[14]	42.2	[2]
Pravastatin	cholestatic jaundice occurs rarely[a]	[73]	268.4	[2]
Verapamil	elevated AP in 0.9% of patients, warning for elevated AP	[74, 75]	20.5	[60]
no cholestasis				
Cerivastatin	cholestasis or elevated AP (≥ 2x ULN) not reported in clinical studies		18.8	[2]
Fluvastatin	cholestasis or elevated AP (≥ 2x ULN) not reported in clinical studies		36.1 – 49.7	[2, 59]
Lovastatin acid	cholestasis or elevated AP (≥ 2x ULN) not reported in clinical studies		19.3	[59]
Rosiglitazone	cholestasis or elevated AP (≥ 2x ULN) not reported in clinical studies		1.9 – 6.4	[53, 59, 60, 66]
Rosuvastatin	cholestasis or elevated AP (≥ 2x ULN) not reported in clinical studies		197.6	[2]
Simvastatin acid	cholestasis or elevated AP (≥ 2x ULN) not reported in clinical studies		20.9	[2]

bid = twice daily. AP = serum alkaline phosphatase, ULN = upper limit of normal. [a] uncommon = 1 – 0.1% of patients, rare = 0.01 – 0.1% of patients, very rare < 0.01% of patients [76]. BSEP IC$_{50}$ data from Hirano et al., 2005 [2] were converted from reported K$_i$ values according to eq. 5. The literature references are shown in brackets.

Supplemental References

1. Kwon, Y., *Handbook of Essential Pharmacokinetics, Pharmacodynamics, and Drug Metabolism for Industrial Scientists*. 2001, New York: Kluwer Academic/Plenum Publishers.

2. Hirano, M., et al., *Bile salt export pump (BSEP/ABCB11) can transport a nonbile acid substrate, pravastatin*. J Pharmacol Exp Ther, 2005. **314**(2): p. 876-82.

3. Giacomini, K.M., et al., *Membrane transporters in drug development*. Nat Rev Drug Discov, 2010. **9**(3): p. 215-36.

4. Umehara, K. and G. Camenisch, *Novel in vitro-in vivo extrapolation (IVIVE) method to predict hepatic organ clearance in rat*. Pharm Res, 2012. **29**(2): p. 603-17.

5. Shin, E., et al., *High-Dose Metformin May Increase the Concentration of Atorvastatin in the Liver by Inhibition of Multidrug Resistance-Associated Protein 2*. J Pharm Sci, 2016.

6. Shitara, Y., et al., *Clinical significance of organic anion transporting polypeptides (OATPs) in drug disposition: their roles in hepatic clearance and intestinal absorption*. Biopharm Drug Dispos, 2013. **34**(1): p. 45-78.

7. Yabe, Y., A. Galetin, and J.B. Houston, *Kinetic characterization of rat hepatic uptake of 16 actively transported drugs*. Drug Metab Dispos, 2011. **39**(10): p. 1808-14.

8. Kawai, R., et al., *Physiologically based pharmacokinetics of cyclosporine A: extension to tissue distribution kinetics in rats and scale-up to human*. J Pharmacol Exp Ther, 1998. **287**(2): p. 457-68.

9. Watanabe, T., et al., *Utility of bilirubins and bile acids as endogenous biomarkers for the inhibition of hepatic transporters*. Drug Metab Dispos, 2015. **43**(4): p. 459-66.

10. Pfeifer, N.D., et al., *Determination of intracellular unbound concentrations and subcellular localization of drugs in rat sandwich-cultured hepatocytes compared with liver tissue*. Drug Metab Dispos, 2013. **41**(11): p. 1949-56.

11. Yamano, K., et al., *Correlation between in vivo and in vitro hepatic uptake of metabolic inhibitors of cytochrome P-450 in rats*. Drug Metab Dispos, 1999. **27**(11): p. 1225-31.

12. Mikkaichi, T., et al., *Liver-selective distribution in rats supports the importance of active uptake into the liver via organic anion transporting polypeptides (OATPs) in humans*. Drug Metab Pharmacokinet, 2015. **30**(5): p. 334-40.

13. DailyMed, *Drug Label Information*; Available from: https://dailymed.nlm.nih.gov.

14. U.S. Food and Drug Administration, *Reyataz NDA 021567/S000 Clinical Pharmacology and Biopharmaceutics Review Part 03*. Available from: www.accessdata.fda.gov.

15. Garcia, M.J., et al., *Clinical pharmacokinetics of statins*. Methods Find Exp Clin Pharmacol, 2003. **25**(6): p. 457-81.

16. van Giersbergen, P.L., et al., *Influence of mild liver impairment on the pharmacokinetics and metabolism of bosentan, a dual endothelin receptor antagonist.* J Clin Pharmacol, 2003. **43**(1): p. 15-22.

17. Fattinger, K., et al., *The endothelin antagonist bosentan inhibits the canalicular bile salt export pump: a potential mechanism for hepatic adverse reactions.* Clin Pharmacol Ther, 2001. **69**(4): p. 223-31.

18. Weber, C., et al., *Pharmacokinetics and pharmacodynamics of the endothelin-receptor antagonist bosentan in healthy human subjects.* Clin Pharmacol Ther, 1996. **60**(2): p. 124-37.

19. Ballantyne, C.M., et al., *Risk for myopathy with statin therapy in high-risk patients.* Arch Intern Med, 2003. **163**(5): p. 553-64.

20. Swiss Compendium, *Prescribing information*; Available from: http://compendium.ch.

21. Lee, M., et al., *Effect of grapefruit juice on pharmacokinetics of microemulsion cyclosporine in African American subjects compared with Caucasian subjects: does ethnic difference matter?* J Clin Pharmacol, 2001. **41**(3): p. 317-23.

22. Miglioli, P.A., et al., *Effect of age on single- and multiple-dose pharmacokinetics of erythromycin.* Eur J Clin Pharmacol, 1990. **39**(2): p. 161-4.

23. U.S. Food and Drug Administration, *Lescol XL NDA 021192/S000 Clinical Pharmacology and Biopharmaceutics Review.* Available from: www.accessdata.fda.gov.

24. Jonsson, A., et al., *Pharmacokinetics of glibenclamide and its metabolites in diabetic patients with impaired renal function.* Eur J Clin Pharmacol, 1998. **53**(6): p. 429-35.

25. U.S. Food and Drug Administration, *Caldolor NDA 022348/S000 Clinical Pharmacology and Biopharmaceutics Review.* Available from: www.accessdata.fda.gov.

26. Gambacorti-Passerini, C., et al., *Alpha1 acid glycoprotein binds to imatinib (STI571) and substantially alters its pharmacokinetics in chronic myeloid leukemia patients.* Clin Cancer Res, 2003. **9**(2): p. 625-32.

27. U.S. Food and Drug Administration, *Edurant NDA 202022/S000 Clinical Pharmacology and Biopharmaceutics Review.* Available from: www.accessdata.fda.gov.

28. Chen, Y., et al., *Effect of a single-dose rifampin on the pharmacokinetics of pitavastatin in healthy volunteers.* Eur J Clin Pharmacol, 2013. **69**(11): p. 1933-8.

29. van Luin, M., et al., *Drug-drug interactions between raltegravir and pravastatin in healthy volunteers.* J Acquir Immune Defic Syndr, 2010. **55**(1): p. 82-6.

30. Kirchheiner, J., et al., *Pharmacokinetics and pharmacodynamics of rosiglitazone in relation to CYP2C8 genotype.* Clin Pharmacol Ther, 2006. **80**(6): p. 657-67.

31. U.S. Food and Drug Administration, *Crestor NDA 021366/S000 Clinical Pharmacology and Biopharmaceutics Review.* Available from: www.accessdata.fda.gov.

32. Ayalasomayajula, S.P., et al., *Evaluation of the potential for steady-state pharmacokinetic interaction between vildagliptin and simvastatin in healthy subjects.* Curr Med Res Opin, 2007. **23**(12): p. 2913-20.

33. van Haarst, A.D., et al., *Clinically important interaction between tedisamil and verapamil.* J Clin Pharmacol, 2009. **49**(5): p. 560-7.

34. Krishna, G., et al., *Effects of oral posaconazole on the pharmacokinetics of atazanavir alone and with ritonavir or with efavirenz in healthy adult volunteers.* J Acquir Immune Defic Syndr, 2009. **51**(4): p. 437-44.

35. Benet, L.Z., F. Broccatelli, and T.I. Oprea, *BDDCS applied to over 900 drugs.* AAPS J, 2011. **13**(4): p. 519-47.

36. Goldsmith, D.R. and C.M. Perry, *Atazanavir.* Drugs, 2003. **63**(16): p. 1679-93.

37. Kunze, A., et al., *Application of the extended clearance concept classification system (ECCCS) to predict the victim drug-drug interaction potential of statins.* Drug Metab Pers Ther, 2015. **30**(3): p. 175-88.

38. Weber, C., R. Gasser, and G. Hopfgartner, *Absorption, excretion, and metabolism of the endothelin receptor antagonist bosentan in healthy male subjects.* Drug Metab Dispos, 1999. **27**(7): p. 810-5.

39. Dingemanse, J. and P.L. van Giersbergen, *Clinical pharmacology of bosentan, a dual endothelin receptor antagonist.* Clin Pharmacokinet, 2004. **43**(15): p. 1089-115.

40. Camenisch, G. and K. Umehara, *Predicting human hepatic clearance from in vitro drug metabolism and transport data: a scientific and pharmaceutical perspective for assessing drug-drug interactions.* Biopharm Drug Dispos, 2012. **33**(4): p. 179-94.

41. Kunze, A., et al., *In vitro-in vivo extrapolation method to predict human renal clearance of drugs.* J Pharm Sci, 2014. **103**(3): p. 994-1001.

42. Yu, K.S., et al., *Ethnic differences and relationships in the oral pharmacokinetics of nifedipine and erythromycin.* Clin Pharmacol Ther, 2001. **70**(3): p. 228-36.

43. Mather, L.E., et al., *Absorption and bioavailability of oral erythromycin.* Br J Clin Pharmacol, 1981. **12**(2): p. 131-40.

44. Manitpisitkul, P., et al., *An open-label drug-drug interaction study of the steady-state pharmacokinetics of topiramate and glyburide in patients with type 2 diabetes mellitus.* Clin Drug Investig, 2013. **33**(12): p. 929-38.

45. U.S. Food and Drug Administration, *Glynase NDA 020051/S003 Label.* Available from: www.accessdata.fda.gov.

46. European Medicine Agency, *Pedea EMEA/H/C/000549 Scientific Discussion.* Available from: http://www.ema.europa.eu/ema.

47. Martin, W., et al., *Pharmacokinetics and absolute bioavailability of ibuprofen after oral administration of ibuprofen lysine in man.* Biopharm Drug Dispos, 1990. **11**(3): p. 265-78.

9

48. European Medicine Agency, *Glivec EMEA/H/C/000406 Scientific Discussion.* Available from: http://www.ema.europa.eu/ema.

49. Peng, B., et al., *Absolute bioavailability of imatinib (Glivec) orally versus intravenous infusion.* J Clin Pharmacol, 2004. **44**(2): p. 158-62.

50. Cox, P.J., et al., *Absorption, disposition, and metabolism of rosiglitazone, a potent thiazolidinedione insulin sensitizer, in humans.* Drug Metab Dispos, 2000. **28**(7): p. 772-80.

51. Miller, A.K., R.A. DiCicco, and M.I. Freed, *The effect of ranitidine on the pharmacokinetics of rosiglitazone in healthy adult male volunteers.* Clin Ther, 2002. **24**(7): p. 1062-71.

52. Duan, J., et al., *Evaluation of atazanavir and darunavir interactions with lipids for developing pH-responsive anti-HIV drug combination nanoparticles.* J Pharm Sci, 2014. **103**(8): p. 2520-9.

53. Dawson, S., et al., *In vitro inhibition of the bile salt export pump correlates with risk of cholestatic drug-induced liver injury in humans.* Drug Metab Dispos, 2012. **40**(1): p. 130-8.

54. Austin, R.P., et al., *The binding of drugs to hepatocytes and its relationship to physicochemical properties.* Drug Metab Dispos, 2005. **33**(3): p. 419-25.

55. Peng, B., P. Lloyd, and H. Schran, *Clinical pharmacokinetics of imatinib.* Clin Pharmacokinet, 2005. **44**(9): p. 879-94.

56. Matsson, P., et al., *A global drug inhibition pattern for the human ATP-binding cassette transporter breast cancer resistance protein (ABCG2).* J Pharmacol Exp Ther, 2007. **323**(1): p. 19-30.

57. Rusinova, R., et al., *Thiazolidinedione insulin sensitizers alter lipid bilayer properties and voltage-dependent sodium channel function: implications for drug discovery.* J Gen Physiol, 2011. **138**(2): p. 249-70.

58. Aleo, M.D., et al., *Human drug-induced liver injury severity is highly associated with dual inhibition of liver mitochondrial function and bile salt export pump.* Hepatology, 2014. **60**(3): p. 1015-22.

59. Morgan, R.E., et al., *A multifactorial approach to hepatobiliary transporter assessment enables improved therapeutic compound development.* Toxicol Sci, 2013. **136**(1): p. 216-41.

60. Warner, D.J., et al., *Mitigating the inhibition of human bile salt export pump by drugs: opportunities provided by physicochemical property modulation, in silico modeling, and structural modification.* Drug Metab Dispos, 2012. **40**(12): p. 2332-41.

61. Kassianides, C., et al., *Liver injury from cyclosporine A.* Dig Dis Sci, 1990. **35**(6): p. 693-7.

62. Kis, E., et al., *Effect of membrane cholesterol on BSEP/Bsep activity: species specificity studies for substrates and inhibitors.* Drug Metab Dispos, 2009. **37**(9): p. 1878-86.

63. *Meyler's Side Effects of Drugs (16th Edition).* 2015: Elsevier Science.

64. U.S. Food and Drug Administration, *Gleevec NDA 021588/S000 Label.* Available from: www.accessdata.fda.gov.

65. European Medicine Agency, *Reyataz EMEA/H/C/000494 -X/0094/G ANNEX I.* Available from: http://www.ema.europa.eu/ema.

66. Chang, J.H., et al., *Evaluating the in vitro inhibition of UGT1A1, OATP1B1, OATP1B3, MRP2, and BSEP in predicting drug-induced hyperbilirubinemia.* Mol Pharm, 2013. **10**(8): p. 3067-75.

67. U.S. Food and Drug Administration, *Lipitor NDA 020702/S042 Label.* Available from: www.accessdata.fda.gov.

68. European Medicine Agency, *Tracleer EMEA/H/C/000401/II/0037 Assessment Report.* Available from: http://www.ema.europa.eu/ema.

69. U.S. Food and Drug Administration, *Micronase NDA 017489/S032 Label.* Available from: www.accessdata.fda.gov.

70. Stricker, B., *Drug Induced Liver Injury.* 2nd ed ed. 1992, Amsterdam: Elsevier.

71. Velayudham, L.S. and G.C. Farrell, *Drug-induced cholestasis.* Expert Opin Drug Saf, 2003. **2**(3): p. 287-304.

72. Stricker, B.H., et al., *Ketoconazole-associated hepatic injury. A clinicopathological study of 55 cases.* J Hepatol, 1986. **3**(3): p. 399-406.

73. U.S. Food and Drug Administration, *Pravachol NDA 019898/S050 Label.* Available from: www.accessdata.fda.gov.

74. U.S. Food and Drug Administration, *Verelan PM NDA 020943/S000 Label.* Available from: www.accessdata.fda.gov.

75. U.S. Food and Drug Administration, *Verelan NDA 19614 Approval Package 1990-04-27.* Available from: www.pharmapendium.com.

76. CIOMS, *Guidelines for preparing core clinical safety information on drug from CIOMS Working Group III.* 1995, Geneva.

4.2. Current *in vitro* methods to determine hepatic Kp_uu: a comparison of their usefulness and limitations

Julia Riede[1,2], Gian Camenisch[1], Jörg Huwyler[2], Birk Poller[1]

[1] Department of PK Sciences, ADME Section, Novartis Institutes for BioMedical Research, Basel, Switzerland

[2] Department of Pharmaceutical Sciences, Division of Pharmaceutical Technology, University of Basel, Basel, Switzerland

ELSEVIER

Pharmacokinetics, Pharmacodynamics and Drug Transport and Metabolism

Current *In Vitro* Methods to Determine Hepatic Kp$_{uu}$: A Comparison of Their Usefulness and Limitations

CrossMark

Julia Riede [1,2], Gian Camenisch [1], Jörg Huwyler [2], Birk Poller [1,*]

[1] *Department of PK Sciences, ADME Section, Novartis Institutes for BioMedical Research, Basel, Switzerland*
[2] *Department of Pharmaceutical Sciences, Division of Pharmaceutical Technology, University of Basel, Basel, Switzerland*

A B S T R A C T

Unbound intrahepatic drug concentrations determine the interaction potential with intracellular targets related to toxicity, pharmacokinetics, or pharmacodynamics. Recently, the unbound liver-to-blood partition coefficient (Kp$_{uu}$) based on the Extended Clearance Model (ECM) has been developed providing indirect estimates of unbound intrahepatic drug concentrations. This study aimed to determine Kp$_{uu}$ for 18 diverse drug compounds by 3 alternative *in vitro* methods and to compare the outcome with the ECM approach. Kp$_{uu}$ was calculated from independent measurements of hepatocellular drug accumulation (Kp) and unbound fraction in hepatocytes (fu$_{hep}$) either assessed from steady-state accumulation at 4°C (temperature method), using equilibrium dialysis (homogenization method), or empirically from logD$_{7.4}$ (logD$_{7.4}$ method). Deviations to ECM-based Kp$_{uu}$ data were closely linked to the absence of intrinsic clearance processes (metabolism, biliary secretion) in the investigated methods. Differences in fu$_{hep}$ additionally contributed to deviations in Kp$_{uu}$. The homogenization method generally provided lowest fu$_{hep}$ values, especially for compounds with high molecular weight or low logD$_{7.4}$. Kp$_{uu}$ values of compounds with low intrinsic clearance correlated well between the ECM and temperature methods independent of physicochemical properties. Therefore, only the ECM provides an integrated quantitative determination of hepatic Kp$_{uu}$. Temperature and homogenization methods, however, represent useful alternatives if compound properties are appropriately considered.

© 2017 American Pharmacists Association®. Published by Elsevier Inc. All rights reserved.

Introduction

Assessments of pharmacological efficacy, drug-drug interaction (DDI) potential, and toxicity of drug candidates were traditionally performed by relating the systemic unbound drug concentration to the respective target inhibition (IC$_{50}$ or Ki). Because of the limited access to human tissue concentrations, the unbound systemic drug concentration served as surrogate for determining intracellular target interactions based on the concept of the "free drug hypothesis."[1,2] This approach assumes a rapid and complete equilibration of the unbound drug between blood and tissue. However, in organs such as the liver or brain, this concept is violated for drugs, which are subject to active cellular transport and metabolic processes.[3,4] Therefore, indirect methods for the determination of unbound intracellular drug concentrations have been developed using the tissue-to-blood partition coefficient for unbound drug at steady-state (Kp$_{uu}$), allowing to account for active processes.[5,6]

Several *in vitro* approaches using cells, tissue slices, and homogenates from different organs have been developed. For the determination of hepatic Kp$_{uu}$, 4 different methods can be applied with primary hepatocytes and subcellular fractions as outlined in Table 1. Three of these methods rely on separate experimental determinations of the liver-to-blood (i.e., hepatocyte-to-media) partition coefficient for total drug at steady-state (Kp) and the unbound fraction in hepatocytes (fu$_{hep}$). Kp can be obtained from cellular drug accumulation experiments usually in the absence of metabolic activity.[7-11] However, different methods have been used to assess fu$_{hep}$: (1) incubations with intact cells on ice (temperature method),[8,12] (2) equilibrium dialysis using homogenized cells or tissue (homogenization method),[3,5,6,10,11,13] and (3) estimation from logD$_{7.4}$ using an empirical correlation with fu$_{hep}$ data[9] (Table 1). Nevertheless,

Table 1
Investigated Methods for the Determination of Kp, fu$_{hep}$, and Kp$_{uu}$

Methods	Kp	fu$_{hep}$	Kp$_{uu}$	Assumptions
Temperature method	Kp (steady-state hepatocyte uptake)	fu$_{hep,temp}$	Kp$_{uu,temp}$ = Kp × fu$_{hep,temp}$	Negligible intrinsic clearance processes Steady-state reached Transporter activity is abolished on ice (for fu$_{hep}$ only) fu$_{hep}$ is not temperature-dependent
Homogenization method		fu$_{hep,hom}$	Kp$_{uu,hom}$ = Kp × fu$_{hep,hom}$	Negligible intrinsic clearance processes Steady-state reached fu$_{hep}$ is not influenced by cell homogenization
logD$_{7.4}$ method		fu$_{hep,logD}$	Kp$_{uu,logD}$ = Kp × fu$_{hep,logD}$	Negligible intrinsic clearance processes Steady-state reached Kp$_{uu}$ depends on cellular volume
ECM method	–	–	Kp$_{uu,ECM}$ = $\frac{PS_{inf,act}+PS_{inf,pas}}{PS_{eff,act}+PS_{eff,pas}+CL_{int,met}+CL_{int,sec}}$	No active sinusoidal efflux Passive sinusoidal influx and efflux are equal

each of the described methods relies on different assumptions, which might affect the assessment's outcome depending on the pharmacokinetic and physicochemical properties of a drug (Table 1).

Alternatively, Kp$_{uu}$ can be calculated from individual *in vitro* hepatic process clearances (i.e., active and passive hepatic uptake and efflux, metabolism, biliary secretion) according to the extended clearance model (ECM) (Table 1).[8,14-19] Our group recently determined ECM-derived Kp$_{uu}$ data and corresponding intrahepatic concentrations for a set of compounds to predict drug-induced cholestasis from bile salt export pump inhibition data.[19] The approach provided superior predictions as compared to using unbound systemic concentrations, thus demonstrating the utility of the ECM-derived Kp$_{uu}$ method. The *in vivo* relevance of the approach was supported by a close *in vitro–in vivo* correlation of Kp$_{uu}$ in rat.[19] Furthermore, the ECM serves as a drug classification system, which is based on *in vitro* hepatic process clearances (sinusoidal membrane permeability and intrinsic clearance). Four ECM classes have been derived based on the processes that govern hepatic drug clearance and disposition (i.e., Kp$_{uu}$).[14,15,19] ECM class 1 and class 2 compounds enter the liver only via passive diffusion, whereas class 3 and class 4 compounds require additional transporter-mediated hepatic uptake. The intrinsic clearance of ECM class 1 and 3 compounds is higher than passive sinusoidal permeability. In contrast, passive sinusoidal permeability exceeds the intrinsic clearance of class 2 and class 4 compounds. According to the ECM concept (Table 1), the Kp$_{uu}$ of ECM class 1 and class 3 compounds is typically <1 (i.e., PS$_{eff}$ + CL$_{int}$ > PS$_{inf}$) due to the predominant role of intrinsic clearance. In contrast, for class 3 compounds that exhibit substantial hepatic uptake, Kp$_{uu}$ is > 1 (i.e., PS$_{eff}$ + CL$_{int}$ < PS$_{inf}$). ECM class 2 compounds display Kp$_{uu}$ values close to 1 because intrinsic clearance is compensated by predominant passive membrane permeability (i.e., PS$_{eff}$ + CL$_{int}$ ≈ PS$_{inf}$). ECM class 4 compounds exhibit Kp$_{uu}$ values > 1 as a result of active hepatic uptake and predominant passive membrane permeability (i.e., PS$_{eff}$ + CL$_{int}$ < PS$_{inf}$).

We recently demonstrated the *in vivo* relevance and usefulness of ECM-derived Kp$_{uu}$ data, which however represents a labor-intensive approach to obtain hepatic Kp$_{uu}$. It was therefore the aim of the present study to compare the ECM method with 3 alternative approaches for hepatic Kp$_{uu}$ determination as outlined in Table 1. A test set of 18 drug compounds with diverse physicochemical and pharmacokinetic properties was analyzed under uniform conditions according to the homogenization, temperature, and logD$_{7.4}$ methods. The obtained Kp$_{uu}$ and fu$_{hep}$ data were compared among the investigated methods and were correlated with ECM-based data. Differences in the outcome were examined with regard to physicochemical and pharmacokinetic compound properties.

Methods

Test Compounds

[^{3}H]Glibenclamide (1.48 MBq/nmol), [^{3}H]rosiglitazone (1.927 MBq/nmol), and [^{3}H]verapamil (3.067 MBq/nmol) were obtained from PerkinElmer (Boston, MA). [^{3}H]Atorvastatin calcium (0.37 MBq/nmol), [^{3}H]cerivastatin sodium (0.185 MBq/nmol), [^{14}C]erythromycin (0.002035 MBq/nmol), [^{3}H]fluvastatin sodium (0.74 MBq/nmol), [^{14}C]ibuprofen (0.002035 MBq/nmol), [^{3}H]ketoconazole (0.37 MBq/nmol), [^{3}H]lovastatin acid sodium (0.37 MBq/nmol), [^{3}H]pitavastatin calcium (0.182 MBq/nmol), [^{3}H]pravastatin calcium (0.37 MBq/nmol), [^{3}H]rosuvastatin calcium (0.37 MBq/nmol), and [^{3}H]simvastatin acid sodium (0.37 MBq/nmol) were obtained from American Radiolabeled Chemicals (St. Louis, MO). [^{3}H]Atazanavir sulfate (0.037 MBq/nmol), [^{3}H]bosentan (0.148 MBq/nmol), and [^{3}H]cyclosporine A (1.295 MBq/nmol) were obtained from Moravek Biochemicals (Brea, CA). [^{14}C]Imatinib mesylate (0.001988 MBq/nmol) was synthesized in the Isotope Laboratories, Novartis Pharma AG (Basel, Switzerland). Radiochemical purity of all compounds was ≥95% as determined in-house by HPLC analysis. All other chemicals were purchased from commercial sources and were of analytical grade.

Thawing and Preparation of Hepatocytes

Cryopreserved primary human hepatocytes (pool of 20 donors, lot: PQP; Bioreclamation IVT, Baltimore, MD) used in steady-state hepatocellular uptake and equilibrium dialysis experiments have been qualified for transporter activity by the vendor. The activity of the most relevant hepatic uptake transporters (organic anion-transporting polypeptides, organic cation transporter 1, sodium taurocholate cotransporting polypeptide) was also confirmed internally by determining the ratio of uptake clearances at 37°C and 4°C for reference substrates. The OATP1B1 substrate estrone-3-sulfate was measured in each experiment and uptake ratios were on average 5.6 ± 1.0.

Upon thawing of the cryopreserved hepatocytes,[20] living and dead cells were counted using a NucleoCounter NC-100 (Chemo-Metec, Allerod, Denmark). The resulting cell viability was on average 88 ± 6%. Hepatocytes were resuspended (2 × 10^6 viable hepatocytes/mL) in prewarmed Krebs-Henseleit buffer (KHB) containing 1 mM of the pan-cytochrome P450 (CYP) inhibitor 1-aminobenzotriazole (ABT). The cell suspensions were pre-incubated for 15 min for complete inhibition of CYP activity.[21]

Determination of Kp From Steady-State Hepatocyte Uptake Experiments

Cellular uptake was initiated by mixing the hepatocyte suspension with the incubation solution (KHB containing 1 mM ABT and test compound) to obtain final concentrations of 1.3×10^5 viable hepatocytes/mL and 0.05 μM or 0.5 μM for ^{3}H- or ^{14}C-labeled compounds, respectively. All incubations were carried out at 37°C under gentle shaking. Incubations were terminated after 30 and 60 min using the oil-spin method (Hepatocyte Transporter Suspension Assay Kit, BD Biosciences, Woburn, MA)[20] and the drug amount in hepatocytes and media was quantified by liquid scintillation counting. Subsequently, Kp was calculated according to Equation 1:

$$Kp = \frac{C_{hep}}{C_{med}} \qquad (1)$$

where C_{hep} and C_{med} are the compound concentrations in hepatocytes and in media, respectively. C_{hep} was calculated based on cell number and volume assuming a cell diameter of 16.2 μm and a spherical cell shape.[10]

Kp was determined at 30 and 60 min. For all compounds, the concentration equilibrium was achieved at 60 min, and Kp was calculated for this time point. To investigate the impact of lysosomal trapping on Kp of positively charged compounds (erythromycin, imatinib, verapamil), additional incubations were performed in the presence of 0.5 mM chloroquine.

Unbound Fraction in Hepatocytes

Temperature Method

Shitara et al.[8] previously described the determination of fu_{hep} from steady-state hepatocyte uptake experiments at 4°C ($fu_{hep,temp}$). Accordingly, hepatocyte uptake experiments were conducted for 60 min as described previously except that incubations were maintained at 4°C. The impact of lysosomal trapping on $fu_{hep,temp}$ of positively charged compounds (erythromycin, imatinib, verapamil) was investigated in additional incubations in the presence of 0.5 mM chloroquine.

Assuming complete inactivation of uptake transporters at 4°C and concentration equilibrium of the unbound drug between media and hepatocytes, the unbound fraction is defined as the ratio of the unbound concentrations in the media ($C_{med,u}$) and in the hepatocytes ($C_{hep,u}$):

$$C_{med,u} = C_{hep,u} = C_{hep} \times fu_{hep,temp} \qquad (2)$$

In the absence of nonspecific binding in the media compartment (i.e., $C_{med} = C_{med,u}$), Equation 2 can be rearranged as follows:

$$fu_{hep,temp} = \frac{C_{med}}{C_{hep}} \qquad (3)$$

Homogenization Method

The determination of fu_{hep} using equilibrium dialysis ($fu_{hep,hom}$) was adapted from Mateus et al.[10] Hepatocyte suspensions were homogenized using a Dounce homogenizer (glass/teflon, tight, 50 strokes) and mixed with incubation solutions (KHB containing 1 mM ABT and test compound). Final concentrations were 0.05 μM or 0.5 μM for ^{3}H- or ^{14}C-labeled compounds, respectively, and 1.3×10^5 homogenized hepatocytes/mL. The impact of lysosomal trapping on $fu_{hep,hom}$ of positively charged compounds (erythromycin, imatinib, verapamil) was investigated in additional incubations in the presence of 0.5 mM chloroquine. Equilibrium

dialysis was performed using a Rapid Equilibrium Dialysis device (molecular weight cutoff: 8 kDa, Thermo Fisher Scientific Inc., Rockford, IL) by placing 300 μL of compound-containing hepatocyte homogenates and 500 μL of KHB buffer containing 1 mM ABT into the respective chambers. The dialysis unit was incubated at 37°C on an orbital shaker (250 rpm) for 4 h. After the incubations, aliquots from both chambers were taken and the drug amount was quantified by liquid scintillation counting. The unbound fraction in the homogenate (fu_{hom}) was calculated as follows:

$$fu_{hom} = \frac{C_{buffer}}{C_{hom}} \qquad (4)$$

where C_{hom} and C_{buffer} are the compound concentrations in the homogenate and in the buffer chamber, respectively. Subsequently, $fu_{hep,hom}$ was calculated according to Equation 5:

$$fu_{hep,hom} = \frac{1}{D \times \left(\frac{1}{fu_{hom}} - 1\right) + 1} \qquad (5)$$

where D is the homogenate dilution factor. D was estimated to be 337 assuming a cell diameter of 16.2 μm and spherical cell shape.[10]

logD$_{7.4}$ Method

The empirical model to predict fu_{hep} from $logD_{7.4}$ ($fu_{hep,logD}$) was developed by Yabe et al.[9] $fu_{hep,logD}$ was calculated as follows:

$$logfu_{hep,logD} = -0.9161 - 0.2567 \times logD_{7.4} \qquad (6)$$

$logD_{7.4}$ values and corresponding literature references are summarized in Table 2.

Calculation of Kp$_{uu}$

For all compounds, Kp_{uu} was calculated using Kp from steady-state hepatocyte uptake experiments and fu_{hep} either based on the temperature method ($Kp_{uu,temp}$), the homogenization method ($Kp_{uu,hom}$), or the $logD_{7.4}$ method ($Kp_{uu,logD}$) according to Equations 7-9:

$$Kp_{uu,temp} = Kp \times fu_{hep,temp} \qquad (7)$$

$$Kp_{uu,hom} = Kp \times fu_{hep,hom} \qquad (8)$$

$$Kp_{uu,logD} = Kp \times fu_{hep,logD} \qquad (9)$$

Determination of Kp$_{uu}$ Using the Extended Clearance Model

The ECM method has been proposed for the prediction of overall intrinsic hepatic clearance ($CL_{int,h}$) using *in vitro* process clearances as follows[8,17,18,22]:

$$CL_{h,int} = $$
$$\frac{PS_{inf,act} + PS_{inf,pas}}{PS_{eff,act} + PS_{eff,pas} + CL_{int,met} + CL_{int,sec}} \times (CL_{int,met} + CL_{int,sec})$$
$$= \frac{PS_{inf}}{PS_{eff} + CL_{int}} \times CL_{int} = Kp_{uu} \times CL_{int} \qquad (10)$$

where PS_{inf} is the sum of active ($PS_{inf,act}$) and passive uptake membrane permeability ($PS_{inf,pas}$), PS_{eff} is the sum of active

Table 2

Parameters for Kp and fu$_{hep}$ Obtained From Temperature, Homogenization, and logD$_{7.4}$ Method and Physicochemical Properties

Compound	Kp[a]	fu$_{hep,temp}$[a]	fu$_{hep,hom}$[a]	fu$_{hep,logD}$	logD$_{7.4}$	MW	Charge at pH 7.4
Atazanavir	180.19 ± 6.82	0.0359 ± 0.0026	0.0049 ± 0.0006	0.0040	5.77[43]	704.9	Neutral
Atorvastatin	240.73 ± 4.79	0.0284 ± 0.0015	0.0027 ± 0.0001	0.0563	1.30[24]	558.6	Negative
Bosentan	38.64 ± 1.90	0.0801 ± 0.0165	0.0025 ± 0.0006	0.0579	1.25[9]	551.6	Negative
Cerivastatin	455.77 ± 21.76	0.0168 ± 0.0007	0.0028 ± 0.0005	0.0395	1.90[24]	459.6	Negative
Cyclosporine A	705.93 ± 47.70	0.0239 ± 0.0023	0.0001 ± 0.0000	0.0216	2.92[44]	1202.6	Neutral
Erythromycin	28.87 ± 1.16	0.3968 ± 0.1378	0.0038 ± 0.0003	0.0633	1.10[9]	733.9	Positive
Fluvastatin	219.22 ± 10.58	0.0150 ± 0.0014	0.0123 ± 0.0027	0.0471	1.60[24]	411.5	Negative
Glibenclamide	142.82 ± 2.51	0.0212 ± 0.0008	0.0072 ± 0.0006	0.0332	2.19[45]	494.0	Negative
Ibuprofen	8.32 ± 0.70	0.1410 ± 0.0298	0.0246 ± 0.0050	0.0752	0.81[46]	206.3	Negative
Imatinib	381.21 ± 17.72	0.0071 ± 0.0008	0.0034 ± 0.0000	0.0294	2.40[47]	493.6	Positive
Ketoconazole	421.11 ± 14.79	0.0023 ± 0.0001	0.0017 ± 0.0002	0.0111	4.05[44]	531.4	Neutral
Lovastatin acid	256.81 ± 38.05	0.0309 ± 0.0017	0.0075 ± 0.0016	0.0497	1.51[24]	404.5	Negative
Pitavastatin	291.61 ± 35.24	0.0221 ± 0.0040	0.0072 ± 0.0019	0.0500	1.50[24]	421.5	Negative
Pravastatin	10.72 ± 1.20	0.1689 ± 0.0066	0.0130 ± 0.0039	0.1537	−0.40[24]	424.5	Negative
Rosiglitazone	37.72 ± 5.40	0.0188 ± 0.0039	0.0097 ± 0.0012	0.0261	2.60[48]	357.4	Neutral
Rosuvastatin	50.08 ± 2.66	0.1317 ± 0.0063	0.0141 ± 0.0081	0.2048	−0.89[24]	481.5	Negative
Simvastatin acid	536.63 ± 15.97	0.0366 ± 0.0010	0.0037 ± 0.0005	0.0399	1.88[24]	436.6	Negative
Verapamil	302.33 ± 14.29	0.0024 ± 0.0002	0.0022 ± 0.0004	0.0431	1.75[44]	454.6	Positive

MW, molecular weight (g/mol).

[a] Data represent mean ± SD of triplicates.

(PS$_{eff,act}$) and passive sinusoidal efflux membrane permeability (PS$_{eff,pas}$) and CL$_{int}$ is the sum of intrinsic metabolic (CL$_{int,met}$) and biliary clearances (CL$_{int,sec}$) (Table 3).

Accordingly, ECM-based Kp$_{uu}$ values (Kp$_{uu,ECM}$) can be calculated according to Equation 11:

$$Kp_{uu,ECM} = \frac{PS_{inf}}{PS_{eff} + CL_{int}} \qquad (11)$$

Kp$_{uu,ECM}$ for the 18 test compounds were taken from Riede et al.[19] The underlying hepatic process clearances were experimentally determined as described in full detail elsewhere.[20,23-25] In brief, PS$_{inf,act}$ and PS$_{inf,pas}$ were determined from incubations with suspended human hepatocytes within the linear time and concentration range using the oil-spin method. PS$_{inf,pas}$ was determined in the presence of uptake transporter inhibitors or at high substrate concentrations where active transport processes are known to be saturated. PS$_{eff}$ was assumed to occur only via passive diffusion and to be equal to PS$_{inf,pas}$ (PS$_{eff,act}$ = 0, PS$_{eff,pas}$ = PS$_{inf,pas}$). CL$_{int,met}$ was determined using human liver microsomes taking the experimentally determined unbound fraction in microsomes into account. CL$_{int,sec}$ was determined in sandwich-cultured human hepatocytes (B-CLEAR® method; Qualyst, Inc., Durham, NC) and was corrected for the unbound fraction in hepatocytes (logD$_{7.4}$ method).

ECM classes were assigned as follows: ECM class 1/2 was assigned if PS$_{eff}$ < CL$_{int}$, otherwise class 3/4. Class 1/3 was assigned if PS$_{eff}$ = PS$_{inf}$, otherwise class 2/4.[14]

Physicochemical Properties

Molecular weight and logD$_{7.4}$ values were obtained from the literature. Molecular charge at pH 7.4 was calculated using ADMET Predictor 8.0 (Simulations Plus, Lancaster, CA).

Statistical Analysis

Experimental data generally represent means of triplicates, and experimental errors are indicated by standard deviations (SDs). SDs of composed parameters (z) upon summation and multiplication of 2 independent parameters (x and y) were calculated according to Equations 12 and 13, respectively:

$$SD_z = \sqrt{SD_x^2 + SD_y^2} \qquad (12)$$

$$\frac{SD_z}{|z|} = \sqrt{\left(\frac{SD_x}{|x|}\right)^2 + \left(\frac{SD_y}{|y|}\right)^2} \qquad (13)$$

The correlation between Kp$_{uu}$ or fu$_{hep}$ values obtained from different methods was assessed by fold-error deviations (% fold deviation <3 or <10) and average fold errors (AFEs) according to Equation 14:

$$AFE = 10^{\frac{1}{n}\sum \log\frac{y}{x}} \qquad (14)$$

where n is the number of data points, and x and y represent corresponding Kp$_{uu}$ or fu$_{hep}$ values on the x-axis and y-axis, respectively.

Results

Determination of Kp and fu$_{hep}$ Values Using the Temperature, Homogenization, and logD$_{7.4}$ Methods

The Kp and fu$_{hep}$ values obtained from the temperature, homogenization, and logD$_{7.4}$ methods for the 18 test compounds are summarized in Table 2. Measured Kp values in human hepatocytes were within a range of 8.32 and 706. The experimental variability (SD) was on average ±7% of the mean Kp values. High Kp values generally correlated with higher logD$_{7.4}$ and positive charge; however, because Kp determinations at 37°C were partially governed by active transport processes, correlations with molecular charge became more evident when Kp was calculated from 4°C incubations, where active transport processes are inactive (where Kp = 1/fu$_{hep,temp}$). The mean Kp values from 4°C experiments were 31.50 (range: 5.92−66.7) for negatively charged compounds and increased to 140 (range: 27.8−436) for neutral compounds and to 188 (range: 2.52−420) for positively charged compounds.

Figure 1 shows the correlation of the fraction unbound in human hepatocytes obtained from the 3 different methods. fu$_{hep}$ values determined with the temperature and logD$_{7.4}$ methods were markedly higher compared to fu$_{hep}$ using the homogenization method for most of the compounds. This observation was supported by AFE values of 6.67 and 9.31, respectively (Figs. 1a and 1b) with only 33% and 11% of the corresponding measured values lying

Table 3
ECM Classification and Hepatic *In Vitro* Process Clearances

Compound	ECM Class	$PS_{inf,act}$	$PS_{inf,pas} = PS_{eff}$	$CL_{int,met}$	$CL_{int,sec}$
		mL/min/kg			
Atazanavir	3	71.8 ± 10.7	20.8 ± 6.0	1240.5 ± 105.5	81.9 ± 29.8
Atorvastatin	3	140.3 ± 88.0	57.7 ± 9.2	64.6^a	11.1 ± 9.0
Bosentan	4	30.7 ± 11.2	61.5 ± 6.6	16.2 ± 3.0	0.8 ± 12.4
Cerivastatin	4	221.5 ± 14.0	243.8 ± 10.3	46.9^a	0
Cyclosporine A	3	113.2 ± 10.6	41.9 ± 4.2	77.6^a	9.1^a
Erythromycin	3	10.2 ± 5.1	20.3 ± 2.4	99.7^a	8.9 ± 1.4
Fluvastatin	4	218.7 ± 49.3	325.5 ± 31.5	146.8^a	0
Glibenclamide	4	66.4 ± 28.8	109.6 ± 13.9	41.1^a	6.3 ± 5.4
Ibuprofen	3	22.2 ± 5.2	21.7 ± 2.4	34.2 ± 3.5	10.3 ± 4.0
Imatinib	2	0	300.9 ± 45.8	40.9 ± 50.7	3.2 ± 4.7
Ketoconazole	1	0	58.5 ± 31.7	97.4^a	29.6^a
Lovastatin acid	3	165.1 ± 16.7	145.5 ± 9.2	459.0^a	0
Pitavastatin	4	364.3 ± 45.3	258.8 ± 36.8	17.7^a	0
Pravastatin	4	58.0 ± 28.5	36.0 ± 2.1	0.9^a	2.1 ± 0.8
Rosiglitazone	3	45.6 ± 38.6	46.6 ± 26.3	98.1 ± 9.3	0
Rosuvastatin	4	27.2 ± 2.1	24.8 ± 1.2	1.5^a	5.8 ± 1.0
Simvastatin acid	3	116.1 ± 12.5	297.9 ± 12.4	769.2^a	1.5 ± 3.0
Verapamil	2	0	258.2 ± 16.6	127.7 ± 3.3	8.1 ± 29.3

Data represent mean $\pm$ SD of triplicates. *In vitro* process clearances were taken from Riede et al.[19] ECM classes were assigned as follows: ECM class 1/2 was assigned if $PS_{eff} < CL_{int}$, otherwise class 3/4. Class 1/3 was assigned if $PS_{eff} = PS_{inf}$, otherwise class 2/4.[14]
$PS_{inf,act}$, active uptake membrane permeability; $PS_{inf,pas}$, passive uptake membrane permeability; PS_{eff}, sinusoidal efflux membrane permeability; $CL_{int,met}$, intrinsic metabolic clearance; $CL_{int,sec}$, intrinsic biliary clearance.
 [a] SD not available.

within a 3-fold deviation. Several compounds (i.e., atorvastatin, bosentan, cerivastatin, cyclosporine A, erythromycin, pravastatin, rosuvastatin, simvastatin acid, and verapamil) showed discrepancies of even more than 10-fold between $fu_{hep,hom}$ and $fu_{hep,temp}$ or $fu_{hep,logD}$, respectively. As illustrated in Figure 1, these compounds were generally characterized by small $logD_{7.4}$ values (<2) or by a high molecular weight (>1200 g/mol). In contrast, fu_{hep} data from the temperature and $logD_{7.4}$ methods provided more comparable values (AFE = 1.39) with 67% and 94% of the values lying within 3-fold and 10-fold deviations (Fig. 1c). Experimental determination of fu_{hep} using the temperature and homogenization methods was associated with average SDs of $\pm11\%$ and $\pm17\%$ of the mean fu_{hep} values, respectively.

Comparison of In Vitro Kp_{uu} Values

Figure 2 and Table 4 provide comparisons of previously determined ECM-based Kp_{uu} values ($Kp_{uu,ECM}$) with measured Kp_{uu} values using either the temperature ($Kp_{uu,temp}$), homogenization ($Kp_{uu,hom}$), or $logD_{7.4}$ method ($Kp_{uu,logD}$). Kp_{uu} values from the temperature method exceeded the corresponding $Kp_{uu,ECM}$ values for most test compounds as indicated by an AFE of 5.01 (Fig. 2a). Here, 44% and 72% of $Kp_{uu,temp}$ values were within a 3-fold or 10-fold deviation from $Kp_{uu,ECM}$ values, respectively. Similarly, Kp_{uu} values from the $logD_{7.4}$ method were higher than the respective $Kp_{uu,ECM}$ values for most of the compounds (AFE = 6.98) with only 22% and 56% of Kp_{uu} values lying within 3-fold or 10-fold deviation, respectively (Fig. 2b). In contrast, Kp_{uu} values from the homogenization method demonstrated the closest correlation with $Kp_{uu,ECM}$ values as indicated by an AFE value close to unity (0.75). More than half of the compounds (61%) deviated by less than 3-fold and 78% were within a 10-fold range (Fig. 2c). In line with fu_{hep} data, relevant negative deviations (>2-fold) between $Kp_{uu,hom}$ and corresponding $Kp_{uu,ECM}$ values were only observed for compounds with a $logD_{7.4}$ <1.5 or a molecular weight >1200 g/mol. Experimental variability of the individual Kp_{uu} methods was generally in a comparable range. Average SDs of $Kp_{uu,temp}$, $Kp_{uu,hom}$, and $Kp_{uu,ECM}$ were $\pm14\%$, $\pm19\%$, and $\pm19\%$ of the respective mean values, whereas $Kp_{uu,logD}$ values were on average associated with lower variability

($\pm7\%$ SD) because the empirical determination of $fu_{hep,logD}$ was not associated with experimental variability.

Among the different methods, Kp_{uu} derived from the ECM represented the only approach that incorporated intrinsic hepatic clearance processes (metabolism and biliary secretion) (Table 3). Hence, we examined whether intrinsic clearance could explain the observed differences in Kp_{uu} between the different methods by plotting the CL_{int}/PS_{eff} ratio against the deviation between the Kp_{uu} methods (Fig. 3). High positive deviations (>5-fold) between $Kp_{uu,temp}$ and $Kp_{uu,ECM}$ values proportionally increased with the contribution of intrinsic clearance (i.e., for the ECM class 3 compounds atazanavir, cyclosporine A, erythromycin, lovastatin acid, simvastatin acid) (Fig. 3a). In contrast, close correlations were obtained for drugs with low CL_{int}/PS_{eff} ratios (ECM class 2, class 4, and several class 1 and class 3 compounds). Similarly, the highest positive deviations between $Kp_{uu,hom}$ and $Kp_{uu,ECM}$ values or $Kp_{uu,logD}$ and $Kp_{uu,ECM}$ values were observed for ECM class 3 compounds (i.e., for atazanavir, lovastatin acid, simvastatin acid), however, no linear correlation with predominant intrinsic clearance processes was observed, and deviations were much lower compared to the temperature method (Figs. 3b and 3c). $Kp_{uu,hom}$ values were on average lower than $Kp_{uu,ECM}$ even for compounds with relevant intrinsic clearance (e.g., cyclosporine A and erythromycin), whereas $Kp_{uu,logD}$ values were generally higher and showed more scattering compared with ECM-based data.

Impact of Lysosomal Trapping on Kp_{uu}

The effect of lysosomal accumulation on Kp, fu_{hep}, and Kp_{uu} was investigated for the positively charged compounds in our data set by incubations in the presence of chloroquine. Chloroquine has previously been shown to reduce the lysosomal trapping of lipophilic bases by increasing the lysosomal pH, thus decreasing cellular drug accumulation.[10,26,27] In the presence of chloroquine, Kp values of verapamil, erythromycin, and imatinib were reduced by 2.3-fold, 3.7-fold, and 8.9-fold, respectively (Table 5). In addition, the unbound fraction increased on average by 2-fold in the presence of chloroquine. The result indicates that the pH gradient between cytosol and lysosomes was partially maintained even at 4°C
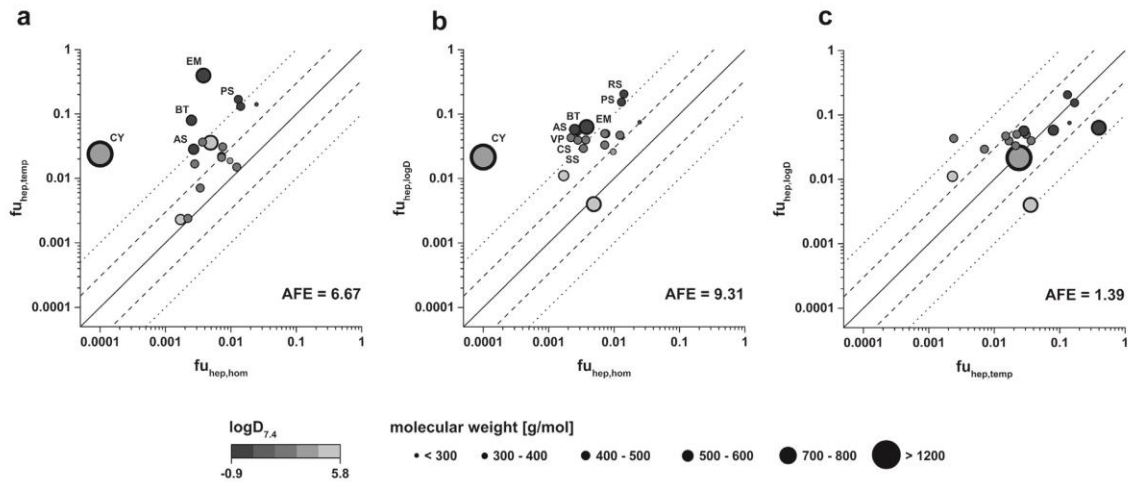
Figure 1. Correlation between fu_{hep} values obtained from temperature and homogenization methods (a), $logD_{7.4}$ and homogenization methods (b), or $logD_{7.4}$ and temperature methods (c). The solid line represents the line of unity, and dashed and dotted lines represent 3-fold and 10-fold deviations, respectively. AS, atorvastatin; BT, bosentan; CS, cerivastatin; CY, cyclosporine A; EM, erythromycin; PS, pravastatin; RS, rosuvastatin; SS, simvastatin; VP, verapamil.

and after cell homogenization. The resulting Kp_{uu} values were 1.6-fold to 5.2-fold lower in the presence of chloroquine, representing distribution of the unbound drug without accumulation in the lysosomal compartment. Only the Kp_{uu} of verapamil, analyzed by the temperature method, was nearly unchanged in the presence of chloroquine.

Discussion

Our group recently established an approach for measuring Kp_{uu} *in vitro* using the ECM and predicted drug-induced cholestasis based on resulting unbound intrahepatic drug concentration and BSEP inhibition data.[19] In the present study, we applied 3 alternative methods for the determination of fu_{hep} and Kp_{uu} (temperature method, homogenization method, and $logD_{7.4}$ method) for comparison with the ECM approach. Differences in the obtained results were mostly related to underlying assumptions and experimental setup as discussed in the following.

Previous work by our group has demonstrated the validity of the *in vitro*–based hepatic ECM for different *in vitro*–*in vivo* extrapolation applications including hepatic clearance and DDI predictions as well as for the estimation of hepatic Kp_{uu} in humans.[19,23-25,28] The ECM concept includes the assumptions that (1) sinusoidal efflux occurs only via passive diffusion and (2) passive sinusoidal influx and efflux permeability is equal. Both factors, however, appear to be of limited relevance for most pharmaceutical drugs because previous work provided successful *in vitro*–*in vivo* extrapolation for hepatic clearance and Kp_{uu} based on the ECM. Moreover, the *in vivo* relevance of this approach has further been corroborated by an *in vitro*–*in vivo* comparison of the ECM-based Kp_{uu} in rat.[19] Therefore, Kp_{uu} data obtained from the investigated alternative methods were primarily compared with ECM-based Kp_{uu} data. The corresponding deviations in Kp_{uu} data were closely linked to the underlying assumptions of each method as outlined in Table 1. Thereby, the most fundamental difference to the ECM approach was the absence of intrinsic hepatic clearance processes (i.e., sum of metabolism and biliary secretion) in Kp
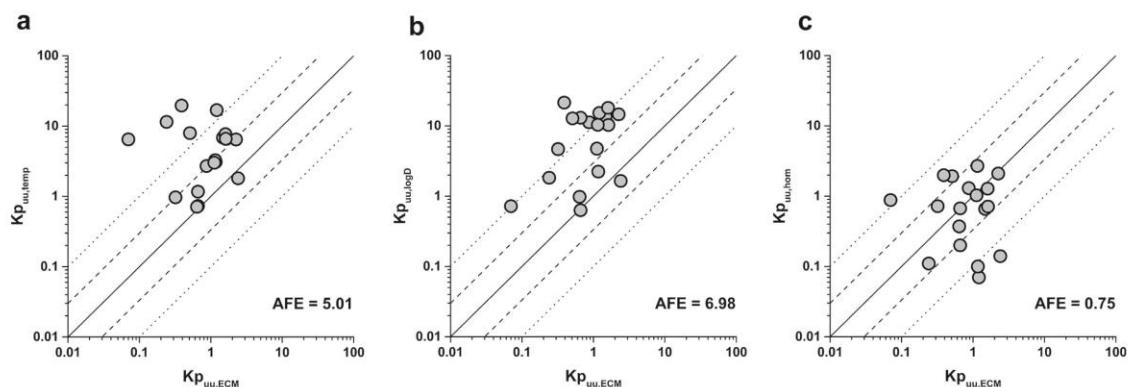

Figure 2. Correlation between Kp_{uu} values obtained from the ECM and either temperature method (a), $logD_{7.4}$ method (b), or homogenization method (c). The solid line represents the line of unity, and dashed and dotted lines represent 3-fold and 10-fold deviations, respectively.

Table 4

Kp_{uu} Values Obtained From the ECM, Temperature, Homogenization, and $logD_{7.4}$ Methods, and ECM Classification

Compounds	ECM Class	Kp_{uu}			
		ECM Method	Temperature Method	Homogenization Method	$logD_{7.4}$ Method
Atazanavir	3	0.07 ± 0.01	6.47 ± 0.53	0.88 ± 0.11	0.72 ± 0.03
Atorvastatin	3	1.48 ± 0.68^a	6.84 ± 0.38	0.66 ± 0.03	13.55 ± 0.27
Bosentan	4	1.17 ± 0.24	3.10 ± 0.66	0.10 ± 0.02	2.24 ± 0.11
Cerivastatin	4	1.60 ± 0.08^a	7.66 ± 0.47	1.28 ± 0.24	18.00 ± 0.86
Cyclosporine A	3	1.21 ± 0.09^a	16.87 ± 1.98	0.07 ± 0.00	15.25 ± 1.03
Erythromycin	3	0.24 ± 0.04^a	11.46 ± 4.01	0.11 ± 0.01	1.83 ± 0.07
Fluvastatin	4	1.15 ± 0.15^a	3.29 ± 0.34	2.70 ± 0.61	10.33 ± 0.50
Glibenclamide	4	1.12 ± 0.19^a	3.03 ± 0.13	1.03 ± 0.09	4.74 ± 0.08
Ibuprofen	3	0.66 ± 0.09	1.17 ± 0.27	0.20 ± 0.04	0.63 ± 0.05
Imatinib	2	0.87 ± 0.18	2.71 ± 0.46	1.30 ± 0.16	11.21 ± 1.40
Ketoconazole	1	0.32 ± 0.18^a	0.97 ± 0.05	0.72 ± 0.09	4.67 ± 0.16
Lovastatin acid	3	0.51 ± 0.03^a	7.94 ± 1.25	1.93 ± 0.50	12.76 ± 1.89
Pitavastatin	4	2.25 ± 0.37^a	6.44 ± 1.40	2.10 ± 0.61	14.58 ± 1.76
Pravastatin	4	2.41 ± 0.74^a	1.81 ± 0.22	0.14 ± 0.04	1.65 ± 0.19
Rosiglitazone	3	0.64 ± 0.23	0.71 ± 0.18	0.37 ± 0.07	0.98 ± 0.14
Rosuvastatin	4	$1.62^a \pm 0.11$	6.59 ± 0.47	0.71 ± 0.41	10.28 ± 0.55
Simvastatin acid	3	$0.39^a \pm 0.02$	19.64 ± 0.80	1.99 ± 0.28	21.41 ± 0.64
Verapamil	2	0.66 ± 0.07	0.73 ± 0.07	0.67 ± 0.13	13.03 ± 0.62

Data represent mean $\pm$ SD of triplicates. ECM-derived Kp_{uu} data were taken from Riede et al.[19]

^{a} No SD available for CL_{int} as indicated in Table 3.

measurements with the temperature, homogenization and $logD_{7.4}$ methods using isolated hepatocytes in suspension. These cells are known to express biliary efflux transporters only to a limited extent on account of the lack cellular polarization.[29] Therefore, an integrated assessment including biliary secretion is not feasible in this *in vitro* system.[30] In addition, the activity of metabolic enzymes was blocked by the pan-CYP inhibitor ABT[21] to achieve steady-state equilibrium of parent drug compound between hepatocytes and media. In contrast, metabolic and biliary clearance processes are integrated in the ECM-based Kp_{uu}, as they are measured in independent liver microsomes and sandwich-cultured hepatocyte (B-CLEAR method) experiments. Incorporation of intrinsic clearance processes generally results in a decreasing hepatic Kp_{uu} (Eq. 11). Nevertheless, a substantial impact on Kp_{uu} is only expected for compounds, where the intrinsic clearance is exceeding the sinusoidal diffusion ($CL_{int} > PS_{eff}$, ECM class 1 and class 3 compounds).[3,14,15,19] Indeed, the largest positive deviations between ECM and the temperature, homogenization, or $logD_{7.4}$ methods were observed for ECM class 3 compounds such as atazanavir or simvastatin acid (Fig. 3). In particular, Kp_{uu} deviations between the temperature and ECM methods indicated a clear correlation with

the extent of intrinsic clearance (Fig. 3a). In contrast, ECM class 1 and class 3 compounds with limited intrinsic clearance as well as ECM class 2 and class 4 compounds, where passive membrane permeability exceeds the intrinsic clearance ($CL_{int} < PS_{eff}$), showed a close correlations in Kp_{uu} between the ECM and the temperature method. Taken together, these aspects explain the different results from the alternative Kp_{uu} methods to the ECM-based approach.

However, also differences in Kp_{uu} among the temperature, homogenization, or $logD_{7.4}$ methods were obtained. As all 3 methods are based on the same experimental determination of Kp, any differences in Kp_{uu} originated accordingly only from differences in the experimental procedures for fu_{hep} (Table 1). The determination of fu_{hep} using temperature method was associated with the following assumptions: (1) transport processes are completely abolished on ice and (2) drug binding is not temperature-dependent. Although the first assumption is a general concept for *in vitro* transport studies, binding properties have been reported to be either increased or reduced at temperatures lower than 37°C.[31-33] To investigate the impact of temperature on binding properties of our test compounds, we performed parallel incubations at 37°C in the presence of an uptake transporter inhibitor cocktail (data not
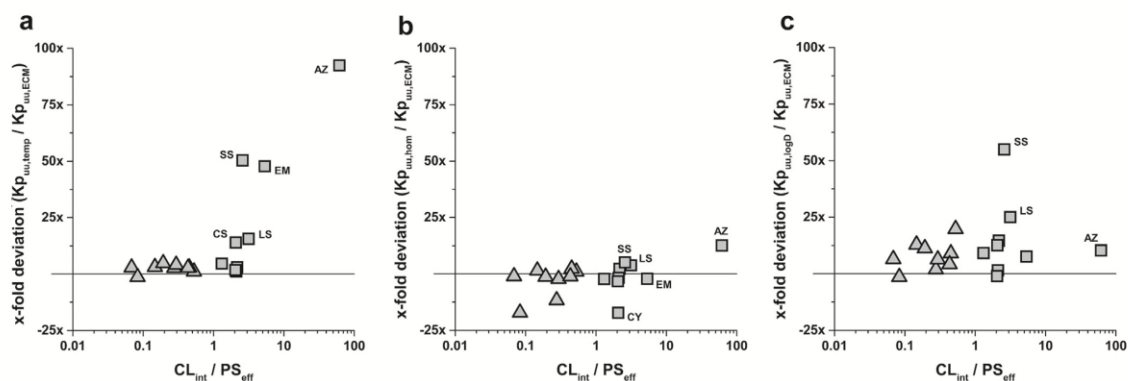

Figure 3. Deviation between either $Kp_{uu,ECM}$ and $Kp_{uu,temp}$ (a), $Kp_{uu,hom}$ (b), or $Kp_{uu,logD}$ (c) depending on the ratio of intrinsic clearance (CL_{int}) to membrane permeability (PS_{eff}). Deviations <1-fold were transformed to negative deviations ($-$x-fold) by the negative reciprocal function. Squares and triangles refer to ECM class 1/3 and class 2/4 compounds, respectively. The solid line represents the line of unity. AZ, atazanavir; CS, cerivastatin; EM, erythromycin; LS, lovastatin; SS, simvastatin.

Table 5
Influence of Chloroquine on Kp, fu$_{hep}$, and Kp$_{uu}$ Values for Basic Drug Compounds

Compounds	Kp	fu$_{hep,temp}$	fu$_{hep,hom}$	Kp$_{uu,temp}$	Kp$_{uu,hom}$
Erythromycin					
−CQ	28.87 ± 1.16	0.3968 ± 0.1378	0.0038 ± 0.0003	11.46 ± 4.01	0.11 ± 0.01
+CQ	7.63 ± 0.98	0.4407 ± 0.0650	0.0082 ± 0.0020	3.36 ± 0.66	0.06 ± 0.02
Imatinib					
−CQ	381.21 ± 47.72	0.0071 ± 0.0008	0.0034 ± 0.0000	2.71 ± 0.46	1.30 ± 0.16
+CQ	42.67 ± 7.31	0.0132 ± 0.0008	0.0058 ± 0.0007	0.56 ± 0.10	0.25 ± 0.05
Verapamil					
−CQ	302.33 ± 14.29	0.0024 ± 0.0002	0.0022 ± 0.0004	0.73 ± 0.07	0.67 ± 0.13
+CQ	129.10 ± 6.75	0.0081 ± 0.0005	0.0032 ± 0.0005	1.05 ± 0.08	0.41 ± 0.07

Data represent mean ± SD of triplicates. −CQ and +CQ refer to the presence or absence of chloroquine (0.5 mM), respectively.
CQ, chloroquine.

shown). The obtained fu$_{hep}$ data correlated well with the corresponding data at 4°C incubations for most test compounds (≤3-fold deviation) suggesting that the temperature only marginally affected the binding in human hepatocytes. Only for cyclosporine A and erythromycin, temperature-dependent deviations of >4-fold were observed, likely resulting from alterations in membrane binding and lysosomal trapping processes, respectively. Izumi et al.[22] recently applied the temperature method to determine Kp$_{uu}$ in human hepatocytes and obtained highly comparable data for an overlapping subset of compounds, thus confirming robustness rather than reproducibility of the data obtained via the temperature method. Because Kp$_{uu}$ from the temperature method correlated well with ECM-based data for drugs in ECM classes 2/4 and 1/3 (with low intrinsic clearance), we conclude that fu$_{hep}$ from the temperature method matches with the corresponding Kp data and provides realistic estimates of Kp$_{uu}$ in the suspended human hepatocytes (Fig. 3a).

The homogenization method has previously been applied to determine fu$_{hep}$ and Kp$_{uu}$ in human embryonic-kidney 293 cells (HEK293).[10] The authors further described generally higher binding in human hepatocytes than in HEK293 cells (average 4.9-fold lower fu$_{hep}$) due to differences in membrane composition and cellular protein content.[10,34] Comparison of our fu$_{hep}$ data for a subset of compounds with the corresponding binding data in HEK293 cells reported by Mateus et al.[10] revealed on average 6.7-fold higher binding in hepatocytes. Therefore, minor differences in experimental procedures such as the homogenization process (ultrasonication as used by Mateus et al.[10] or using a Dounce homogenizer as in the present study) or the cell number in the incubations (0.13 × 10^6 vs. 10 × 10^6 hepatocytes/mL)[10] did not appear to affect fu$_{hep}$ results. The homogenization method implies the fundamental assumption that drug binding to intracellular structures is not affected by the cell homogenization process. Nevertheless, mechanical cell homogenization by ultrasonication or douncing is known to not only disrupt the plasma membrane but also to break cell organelles including intracellular membranes thereby increasing the number of intracellular binding structures.[35,36] This aspect provides a likely explanation for the significantly lower fu$_{hep}$ data obtained with the homogenization method compared with the temperature and logD$_{7.4}$ methods. Among the investigated compounds, low lipophilicity and high molecular weight were associated with the highest deviation in fu$_{hep}$ between the homogenization and temperature or logD$_{7.4}$ methods (Fig. 1). In intact cells, the intracellular distribution of large hydrophobic compounds is likely more restricted compared with drugs with lower molecular weight and higher lipophilicity, which feature high passive membrane permeability[37,38] and thus unlimited access to binding sites of integral membrane proteins. Consequently, upon breakdown of cellular structures, the binding of such molecules to the cell homogenate may be particularly increased which

results in very low fu$_{hep}$ values as shown in Figures 1a and 1b (i.e., for atorvastatin, bosentan, cerivastatin, cyclosporine A, erythromycin, pravastatin, rosuvastatin, simvastatin acid, verapamil). These observations are also linked to the generally lower Kp$_{uu}$ values from the homogenization method compared with the ECM-derived Kp$_{uu}$, and it cannot be excluded that good correlations for compounds with the described properties might result from simultaneous overestimation of Kp and underestimation of fu$_{hep}$. Thus, the homogenization method likely provides good fu$_{hep}$ estimates for compounds with moderate or high logD$_{7.4}$ and rather small molecular weight, whereas the temperature method seems to be reasonably applicable for compounds with low logD$_{7.4}$ and high molecular weight. Further research on a larger set of compounds will be required though to refine these anticipated relationships between physicochemical compound properties and the different fu$_{hep}$ prediction methods.

The logD$_{7.4}$ method is an empirical equation, which has been established by Yabe et al.[9] based on the correlation of experimental fu$_{hep}$ and logD$_{7.4}$ data from 13 drugs and consequently allows to predict fu$_{hep}$ solely from the logD$_{7.4}$ of a compound without requiring any experimental data. The obtained fu$_{hep}$ data for our test compounds showed significant deviations from fu$_{hep}$ derived from the homogenization method but a better correlation with the data from the temperature method. This behavior is likely explained by the fact that fu$_{hep}$ values in the original publication were generated using highly comparable experimental conditions as used for the temperature method in our study. Consequently, we also observed the correlation of Kp at 4°C with logD$_{7.4}$. Resulting Kp$_{uu}$ data derived from the logD$_{7.4}$ method showed the largest deviation to the corresponding data using the ECM or homogenization methods (44% of compounds deviating >10-fold). Although deviations observed with the other methods could mechanistically be explained, the logD$_{7.4}$-based results did not follow a distinct pattern and are considered to be due to the nature of the empirical approach, which does not account for factors such as molecular weight or intrinsic clearance (Figs. 1c and 3b). Nevertheless, the logD$_{7.4}$ method can provide an initial estimate of fu$_{hep}$ in the absence of *in vitro* data. It is also worth noting that the hepatocyte cell volume is a critical parameter for the logD$_{7.4}$ method because calculated Kp and resulting Kp$_{uu}$ values are inversely proportional to the applied cell volume. In the present study, we used a cellular volume of 2.2 µL/10^6 hepatocytes in line with the study by Mateus et al.[10]; however, a range of 2.2-4.5 µL/10^6 hepatocytes has been reported in the literature.[10,12,39-41] Applying a cell volume of 4.5 µL/10^6 hepatocytes[9,41,42] would result in 2-fold lower Kp$_{uu,\,logD}$ values and a closer correlation with Kp$_{uu,ECM}$ data. In contrast, Kp$_{uu}$ estimations using the temperature and homogenization methods are not affected by changing cellular volumes. Although this parameter is also required for the determination of Kp and fu$_{hep}$, the cell volume is ultimately canceled out in the calculation of Kp$_{uu}$ using these methods.

Lysosomal trapping has previously been shown to especially increase the overall cellular accumulation of lipophilic bases with pK_a values in a pH-sensitive range.[10,26] We confirmed these results by inhibiting the lysosomal accumulation of erythromycin, imatinib, and verapamil using chloroquine. In addition, however, we found that also experimentally determined fu_{hep} data were partially affected by lysosomal trapping effects. These data suggest that residual pH gradients between the cytosolic and lysosomal compartments are maintained even on mechanical disruption or at low temperature. Because lysosomal trapping affected the determination of Kp and fu_{hep} to a different extent, special attention is required if the temperature and homogenization methods are applied to lipophilic basic compounds. In contrast, Kp_{uu} based on the ECM represents the distribution of the unbound uncharged drug species only because the charged fraction is assumed to be unable to permeate across membranes. Mechanistic modeling would be required to incorporate the fraction of the unbound charged drug.[10] The unbound charged fraction in the cytosol, which is relevant for DDI or toxicity assessments, however, is assumed to be of limited relevance based on the small pH difference between medium/plasma and cytosol (~0.2 pH units).

Taking into account the assumptions and limitations of the investigated methods (ECM, temperature, homogenization, and $logD_{7.4}$ methods), comparable Kp_{uu} data were obtained for a significant fraction of test compounds. The alternative methods require markedly less experimental effort compared with the resource-intensive ECM-based approach, which involves 4 independent experiments (hepatic uptake in suspended hepatocytes, metabolic clearance in liver microsomes, fraction unbound in microsomes, biliary secretion in sandwich-cultured hepatocytes). However, for compounds with predominant intrinsic clearance (i.e., ECM class 1 and class 3 compounds), unreasonably high Kp_{uu} values were obtained by the alternative methods, and knowledge of the contribution of intrinsic clearance to the overall hepatic drug disposition is only available once the corresponding *in vitro* experiments have been performed. In conclusion, the ECM is considered as the preferred approach for an integrated quantitative determination of hepatic Kp_{uu}. Nevertheless, the alternative methods, in particular the temperature method, provide valid fu_{hep} data if the methods are appropriately selected based on the physicochemical properties of a compound.

Acknowledgments

References

1. Muller PY, Milton MN. The determination and interpretation of the therapeutic index in drug development. *Nat Rev Drug Discov.* 2012;11(10):751-761.
2. Zamek-Gliszczynski MJ, Lee CA, Poirier A, et al. ITC recommendations for transporter kinetic parameter estimation and translational modeling of transport-mediated PK and DDIs in humans. *Clin Pharmacol Ther.* 2013;94(1):64-79.
3. Pfeifer ND, Harris KB, Yan GZ, Brouwer KL. Determination of intracellular unbound concentrations and subcellular localization of drugs in rat sandwich-cultured hepatocytes compared with liver tissue. *Drug Metab Dispos.* 2013;41(11):1949-1956.
4. Chu X, Korzekwa K, Elsby R, et al. Intracellular drug concentrations and transporters: measurement, modeling, and implications for the liver. *Clin Pharmacol Ther.* 2013;94(1):126-141.
5. Friden M, Bergstrom F, Wan H, et al. Measurement of unbound drug exposure in brain: modeling of pH partitioning explains diverging results between the brain slice and brain homogenate methods. *Drug Metab Dispos.* 2011;39(3):353-362.
6. Friden M, Gupta A, Antonsson M, Bredberg U, Hammarlund-Udenaes M. In vitro methods for estimating unbound drug concentrations in the brain interstitial and intracellular fluids. *Drug Metab Dispos.* 2007;35(9):1711-1719.
7. Parker AJ, Houston JB. Rate-limiting steps in hepatic drug clearance: comparison of hepatocellular uptake and metabolism with microsomal metabolism of saquinavir, nelfinavir, and ritonavir. *Drug Metab Dispos.* 2008;36(7):1375-1384.
8. Shitara Y, Maeda K, Ikejiri K, Yoshida K, Horie T, Sugiyama Y. Clinical significance of organic anion transporting polypeptides (OATPs) in drug disposition: their roles in hepatic clearance and intestinal absorption. *Biopharm Drug Dispos.* 2013;34(1):45-78.
9. Yabe Y, Galetin A, Houston JB. Kinetic characterization of rat hepatic uptake of 16 actively transported drugs. *Drug Metab Dispos.* 2011;39(10):1808-1814.
10. Mateus A, Matsson P, Artursson P. Rapid measurement of intracellular unbound drug concentrations. *Mol Pharm.* 2013;10(6):2467-2478.
11. Morse BL, Cai H, MacGuire JG, et al. Rosuvastatin liver partitioning in cynomolgus monkeys: measurement in vivo and prediction using in vitro monkey hepatocyte uptake. *Drug Metab Dispos.* 2015;43(11):1788-1794.
12. Riccardi K, Li Z, Brown JA, et al. Determination of unbound partition coefficient and in vitro-in vivo extrapolation for SLC13A transporter-mediated uptake. *Drug Metab Dispos.* 2016;44(10):1633-1642.
13. Schuhmann G, Fichtl B, Kurz H. Prediction of drug distribution in vivo on the basis of in vitro binding data. *Biopharm Drug Dispos.* 1987;8(1):73-86.
14. Camenisch G, Riede J, Kunze A, Huwyler J, Poller B, Umehara K. The extended clearance model and its use for the interpretation of hepatobiliary elimination data. *ADMET & DMPK.* 2015;3(1):1-14.
15. Camenisch GP. Drug disposition classification systems in discovery and development: a comparative review of the BDDCS, ECCS and ECCCS concepts. *Pharm Res.* 2016;33(11):2583-2593.
16. Varma MV, Bi YA, Kimoto E, Lin J. Quantitative prediction of transporter- and enzyme-mediated clinical drug-drug interactions of organic anion-transporting polypeptide 1B1 substrates using a mechanistic net-effect model. *J Pharmacol Exp Ther.* 2014;351(1):214-223.
17. Kusuhara H, Sugiyama Y. In vitro-in vivo extrapolation of transporter-mediated clearance in the liver and kidney. *Drug Metab Pharmacokinet.* 2009;24(1):37-52.
18. Shitara Y, Horie T, Sugiyama Y. Transporters as a determinant of drug clearance and tissue distribution. *Eur J Pharm Sci.* 2006;27(5):425-446.
19. Riede J, Poller B, Huwyler J, Camenisch G. Assessing the risk of drug-induced cholestasis using unbound intrahepatic concentrations. *Drug Metab Dispos.* 2017;45(5):523-553.
20. Kunze A, Huwyler J, Camenisch G, Poller B. Prediction of organic anion-transporting polypeptide 1B1- and 1B3-mediated hepatic uptake of statins based on transporter protein expression and activity data. *Drug Metab Dispos.* 2014;42(9):1514-1521.
21. Kimoto E, Walsky R, Zhang H, et al. Differential modulation of cytochrome P450 activity and the effect of 1-aminobenzotriazole on hepatic transport in sandwich-cultured human hepatocytes. *Drug Metab Dispos.* 2012;40(2):407-411.
22. Izumi S, Nozaki Y, Komori T, et al. Comparison of the predictability of human hepatic clearance for organic anion transporting polypeptide substrate drugs between different in vitro-in vivo extrapolation approaches. *J Pharm Sci.* 2017 [Epub ahead of print].
23. Umehara K, Camenisch G. Novel in vitro-in vivo extrapolation (IVIVE) method to predict hepatic organ clearance in rat. *Pharm Res.* 2012;29(2):603-617.
24. Kunze A, Poller B, Huwyler J, Camenisch G. Application of the extended clearance concept classification system (ECCCS) to predict the victim drug-drug interaction potential of statins. *Drug Metab Pers Ther.* 2015;30(3):175-188.
25. Camenisch G, Umehara K. Predicting human hepatic clearance from in vitro drug metabolism and transport data: a scientific and pharmaceutical perspective for assessing drug-drug interactions. *Biopharm Drug Dispos.* 2012;33(4):179-194.
26. Kazmi F, Hensley T, Pope C, et al. Lysosomal sequestration (trapping) of lipophilic amine (cationic amphiphilic) drugs in immortalized human hepatocytes (Fa2N-4 cells). *Drug Metab Dispos.* 2013;41(4):897-905.
27. Ohkuma S, Poole B. Cytoplasmic vacuolation of mouse peritoneal macrophages and the uptake into lysosomes of weakly basic substances. *J Cell Biol.* 1981;90(3):656-664.
28. Riede J, Poller B, Umehara K, Huwyler J, Camenisch G. New IVIVE method for the prediction of total human clearance and relative elimination pathway contributions from in vitro hepatocyte and microsome data. *Eur J Pharm Sci.* 2016;86:96-102.
29. Lundquist P, Englund G, Skogastierna C, et al. Functional ATP-binding cassette drug efflux transporters in isolated human and rat hepatocytes significantly affect assessment of drug disposition. *Drug Metab Dispos.* 2014;42(3):448-458.
30. Swift B, Pfeifer ND, Brouwer KL. Sandwich-cultured hepatocytes: an in vitro model to evaluate hepatobiliary transporter-based drug interactions and hepatotoxicity. *Drug Metab Rev.* 2010;42(3):446-471.
31. Igari Y, Sugiyama Y, Awazu S, Hanano M. Interspecies difference in drug protein binding-temperature and protein concentration dependency: effect on calculation of effective protein fraction. *J Pharm Sci.* 1981;70(9):1049-1053.
32. Kodama H, Kodama Y, Shinozawa S, Kanemaru R, Todaka K, Mitsuyama Y. Temperature effect on serum protein binding kinetics of phenytoin in monotherapy patients with epilepsy. *Eur J Pharm Biopharm.* 1999;47(3):295-298.

J. Riede et al. / Journal of Pharmaceutical Sciences 106 (2017) 2805-2814

33. Kurz H, Fichtl B. Binding of drugs to tissues. *Drug Metab Rev*. 1983;14(3):467-510.
34. Ahlin G, Hilgendorf C, Karlsson J, Szigyarto CA, Uhlen M, Artursson P. Endogenous gene and protein expression of drug-transporting proteins in cell lines routinely used in drug discovery programs. *Drug Metab Dispos*. 2009;37(12):2275-2283.
35. de Araujo ME, Lamberti G, Huber LA. Homogenization of mammalian cells. *Cold Spring Harb Protoc*. 2015;2015(11):1009-1012.
36. Keemink J, Augustijns P, Annaert P. Unbound ritonavir concentrations in rat and human hepatocytes. *J Pharm Sci*. 2015;104(7):2378-2387.
37. Camenisch G, Alsenz J, van de Waterbeemd H, Folkers G. Estimation of permeability by passive diffusion through Caco-2 cell monolayers using the drugs' lipophilicity and molecular weight. *Eur J Pharm Sci*. 1998;6(4):317-324.
38. Camenisch G, Folkers G, van de Waterbeemd H. Comparison of passive drug transport through Caco-2 cells and artificial membranes. *Int J Pharm*. 1997;147(1):61-70.
39. Nordell P, Svanberg P, Bird J, Grime K. Predicting metabolic clearance for drugs that are actively transported into hepatocytes: incubational binding as a consequence of in vitro hepatocyte concentration is a key factor. *Drug Metab Dispos*. 2013;41(4):836-843.
40. Reinoso RF, Telfer BA, Brennan BS, Rowland M. Uptake of teicoplanin by isolated rat hepatocytes: comparison with in vivo hepatic distribution. *Drug Metab Dispos*. 2001;29(4 Pt 1):453-459.
41. Hallifax D, Houston JB. Saturable uptake of lipophilic amine drugs into isolated hepatocytes: mechanisms and consequences for quantitative clearance prediction. *Drug Metab Dispos*. 2007;35(8):1325-1332.
42. Hallifax D, Houston JB. Uptake and intracellular binding of lipophilic amine drugs by isolated rat hepatocytes and implications for prediction of in vivo metabolic clearance. *Drug Metab Dispos*. 2006;34(11):1829-1836.
43. Duan J, Freeling JP, Koehn J, Shu C, Ho RJ. Evaluation of atazanavir and darunavir interactions with lipids for developing pH-responsive anti-HIV drug combination nanoparticles. *J Pharm Sci*. 2014;103(8):2520-2529.
44. Kunze A, Huwyler J, Poller B, Gutmann H, Camenisch G. In vitro-in vivo extrapolation method to predict human renal clearance of drugs. *J Pharm Sci*. 2014;103(3):994-1001.
45. Austin RP, Barton P, Mohmed S, Riley RJ. The binding of drugs to hepatocytes and its relationship to physicochemical properties. *Drug Metab Dispos*. 2005;33(3):419-425.
46. Benet LZ, Broccatelli F, Oprea TI. BDDCS applied to over 900 drugs. *AAPS J*. 2011;13(4):519-547.
47. Mattson P, Englund G, Ahlin G, Bergstrom CA, Norinder U, Artursson P. A global drug inhibition pattern for the human ATP-binding cassette transporter breast cancer resistance protein (ABCG2). *J Pharmacol Exp Ther*. 2007;323(1):19-30.
48. Rusinova R, Herold KF, Sanford RL, Greathouse DV, Hemmings Jr HC, Andersen OS. Thiazolidinedione insulin sensitizers alter lipid bilayer properties and voltage-dependent sodium channel function: implications for drug discovery. *J Gen Physiol*. 2011;138(2):249-270.

4.3. New IVIVE method for the prediction of total human clearance and relative elimination pathway contributions from *in vitro* hepatocyte and microsome data

Julia Riede[1,2], Birk Poller[1], Ken-ichi Umehara[1], Jörg Huwyler[2], Gian Camenisch[1]

[1] Division of Drug Metabolism and Pharmacokinetics, Integrated Drug Disposition Section, Novartis Institutes for BioMedical Research, CH-4056 Basel, Switzerland

[2] Department of Pharmaceutical Sciences, Division of Pharmaceutical Technology, University of Basel, CH-4056 Basel, Switzerland

Contents lists available at ScienceDirect

European Journal of Pharmaceutical Sciences

New IVIVE method for the prediction of total human clearance and relative elimination pathway contributions from *in vitro* hepatocyte and microsome data

Julia Riede [a,b], Birk Poller [a], Ken-ichi Umehara [a], Jörg Huwyler [b], Gian Camenisch [a,*]

[a] *Division of Drug Metabolism and Pharmacokinetics, Integrated Drug Disposition Section, Novartis Institutes for BioMedical Research, CH-4056 Basel, Switzerland*
[b] *Department of Pharmaceutical Sciences, Division of Pharmaceutical Technology, University of Basel, CH-4056 Basel, Switzerland*

ARTICLE INFO

ABSTRACT

Total human clearance is a key determinant for the pharmacokinetic behavior of drug candidates. Our group recently introduced the Extended Clearance Model (ECM) as an accurate *in vitro–in vivo* extrapolation (IVIVE) method for the prediction of hepatic clearance. Yet, knowledge about relative elimination pathway contributions is needed in order to predict the total human clearance of drug candidates. In the present work, a training set of 18 drug compounds was used to describe the affiliations between *in vitro* sinusoidal uptake clearance and the fractional contributions of hepatic (metabolic and biliary) or renal clearance to overall *in vivo* elimination. By means of these quantitative relationships and using a validation set of 10 diverse drug molecules covering different (sub)classes of the Extended Clearance Concept Classification System (ECCCS), the relative contributions of elimination pathways were calculated and demonstrated to well correlate with human reference data. Likewise, ECM- and pathway-based predictions of total clearances from both data sets demonstrated a strong correlation with the observed clinical values with 26 out of 28 compounds within a three-fold deviation. Hence, total human clearance and relative contributions of elimination pathways were successfully predicted by the presented method using solely hepatocyte and microsome *in vitro* data.

© 2016 Elsevier B.V. All rights reserved.

1. Introduction

Clearance describes the capacity by which a compound is eliminated from the body via metabolism or direct excretion. The liver is the major

organ involved in the metabolism. In general, lipophilic compounds are enzymatically converted into more hydrophilic metabolites in order to facilitate their excretion. Alternatively, parent compounds may be subject to biliary and/or renal secretion. Biliary excretion is generally mediated by canalicular efflux transporter proteins and depends on physicochemical properties such as molecular weight, polarity or ionization (Varma et al., 2012). Renal excretion typically occurs for small, hydrophilic compounds (Fan and de Lannoy, 2014). It involves passive filtration through the glomerulus and, depending on the respective compound properties, active and/or passive carrier-mediated tubular secretion as well as reabsorption back into the blood.

Early knowledge of the predominant clearance mechanism(s) of a drug candidate in human has increasingly gained importance during drug development since efficacy and safety are directly impacted by the pharmacokinetic behavior of a drug (Varma et al., 2015). Recently, the so-called Extended Clearance Concept Classification System (ECCCS)

was demonstrated to allow a qualitative anticipation of hepatic and extra-hepatic clearance pathway contributions for new chemical entities based on *in vitro* data for (passive) sinusoidal uptake and intrinsic hepatic clearance (Camenisch et al., 2015). ECCCS class 1/2 compounds are known to be predominantly cleared in the liver, mainly by metabolism. Renal clearance is a minor elimination route (≤20% contribution) for these compounds due to a high degree of plasma protein binding and extensive reabsorption *via* passive diffusion from the renal tubules back into the blood (Camenisch et al., 2015; Kunze et al., 2014). In contrast, the less permeable ECCCS class 3/4 compounds are much less undergoing hepatic metabolism and, as a consequence, direct elimination as unchanged drug *via* the renal and/or biliary routes becomes of increasing importance. Yet, a numerical quantification of all the clearance pathway contributions is still missing although over the past decades, several empirical and mechanistic approaches using preclinical species (allometric scaling) and *in vitro* data have been developed (Lave et al., 1999; Ring et al., 2011; Varma et al., 2015). Allometric scaling based on body weight has been used to predict renal, hepatic and total clearance in human from preclinical animal data from single or multiple species. However, the predictability of this approach has been limited for compounds, which show species disconnects due to differences in transporter and/or enzyme expression and specificity, in the contribution of elimination pathways or in plasma protein binding (Chaturvedi et al., 2001; Deguchi et al., 2011; Feng et al., 2010; Ring et al., 2011). More mechanistic methods, generally referred as *in vitro–in vivo* extrapolation (IVIVE) approaches, use *in vitro* data to predict *in vivo* clearances. (Metabolic) *in vitro* clearances from human liver microsomes (HLM) or primary hepatocytes are routinely measured during early drug development and converted to hepatic *in vivo* clearances according to the "well-stirred" liver model (Chao et al., 2010; Obach, 2001; Pang and Rowland, 1977). Improved IVIVE methods, based on the Extended Clearance Model (ECM) concept describing hepatic elimination as the interplay of sinusoidal uptake, intracellular metabolism, biliary secretion and sinusoidal efflux, have recently been demonstrated to provide much more accurate predictions of hepatic clearance though (Camenisch et al., 2015). Yet, all these IVIVE approaches still neglect renal clearance as a frequently occurring important elimination pathway.

The objective of this work was to develop a novel concept for the prediction of total body clearance in human. A training set of 18 drug compounds was used to establish the mathematical relationships between *in vitro* hepatocyte uptake clearance and the fractional elimination pathway contributions. For a diverse dataset of 28 compounds (including an independent validation set of 10 in-house compounds) total body clearances were subsequently obtained from ECM-based predictions of hepatic clearance and the anticipated fractional contributions of hepatic and renal clearance to total elimination as illustrated in Fig. 1.

2. Methods

2.1. Test compounds

The entire training set information (namely for lovastatin acid, simvastatin acid, cerivastatin, fluvastatin, ketoconazole, pitavastatin, propranolol, quinidine, verapamil, aliskiren, cimetidine, digoxin, atorvastatin, ciprofloxacin, cyclosporine A, furosemide, pravastatin and valsartan) was published elsewhere (Camenisch et al., 2015; Camenisch and Umehara, 2012; Kunze et al., 2014; Kunze et al., 2015). Our validation/test set consisted of 10 diverse Novartis developmental compounds (NVS 1 to 10). All [^{14}C]- or [^{3}H]-labeled drug candidates were synthesized in the Isotope Laboratories, Drug Metabolism and Pharmacokinetics, Novartis Pharma AG (Basel, Switzerland). The corresponding unlabeled Novartis compounds were chemically synthesized at Novartis Pharma AG. All other chemicals and reagents were of analytical grade and purchased from commercial sources.
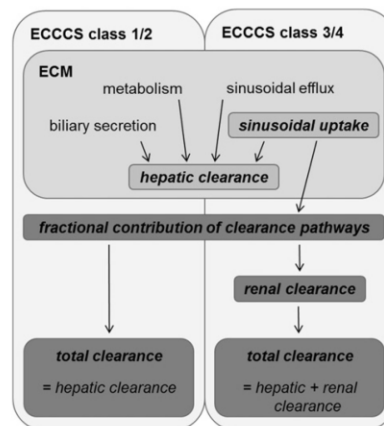

Fig. 1. Workflow for the prediction of total human clearance according to the novel IVIVE approach described in this manuscript. Shortly, in accordance with Extended Clearance Model (ECM), hepatic clearance is projected using *in vitro* parameters for sinusoidal uptake, hepatic metabolism, biliary secretion and sinusoidal efflux back into the blood. The fractional contribution of hepatic and, consequently, of renal elimination can be quantitatively assessed based on their numerical relationship with the *in vitro* hepatic uptake clearance. Subsequently, at least for compounds undergoing significant extra-hepatic elimination (*i.e.* ECCCS class 3/4 compounds), the predicted hepatic clearance needs to be completed with fractional renal clearance information to derive total systemic clearance.

2.2. Determination of in vitro hepatic clearance parameters

All experimental methods and calculation procedures have been described in full detail previously (Camenisch and Umehara, 2012; Kunze et al., 2015). Shortly, metabolic clearances ($CL_{int,met}$) were generally measured in nicotinamide adenine diphosphate (NADPH)-containing HLM. For simvastatin acid, pitavastatin, cerivastatin and fluvastatin $CL_{int,met}$ was additionally analyzed in uridine diphosphate glucuronic acid (UDPGA)-containing HLM. Biliary secretion ($CL_{int,sec}$) was determined in sandwich-cultured human hepatocytes (B-CLEAR® method, Qualyst, Inc., Durham, NC). Active ($PS_{inf,act}$) and passive ($PS_{inf,pas}$) hepatic uptake data were determined using suspensions of pooled human hepatocytes. Sinusoidal efflux from hepatocytes back into blood (PS_{eff}) was assumed to occur *via* passive diffusion so that PS_{eff} is equal to $PS_{inf,pas}$. The *in vitro* process clearances were up-scaled to human organ level using the following scaling factors: 99 [10^6 cells/g liver] for suspended hepatocytes, 53 [mg protein/g liver] for HLM, 116 [mg protein/g liver] for sandwich-cultured hepatocytes and 25.7 [g liver/kg body weight] for liver weight. All *in vitro* parameters for all our training and test set compounds are provided in Table 1. ECCCS class assignments were carried out as depicted in Fig. 2 and as described previously (Camenisch et al., 2015; Camenisch and Umehara, 2012; Kunze et al., 2015).

2.3. Anticipation of fractional elimination pathways

Assuming absence of extra-hepatic/renal elimination pathways (*e.g.* lung metabolism) the fractional contribution of renal elimination to overall *in vivo* body clearance (fn_{ren}) is defined as follows:

$$fn_{ren} = 1 - fn_h \tag{1}$$

where, fn_h is the fractional contribution of total hepatic elimination to overall clearance.

Therefore, the fractional contribution of biliary (fn_{sec}) elimination to overall clearance can be calculated with:

$$fn_{sec} = fn_h - fn_{met} \tag{2}$$

where, fn_{met} denotes the fractional contribution of metabolic hepatic elimination to total body clearance.

fn_h as well as fn_{met} are both highly dependent on the *in vitro* sinusoidal membrane permeability due to the gatekeeper role of hepatic uptake as discussed previously (Camenisch et al., 2015). To establish the proper correlations, a regression analysis was performed by fitting the corresponding *in vitro* and *in vivo* training set data (Tables 1 and 2) to the inverse exponential equations $fn_h = 1 - exp^{-b \cdot PS_{inf}}$ (where, PS_{inf} is the sum of $PS_{inf,act}$ and $PS_{inf,pas}$) and $fn_{met} = 1 - exp^{-b \cdot PS_{inf,pas}}$, respectively (OriginPro 9.1 (OriginLab Corporation, Northampton, USA)). These non-linear relationships, as depicted in Fig. 3, were used to predict fn_h and fn_{met} for all the training and validation compounds (Table 2). Subsequently, fn_{ren} and fn_{sec} were calculated according to Eqs. (1) and (2).

2.4. Prediction of hepatic organ and total body clearances

The overall hepatic intrinsic clearance ($CL_{h,int}$) was calculated by feeding the up-scaled *in vitro* process clearances into the ECM (Camenisch and Umehara, 2012; Kunze et al., 2015):

$$CL_{h,int} = \frac{(PS_{inf,act} + PS_{inf,pas}) \cdot (CL_{int,sec} + CL_{int,met})}{(PS_{eff} + CL_{int,sec} + CL_{int,met})}. \tag{3}$$

Table 1
In vitro process clearances and ECCCS class assignments.

Compounds	ECCCS	$PS_{inf,act}$	$PS_{inf,pas} = PS_{eff}$	$CL_{int,met}$	$CL_{int,sec}$	fu_b
Training set						
Lovastatin acid	1	165.1	145.5	459.0	0.0	0.08
Simvastatin acid	1	116.1	297.9	769.2	1.7	0.11
Cerivastatin	2	221.5	243.8	46.9	0.0	0.02
Fluvastatin	2	218.7	325.5	146.8	0.0	0.04
Ketoconazole	2	0.0	1568.5	97.4	29.6	0.02
Pitavastatin	2	364.3	258.7	17.7	0.0	0.07
Propranolol	2	300.7	276.3	110.8	6.8	0.11
Quinidine	2	229.4	109.3	28.4	5.1	0.27
Verapamil	2	0.0	258.2	127.7	8.1	0.13
Aliskiren	3	32.3	25.4	89.2	31.2	0.70
Cimetidine	3	3.0	3.6	528.7	0.2	0.84
Digoxin	3	20.0	6.9	24.2	18.4	0.82
Atorvastatin	4	140.4	57.7	64.6	11.8	0.08
Ciprofloxacin	4	7.0	22.9	22.0	0.0	0.69
Cyclosporine A	4	113.2	41.9	77.6	9.1	0.03
Furosemide	4	11.1	23.9	19.0	1.2	0.03
Pravastatin	4	57.9	36.0	0.9	2.2	0.97
Valsartan	4	16.0	18.5	4.1	21.5	0.09
Validation set						
NVS 1	2	0.0	332.0	524.4	nd	0.05
NVS 2	2	0.0	114.7	30.0	nd	0.07
NVS 3	2	0.0	457.2	111.6	nd	0.02
NVS 4	2	0.0	407.1	235.6	nd	0.02
NVS 5	2	140.2	154.2	36.0	nd	0.30
NVS 6	2	0.0	300.2	82.3	3.2	0.08
NVS 7	3	0.0	94.1	207.0	nd	0.05
NVS 8	3	56.0	28.0	1.7	945.3	0.20
NVS 9	4	0.0	88.0	42.2	nd	0.02
NVS 10	4	2.5	2.0	0.7	nd	0.10

nd: not determined. All process clearances are expressed in [ml/min/kg] and were determined as described under "Methods". ECCCS classification was performed as outlined in Fig. 2 and as described previously (Camenisch et al., 2015). The unbound fraction in blood (fu_b) was taken from literature (Camenisch and Umehara, 2012; Kunze et al., 2015) or, for all compounds in the validation set, was calculated from in-house plasma protein binding (fu_p) and blood-to-plasma partition coefficient (R_b) data with $fu_b = fu_p/R_b$.
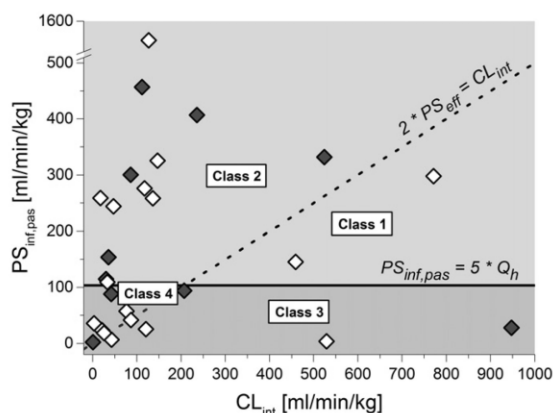

Fig. 2. Schematic Extended Clearance Concept Classification (ECCCS) diagram. $PS_{inf,pas}$ denotes the passive sinusoidal uptake permeability, PS_{eff} is the sinusoidal efflux permeability and CL_{int} describes the sum of intrinsic metabolic ($CL_{int,met}$) and biliary ($CL_{int,sec}$) clearances. The solid line defines the previously defined ECCCS class 1/2 vs class 3/4 permeability threshold at $PS_{inf,pas}$ ~ five-times Q_h whereas the dotted line represents ECCCS class 1/3 vs class 2/4 threshold where $2*PS_{eff} = CL_{int}$ (Camenisch et al., 2015). Dark gray and white diamonds represent the compounds of the validation and the training sets, respectively (Table 1).

Subsequently, the hepatic organ clearance (CL_h) can be predicted based on the "well-stirred" liver model as follows:

$$CL_h = \frac{Q_h \cdot fu_b \cdot CL_{h,int}}{Q_h + fu_b \cdot CL_{h,int}} \tag{4}$$

where, Q_h is the hepatic blood flow (20.7 ml/min/kg) and fu_b is the unbound fraction in blood (Table 1).

The total human body clearance (CL_{tot}) can be anticipated according to Eq. (5):

$$CL_{tot} = \frac{CL_h}{fn_h}. \tag{5}$$

Accordingly, renal organ clearance (CL_{ren}) can be calculated as follows:

$$CL_{ren} = CL_{tot} - CL_h. \tag{6}$$

For all training and validation compounds Eqs. (3) to (6) were used to predict CL_h, CL_{ren} and CL_{tot} as summarized in Table 2.

2.5. Statistical analysis

The non-linear relationships between sinusoidal permeability and fractional hepatic or metabolic contributions as well as the linear correlations between observed (obs) and predicted (pred) fractional pathway contributions were investigated by regression analysis to obtain the regression equations and the correlation coefficients (r^2) (OriginPro 9.1). To indicate the accuracy of the total clearance predictions, fold-error deviations (% fold error < 2 or <3) were determined. Average fold errors (AFE) were calculated as follows:

$$AFE = 10^{\frac{1}{n}\sum \log \frac{pred}{obs}} \tag{7}$$

where, n is the number of data points.

Table 2
Predicted and observed *in vivo* clearance/elimination pathway information.

Compounds	fn_h	fn_{met}	fn_{ren}	fn_{sec}	CL_h	CL_{ren}	CL_{tot}	fn_h	fn_{met}	fn_{ren}	fn_{sec}	CL_h	CL_{ren}	CL_{tot}
				Predicted (pred)								Observed (obs)		
Training set														
Lovastatin acid	1.00	0.89	0.00	0.10	9.9	0.0	9.9	0.90	0.90	0.10	0.00	11.4	1.3	12.6
Simvastatin acid	1.00	0.99	0.00	0.01	12.7	0.0	12.7	0.87	0.87	0.13	0.00	25.2	3.8	29.0
Cerivastatin	1.00	0.98	0.00	0.02	1.4	0.0	1.4	1.00	1.00	0.00	0.00	3.4	0.0	3.4
Fluvastatin	1.00	0.99	0.00	0.01	5.1	0.0	5.1	0.94	0.94	0.06	0.00	7.0	0.4	7.5
Ketoconazole	1.00	1.00	0.00	0.00	1.7	0.0	1.7	0.97	0.97	0.03	0.00	3.9	0.1	4.0
Pitavastatin	1.00	0.98	0.00	0.02	2.5	0.0	2.5	1.00	na	0.00	na	3.5	0.0	3.5
Propranolol	1.00	0.99	0.00	0.01	9.9	0.0	9.9	0.99	0.99	0.01	0.00	12.8	0.1	12.9
Quinidine	1.00	0.81	0.00	0.19	10.5	0.0	10.5	0.81	0.81	0.19	0.00	8.7	2.0	10.7
Verapamil	0.99	0.98	0.01	0.01	7.4	0.1	7.5	0.97	0.97	0.03	0.00	13.7	0.4	14.1
Aliskiren	0.63	0.32	0.37	0.31	12.8	7.4	20.2	0.75	0.10	0.25	0.65	11.3	3.8	15.1
Cimetidine	0.11	0.05	0.89	0.06	4.3	35.6	39.9	0.16	0.14	0.84	0.02	2.7	14.2	16.9
Digoxin	0.37	0.10	0.63	0.27	9.9	16.5	26.4	0.34	0.04	0.66	0.30	4.6	8.9	13.5
Atorvastatin	0.97	0.58	0.03	0.38	6.5	0.2	6.7	0.98	0.70	0.02	0.28	5.9	0.1	6.0
Ciprofloxacin	0.41	0.29	0.59	0.11	6.8	9.9	16.7	0.40	0.12	0.60	0.28	4.5	6.8	11.3
Cyclosporine A	0.93	0.47	0.07	0.46	2.7	0.2	2.9	0.99	0.96	0.01	0.03	3.1	0.0	3.1
Furosemide	0.46	0.30	0.54	0.15	0.5	0.6	1.1	0.34	0.17	0.66	0.17	0.4	0.8	1.2
Pravastatin	0.81	0.42	0.19	0.38	5.4	1.3	6.7	0.53	0.30	0.47	0.23	10.4	9.3	19.8
Valsartan	0.45	0.25	0.55	0.21	1.7	2.0	3.7	0.71	0.11	0.29	0.60	0.7	0.3	0.9
Validation set														
NVS 1	1.00	0.99	0.00	0.00	6.8	0.0	6.8	1.00	1.00	0.00	0.00	3.0	0.0	3.0
NVS 2	0.86	0.83	0.14	0.04	1.6	0.2	1.8	0.99	0.99	0.01	0.00	1.5	0.0	1.5
NVS 3	1.00	1.00	0.00	0.00	1.4	0.0	1.4	1.00	0.99	0.00	0.01	2.7	0.0	2.7
NVS 4	1.00	1.00	0.00	0.00	3.0	0.0	3.0	1.00	0.99	0.00	0.01	4.7	0.0	4.7
NVS 5	0.99	0.90	0.01	0.09	9.2	0.1	9.3	0.94	0.88	0.06	0.06	6.0	0.4	6.4
NVS 6	0.99	0.99	0.01	0.01	4.2	0.0	4.2	0.95	0.85	0.05	0.10	4.0	0.2	4.3
NVS 7	0.81	0.76	0.19	0.04	2.8	0.7	3.4	1.00	1.00	0.00	0.00	12.0	0.0	12.0
NVS 8	0.77	0.35	0.23	0.42	9.0	2.7	11.8	0.78	0.55	0.22	0.23	10.6	3.0	13.6
NVS 9	0.78	0.74	0.22	0.05	0.7	0.2	0.9	0.96	0.87	0.04	0.09	0.8	0.0	0.9
NVS 10	0.08	0.03	0.92	0.05	0.1	1.4	1.5	0.10	0.06	0.90	0.04	0.2	1.9	2.1

na: information not available. Clearance values are generally expressed in [ml/min/kg] and refer to systemic elimination from blood. All predicted values were derived as described under "Methods". For the training set all observed values were taken from literature (Camenisch and Umehara, 2012; Kunze et al., 2014; Kunze et al., 2015). $fn_{met,obs}$ ($=CL_{met,obs}/CL_{tot,obs}$) and $fn_{ren,obs}$ ($=CL_{ren,obs}/CL_{tot,obs}$) values for the validation set were calculated from the observed total ($CL_{tot,obs}$), renal ($CL_{ren,obs}$) and metabolic ($CL_{met,obs}$) clearances as derived from peroral human mass balance studies taking into consideration the estimated absolute oral bioavailabilities (F) (unpublished data). Thereof, $fn_{h,obs}$ ($=1-fn_{ren,obs}$) and $fn_{sec,obs}$ ($=fn_{h,obs}-fn_{met,obs}$) values were calculated.

3. Results

3.1. Quantitative assessment of fractional pathway contributions

The non-linear regression relationship between the observed fractional hepatic elimination ($fn_{h,obs}$) and the total *in vitro* sinusoidal membrane permeability (PS_{inf}) for the 18 training compounds demonstrated a good quantitative correlation ($r^2 = 0.82$, Fig. 3A). Similarly, a strong correlation was obtained between the metabolic pathway contribution in human ($fn_{met,obs}$) and the passive sinusoidal membrane permeability ($PS_{inf,pas}$) ($r^2 = 0.84$, Fig. 3B). In the latter case, $PS_{inf,pas}$ was considered to be more appropriate than PS_{inf} given that an increase in lipophilicity promotes both high passive permeability and the affinity to drug metabolizing enzymes (Benet et al., 2008; Camenisch et al., 2015).

Pitavastatin was excluded from this analysis due to lack of human reference data for fn_{met} and fn_{sec}.

Using Eqs. (1) and (2), the fractional pathway contributions to overall elimination were derived from the inverse exponential relationships given in Fig. 3 for all 28 validation and training compounds. Fig. 4A and B show the comparison between predicted and *in vivo* observed human fn_h and fn_{met} values, respectively, providing excellent correlations close to the line of unity ($r^2 = 0.85$ *vs.* $r^2 = 0.84$). The corresponding relationships for fn_{ren} and fn_{sec} are given in Fig. 4C and D, respectively. While the correlation between calculated and observed fn_{ren} parameters was also excellent ($r^2 = 0.85$) it was somewhat weaker for the anticipation of fn_{sec} ($r^2 = 0.33$). Just referring to the validation set, the correlations between predicted and observed values for fn_h, fn_{ren}, fn_{met} and fn_{sec} in terms of r^2 were 0.90, 0.90, 0.86 and 0.74, respectively.
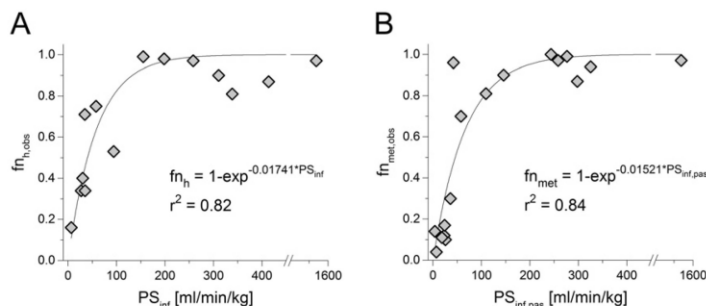

Fig. 3. Correlation between *in vitro* sinusoidal membrane permeability (PS_{inf} or $PS_{inf,pas}$) and observed fractional total hepatic ($fn_{h,obs}$) (A) or metabolic hepatic ($fn_{met,obs}$) (B) elimination for the training set. Solid lines show the non-linear inverse exponential regressions as described under "Methods".

All the predicted and observed fn values for hepatic, metabolic, renal and biliary elimination are given in Table 2.

In agreement with the *in vivo* data and in accordance with ECCCS, all class 1/2 compounds from both data sets were predicted to be predominantly cleared *via* the liver, or more precisely by metabolism ($fn_{h,pred} = 0.86–1.00$ and $fn_{met,pred} = 0.81–1.00$ *vs* $fn_{h,obs} = 0.81–1.00$ and $fn_{met,obs} = 0.81–1.00$). Significant contributions of renal ($fn_{ren,pred} = 0.03–0.92$) and partly also of biliary elimination ($fn_{sec,pred} = 0.04–0.42$) were predicted for most of the class 3/4 compounds in both datasets. All these projections are well in line with the respective *in vivo* observations with exception of NVS 7 ($fn_{ren,pred} = 0.22$) and NVS 9 ($fn_{ren,pred} = 0.19$) for which no significant renal elimination was determined in human (<5%).

3.2. Total body clearance prediction

For both compound sets ECM-based CL_h values were calculated according to Eqs. (3) and (4). Subsequently, CL_{tot} and CL_{ren} were derived according to Eqs. (5) and (6). The corresponding predicted and observed clearance estimates are given in Table 2. Fig. 5 shows the correlation between predicted and observed (total) body clearances for ECCCS class 1/2 (Fig. 5A) and class 3/4 compounds (Fig. 5B). For ECCCS class 1/2 compounds, well known to be almost exclusively cleared by hepatic metabolism, all predictions in the absence of a correction for a fractional renal clearance contribution (*i.e.* based only on CL_h) generally provided very accurate CL_{tot} estimations (AFE of 1.02 and 0.75 for the validation compounds and the complete dataset, respectively) as already shown previously (Camenisch and Umehara,

2012, Camenisch et al., 2015). In contrast, due to the substantial role of renal elimination, for the class 3/4 compounds in our dataset the *in vivo* observed total clearances were generally under-estimated just using CL_h (AFE = 0.28 for the validation set, AFE = 0.50 for the complete dataset, Fig. 5B). Taking renal elimination according to Eq. (5) into account, the accuracy could significantly be improved for this ECCCS subclass (AFE of 0.65 and 1.06 for the validation and entire dataset, respectively). Including all 28 compounds the comparison of predicted and observed total clearance demonstrated overall a good predictability (AFE = 0.88). 20 (71%) and 26 (93%) out of 28 compounds were predicted within two-fold and three-fold errors, respectively. Exceptions were NVS 7 and valsartan for which CL_{tot} was significantly under- (3.4-fold) and over- (4-fold) predicted, respectively.

4. Discussion

In previous studies, our group has developed an ECM-based IVIVE method for the prediction of hepatic drug clearance from the different process clearances driving liver elimination (Camenisch and Umehara, 2012; Kunze et al., 2015; Umehara and Camenisch, 2012). Here we present a novel extension of this IVIVE approach, which allows the prediction of the relevant elimination pathways and the total drug clearance in human purely based on *in vitro* data and in alignment with the ECCCS class assignment of drug compounds.

The proposed prediction method is based on the observed non-linear association between the *in vitro* sinusoidal membrane permeability from suspended hepatocytes and the *in vivo* fractional hepatic as
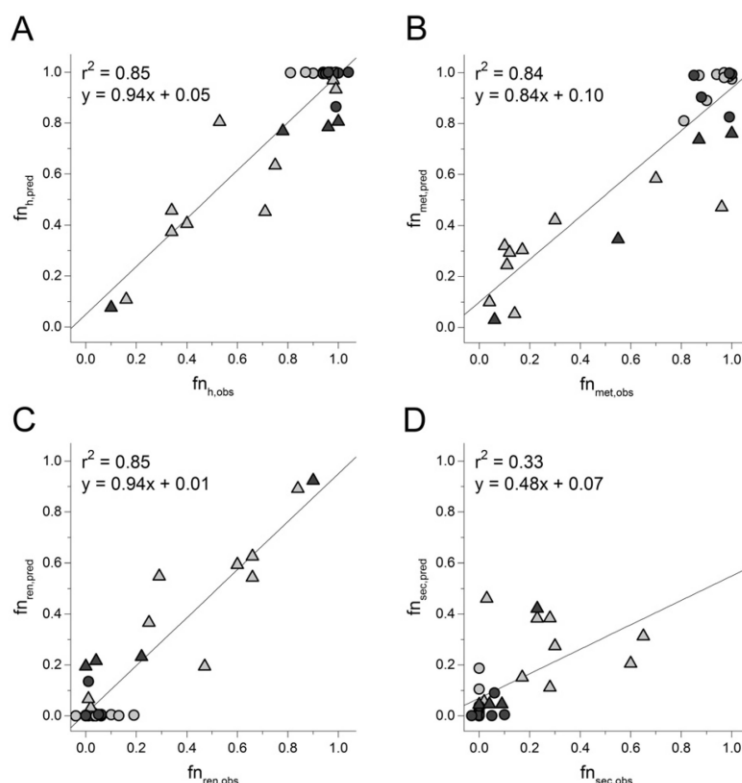

Fig. 4. Correlation between predicted (pred) and observed (obs) human fractional total hepatic (fn_h) (A), metabolic hepatic (fn_{met}) (B), renal (fn_{ren}) (C) and biliary (fn_{sec}) (D) elimination for the validation (dark gray) and training sets (light gray). Circles and triangles characterize ECCCS class 1/2 and 3/4, respectively. Solid lines represent the linear regression as described under "Methods".
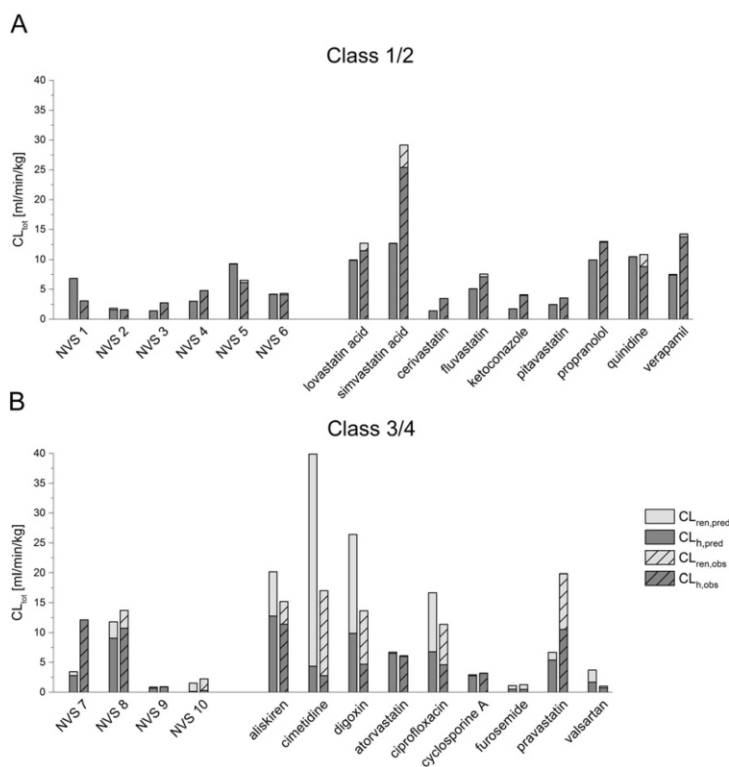
Fig. 5. Comparison of observed (obs) and predicted (pred) human renal (ren), hepatic (h) and total (tot) clearances for the entire data set as described in under "Methods". Panels (A) and (B) refer to the predictions for ECCCS class 1/2 and class 3/4 compounds, respectively.

well as metabolic contributions to total clearance (Camenisch et al., 2015). Taking into consideration these relationships the fractional hepatic, renal, metabolic and biliary elimination pathway contributions as well as the total human body clearances could successfully be estimated for a set of 28 compounds. For the investigated compounds $fn_{h,pred}$, $fn_{ren,pred}$ as well as $fn_{met,pred}$ values were anticipated with high accuracy ($r^2 \geq 0.84$, Fig. 4A, 4B and 4C). $fn_{sec,pred}$ revealed slightly higher deviations to observed values in human though ($r^2 = 0.33$, Fig. 4D). However, considering that the biliary excretion by humans is often uncharacterized (*i.e.* indirectly estimated instead of directly measured) and that $fn_{sec,pred}$ was derived from two independently predicted values ($fn_{ren,pred}$ and $fn_{met,pred}$) this is not further surprising. Yet, the current approach still provides a very reliable qualitative indication for the relevance of biliary elimination.

The *in vitro* metabolic profile of drug candidates is usually characterized in the early phase of drug development using liver preparations such as HLM with special emphasis on CYP-mediated elimination due to its predominant role in metabolic drug elimination (Zientek and Youdim, 2015). This approach, however, is expected to provide accurate hepatic clearance predictions only for compounds where enzymatic (oxidative) metabolism is the predominant clearance pathway. Here, we propose a new strategy for tailor-made evaluations based on the ECCCS compound classification system, taking into account all relevant human clearance processes including direct biliary and renal secretion. Thereby, the passive sinusoidal uptake clearance into suspended human hepatocytes ($PS_{inf,pas}$) represents a key parameter to assign compounds into class 1/2 and class 3/4 as well as to derive the related clearance mechanisms (Fig. 2). The highly permeable ECCCS class 1/2 compounds ($PS_{inf,pas}$ above ~100 ml/min/kg) are expected to be mainly cleared *via* hepatic elimination ($fn_{h,obs} = 0.81$–1.0) (Camenisch and Umehara, 2012). For compounds with $PS_{inf,pas}$ above the 100 ml/min/ kg threshold the likelihood for biliary and/or renal secretion of unchanged drug is low (Camenisch et al., 2015). Consequently, hepatic metabolism represents the predominant elimination pathway for ECCCS class 1/2 compounds and clearance data from HLM generally provide sufficient information to anticipate the hepatic clearance of this subclass as illustrated in Fig. 5A and as reviewed in detail elsewhere (Camenisch et al., 2015). In contrast, for class 3/4 compounds ($PS_{inf,pas}$ below ~100 ml/min/kg, Fig. 2) renal secretion of unchanged drug often represents an important elimination process besides hepatic elimination (*via* metabolism and/or biliary secretion) (Camenisch et al., 2015; Kunze et al., 2014). Therefore, a correction for renal clearance has to be taken into consideration to anticipate the total clearance of such compounds. Thus, ECM-based hepatic clearance anticipation alone would clearly under-predict total body clearance for most of the class 3/4 compounds as illustrated in Fig. 5B. Pooling all compounds from the training and validation sets, the total body clearances for 26 out of 28 compounds were predicted within a three-fold error independent of the major elimination pathway and the extent of overall clearance. Exceptions were NVS 7 and valsartan, for which the total clearances were 3.4-fold under-predicted and 4-fold over-predicted, respectively. Based on present predictions NVS 7 is expected to be predominantly cleared by the hepatic metabolic pathway ($fn_{met,pred} = 0.76$). In clinics, NVS 7 was truly identified to be predominantly cleared by metabolism ($fn_{met,obs} = 1.0$). However, a considerable fraction (estimated 50%) was due to extra-hepatic metabolism, likely in lung *via* CYP1A1. As our prediction model bases on the fundamental assumption that no extra-hepatic/renal clearance pathways are involved in overall elimination, the non-hepatic metabolic clearance of NVS 7 is neglected resulting in an over-estimation of fn_h and consequently in a significant

under-prediction of CL_{tot}. Taking a lung clearance pathway as outlined above into account, CL_{tot} for NVS 7 would have been under-predicted by 1.1-fold only. Valsartan was previously demonstrated to undergo transporter-mediated sinusoidal efflux (Camenisch and Umehara, 2012). Consequently, as active sinusoidal elimination is neglected with the current approach, the determined over-prediction in total human valsartan clearance mainly results from a discrepancy in the calculation of hepatic clearance rather than from an inaccurate fn_h prediction. Excluding NVS 7 and valsartan from the analysis the overall prediction accuracy for total clearance is excellent (AFE = 0.87). ECCCS class 1/2 compounds are somewhat under-predicted (AFE = 0.76) while for ECCCS class 3/4 compounds a slight over-prediction is observed (AFE = 1.06). Still, the overall quality of presented human clearance anticipation is comparable to or even exceeding currently available allometry-based methods for total clearance and previous IVIVE prediction methods for renal or hepatic clearance at least with regard to accuracy as demonstrated in a large comparative assessment of different methods for human clearance estimation (Ring et al., 2011).

To further improve the above predictions of total clearance, non-hepatic/renal elimination, entero-hepatic circulation and/or non-cytochrome P450 (CYP) metabolism pathways would have to be considered though. While extra-hepatic/renal elimination processes (such as lung metabolism or intestinal secretion) or entero-hepatic cycling remain difficult to anticipate, the likelihood for the involvement of non-CYP mediated metabolism pathways seems to increase for compounds with low metabolic clearance in HLM ($CL_{int,met}$ below ~10 ml/min/kg). This surely holds true for pravastatin in our training set or for NVS 8 and NVS 10 in our validation set. Pravastatin has a low reported metabolic *in vivo* clearance (CL_{met} = 5.9 ml/min/kg) which contributes with 30% to total clearance in human (Hatanaka, 2000). Pravastatin is considered to be metabolized by non-CYP enzymes, possibly by UDP-glucuronosyltransferases (UGTs) and sulfutransferases (Elsby et al., 2012; Hatanaka, 2000), and hepatic clearance is ~2-fold underestimated using only NADPH-containing HLM (note: other statins like simvastatin acid, cerivastatin and pitavastatin are also well-known substrates of UGTs. However, for these compounds, in contrast to pravastatin, available *in vitro* data account for CYP as well as non-CYP mediated metabolism as described under "Methods"). Similarly, NVS 8 as well as NVS 10 were demonstrated to be strongly eliminated *via* direct glucuronidation in the clinics although hepatic clearance was only slightly under-predicted (1.2-fold and 1.8-fold, respectively) using the ECM-based approach according to Eq. (4) (as sinusoidal uptake was identified to be the rate-determining hepatic clearance process for both compounds this is not further surprising though (Camenisch et al., 2015)). For compounds with the described properties, metabolic clearance assessments might therefore be extended to *in vitro* systems such as hepatocytes or S9 fractions, which express additional cytosolic enzyme families in addition to the CYP enzymes. However, further research will be required to support this theory and to optimize the *in vitro* assessment of non-CYP mediated metabolism.

5. Conclusion

The presented correlations allow a quantitative estimation of elimination routes in human for (new) drug candidates at an early stage of drug development. Depending on the compounds ECCCS class assignments it further enables a tailor-made pharmacokinetic evaluation in order to simplify and to refine human clearance predictions during drug development. Especially, since bottom–up IVIVE approaches for the prediction of human renal clearance are currently limited, our novel method provides a fast and simple, yet highly reliable alternative to anticipate the involvement of metabolic and secretory drug elimination pathways. Moreover, it allows the quantitative prediction of the total body clearance in human solely from *in vitro* clearance data.

References

Benet, L.Z., Amidon, G.L., Barends, D.M., Lennernas, H., Polli, J.E., Shah, V.P., Stavchansky, S.A., Yu, L.X., 2008. The use of BDDCS in classifying the permeability of marketed drugs. Pharm. Res. 25, 483–488.

Camenisch, G., Umehara, K., 2012. Predicting human hepatic clearance from *in vitro* drug metabolism and transport data: a scientific and pharmaceutical perspective for assessing drug–drug interactions. Biopharm. Drug Dispos. 33, 179–194.

Camenisch, G., Riede, J., Kunze, A., Huwyler, J., Poller, B., Umehara, K., 2015. The Extended Clearance Model and Its use for the Interpretation of Hepatobiliary Elimination Data. ADMET & DMPK 3 pp. 1–14.

Chao, P., Uss, A.S., Cheng, K.C., 2010. Use of intrinsic clearance for prediction of human hepatic clearance. Expert Opin. Drug Metab. Toxicol. 6, 189–198.

Chaturvedi, P.R., Decker, C.J., Odinecs, A., 2001. Prediction of pharmacokinetic properties using experimental approaches during early drug discovery. Curr. Opin. Chem. Biol. 5, 452–463.

Deguchi, T., Watanabe, N., Kurihara, A., Igeta, K., Ikenaga, H., Fusegawa, K., Suzuki, N., Murata, S., Hirouchi, M., Furuta, Y., Iwasaki, M., Okazaki, O., Izumi, T., 2011. Human Pharmacokinetic Prediction of UDP-glucuronosyltransferase Substrates With an Animal Scale-up Approach. *Drug Metab. Dispos.* 39 pp. 820–829.

Elsby, R., Hilgendorf, C., Fenner, K., 2012. Understanding the critical disposition pathways of statins to assess drug–drug interaction risk during drug development: it's not just about OATP1B1. Clin. Pharmacol. Ther. 92, 584–598.

Fan, J., de Lannoy, I.A., 2014. Pharmacokinetics. Biochem. Pharmacol. 87, 93–120.

Feng, B., LaPerle, J.L., Chang, G., Varma, M.V., 2010. Renal clearance in drug discovery and development: molecular descriptors, drug transporters and disease state. Expert Opin. Drug Metab. Toxicol. 6, 939–952.

Hatanaka, T., 2000. Clinical pharmacokinetics of pravastatin: mechanisms of pharmacokinetic events. Clin. Pharmacokinet. 39, 397–412.

Kunze, A., Huwyler, J., Poller, B., Gutmann, H., Camenisch, G., 2014. *In vitro–in vivo* extrapolation method to predict human renal clearance of drugs. J. Pharm. Sci. 103, 994–1001.

Kunze, A., Poller, B., Huwyler, J., Camenisch, G., 2015. Application of the extended clearance concept classification system (ECCCS) to predict the victim drug–drug interaction potential of statins. Drug Metabol Personal Ther.

Lave, T., Coassolo, P., Reigner, B., 1999. Prediction of hepatic metabolic clearance based on interspecies allometric scaling techniques and *in vitro–in vivo* correlations. Clin. Pharmacokinet. 36, 211–231.

Obach, R.S., 2001. The prediction of human clearance from hepatic microsomal metabolism data. Curr. Opin. Drug Discov. Devel. 4, 36–44.

Pang, K.S., Rowland, M., 1977. Hepatic clearance of drugs. I. Theoretical considerations of a "well-stirred" model and a "parallel tube" model. Influence of hepatic blood flow, plasma and blood cell binding, and the hepatocellular enzymatic activity on hepatic drug clearance. J. Pharmacokinet. Biopharm. 5, 625–653.

Ring, B.J., Chien, J.Y., Adkison, K.K., Jones, H.M., Rowland, M., Jones, R.D., Yates, J.W., Ku, M.S., Gibson, C.R., He, H., Vuppugalla, R., Marathe, P., Fischer, V., Dutta, S., Sinha, V.K., Bjornsson, T., Lave, T., Poulin, P., 2011. PhRMA CPCDC initiative on predictive models of human pharmacokinetics, part 3: comparative assessement of prediction methods of human clearance. J. Pharm. Sci. 100, 4090–4110.

Umehara, K., Camenisch, G., 2012. Novel *in vitro–in vivo* extrapolation (IVIVE) method to predict hepatic organ clearance in rat. Pharm. Res. 29, 603–617.

Varma, M.V., Chang, G., Lai, Y., Feng, B., El-Kattan, A.F., Litchfield, J., Goosen, T.C., 2012. Physicochemical property space of hepatobiliary transport and computational models for predicting rat biliary excretion. Drug Metab. Dispos. 40, 1527–1537.

Varma, M.V., Steyn, S.J., Allerton, C., El-Kattan, A.F., 2015. Predicting clearance mechanism in drug discovery: extended clearance classification system (ECCS). Pharm. Res. 32, 3785–3802.

Zientek, M.A., Youdim, K., 2015. Reaction phenotyping: advances in the experimental strategies used to characterize the contribution of drug-metabolizing enzymes. Drug Metab. Dispos. 43, 163–181.

CHAPTER 5

Discussion and future perspectives

In the present work, new IVIVE models for the prediction of drug disposition in humans were successfully established and validated. Furthermore, the utility of the drug classification systems ECM and ECCCS for the design and translation of pharmacokinetic *in vitro* assessments was demonstrated. In the context of hepatic drug distribution, the applicability of four *in vitro* methods to determine hepatic drug partitioning, intracellular drug binding, and unbound intrahepatic drug concentrations were investigated (sections 4.1 and 4.2). In particular, the mechanistic model based on the ECM concept indicated high *in vivo* relevance with regard to the prediction of clinical cholestasis manifestation upon BSEP inhibition and close *in vitro-in vivo* correlation (IVIVC) of Kp_{uu} in rats. The temperature and homogenization methods demonstrated usefulness in the investigation of intracellular drug binding to determine the unbound fraction in hepatocytes. In addition, a straightforward IVIVE approach for the prediction of total drug clearance was developed (section 4.3). Determining the hepatic drug clearance together with the relative elimination pathway contributions from *in vitro* experiments provided good predictability of total and renal drug clearance in humans.

Further perspectives and limitations of the investigated IVIVE models for assessments of the unbound intrahepatic drug concentration and total drug clearance are discussed in the following sections.

5.1.   ECM-based Kp_{uu} and the prediction of drug-induced cholestasis

Over the last years, several attempts have been made to predict drug-induced cholestasis using *in vitro* data on BSEP inhibition and clinical systemic drug exposure (Dawson et al., 2012; Morgan et al., 2013; Shah et al., 2015). Nevertheless, no complete correlation between BSEP inhibition *in vitro* and clinical risk of cholestasis could be established. This outcome is likely attributed to the use of systemic drug exposure, which is not expected to represent the unbound intrahepatic drug concentrations due to active transport or metabolic processes in the liver (Muller and Milton, 2012; Chu et al., 2013). In contrast, the ECM-based model provides estimates of Kp_{uu} under consideration of all active and passive hepatic clearance processes. This assessment allows the calculation of unbound intrahepatic concentrations and thus the direct translation of BSEP inhibition *in vitro* to the clinical incidence of drug-induced cholestasis. Moreover, the ECM-based approach supports the evaluation of genetic polymorphisms, disease state, or other potential factors that contribute to the risk of drug-induced cholestasis.

Although not directly evident in the present analysis, other processes might contribute to the development of cholestasis. These are, on the one hand, BSEP-independent pathways that are involved in maintaining the hepatocellular bile acid homeostasis and, on the other hand, additional processes that affect intrahepatic drug concentrations. Besides BSEP-mediated canalicular efflux, hepatic bile acid levels are regulated by other sinusoidal and canalicular transporters. Under physiological conditions, bile acids are taken up from the sinusoidal blood into the hepatocytes by NTCP and OATPs followed by canalicular secretion via BSEP and MRP2, whereby NTCP and BSEP are the driving force in the vectorial bile acid transport. Sinusoidal MRP3, MRP4, and heteromeric organic solute transporter OSTα-OSTβ mediate back-flux of bile acids into the systemic circulation (Dawson et al., 2009). This process, however, seems to have only a minor contribution to the overall hepatocellular bile acid disposition under normal conditions. Yet, increases in the intrahepatic bile acid levels upon BSEP inhibition generally induce an upregulation of processes that contribute to bile acid clearance from hepatocytes in order to protect the cells. The bile acid efflux transporter system is induced via activation of the bile-acid sensitive nuclear receptors FXR, pregnane X receptor (PXR), and constitutive androstane receptor (CAR), whereas sinusoidal bile acid uptake transporters are down-regulated (Soroka et al., 2001; Gradhand et al., 2008; Rodrigues et al., 2014). Similarly, activation of FXR, PXR, and CAR regulates bile acid synthesis and conjugation by gene repression of CYP7A1 or induction of UGT1A1 and SULT2A1, respectively (Li and Chiang, 2014). Hence, these protective pathways may compensate reduced BSEP function and prevent intrahepatic bile acid accumulation by increased sinusoidal efflux and conjugation or decreased sinusoidal uptake and synthesis. On the other hand, concurrent inhibition of BSEP and the described protective pathways such as MRP3 or MRP4-mediated efflux likely increases the risk of drug-induced cholestasis (Morgan et al., 2013; Kock et al., 2014). The ECM-based assessment, however, only considers the inhibition of BSEP, while the involvement of any protective pathway probably alters the actual cholestasis risk. Nevertheless, quantitative information about bile acid transport and metabolism under cholestatic conditions in humans is currently limited and further research is required in order to refine mechanistic models for hepatic and systemic bile acid disposition (Woodhead et al., 2014; Guo et al., 2016).

In the context of hepatic drug disposition and resulting unbound intrahepatic drug concentrations, different processes are not considered within the ECM approach. Active sinusoidal efflux permeability as mediated by MRPs is neglected in the assessment. The physiological relevance of MRP3 and MRP4-mediated drug transport during cholestasis is so far largely unknown and requires additional investigations. In general, no significant impact on hepatic drug distribution is expected as discussed in the sections 4.1 and 4.2. However, experimental *in vitro* setups in combination with complex modeling approaches have been developed and could be applied on a case-by-case basis (Pfeifer et al., 2013b).

Besides alterations in transporter and enzyme expression during cholestasis, a number of drugs are known to induce or inhibit in a time-dependent manner certain elimination pathways.

For instance, rifampicin or bosentan induce the expression of CYP3A4 via PXR activation and thus enhance their own metabolic elimination in humans (Dingemanse and van Giersbergen, 2004; Xu et al., 2005). Under such circumstances intrahepatic drug and bile acid concentrations can change. Depending on the affected pathways, this might result in an increased or reduced cholestasis risk. Furthermore, co-medication can affect hepatic drug elimination due to inhibition or induction of drug-metabolizing enzymes and transporters. Consequently, Kp_{uu} and unbound intrahepatic concentration of victim drugs are likewise affected in the presence of a perpetrator drug. However, the ECM approach will allow accounting for DDI effects on Kp_{uu} in the same way as demonstrated for transporter and enzyme polymorphisms (section 4.1) or for DDI effects on the hepatic clearance (Camenisch and Umehara, 2012; Kunze et al., 2015). Nevertheless, quantitative information about the extent and the contribution of all underlying hepatic clearance processes of the victim drug are required to calculate Kp_{uu} for a DDI scenario.

In addition, the assessment is focused on parent drug alone whereas potential effects of metabolites are neglected. For certain drugs, metabolites exhibit the greater risk for BSEP inhibition compared to the parent drug compound such as in the case of troglitazone and its metabolite troglitazone sulfate. Troglitazone is a potent BSEP inhibitor that has been withdrawn from the market due to several cases of severe liver injury. Studies in rat have shown that male rats are more sensitive to troglitazone-induced intrahepatic cholestasis and liver toxicity. This correlated with higher liver tissue concentrations of the major metabolite troglitazone sulfate due to higher formation rate in male rats. Taking into account the high liver tissue accumulation and that troglitazone sulfate is a 10-fold more potent BSEP inhibitor compared to the parent drug, troglitazone-induced cholestasis is likely predominately mediated by troglitazone sulfate (Funk et al., 2001a; Funk et al., 2001b; Padda et al., 2011). Hence, BSEP inhibition potential and unbound intrahepatic concentrations should be additionally investigated for metabolites with substantial exposure (FDA, 2016). However, to the best of our knowledge, the present data set did not include drugs with metabolites that are associated with a higher BSEP inhibition risk compared to the parent compound.

The use of ECM-based unbound intrahepatic drug concentrations is not only expected to enable the risk assessment of BSEP inhibition. Besides that, the ECM can likely also be applied in order to improve the evaluation of intrahepatic drug interactions with therapeutic targets or other transporters and drug-metabolizing enzymes that influence the pharmacokinetic, pharmacodynamics, and toxicological properties of drugs. Taking into account that underlying hepatic processes need to be determined *in vitro* once only, Kp_{uu} for a certain drug compound can be additionally used to evaluate substrate or inhibitor interactions with any other intrahepatic transporter and enzyme. For instance, in a recent study, the use of Kp_{uu} allowed to improve DDI predictions for CYP inhibition (Iwasaki et al., 2017). Similarly, improved translation of efficacy data have been observed in the context of inhibition of HMG-CoA reductase and the lipid-lowering effect of statins (Riccardi et al., 2017). Also drug-induced hyperbilirubinemia due to inhibition of MRP2 (conjugated hyperbilirubinemia) and UGT1A1 (unconjugated hyperbilirubinemia) depends

on the unbound intrahepatic drug concentration and can be likely evaluated using the ECM approach (Brouwer et al., 2013). Furthermore, the ECM concept might also be applicable to other organs like kidney or brain where Kp_{uu} depends on similar processes. However appropriate *in vitro* systems are currently not available that would allow determining all relevant active metabolic and transport processes.

5.2. Comparison of Kp_{uu} methods

The validity of ECM-based Kp_{uu} approach and the underlying experimental data was reliably demonstrated by the prediction of drug-induced cholestasis in humans and IVIVC in rats (section 4.1). Nevertheless, the ECM approach requires the labor and cost-intensive determination of several *in vitro* parameters. Therefore, additional *in vitro* approaches were investigated, which require less experimental efforts, namely the temperature method, the homogenization method, and the $logD_{7.4}$ method. For all three approaches, the absence of metabolism and biliary secretion in Kp determinations was identified as the main limitation. Hence, hepatic Kp_{uu} cannot be correctly predicted for compounds with predominant intrinsic clearance (ECM class 1 and 3 compounds). In contrast, the hepatic Kp_{uu} of ECM class 2 and 4 compounds is assessable at least using the temperature method (section 4.2). Therefore, knowledge of a drugs ECM class could guide the selection of the appropriate Kp_{uu} *in vitro* method. Yet, the assignment of a preliminary ECM class already requires experimental hepatic uptake and metabolic clearance data (section 4.3). Having determined these parameters, however, allows the calculation of the ECM-based Kp_{uu} for class 2 and 4 compounds without need for additional experimental work. For ECM class 1 and 3 compounds, *in vitro* measurements of biliary secretion are required to correctly calculate the ECM-based Kp_{uu}. A preliminary EMC class assignment thus might reduce the number of sandwich-culture hepatocyte assays but cannot facilitate the selection of the appropriate Kp_{uu} approaches. Therefore, the ECM remains the preferred approach for the determination of hepatic Kp_{uu} irrespective of the ECM class. The alternative Kp_{uu} approaches might be applicable to evaluate drug efficacy or toxicity in cell types where Kp is only determined by transport processes and not by metabolism as previously demonstrated by Mateus et al. (2013).

In contrast, the alternative approaches allowed determining the binding parameter fu_{hep}, which is not directly available from the ECM-based method. Knowledge of fu_{hep} is considered to be important for physiologically-based pharmacokinetic (PBPK) modeling purposes or for binding correction in hepatocyte incubations (i.e. for the correction of apparent metabolic or biliary clearance parameters). Among the three investigated approaches, the temperature method indicated the best applicability, which was suggested by close correlation to ECM-derived data for ECM class 2 and 4 compounds as discussed in section 4.2. The homogenization method provided comparable results to the temperature method for small lipophilic compounds. In contrast, the binding properties of large or hydrophilic compounds were not correctly predicted. Thus, the homogenization method is likely applicable to compounds with the appropriate

physicochemical properties, in particular when taking into account that this approach requires minor experimental effort and is suitable for high-throughput screenings (Mateus et al., 2014). However, for compounds that not fulfill the described physicochemical requirements, fu_{hep} should be preferably determined using the temperature method.

Though, a potential influence of temperature cannot generally be excluded. Membrane fluidity and permeability are known to be temperature-sensitive (Frezard and Garnier-Suillerot, 1998; Pang et al., 2010; Brouwer et al., 2013; Zamek-Gliszczynski et al., 2013). Yet, altered membrane permeability will not affect the determination of fu_{hep} using the temperature method since uptake and efflux permeability are equilibrated at steady-state and in the absence of active processes (i.e. $PS_{inf} = PS_{eff}$). As a consequence, temperature would affect uptake and efflux permeability to the same extent, which will not influence fu_{hep}. However, temperature-dependent changes in binding to cellular structures need to be considered which was therefore investigated in control incubations at 37°C in the presence of a cocktail of uptake transporter inhibitors. This analysis indicated that binding properties were not affected to a relevant extent with exception of few compounds, which are associated with extensive binding or lysosomal trapping processes. For instance, lysosomal trapping processes are reduced at lower temperature, which is expected to cause an overestimation of fu_{hep} when using the temperature method. Hence, to assure the determination of physiologically relevant data, control incubations at 37°C in the presence of uptake transporter inhibitors could be conducted for susceptible drugs. This concerns in particular compounds, which likely undergo lysosomal trapping (i.e. positively charged compounds with $pK_a > 6$ (Kazmi et al., 2013)) or exhibit extensive binding. However, incubations at 37°C with inhibitors for transporters and drug-metabolizing enzymes hold the risk of incomplete inhibition of potentially unknown active processes, resulting in erroneous fu_{hep} data. Therefore, knowledge of the compound properties as well as careful selection of the experimental method is recommended in order to reliably determine fu_{hep}.

5.3. Prediction of total drug clearance

Hepatic clearance of drug compounds is routinely predicted during drug development using IVIVE approaches like the ECM. Renal drug elimination represents the second major clearance pathway in humans and has to be likewise investigated. Yet, suitable renal IVIVE approaches are currently limited and allometric scaling from preclinical animals can be impaired by species differences (Chaturvedi et al., 2001; Deguchi et al., 2011; Watanabe et al., 2011; Kunze et al., 2014b; Dave and Morris, 2015). In addition, PBPK models have been developed (Neuhoff et al., 2013). However, such complex approaches are not applicable for bottom-up predictions at early drug development stages due to the need of extensive experimental data. In this context, the presented model is a reliable alternative for the prediction of renal and total clearance at early development stages. The approach is based on the prediction of elimination pathway contributions estimated from *in vitro* sinusoidal uptake data. Since this parameter is routinely measured for hepatic clearance predictions, no further *in vitro* experiments are required.

The obtained total clearance thus represents a crucial parameter for human pharmacokinetic predictions in order to anticipate the pharmacologically effective human dose and the systemic drug exposure. In addition, information about the contribution of hepatic and renal elimination pathways is valuable during early drug development. The identification of transporter and enzyme substrates is requested by health authorities, however, only for transporters and enzymes, which are involved in major elimination pathways with more than 25% contribution to overall drug elimination (EMA, 2012; FDA, 2012; Hillgren et al., 2013). Hence, ECCCS classification and knowledge about the contribution of elimination pathways supports the selection of follow-up phenotyping studies in order to identify potential DDI victim drugs.

Nevertheless, the presented approach does not provide mechanistic insights of the underlying renal elimination processes. Renal elimination represents the net effect of glomerular filtration, tubular secretion, and tubular reabsorption and a mechanistic renal IVIVE approach would be desirable to elucidate the interplay between the individual processes. However, currently available *in vitro* cell lines and primary cells are lacking functional expression of several transporters, in particular OAT1 and OAT3, thus limiting the investigation of anionic compounds (Hilgendorf et al., 2007; Kunze et al., 2014b). However, adjustments in transporter expression can be realized by genetic engineering (Nieskens et al., 2016). In addition, emerging 3D models of the human renal proximal tubules may have the potential to fill this gap in the future (Weber et al., 2016).

A further limitation of the model is related to neglected non-hepatic/non-renal elimination pathways as discussed in section 4.3. Although only relevant for a small fraction of drugs, elimination pathways such as non-CYP-mediated metabolism, extra-hepatic metabolism, enterohepatic circulation, or intestinal secretion have been observed. Similar to hepatic and renal elimination, the occurrence of these alternative elimination pathways seems to correlate to *in vitro* hepatic process clearances (i.e extent of intrinsic clearance and sinusoidal uptake permeability) and ECCCS classification (Camenisch, 2016). For instance, low CYP-mediated clearance *in vitro* is likely an indication for non-CYP-mediated metabolism. In this case, follow-up studies should be conducted using microsomal incubations with additional co-factors or using hepatocytes or S9 fractions that contain additional cytosolic drug-metabolizing enzymes in order to account for enzymes such as UGTs or SULTs. Very high passive uptake permeability seems to be a prerequisite for extra-hepatic metabolism such as lung metabolism, which can further be investigated using lung microsomes or slices. In addition, direct intestinal secretion seems to be relevant only for highly permeable efflux transporter substrates, whereas enterohepatic circulation is rather significant for low permeable efflux transporter substrates. Nevertheless, *in vitro* methods for the described alternative clearance mechanisms must be established and validated in order to provide quantitative predictions. Hence, extensive research will be required to confirm these relationships and to implement novel *in vitro* approaches for the characterization of non-hepatic/non-renal elimination pathways during drug development.

5.4. Conclusion

Within the scope of this work, new IVIVE approaches were investigated in order to facilitate the study of hepatic drug distribution and total drug elimination in humans during preclinical drug development. *In vitro* determination of the hepatic process clearances for a drug compound allows the prediction of hepatic Kp_{uu} based on the ECM concept. This assessment provides the basis for the evaluation of intracellular drug interactions with hepatic transporters, enzymes, and drug targets and is expected to significantly improve the translation of *in vitro* data related to toxicity, pharmacokinetics, and pharmacodynamics. Information about fu_{hep}, on the other hand, is needed for modeling purposes or the correction of intrahepatic process clearances and is preferably obtained by the temperature method.

In parallel, the same hepatic *in vitro* parameters allow the determination of total drug clearance and relative pathway contributions. Knowledge about the total drug clearance will provide valuable information for the estimation of systemic drug exposure and to support dose anticipation for first-in-human studies. In accordance with the ECCCS classification, quantitative information about renal and hepatic pathway contributions will additionally provide guidance for selecting the appropriate phenotyping strategy in order to evaluate the DDI potential of victim drugs.

The results of this thesis are therefore expected to improve the translation of *in vitro* safety and efficacy data for new drug candidates. Furthermore, the investigated *in vitro* models and classification systems will facilitate integrated and tailor-made pharmacokinetic assessments during early drug development stages.

References

Austin RP, Barton P, Mohmed S, and Riley RJ (2005) The binding of drugs to hepatocytes and its relationship to physicochemical properties. *Drug metabolism and disposition: the biological fate of chemicals* **33:**419-425.

Bailey DN (1997) Relative binding of acetaminophen, lidocaine, phenobarbital, phenytoin, quinidine, and theophylline to human tissues in vitro. *J Anal Toxicol* **21:**1-4.

Benet LZ, Amidon GL, Barends DM, Lennernas H, Polli JE, Shah VP, Stavchansky SA, and Yu LX (2008) The use of BDDCS in classifying the permeability of marketed drugs. *Pharmaceutical research* **25:**483-488.

Benet LZ, Cummins CL, and Wu CY (2004) Unmasking the dynamic interplay between efflux transporters and metabolic enzymes. *Int J Pharm* **277:**3-9.

Bjornsson E and Olsson R (2005) Outcome and prognostic markers in severe drug-induced liver disease. *Hepatology* **42:**481-489.

Bohnert T and Gan LS (2013) Plasma protein binding: from discovery to development. *Journal of pharmaceutical sciences* **102:**2953-2994.

Bow DA, Perry JL, Miller DS, Pritchard JB, and Brouwer KL (2008) Localization of P-gp (Abcb1) and Mrp2 (Abcc2) in freshly isolated rat hepatocytes. *Drug metabolism and disposition: the biological fate of chemicals* **36:**198-202.

Brouwer KL, Keppler D, Hoffmaster KA, Bow DA, Cheng Y, Lai Y, Palm JE, Stieger B, Evers R, and International Transporter C (2013) In vitro methods to support transporter evaluation in drug discovery and development. *Clin Pharmacol Ther* **94:**95-112.

Camenisch G, Folkers G, and van de Waterbeemd H (1997) Comparison of passive drug transport through Caco-2 cells and artificial membranes. *Int J Pharm* **147:**61-70.

Camenisch G and Umehara K (2012) Predicting human hepatic clearance from in vitro drug metabolism and transport data: a scientific and pharmaceutical perspective for assessing drug-drug interactions. *Biopharmaceutics & drug disposition* **33:**179-194.

Camenisch GP (2016) Drug Disposition Classification Systems in Discovery and Development: A Comparative Review of the BDDCS, ECCS and ECCCS Concepts. *Pharmaceutical research* **33:**2583-2593.

Carlile DJ, Zomorodi K, and Houston JB (1997) Scaling factors to relate drug metabolic clearance in hepatic microsomes, isolated hepatocytes, and the intact liver: studies with induced livers

involving diazepam. *Drug metabolism and disposition: the biological fate of chemicals* **25:**903-911.

Cesar-Razquin A, Snijder B, Frappier-Brinton T, Isserlin R, Gyimesi G, Bai X, Reithmeier RA, Hepworth D, Hediger MA, Edwards AM, and Superti-Furga G (2015) A Call for Systematic Research on Solute Carriers. *Cell* **162:**478-487.

Chan LM, Lowes S, and Hirst BH (2004) The ABCs of drug transport in intestine and liver: efflux proteins limiting drug absorption and bioavailability. *European journal of pharmaceutical sciences : official journal of the European Federation for Pharmaceutical Sciences* **21:**25-51.

Chang JH, Plise E, Cheong J, Ho Q, and Lin M (2013) Evaluating the in vitro inhibition of UGT1A1, OATP1B1, OATP1B3, MRP2, and BSEP in predicting drug-induced hyperbilirubinemia. *Mol Pharm* **10:**3067-3075.

Chaturvedi PR, Decker CJ, and Odinecs A (2001) Prediction of pharmacokinetic properties using experimental approaches during early drug discovery. *Curr Opin Chem Biol* **5:**452-463.

Chen Q, Zhang T, Wang JF, and Wei DQ (2011) Advances in human cytochrome p450 and personalized medicine. *Curr Drug Metab* **12:**436-444.

Cheng Y, Woolf TF, Gan J, and He K (2016) In vitro model systems to investigate bile salt export pump (BSEP) activity and drug interactions: A review. *Chem Biol Interact* **255:**23-30.

Chiba M, Ishii Y, and Sugiyama Y (2009) Prediction of hepatic clearance in human from in vitro data for successful drug development. *AAPS J* **11:**262-276.

Chu X, Korzekwa K, Elsby R, Fenner K, Galetin A, Lai Y, Matsson P, Moss A, Nagar S, Rosania GR, Bai JP, Polli JW, Sugiyama Y, Brouwer KL, and International Transporter C (2013) Intracellular drug concentrations and transporters: measurement, modeling, and implications for the liver. *Clin Pharmacol Ther* **94:**126-141.

CIOMS (1999) *Reporting Adverse Drug Reactions - Definitions of Terms and Criteria for their Use*, Geneva.

Corless JK and Middleton HM, 3rd (1983) Normal liver function. A basis for understanding hepatic disease. *Arch Intern Med* **143:**2291-2294.

Costa A, Sarmento B, and Seabra V (2014) An evaluation of the latest in vitro tools for drug metabolism studies. *Expert opinion on drug metabolism & toxicology* **10:**103-119.

Coughtrie MWH (2016) Function and organization of the human cytosolic sulfotransferase (SULT) family. *Chem-Biol Interact* **259:**2-7.

Dave RA and Morris ME (2015) Quantitative structure-pharmacokinetic relationships for the prediction of renal clearance in humans. *Drug metabolism and disposition: the biological fate of chemicals* **43:**73-81.

Dawson PA, Lan T, and Rao A (2009) Bile acid transporters. *J Lipid Res* **50:**2340-2357.

Dawson S, Stahl S, Paul N, Barber J, and Kenna JG (2012) In vitro inhibition of the bile salt export pump correlates with risk of cholestatic drug-induced liver injury in humans. *Drug metabolism and disposition: the biological fate of chemicals* **40:**130-138.

De Bruyn T, Chatterjee S, Fattah S, Keemink J, Nicolai J, Augustijns P, and Annaert P (2013) Sandwich-cultured hepatocytes: utility for in vitro exploration of hepatobiliary drug disposition and drug-induced hepatotoxicity. *Expert opinion on drug metabolism & toxicology* **9:**589-616.

DeGorter MK, Xia CQ, Yang JJ, and Kim RB (2012) Drug transporters in drug efficacy and toxicity. *Annu Rev Pharmacol Toxicol* **52:**249-273.

Deguchi T, Watanabe N, Kurihara A, Igeta K, Ikenaga H, Fusegawa K, Suzuki N, Murata S, Hirouchi M, Furuta Y, Iwasaki M, Okazaki O, and Izumi T (2011) Human pharmacokinetic prediction of UDP-glucuronosyltransferase substrates with an animal scale-up approach. *Drug metabolism and disposition: the biological fate of chemicals* **39:**820-829.

Di L (2014) The role of drug metabolizing enzymes in clearance. *Expert opinion on drug metabolism & toxicology* **10:**379-393.

Di L, Feng B, Goosen TC, Lai Y, Steyn SJ, Varma MV, and Obach RS (2013) A perspective on the prediction of drug pharmacokinetics and disposition in drug research and development. *Drug metabolism and disposition: the biological fate of chemicals* **41:**1975-1993.

Di L, Keefer C, Scott DO, Strelevitz TJ, Chang G, Bi YA, Lai YR, Duckworth J, Fenner K, Troutman MD, and Obach RS (2012) Mechanistic insights from comparing intrinsic clearance values between human liver microsomes and hepatocytes to guide drug design. *European Journal of Medicinal Chemistry* **57:**441-448.

Dietrich CG and Geier A (2014) Effect of drug transporter pharmacogenetics on cholestasis. *Expert opinion on drug metabolism & toxicology* **10:**1533-1551.

Ding X and Kaminsky LS (2003) Human extrahepatic cytochromes P450: function in xenobiotic metabolism and tissue-selective chemical toxicity in the respiratory and gastrointestinal tracts. *Annu Rev Pharmacol Toxicol* **43:**149-173.

Dingemanse J and van Giersbergen PL (2004) Clinical pharmacology of bosentan, a dual endothelin receptor antagonist. *Clin Pharmacokinet* **43:**1089-1115.

Eipel C, Abshagen K, and Vollmar B (2010) Regulation of hepatic blood flow: The hepatic arterial buffer response revisited. *World J Gastroentero* **16:**6046-6057.

Elsby R, Hilgendorf C, and Fenner K (2012) Understanding the critical disposition pathways of statins to assess drug-drug interaction risk during drug development: it's not just about OATP1B1. *Clin Pharmacol Ther* **92:**584-598.

EMA (2012) Guideline on the Investigation of Drug Interactions.

Erlinger S, Arias IM, and Dhumeaux D (2014) Inherited Disorders of Bilirubin Transport and Conjugation: New Insights Into Molecular Mechanisms and Consequences. *Gastroenterology* **146:**1625-1638.

Estudante M, Morais JG, Soveral G, and Benet LZ (2013) Intestinal drug transporters: an overview. *Adv Drug Deliv Rev* **65:**1340-1356.

Fan J and de Lannoy IA (2014) Pharmacokinetics. *Biochemical pharmacology* **87:**93-120.

Fasinu P, Bouic PJ, and Rosenkranz B (2012) Liver-based in vitro technologies for drug biotransformation studies - a review. *Curr Drug Metab* **13:**215-224.

Fattinger K, Funk C, Pantze M, Weber C, Reichen J, Stieger B, and Meier PJ (2001) The endothelin antagonist bosentan inhibits the canalicular bile salt export pump: a potential mechanism for hepatic adverse reactions. *Clin Pharmacol Ther* **69:**223-231.

FDA (2012) Guidance for Industry. Drug Interaction Studies - Study Design, Data Analysis, Implications for Dosing, and Labeling Recommendations.

FDA (2016) Guidance for Industry. Safety Testing of Drug Metabolites.

Feng B, LaPerle JL, Chang G, and Varma MV (2010) Renal clearance in drug discovery and development: molecular descriptors, drug transporters and disease state. *Expert opinion on drug metabolism & toxicology* **6:**939-952.

Foti RS, Tyndale RF, Garcia KL, Sweet DH, Nagar S, Sharan S, and Rock DA (2015) "Target-Site" Drug Metabolism and Transport. *Drug metabolism and disposition: the biological fate of chemicals* **43:**1156-1168.

Frezard F and Garnier-Suillerot A (1998) Permeability of lipid bilayer to anthracycline derivatives. Role of the bilayer composition and of the temperature. *Biochimica et biophysica acta* **1389:**13-22.

Fujiwara R, Nakajima M, Yamanaka H, Katoh M, and Yokoi T (2008) Product inhibition of UDP-glucuronosyltransferase (UGT) enzymes by UDP obfuscates the inhibitory effects of UGT substrates. *Drug metabolism and disposition: the biological fate of chemicals* **36:**361-367.

Funk C, Pantze M, Jehle L, Ponelle C, Scheuermann G, Lazendic M, and Gasser R (2001a) Troglitazone-induced intrahepatic cholestasis by an interference with the hepatobiliary export of bile acids in male and female rats. Correlation with the gender difference in troglitazone sulfate formation and the inhibition of the canalicular bile salt export pump (Bsep) by troglitazone and troglitazone sulfate. *Toxicology* **167:**83-98.

Funk C, Ponelle C, Scheuermann G, and Pantze M (2001b) Cholestatic potential of troglitazone as a possible factor contributing to troglitazone-induced hepatotoxicity: in vivo and in vitro interaction at the canalicular bile salt export pump (Bsep) in the rat. *Molecular pharmacology* **59:**627-635.

Gao Y, Shao JW, Jiang Z, Chen JZ, Gu SG, Yu SH, Zheng K, and Jia L (2014) Drug enterohepatic circulation and disposition: constituents of systems pharmacokinetics. *Drug Discovery Today* **19:**326-340.

Gertz M, Harrison A, Houston JB, and Galetin A (2010) Prediction of human intestinal first-pass metabolism of 25 CYP3A substrates from in vitro clearance and permeability data. *Drug metabolism and disposition: the biological fate of chemicals* **38:**1147-1158.

Giacomini KM, Huang SM, Tweedie DJ, Benet LZ, Brouwer KL, Chu X, Dahlin A, Evers R, Fischer V, Hillgren KM, Hoffmaster KA, Ishikawa T, Keppler D, Kim RB, Lee CA, Niemi M, Polli JW, Sugiyama Y, Swaan PW, Ware JA, Wright SH, Yee SW, Zamek-Gliszczynski MJ, and Zhang L (2010) Membrane transporters in drug development. *Nat Rev Drug Discov* **9:**215-236.

Godoy P, Hewitt NJ, Albrecht U, Andersen ME, Ansari N, Bhattacharya S, Bode JG, Bolleyn J, Borner C, Bottger J, Braeuning A, Budinsky RA, Burkhardt B, Cameron NR, Camussi G, Cho CS, Choi YJ, Craig Rowlands J, Dahmen U, Damm G, Dirsch O, Donato MT, Dong J, Dooley S, Drasdo D, Eakins R, Ferreira KS, Fonsato V, Fraczek J, Gebhardt R, Gibson A, Glanemann M, Goldring CE, Gomez-Lechon MJ, Groothuis GM, Gustavsson L, Guyot C, Hallifax D, Hammad S, Hayward A, Haussinger D, Hellerbrand C, Hewitt P, Hoehme S, Holzhutter HG, Houston JB, Hrach J, Ito K, Jaeschke H, Keitel V, Kelm JM, Kevin Park B, Kordes C, Kullak-Ublick GA, LeCluyse EL, Lu P, Luebke-Wheeler J, Lutz A, Maltman DJ, Matz-Soja M, McMullen P, Merfort I, Messner S, Meyer C, Mwinyi J, Naisbitt DJ, Nussler AK, Olinga P, Pampaloni F, Pi J, Pluta L, Przyborski SA, Ramachandran A, Rogiers V, Rowe C, Schelcher C, Schmich K, Schwarz M, Singh B, Stelzer EH, Stieger B, Stober R, Sugiyama Y, Tetta C, Thasler WE, Vanhaecke T, Vinken M, Weiss TS, Widera A, Woods CG, Xu JJ, Yarborough KM, and Hengstler JG (2013) Recent advances in 2D and 3D in vitro systems using primary hepatocytes, alternative

hepatocyte sources and non-parenchymal liver cells and their use in investigating mechanisms of hepatotoxicity, cell signaling and ADME. *Arch Toxicol* **87:**1315-1530.

Gorboulev V, Ulzheimer JC, Akhoundova A, Ulzheimer-Teuber I, Karbach U, Quester S, Baumann C, Lang F, Busch AE, and Koepsell H (1997) Cloning and characterization of two human polyspecific organic cation transporters. *DNA Cell Biol* **16:**871-881.

Gradhand U, Lang T, Schaeffeler E, Glaeser H, Tegude H, Klein K, Fritz P, Jedlitschky G, Kroemer HK, Bachmakov I, Anwald B, Kerb R, Zanger UM, Eichelbaum M, Schwab M, and Fromm MF (2008) Variability in human hepatic MRP4 expression: influence of cholestasis and genotype. *Pharmacogenomics J* **8:**42-52.

Gundert-Remy U, Bernauer U, Blomeke B, Doring B, Fabian E, Goebel C, Hessel S, Jackh C, Lampen A, Oesch F, Petzinger E, Volkel W, and Roos PH (2014) Extrahepatic metabolism at the body's internal-external interfaces. *Drug Metab Rev* **46:**291-324.

Guo C, Yang K, Brouwer KR, St Claire RL, 3rd, and Brouwer KL (2016) Prediction of Altered Bile Acid Disposition Due to Inhibition of Multiple Transporters: An Integrated Approach Using Sandwich-Cultured Hepatocytes, Mechanistic Modeling, and Simulation. *J Pharmacol Exp Ther* **358:**324-333.

Hardwick RN, Ferreira DW, More VR, Lake AD, Lu ZQ, Manautou JE, Slitt AL, and Cherrington NJ (2013) Altered UDP-Glucuronosyltransferase and Sulfotransferase Expression and Function during Progressive Stages of Human Nonalcoholic Fatty Liver Disease. *Drug Metabolism and Disposition* **41:**554-561.

Hediger MA, Clemencon B, Burrier RE, and Bruford EA (2013) The ABCs of membrane transporters in health and disease (SLC series): introduction. *Mol Aspects Med* **34:**95-107.

Hilgendorf C, Ahlin G, Seithel A, Artursson P, Ungell AL, and Karlsson J (2007) Expression of thirty-six drug transporter genes in human intestine, liver, kidney, and organotypic cell lines. *Drug metabolism and disposition: the biological fate of chemicals* **35:**1333-1340.

Hillgren KM, Keppler D, Zur AA, Giacomini KM, Stieger B, Cass CE, Zhang L, and International Transporter C (2013) Emerging transporters of clinical importance: an update from the International Transporter Consortium. *Clin Pharmacol Ther* **94:**52-63.

Hinderling PH (1997) Red blood cells: a neglected compartment in pharmacokinetics and pharmacodynamics. *Pharmacol Rev* **49:**279-295.

Houston JB and Galetin A (2008) Methods for Predicting In Vivo Pharmacokinetics Using Data from In Vitro Assays. *Current Drug Metabolism* **9:**940-951.

Hussaini SH and Farrington EA (2007) Idiosyncratic drug-induced liver injury: an overview. *Expert Opin Drug Saf* **6:**673-684.

Ishigami M, Tokui T, Komai T, Tsukahara K, Yamazaki M, and Sugiyama Y (1995) Evaluation of the uptake of pravastatin by perfused rat liver and primary cultured rat hepatocytes. *Pharmaceutical research* **12:**1741-1745.

Iusuf D, van de Steeg E, and Schinkel AH (2012) Hepatocyte hopping of OATP1B substrates contributes to efficient hepatic detoxification. *Clin Pharmacol Ther* **92:**559-562.

Iwasaki S, Hirabayashi H, Funami M, and Amano N (2017) Unbound liver concentration is the true inhibitor concentration that determines cytochrome P450-mediated drug-drug interactions in rat liver. *Xenobiotica; the fate of foreign compounds in biological systems* **47:**488-497.

Jia L and Liu X (2007) The conduct of drug metabolism studies considered good practice (II): in vitro experiments. *Curr Drug Metab* **8:**822-829.

Jones CR, Hatley OJ, Ungell AL, Hilgendorf C, Peters SA, and Rostami-Hodjegan A (2016) Gut Wall Metabolism. Application of Pre-Clinical Models for the Prediction of Human Drug Absorption and First-Pass Elimination. *AAPS J* **18:**589-604.

Jones HM, Barton HA, Lai Y, Bi YA, Kimoto E, Kempshall S, Tate SC, El-Kattan A, Houston JB, Galetin A, and Fenner KS (2012) Mechanistic pharmacokinetic modeling for the prediction of transporter-mediated disposition in humans from sandwich culture human hepatocyte data. *Drug metabolism and disposition: the biological fate of chemicals* **40:**1007-1017.

Kazmi F, Hensley T, Pope C, Funk RS, Loewen GJ, Buckley DB, and Parkinson A (2013) Lysosomal sequestration (trapping) of lipophilic amine (cationic amphiphilic) drugs in immortalized human hepatocytes (Fa2N-4 cells). *Drug metabolism and disposition: the biological fate of chemicals* **41:**897-905.

Keppler D (2014) The roles of MRP2, MRP3, OATP1B1, and OATP1B3 in conjugated hyperbilirubinemia. *Drug metabolism and disposition: the biological fate of chemicals* **42:**561-565.

Kilford PJ, Gertz M, Houston JB, and Galetin A (2008) Hepatocellular binding of drugs: correction for unbound fraction in hepatocyte incubations using microsomal binding or drug lipophilicity data. *Drug metabolism and disposition: the biological fate of chemicals* **36:**1194-1197.

Kimoto E, Yoshida K, Balogh LM, Bi YA, Maeda K, El-Kattan A, Sugiyama Y, and Lai Y (2012) Characterization of organic anion transporting polypeptide (OATP) expression and its functional contribution to the uptake of substrates in human hepatocytes. *Mol Pharm* **9:**3535-3542.

Kock K and Brouwer KL (2012) A perspective on efflux transport proteins in the liver. *Clin Pharmacol Ther* **92:**599-612.

Kock K, Ferslew BC, Netterberg I, Yang K, Urban TJ, Swaan PW, Stewart PW, and Brouwer KL (2014) Risk factors for development of cholestatic drug-induced liver injury: inhibition of hepatic basolateral bile acid transporters multidrug resistance-associated proteins 3 and 4. *Drug metabolism and disposition: the biological fate of chemicals* **42:**665-674.

Koepsell H (2013) The SLC22 family with transporters of organic cations, anions and zwitterions. *Mol Aspects Med* **34:**413-435.

Konig J, Muller F, and Fromm MF (2013) Transporters and drug-drug interactions: important determinants of drug disposition and effects. *Pharmacol Rev* **65:**944-966.

Konig J, Nies AT, Cui Y, Leier I, and Keppler D (1999) Conjugate export pumps of the multidrug resistance protein (MRP) family: localization, substrate specificity, and MRP2-mediated drug resistance. *Biochimica et biophysica acta* **1461:**377-394.

Kosters A and Karpen SJ (2008) Bile acid transporters in health and disease. *Xenobiotica; the fate of foreign compounds in biological systems* **38:**1043-1071.

Kotani N, Maeda K, Watanabe T, Hiramatsu M, Gong LK, Bi YA, Takezawa T, Kusuhara H, and Sugiyama Y (2011) Culture period-dependent changes in the uptake of transporter substrates in sandwich-cultured rat and human hepatocytes. *Drug metabolism and disposition: the biological fate of chemicals* **39:**1503-1510.

Kriz W (1981) Structural Organization of the Renal Medulla - Comparative and Functional-Aspects. *American Journal of Physiology* **241:**R3-R16.

Kuehl GE, Lampe JW, Potter JD, and Bigler J (2005) Glucuronidation of nonsteroidal anti-inflammatory drugs: identifying the enzymes responsible in human liver microsomes. *Drug metabolism and disposition: the biological fate of chemicals* **33:**1027-1035.

Kullak-Ublick GA, Andrade RJ, Merz M, End P, Benesic A, Gerbes AL, and Aithal GP (2017) Drug-induced liver injury: recent advances in diagnosis and risk assessment. *Gut* **66:**1154-1164.

Kullak-Ublick GA, Ismair MG, Stieger B, Landmann L, Huber R, Pizzagalli F, Fattinger K, Meier PJ, and Hagenbuch B (2001) Organic anion-transporting polypeptide B (OATP-B) and its functional comparison with three other OATPs of human liver. *Gastroenterology* **120:**525-533.

Kullak-Ublick GA, Stieger B, Hagenbuch B, and Meier PJ (2000) Hepatic transport of bile salts. *Semin Liver Dis* **20:**273-292.

Kunze A, Huwyler J, Camenisch G, and Poller B (2014a) Prediction of organic anion-transporting polypeptide 1B1- and 1B3-mediated hepatic uptake of statins based on transporter protein expression and activity data. *Drug metabolism and disposition: the biological fate of chemicals* **42:**1514-1521.

Kunze A, Huwyler J, Poller B, Gutmann H, and Camenisch G (2014b) In vitro-in vivo extrapolation method to predict human renal clearance of drugs. *Journal of pharmaceutical sciences* **103:**994-1001.

Kunze A, Poller B, Huwyler J, and Camenisch G (2015) Application of the extended clearance concept classification system (ECCCS) to predict the victim drug-drug interaction potential of statins. *Drug Metab Pers Ther* **30:**175-188.

Kusuhara H and Sugiyama Y (2009) In vitro-in vivo extrapolation of transporter-mediated clearance in the liver and kidney. *Drug Metab Pharmacokinet* **24:**37-52.

Kwon Y (2001) *Handbook of Essential Pharmacokinetics, Pharmacodynamics, and Drug Metabolism for Industrial Scientists*. Kluwer Academic/Plenum Publishers, New York.

Launay-Vacher V, Izzedine H, Karie S, Hulot JS, Baumelou A, and Deray G (2006) Renal tubular drug transporters. *Nephron Physiol* **103:**p97-106.

Laznicek M and Laznickova A (1995) The Effect of Lipophilicity on the Protein-Binding and Blood-Cell Uptake of Some Acidic Drugs. *J Pharmaceut Biomed* **13:**823-828.

Lecluyse EL and Alexandre E (2010) Isolation and culture of primary hepatocytes from resected human liver tissue. *Methods in molecular biology* **640:**57-82.

Lee PS, Song IS, Shin TH, Chung SJ, Shim CK, Song S, and Chung YB (2003) Kinetic analysis about the bidirectional transport of 1-anilino-8-naphthalene sulfonate (ANS) by isolated rat hepatocytes. *Archives of Pharmacal Research* **26:**338-343.

Levine WG (1978) Biliary-Excretion of Drugs and Other Xenobiotics. *Annu Rev Pharmacol* **18:**81-96.

Levy G (1976) Pharmacokinetic approaches to the study of drug interactions. *Ann N Y Acad Sci* **281:**24-39.

Li T and Chiang JY (2014) Bile acid signaling in metabolic disease and drug therapy. *Pharmacol Rev* **66:**948-983.

Lin L, Yee SW, Kim RB, and Giacomini KM (2015) SLC transporters as therapeutic targets: emerging opportunities. *Nat Rev Drug Discov* **14:**543-560.

Link E, Parish S, Armitage J, Bowman L, Heath S, Matsuda F, Gut I, Lathrop M, and Collins R (2008) SLCO1B1 variants and statin-induced myopathy--a genomewide study. *N Engl J Med* **359:**789-799.

Lips KS, Volk C, Schmitt BM, Pfeil U, Arndt P, Miska D, Ermert L, Kummer W, and Koepsell H (2005) Polyspecific cation transporters mediate luminal release of acetylcholine from bronchial epithelium. *American journal of respiratory cell and molecular biology* **33:**79-88.

Liu HC, Goldenberg A, Chen Y, Lun C, Wu W, Bush KT, Balac N, Rodriguez P, Abagyan R, and Nigam SK (2016) Molecular Properties of Drugs Interacting with SLC22 Transporters OAT1, OAT3, OCT1, and OCT2: A Machine-Learning Approach. *J Pharmacol Exp Ther* **359:**215-229.

Liu X, Wright M, and Hop CE (2014) Rational use of plasma protein and tissue binding data in drug design. *J Med Chem* **57:**8238-8248.

Liu XR, Lecluyse EL, Brouwer KR, Lightfoot RM, Lee JI, and Brouwer KLR (1999) Use of Ca2+ modulation to evaluate biliary excretion in sandwich-cultured rat hepatocytes. *Journal of Pharmacology and Experimental Therapeutics* **289:**1592-1599.

Lote CJ (2012) *Principles of Renal Physiology*. Springer, New York.

Lundquist P, Englund G, Skogastierna C, Loof J, Johansson J, Hoogstraate J, Afzelius L, and Andersson TB (2014a) Functional ATP-binding cassette drug efflux transporters in isolated human and rat hepatocytes significantly affect assessment of drug disposition. *Drug metabolism and disposition: the biological fate of chemicals* **42:**448-458.

Lundquist P, Loof J, Sohlenius-Sternbeck AK, Floby E, Johansson J, Bylund J, Hoogstraate J, Afzelius L, and Andersson TB (2014b) The impact of solute carrier (SLC) drug uptake transporter loss in human and rat cryopreserved hepatocytes on clearance predictions. *Drug metabolism and disposition: the biological fate of chemicals* **42:**469-480.

Lynch T and Price A (2007) The effect of cytochrome P450 metabolism on drug response, interactions, and adverse effects. *Am Fam Physician* **76:**391-396.

Malarkey DE, Johnson K, Ryan L, Boorman G, and Maronpot RR (2005) New insights into functional aspects of liver morphology. *Toxicologic pathology* **33:**27-34.

Marchetti S, Mazzanti R, Beijnen JH, and Schellens JH (2007) Concise review: Clinical relevance of drug drug and herb drug interactions mediated by the ABC transporter ABCB1 (MDR1, P-glycoprotein). *Oncologist* **12:**927-941.

Masereeuw R and Russel FG (2001a) Mechanisms and clinical implications of renal drug excretion. *Drug Metab Rev* **33:**299-351.

Masereeuw R and Russel FGM (2001b) Mechanisms and clinical implications of renal drug excretion. *Drug Metabolism Reviews* **33:**299-351.

Masuda S, Terada T, Yonezawa A, Tanihara Y, Kishimoto K, Katsura T, Ogawa O, and Inui K (2006) Identification and functional characterization of a new human kidney-specific H+/organic cation antiporter, kidney-specific multidrug and toxin extrusion 2. *J Am Soc Nephrol* **17:**2127-2135.

Mateus A, Matsson P, and Artursson P (2013) Rapid measurement of intracellular unbound drug concentrations. *Mol Pharm* **10:**2467-2478.

Mateus A, Matsson P, and Artursson P (2014) A high-throughput cell-based method to predict the unbound drug fraction in the brain. *J Med Chem* **57:**3005-3010.

Mathijs K, Kienhuis AS, Brauers KJ, Jennen DG, Lahoz A, Kleinjans JC, and van Delft JH (2009) Assessing the metabolic competence of sandwich-cultured mouse primary hepatocytes. *Drug metabolism and disposition: the biological fate of chemicals* **37:**1305-1311.

McCuskey RS (2008) The hepatic microvascular system in health and its response to toxicants. *Anat Rec (Hoboken)* **291:**661-671.

Morgan RE, Trauner M, van Staden CJ, Lee PH, Ramachandran B, Eschenberg M, Afshari CA, Qualls CW, Jr., Lightfoot-Dunn R, and Hamadeh HK (2010) Interference with bile salt export pump function is a susceptibility factor for human liver injury in drug development. *Toxicological sciences : an official journal of the Society of Toxicology* **118:**485-500.

Morgan RE, van Staden CJ, Chen Y, Kalyanaraman N, Kalanzi J, Dunn RT, 2nd, Afshari CA, and Hamadeh HK (2013) A multifactorial approach to hepatobiliary transporter assessment enables improved therapeutic compound development. *Toxicological sciences : an official journal of the Society of Toxicology* **136:**216-241.

Morrissey KM, Stocker SL, Wittwer MB, Xu L, and Giacomini KM (2013) Renal transporters in drug development. *Annu Rev Pharmacol Toxicol* **53:**503-529.

Morse BL, Cai H, MacGuire JG, Fox M, Zhang L, Zhang Y, Gu X, Shen H, Dierks EA, Su H, Luk CE, Marathe P, Shu YZ, Humphreys WG, and Lai Y (2015) Rosuvastatin Liver Partitioning in Cynomolgus Monkeys: Measurement In Vivo and Prediction Using In Vitro Monkey Hepatocyte Uptake. *Drug metabolism and disposition: the biological fate of chemicals* **43:**1788-1794.

Muller F and Fromm MF (2011) Transporter-mediated drug-drug interactions. *Pharmacogenomics* **12:**1017-1037.

Muller J, Lips KS, Metzner L, Neubert RH, Koepsell H, and Brandsch M (2005) Drug specificity and intestinal membrane localization of human organic cation transporters (OCT). *Biochemical pharmacology* **70:**1851-1860.

Muller PY and Milton MN (2012) The determination and interpretation of the therapeutic index in drug development. *Nat Rev Drug Discov* **11:**751-761.

Nagar S and Korzekwa K (2012) Commentary: nonspecific protein binding versus membrane partitioning: it is not just semantics. *Drug metabolism and disposition: the biological fate of chemicals* **40:**1649-1652.

Neuhoff S, Gaohua L, Burt H, Jamei M, Li L, Tucker GT, and Rostami-Hodjeagan A (2013) Accounting for Transporters in Renal Clearance: Towards a Mechanistic Kidney Model (Mech KiM), in: *In Transporters in drug development; Yuichi Sugiyama BS, Ed New York: Springer Science+Business Media*, pp 155– 177.

Neuvonen PJ (2010) Drug interactions with HMG-CoA reductase inhibitors (statins): the importance of CYP enzymes, transporters and pharmacogenetics. *Curr Opin Investig Drugs* **11:**323-332.

Neve EP and Ingelman-Sundberg M (2010) Cytochrome P450 proteins: retention and distribution from the endoplasmic reticulum. *Current opinion in drug discovery & development* **13:**78-85.

Niemi M, Neuvonen PJ, Hofmann U, Backman JT, Schwab M, Lutjohann D, von Bergmann K, Eichelbaum M, and Kivisto KT (2005) Acute effects of pravastatin on cholesterol synthesis are associated with SLCO1B1 (encoding OATP1B1) haplotype *17. *Pharmacogenet Genomics* **15:**303-309.

Nies AT, Herrmann E, Brom M, and Keppler D (2008) Vectorial transport of the plant alkaloid berberine by double-transfected cells expressing the human organic cation transporter 1 (OCT1, SLC22A1) and the efflux pump MDR1 P-glycoprotein (ABCB1). *Naunyn Schmiedebergs Arch Pharmacol* **376:**449-461.

Nies AT, Koepsell H, Winter S, Burk O, Klein K, Kerb R, Zanger UM, Keppler D, Schwab M, and Schaeffeler E (2009) Expression of organic cation transporters OCT1 (SLC22A1) and OCT3 (SLC22A3) is affected by genetic factors and cholestasis in human liver. *Hepatology* **50:**1227-1240.

Nieskens TT, Peters JG, Schreurs MJ, Smits N, Woestenenk R, Jansen K, van der Made TK, Roring M, Hilgendorf C, Wilmer MJ, and Masereeuw R (2016) A Human Renal Proximal Tubule Cell Line with Stable Organic Anion Transporter 1 and 3 Expression Predictive for Antiviral-Induced Toxicity. *AAPS J* **18:**465-475.

Nordell P, Winiwarter S, and Hilgendorf C (2013) Resolving the distribution-metabolism interplay of eight OATP substrates in the standard clearance assay with suspended human cryopreserved hepatocytes. *Mol Pharm* **10:**4443-4451.

Obach RS (2001) The prediction of human clearance from hepatic microsomal metabolism data. *Current opinion in drug discovery & development* **4:**36-44.

Obach RS (2011) Predicting Clearance in Humans from In Vitro Data. *Current Topics in Medicinal Chemistry* **11:**334-339.

Ohkuma S and Poole B (1981) Cytoplasmic vacuolation of mouse peritoneal macrophages and the uptake into lysosomes of weakly basic substances. *The Journal of cell biology* **90:**656-664.

Oostendorp RL, Beijnen JH, and Schellens JH (2009) The biological and clinical role of drug transporters at the intestinal barrier. *Cancer Treat Rev* **35:**137-147.

Otsuka M, Matsumoto T, Morimoto R, Arioka S, Omote H, and Moriyama Y (2005) A human transporter protein that mediates the final excretion step for toxic organic cations. *Proceedings of the National Academy of Sciences of the United States of America* **102:**17923-17928.

Overington JP, Al-Lazikani B, and Hopkins AL (2006) How many drug targets are there? *Nat Rev Drug Discov* **5:**993-996.

Padda MS, Sanchez M, Akhtar AJ, and Boyer JL (2011) Drug-induced cholestasis. *Hepatology* **53:**1377-1387.

Pade V and Stavchansky S (1997) Estimation of the relative contribution of the transcellular and paracellular pathway to the transport of passively absorbed drugs in the Caco-2 cell culture model. *Pharmaceutical research* **14:**1210-1215.

Paine MF, Hart HL, Ludington SS, Haining RL, Rettie AE, and Zeldin DC (2006) The human intestinal cytochrome P450 "pie". *Drug metabolism and disposition: the biological fate of chemicals* **34:**880-886.

Pan GY, Boiselle C, and Wang JL (2012) Assessment of Biliary Clearance in Early Drug Discovery Using Sandwich-Cultured Hepatocyte Model. *Journal of pharmaceutical sciences* **101:**1898-1908.

Pang KS, Rodrigues AD, and Peter RM (2010) *Enzyme- and Trnsporter-based drug-drug interactions - Progress and Future Challenges*. Springer, New York.

Pang KS and Rowland M (1977) Hepatic clearance of drugs. I. Theoretical considerations of a "well-stirred" model and a "parallel tube" model. Influence of hepatic blood flow, plasma and

blood cell binding, and the hepatocellular enzymatic activity on hepatic drug clearance. *Journal of pharmacokinetics and biopharmaceutics* **5:**625-653.

Parker AJ and Houston JB (2008) Rate-limiting steps in hepatic drug clearance: comparison of hepatocellular uptake and metabolism with microsomal metabolism of saquinavir, nelfinavir, and ritonavir. *Drug metabolism and disposition: the biological fate of chemicals* **36:**1375-1384.

Pedersen JM, Matsson P, Bergstrom CA, Hoogstraate J, Noren A, LeCluyse EL, and Artursson P (2013) Early identification of clinically relevant drug interactions with the human bile salt export pump (BSEP/ABCB11). *Toxicological sciences : an official journal of the Society of Toxicology* **136:**328-343.

Pelkonen O and Turpeinen M (2007) In vitro-in vivo extrapolation of hepatic clearance: Biological tools, scaling factors, model assumptions and correct concentrations. *Xenobiotica; the fate of foreign compounds in biological systems* **37:**1066-1089.

Pfeifer ND, Hardwick RN, and Brouwer KL (2014) Role of hepatic efflux transporters in regulating systemic and hepatocyte exposure to xenobiotics. *Annu Rev Pharmacol Toxicol* **54:**509-535.

Pfeifer ND, Harris KB, Yan GZ, and Brouwer KL (2013a) Determination of intracellular unbound concentrations and subcellular localization of drugs in rat sandwich-cultured hepatocytes compared with liver tissue. *Drug metabolism and disposition: the biological fate of chemicals* **41:**1949-1956.

Pfeifer ND, Yang K, and Brouwer KL (2013b) Hepatic basolateral efflux contributes significantly to rosuvastatin disposition I: characterization of basolateral versus biliary clearance using a novel protocol in sandwich-cultured hepatocytes. *J Pharmacol Exp Ther* **347:**727-736.

Poulin P (2015) Drug Distribution to Human Tissues: Prediction and Examination of the Basic Assumption in In Vivo Pharmacokinetics-Pharmacodynamics (PK/PD) Research. *Journal of pharmaceutical sciences* **104:**2110-2118.

Radominska-Pandya A, Czernik PJ, Little JM, Battaglia E, and Mackenzie PI (1999) Structural and functional studies of UDP-glucuronosyltransferases. *Drug Metabolism Reviews* **31:**817-899.

Riccardi K, Li Z, Brown JA, Gorgoglione MF, Niosi M, Gosset J, Huard K, Erion DM, and Di L (2016) Determination of Unbound Partition Coefficient and in Vitro-in Vivo Extrapolation for SLC13A Transporter-Mediated Uptake. *Drug metabolism and disposition: the biological fate of chemicals* **44:**1633-1642.

Riccardi K, Lin J, Li Z, Niosi M, Ryu S, Hua W, Atkinson K, Kosa RE, Litchfield J, and Di L (2017) Novel Method to Predict In Vivo Liver-to-Plasma Kpuu for OATP Substrates Using Suspension Hepatocytes. *Drug metabolism and disposition: the biological fate of chemicals* **45:**576-580.

Richardson SJ, Bai A, Kulkarni AA, and Moghaddam MF (2016) Efficiency in Drug Discovery: Liver S9 Fraction Assay As a Screen for Metabolic Stability. *Drug Metab Lett* **10:**83-90.

Robey RW, To KK, Polgar O, Dohse M, Fetsch P, Dean M, and Bates SE (2009) ABCG2: a perspective. *Adv Drug Deliv Rev* **61:**3-13.

Rodrigues AD, Lai Y, Cvijic ME, Elkin LL, Zvyaga T, and Soars MG (2014) Drug-induced perturbations of the bile acid pool, cholestasis, and hepatotoxicity: mechanistic considerations beyond the direct inhibition of the bile salt export pump. *Drug metabolism and disposition: the biological fate of chemicals* **42:**566-574.

Roth M, Obaidat A, and Hagenbuch B (2012) OATPs, OATs and OCTs: the organic anion and cation transporters of the SLCO and SLC22A gene superfamilies. *Br J Pharmacol* **165:**1260-1287.

Rowland A, Miners JO, and Mackenzie PI (2013) The UDP-glucuronosyltransferases: Their role in drug metabolism and detoxification. *Int J Biochem Cell B* **45:**1121-1132.

Rowland M and Tozer TN (1995) *Clinical Pharmacokinetics - Concenpts and Applications*. Lippincott Williams & Wilkins, Philadelphia.

Sahi J, Grepper S, and Smith C (2010) Hepatocytes as a tool in drug metabolism, transport and safety evaluations in drug discovery. *Curr Drug Discov Technol* **7:**188-198.

Sahoo S, Aurich MK, Jonsson JJ, and Thiele I (2014) Membrane transporters in a human genome-scale metabolic knowledgebase and their implications for disease. *Front Physiol* **5:**91.

Saier MH, Jr., Reddy VS, Tsu BV, Ahmed MS, Li C, and Moreno-Hagelsieb G (2016) The Transporter Classification Database (TCDB): recent advances. *Nucleic acids research* **44:**D372-379.

Schaefer O, Ohtsuki S, Kawakami H, Inoue T, Liehner S, Saito A, Sakamoto A, Ishiguro N, Matsumaru T, Terasaki T, and Ebner T (2012) Absolute quantification and differential expression of drug transporters, cytochrome P450 enzymes, and UDP-glucuronosyltransferases in cultured primary human hepatocytes. *Drug metabolism and disposition: the biological fate of chemicals* **40:**93-103.

Schinkel AH and Jonker JW (2003) Mammalian drug efflux transporters of the ATP binding cassette (ABC) family: an overview. *Adv Drug Deliv Rev* **55:**3-29.

Scotcher D, Jones C, Posada M, Rostami-Hodjegan A, and Galetin A (2016) Key to Opening Kidney for In Vitro-In Vivo Extrapolation Entrance in Health and Disease: Part I: In Vitro Systems and Physiological Data. *Aaps Journal* **18:**1067-1081.

Shah F, Leung L, Barton HA, Will Y, Rodrigues AD, Greene N, and Aleo MD (2015) Setting Clinical Exposure Levels of Concern for Drug-Induced Liver Injury (DILI) Using Mechanistic in vitro Assays. *Toxicological sciences : an official journal of the Society of Toxicology* **147:**500-514.

Shen Q, Wang L, Zhou H, Jiang HD, Yu LS, and Zeng S (2013) Stereoselective binding of chiral drugs to plasma proteins. *Acta Pharmacol Sin* **34:**998-1006.

Sherwood L (2015) *Human Physiology: From Cells to Systems*. Cengage Learning.

Shitara Y, Horie T, and Sugiyama Y (2006) Transporters as a determinant of drug clearance and tissue distribution. *European journal of pharmaceutical sciences : official journal of the European Federation for Pharmaceutical Sciences* **27:**425-446.

Shitara Y, Maeda K, Ikejiri K, Yoshida K, Horie T, and Sugiyama Y (2013) Clinical significance of organic anion transporting polypeptides (OATPs) in drug disposition: their roles in hepatic clearance and intestinal absorption. *Biopharmaceutics & drug disposition* **34:**45-78.

Slot AJ, Molinski SV, and Cole SP (2011) Mammalian multidrug-resistance proteins (MRPs). *Essays Biochem* **50:**179-207.

Smith DA, Di L, and Kerns EH (2010) The effect of plasma protein binding on in vivo efficacy: misconceptions in drug discovery. *Nat Rev Drug Discov* **9:**929-939.

Soroka CJ, Lee JM, Azzaroli F, and Boyer JL (2001) Cellular localization and up-regulation of multidrug resistance-associated protein 3 in hepatocytes and cholangiocytes during obstructive cholestasis in rat liver. *Hepatology* **33:**783-791.

Srivastava A (2014) Progressive familial intrahepatic cholestasis. *J Clin Exp Hepatol* **4:**25-36.

Stieger B (2010) Role of the bile salt export pump, BSEP, in acquired forms of cholestasis. *Drug Metab Rev* **42:**437-445.

Stieger B, Fattinger K, Madon J, Kullak-Ublick GA, and Meier PJ (2000) Drug- and estrogen-induced cholestasis through inhibition of the hepatocellular bile salt export pump (Bsep) of rat liver. *Gastroenterology* **118:**422-430.

Sugano K, Kansy M, Artursson P, Avdeef A, Bendels S, Di L, Ecker GF, Faller B, Fischer H, Gerebtzoff G, Lennernaes H, and Senner F (2010) Coexistence of passive and carrier-mediated processes in drug transport. *Nat Rev Drug Discov* **9:**597-614.

Swift B, Pfeifer ND, and Brouwer KL (2010) Sandwich-cultured hepatocytes: an in vitro model to evaluate hepatobiliary transporter-based drug interactions and hepatotoxicity. *Drug Metab Rev* **42:**446-471.

Takeda M, Noshiro R, Onozato ML, Tojo A, Hasannejad H, Huang XL, Narikawa S, and Endou H (2004) Evidence for a role of human organic anion transporters in the muscular side effects of HMG-CoA reductase inhibitors. *Eur J Pharmacol* **483:**133-138.

Tanihara Y, Masuda S, Sato T, Katsura T, Ogawa O, and Inui K (2007) Substrate specificity of MATE1 and MATE2-K, human multidrug and toxin extrusions/H(+)-organic cation antiporters. *Biochemical pharmacology* **74:**359-371.

Terasaki T, Iga T, Sugiyama Y, Sawada Y, and Hanano M (1984) Nuclear-Binding as a Determinant of Tissue Distribution of Adriamycin, Daunomycin, Adriamycinol, Daunorubicinol and Actinomycin-D. *J Pharmacobio-Dynam* **7:**269-277.

Trapp S and Horobin RW (2005) A predictive model for the selective accumulation of chemicals in tumor cells. *Eur Biophys J* **34:**959-966.

Trapp S, Rosania GR, Horobin RW, and Kornhuber J (2008) Quantitative modeling of selective lysosomal targeting for drug design. *Eur Biophys J* **37:**1317-1328.

Tweedie D, Polli JW, Berglund EG, Huang SM, Zhang L, Poirier A, Chu X, Feng B, and International Transporter C (2013) Transporter studies in drug development: experience to date and follow-up on decision trees from the International Transporter Consortium. *Clin Pharmacol Ther* **94:**113-125.

Tzvetkov MV, Vormfelde SV, Balen D, Meineke I, Schmidt T, Sehrt D, Sabolic I, Koepsell H, and Brockmoller J (2009) The effects of genetic polymorphisms in the organic cation transporters OCT1, OCT2, and OCT3 on the renal clearance of metformin. *Clin Pharmacol Ther* **86:**299-306.

Umehara K and Camenisch G (2012) Novel in vitro-in vivo extrapolation (IVIVE) method to predict hepatic organ clearance in rat. *Pharmaceutical research* **29:**603-617.

Vallon V, Platt KA, Cunard R, Schroth J, Whaley J, Thomson SC, Koepsell H, and Rieg T (2011) SGLT2 mediates glucose reabsorption in the early proximal tubule. *J Am Soc Nephrol* **22:**104-112.

van de Steeg E, Stranecky V, Hartmannova H, Noskova L, Hrebicek M, Wagenaar E, van Esch A, de Waart DR, Oude Elferink RP, Kenworthy KE, Sticova E, al-Edreesi M, Knisely AS, Kmoch S, Jirsa M, and Schinkel AH (2012) Complete OATP1B1 and OATP1B3 deficiency causes human Rotor syndrome by interrupting conjugated bilirubin reuptake into the liver. *The Journal of clinical investigation* **122:**519-528.

van de Waterbeemd H and Gifford E (2003) ADMET in silico modelling: towards prediction paradise? *Nat Rev Drug Discov* **2:**192-204.

van der Woerd WL, van Mil SW, Stapelbroek JM, Klomp LW, van de Graaf SF, and Houwen RH (2010) Familial cholestasis: progressive familial intrahepatic cholestasis, benign recurrent intrahepatic cholestasis and intrahepatic cholestasis of pregnancy. *Best Pract Res Clin Gastroenterol* **24:**541-553.

van Leeuwen N, Swen JJ, Guchelaar HJ, and t Hart LM (2013) The role of pharmacogenetics in drug disposition and response of oral glucose-lowering drugs. *Clin Pharmacokinet* **52:**833-854.

van Staden CJ, Morgan RE, Ramachandran B, Chen Y, Lee PH, and Hamadeh HK (2012) Membrane vesicle ABC transporter assays for drug safety assessment. *Curr Protoc Toxicol* **Chapter 23:**Unit 23 25.

Varma MV, Bi YA, Kimoto E, and Lin J (2014) Quantitative prediction of transporter- and enzyme-mediated clinical drug-drug interactions of organic anion-transporting polypeptide 1B1 substrates using a mechanistic net-effect model. *J Pharmacol Exp Ther* **351:**214-223.

Varma MV, Chang G, Lai Y, Feng B, El-Kattan AF, Litchfield J, and Goosen TC (2012) Physicochemical property space of hepatobiliary transport and computational models for predicting rat biliary excretion. *Drug metabolism and disposition: the biological fate of chemicals* **40:**1527-1537.

Varma MV, Steyn SJ, Allerton C, and El-Kattan AF (2015) Predicting Clearance Mechanism in Drug Discovery: Extended Clearance Classification System (ECCS). *Pharmaceutical research* **32:**3785-3802.

Vildhede A, Wisniewski JR, Noren A, Karlgren M, and Artursson P (2015) Comparative Proteomic Analysis of Human Liver Tissue and Isolated Hepatocytes with a Focus on Proteins Determining Drug Exposure. *Journal of Proteome Research* **14:**3305-3314.

Vlaming ML, Mohrmann K, Wagenaar E, de Waart DR, Elferink RP, Lagas JS, van Tellingen O, Vainchtein LD, Rosing H, Beijnen JH, Schellens JH, and Schinkel AH (2006) Carcinogen and anticancer drug transport by Mrp2 in vivo: studies using Mrp2 (Abcc2) knockout mice. *J Pharmacol Exp Ther* **318:**319-327.

Volpe DA, Hamed SS, and Zhang LK (2014) Use of Different Parameters and Equations for Calculation of IC50 Values in Efflux Assays: Potential Sources of Variability in IC50 Determination. *Aaps Journal* **16:**172-180.

Walsh AA, Szklarz GD, and Scott EE (2013) Human cytochrome P450 1A1 structure and utility in understanding drug and xenobiotic metabolism. *The Journal of biological chemistry* **288:**12932-12943.

Walsky RL, Bauman JN, Bourcier K, Giddens G, Lapham K, Negahban A, Ryder TF, Obach RS, Hyland R, and Goosen TC (2012) Optimized assays for human UDP-glucuronosyltransferase (UGT) activities: altered alamethicin concentration and utility to screen for UGT inhibitors. *Drug metabolism and disposition: the biological fate of chemicals* **40:**1051-1065.

Watanabe T, Kusuhara H, Watanabe T, Debori Y, Maeda K, Kondo T, Nakayama H, Horita S, Ogilvie BW, Parkinson A, Hu Z, and Sugiyama Y (2011) Prediction of the overall renal tubular secretion and hepatic clearance of anionic drugs and a renal drug-drug interaction involving organic anion transporter 3 in humans by in vitro uptake experiments. *Drug metabolism and disposition: the biological fate of chemicals* **39:**1031-1038.

Weber EJ, Chapron A, Chapron BD, Voellinger JL, Lidberg KA, Yeung CK, Wang Z, Yamaura Y, Hailey DW, Neumann T, Shen DD, Thummel KE, Muczynski KA, Himmelfarb J, and Kelly EJ (2016) Development of a microphysiological model of human kidney proximal tubule function. *Kidney Int* **90:**627-637.

Wessler JD, Grip LT, Mendell J, and Giugliano RP (2013) The P-glycoprotein transport system and cardiovascular drugs. *J Am Coll Cardiol* **61:**2495-2502.

Woodhead JL, Yang K, Brouwer KL, Siler SQ, Stahl SH, Ambroso JL, Baker D, Watkins PB, and Howell BA (2014) Mechanistic Modeling Reveals the Critical Knowledge Gaps in Bile Acid-Mediated DILI. *CPT Pharmacometrics Syst Pharmacol* **3:**e123.

Xu C, Li CY, and Kong AN (2005) Induction of phase I, II and III drug metabolism/transport by xenobiotics. *Arch Pharm Res* **28:**249-268.

Yabe Y, Galetin A, and Houston JB (2011) Kinetic characterization of rat hepatic uptake of 16 actively transported drugs. *Drug metabolism and disposition: the biological fate of chemicals* **39:**1808-1814.

Yang K, Guo C, Woodhead JL, St Claire RL, 3rd, Watkins PB, Siler SQ, Howell BA, and Brouwer KL (2016) Sandwich-Cultured Hepatocytes as a Tool to Study Drug Disposition and Drug-Induced Liver Injury. *Journal of pharmaceutical sciences* **105:**443-459.

Yang K, Kock K, Sedykh A, Tropsha A, and Brouwer KL (2013) An updated review on drug-induced cholestasis: mechanisms and investigation of physicochemical properties and pharmacokinetic parameters. *Journal of pharmaceutical sciences* **102:**3037-3057.

Yang XN, Gandhi YA, Duignan DB, and Morris ME (2009) Prediction of Biliary Excretion in Rats and Humans Using Molecular Weight and Quantitative Structure-Pharmacokinetic Relationships. *Aaps Journal* **11:**511-525.

Yonezawa A and Inui K (2011) Importance of the multidrug and toxin extrusion MATE/SLC47A family to pharmacokinetics, pharmacodynamics/toxicodynamics and pharmacogenomics. *Br J Pharmacol* **164:**1817-1825.

Zamek-Gliszczynski MJ, Lee CA, Poirier A, Bentz J, Chu X, Ellens H, Ishikawa T, Jamei M, Kalvass JC, Nagar S, Pang KS, Korzekwa K, Swaan PW, Taub ME, Zhao P, and Galetin A (2013) ITC recommendations for transporter kinetic parameter estimation and translational modeling of transport-mediated PK and DDIs in humans. *Clin Pharmacol Ther* **94:**64-79.

Zhou SF (2008) Drugs behave as substrates, inhibitors and inducers of human cytochrome P450 3A4. *Current Drug Metabolism* **9:**310-322.

Acknowledgements

First of all, I would like to thank my academic supervisor **Prof. Dr. Jörg Huwyler** for providing me the opportunity to be part of his group and to realize this collaborative PhD project. I greatly appreciated your enthusiasm for my work and our interesting discussions. Thank you for your support throughout the last three years and our nice trip to Bad Herrenalb.

I would like to express my deepest gratitude to **Dr. Gian Camenisch** for giving me the chance to complete my PhD studies in his group and for my exciting PhD project. It was a great pleasure to resolve the cholestasis! Thank you for your passion about unbound intrahepatic drug concentrations and your scientific advice to achieve them. In addition, I would like to thank you for your trust in me and your continuous support for the accomplishment of all publications and presentations.

A very special thank you goes to **Dr. Birk Poller** for being my patient supervisor and friend over the last years. Thank you for your commitment to this work, for your guidance through all challenges in my PhD, for sharing your expert knowledge about drug transporters and pharmacokinetics with me, and for the nice, educational, and funny time in and outside of your lab. May the Kp be with uu!

I would like to thank **Dr. Olivier Kretz** and **Dr. Vijay Bhargava** for the great opportunity to conduct my PhD studies in the PK Sciences / DMPK department of Novartis.

I am very grateful to my co-referee **Prof. Dr. Gerd Kullak-Ublick** for being part of my thesis committee and the evaluation of this work. I highly appreciated your interest for my PhD projects and the valuable advice for the classification of cholestatic drugs. In addition, I would like to thank **Prof. Dr. Stephan Krähenbühl** for overtaking the role of chair for my PhD defense.

Many thanks to **Dr. Kenichi Umehara** for his scientific advice regarding the metabolism studies and providing me access to his laboratory and equipment. I would also like to thank you for your help with all modeling issues as well as for your contribution to the efflux transporter project and our upcoming publication. In addition, I would like to thank **Marc Witschi** and **Claire Juif** for introducing me into the field of enzyme kinetics, microsomes, and HPLC analysis and their help with all technical and experimental difficulties. It was a great pleasure to learn from and work with you, thank you for the nice time in your lab!

I would like to thank **Dr. Hilmar Schiller** for his scientific advice in order to implement the binding assays. Thank you for your guidance and sharing your extensive knowledge about enzymes and